UNIVERSITÉ
LAVAL

Modélisation de la consolidation au dégel à grandes déformations

Thèse

Simon Dumais

Doctorat en génie civil
Philosophiæ doctor (Ph. D.)

Québec, Canada

Modélisation de la consolidation au dégel à grandes déformations

Thèse

Simon Dumais

Sous la direction de :

Jean-Marie Konrad, directeur de recherche

Résumé

Cette thèse présente le développement d'une méthode d'ingénierie pour la modélisation de la consolidation au dégel non linéaire à grandes déformations. Les travaux qui y sont présentés s'inscrivent à la suite des théories et de modèles de consolidation existants. Les bases de la théorie de consolidation au dégel à une dimension sont donc reprises. En premier lieu, un modèle numérique de consolidation au dégel non linéaire à grandes déformations est formulé en combinant la théorie de consolidation à grandes déformations de Gibson et des équations de transferts de chaleur. Ces deux composantes sont couplées au sein d'un domaine de modélisation défini en coordonnées lagrangiennes qui s'adaptent aux déformations de sol. Il en résulte donc l'introduction d'une seconde frontière mobile à la surface pour la modélisation de la consolidation au dégel en plus de la frontière mobile au front de dégel. Le modèle utilise des relations non linéaires $\sigma_v' - e - k_v$ pour définir les propriétés des sols dégelés. Une étude de cas du pipeline expérimentale d'Inuvik est réalisée avec le modèle numérique. Cette étude de cas permet de démontrer l'utilisation du modèle pour un problème pratique et de valider le modèle. Les résultats obtenus sont comparés aux résultats de la théorie de consolidation au dégel linéaire à petites déformations et aux mesures de terrain. Le modèle non linéaire à grandes déformations offre une augmentation importante de la précision lors du calcul des tassements de fonte, du taux de tassement et des pressions interstitielles excédentaires. En second lieu, un modèle conceptuel pour la consolidation au dégel des sols dégelés à grains fins est proposé. Ce modèle permet de définir les caractéristiques des relations $\sigma_v' - e - k_v$ utilisées comme intrants au modèle numérique de consolidation au dégel. Le concept de la contrainte résiduelle y est généralisé aux sols riches en glace en spécifiant qu'il s'agit de la contrainte effective au sein des éléments de sol plutôt que de la contrainte effective globale du sol. Ensuite, des relations empiriques sont formulées pour déterminer les caractéristiques des relations $\sigma_v' - e - k_v$ à partir de l'indice des vides initial du sol dégelé et de propriétés d'indice du sol.

Abstract

This thesis presents the development of an engineering method for the modelling of large strain nonlinear thaw consolidation. The work presented herein follows existing thaw consolidation theories and models. The foundations of one-dimensional thaw consolidation theory are therefore used. First, a numerical model for large strain nonlinear thaw consolidation is formulated by combining the Gibson large strain consolidation theory to heat transfer equations. The two components are coupled in a modelling domain formulated in Lagrangian coordinates that adapts to the soil deformation. This results in the introduction of a second moving boundary at the soil surface to model thaw consolidation in addition to the moving boundary at the thaw front. The model uses nonlinear $\sigma'_v - e - k_v$ relationships to define the properties of thawed soils. A case study of the Inuvik experimental pipeline with the numerical model is presented. The case study demonstrates the use of the model for a practical problem and it is used to validate the model. The modelling results are compared to the results obtained with the small strain linear thaw consolidation theory and with the field data. The results obtained with the large strain nonlinear model for thaw settlement, the rate of thaw settlement and the excess pore pressures compare favourably with the field data. Second, a conceptual model for thaw consolidation of thawed fine-grained soils is proposed. The model is used to define the characteristics of the nonlinear $\sigma'_v - e - k_v$ relationships used as input for the numerical modelling of thaw consolidation. The concept of the residual stress is generalized to ice rich soils by specifying that it is the effective stress within the soil element rather than the effective stress of the bulk soil. Then, empirical relationships are formulated to determine the characteristics of the $\sigma'_v - e - k_v$ relationships as a function of the initial thawed void ratio and soil index properties.

Table des matières

Liste des figures

Liste des tableaux

Liste des symboles

a	Profondeur en coordonnées Lagrangiennes /*depth in Lagrangian coordinates*
A	Section transversale d'un élément de sol /*cross-section of a soil element*
B et n	Coefficients thermiques du sol pour la profondeur de dégel /*thermal coefficients of soil for thaw depth*
C_c^*	Indice de compressibilité du sol dégelé /*compression index of the thawed soil*
C_k^*	Indice de changement de la conductivité hydraulique du sol dégelé /*hydraulic conductivity change index of the thawed soil*
C	Capacité thermique volumétrique du sol / *volumetric heat capacity of the soil*
c_u	Capacité thermique volumétrique du sol dégelé /*volumetric heat capacity of unfrozen soil*
c_i	Capacité thermique massique de la glace / *heat capacity of ice by mass*
c_s	Capacité thermique massique des solides / *heat capacity of solids by mass*
c_w	Capacité thermique massique de l'eau / *heat capacity of water by mass*
c_v	Coefficient de consolidation /*coefficient of consolidation*
d_{50_ff}	Taille médiane des grains de la fraction fine / *median grain size of the fine fraction*
e	Indice des vides/*void ratio*
e_{LL}	Indice des vides à la limite de liquidité/ *void ratio at the liquid limit*
e_f	Indice des vides du sol gelé/*void ratio of frozen soil*
e_i^*	Indice des vides initial du sol dégelé/*initial thawed void ratio*
e_0^*	Indice des vides du sol dégelé/*thawed void ratio*
g et λ	Coefficients hydromécaniques du sol /*hydromechanical coefficients of soil*
G	Gradient géothermique / *geothermal gradient*
G_s	Densité des particules solides / *specific gravity of solid particles*
H	Épaisseur de sol dégelé/*thickness of thawed layer*
H_w	Épaisseur d'eau à la surface du sol/ *thickness of water accumulating at the surface*
K	Perméabilité du sol dégelé /*permeability of unfrozen soil*
k_f	Conductivité thermique du sol gelé /*thermal conductivity of frozen soil*
k_g	Conductivité thermique du sol /*thermal conductivity of the ground*
k_u	Conductivité thermique du sol dégelé/*thermal conductivity of unfrozen soil*
k_v	Conductivité hydraulique verticale /*vertical hydraulic conductivity*
k_{v0}^*	Conductivité hydraulique verticale initiale du sol dégelé /*initial vertical hydraulic conductivity of the thawed soil*
L	Chaleur latente de fusion de l'eau / *latent heat of fusion of water*
L_s	Chaleur latente du *sol* / *latent heat of the soil*
m_v	Coefficient de changement de volume / *coefficient of volume change*
P_0	Charge appliquée /*applied load*
P_i	Pression de la glace / *ice pressure*

q	Flux thermique / *heat flux*
R	Ratio de consolidation au dégel /*thaw consolidation ratio*
s	Tassement /*settlement*
t	Temps /*time*
t_{thaw}	Temps pour que le dégel atteigne le bas de l'échantillon / *time for thaw depth to reach bottom of the sample*
T	Température / *temperature*
T_0	Température initiale / *inital temperature*
T_f	Point de congélation du sol / *freezing point of the soil*
T_g	Température du sol /*ground temperature*
T_s	Température à la surface /*surface temperature*
u	Pression interstitielle /*pore pressure*
u_h	Pression hydrostatique / *hydrostatic pore pressure*
u_e	Pression interstitielle excédentaire / *excess pore pressure*
U	Degré de consolidation / *degree of consolidation*
v_a	Vitesse d'écoulement d'eau dans la direction a / *water flow velocity in the direction of a*
v_s	Vitesse des particules de sol / *velocity of soil particles*
v_w	Vitesse de l'eau interstitielle / *velocity of pore water*
V_i	Volume spécifique de la glace / s*pecific volume of ice*
V_w	Volume spécifique de l'eau / *specific volume of water*
w_L	Limite de liquidité/ *liquid limit*
w_P	Limite de plasticité/ plastic *limit*
w_u	Teneur en eau non gelée / *Unfrozen water content*
X	Profondeur de dégel /*thaw penetration depth*
Z	Profondeur normalisée /*normalized depth*
Z_z	Profondeur de dégel à petites déformations / *small strain thaw depth*
α ou α_T	Taux de pénétration au dégel /*rate of thaw penetration*
α_u et β_u	Coefficients du sol pour la teneur en eau non gelée / *characteristic coefficients of the soil for the unfrozen water content*
γ'	Poids volumique déjaugé /*buoyant unit weight*
γ_i	Poids volumique de la glace /*unit weight of ice*
γ_s	Poids volumique des solides /*unit weight of solids*
γ_w	Poids volumiques de l'eau /*unit weight of water*
δ	Déformation au dégel /*thaw strain*
θ_i	Fraction volumique de glace / *volumetric fraction of ice*
θ_s	Fraction volumique de solide / *volumetric fraction of the soil particles*
θ_u	Fraction volumique d'eau non gelée /*volumetric fraction of unfrozen water*

θ_v Fraction volumique des vides / *volumetric fraction of the voids*

θ_w Fraction volumique de l'eau / *volumetric fraction of water*

κ_f Diffusivité du sol gelé /*diffusivity of frozen soil*

κ_u Diffusivité du sol dégelé /*diffusivity of unfrozen soil*

λ Conductivité thermique du sol / *thermal conductivity of the soil*

λ_s Conductivité thermique des particules solides / *thermal conductivity of solid particles*

ρ_i Masse volumique de la glace / *density of ice*

ρ_s Masse volumique des solides / *density of solids*

ρ_w Masse volumique de l'eau / *density of water*

σ'_0 Contrainte résiduelle /*residual stress*

σ_v Contrainte total verticale / *total vertical stress*

σ'_v Contrainte effective verticale/*vertical effective stress*

ξ Profondeur en coordonnées convectives /*depth in convective coordinates*

ΔV Évacuation volumétrique de l'eau au front de dégel / *volumetric discharge of water at the thaw front*

ΔZ Épaisseur d'une couche de sol / *soil layer thickness*

Δt Incrément de temps /*time increment*

Remerciements

Mes premiers remerciements vont à mon directeur de recherche, Jean-Marie Konrad. Je vous remercie de m'avoir confié ce projet de recherche auquel vous teniez tant. Grâce à vous, j'ai appris la rigueur et l'importance de s'appuyer des fondements théoriques solides. Je vous remercie d'avoir été aussi exigeant avec moi que je devrais toujours l'être envers moi-même et de m'avoir appris à devenir mon plus sévère critique. Ça a été un énorme plaisir de participer à ce réel travail de collaboration au cours duquel vous m'avez transmis beaucoup au niveau scientifique et professionnel.

Je remercie mes collègues étudiants d'avoir rendu l'expérience plus qu'agréable. En réalisant d'aussi longues études graduées, j'ai eu la chance de croiser le chemin de plusieurs étudiants de très grande qualité. J'espère que j'aurai l'occasion de travailler à nouveau avec eux au cours de ma carrière dans le domaine de la géotechnique.

Je remercie les professeurs du département de génie civil et de génie des eaux de l'Université Laval et plus précisément les professeurs du domaine de la géotechnique grâce à qui j'ai reçu une formation de très haute qualité. C'est réellement inspirant pour moi d'avoir pu mener mes études graduées au sein d'un département aussi prestigieux. J'aimerais particulièrement remercier Guy Doré grâce à qui j'ai eu la piqure de la recherche scientifique.

Je remercie ma famille et plus particulièrement mes parents, Denis et Suzanne. Je vous remercie du soutien inconditionnel que vous m'avez toujours offert. Deux valeurs que vous m'avez inculquées m'ont particulièrement été utiles durant mes études : papa, tu m'as toujours dit « ce qui mérite d'être fait, mérite d'être bien fait » et maman, « quand on commence quelque chose, on le finit ».

Mes derniers remerciements sont sans aucun doute les plus importants. Ils vont à la personne sans qui tout ça n'aurait pas été possible, à ma femme, Loriane. Merci de m'avoir forcé à travailler quand je manquais de motivation et de m'avoir forcé à me reposer quand j'en avais besoin. Merci de m'avoir supporté à travers les hauts et les bas que j'ai connus durant mes études. Surtout, merci d'avoir enduré mon caractère durant les moments plus difficiles. Merci de m'avoir soutenu lorsque je recevais des commentaires plus durs sur mon travail et de m'avoir rappelé l'importance de ces commentaires. Merci de m'avoir permis de parler d'indice des vides pendant qu'on soupait après de longues journées de travail. Merci de m'avoir poussé à réaliser plusieurs projets professionnels qui m'ont permis de vivre des expériences très enrichissantes. C'est tellement important d'avoir pu compter sur quelqu'un comme toi qui a toujours compris tout ce que ça représente de faire un doctorat. Enfin, je te remercie d'être une mère extraordinaire pour notre fils Roman. Merci de t'être occupé de lui à temps double alors que je terminais ma thèse. Et, un petit gros merci à toi, Roman, sans trop le savoir, tu m'as donné un second souffle afin de compléter mon doctorat en donnant un sens tout particulier à ma vie.

Avant-propos

Cette thèse de doctorat est rédigée sous la forme d'une thèse par insertion d'articles. Ce type de thèse dite de forme hybride comprend donc des chapitres de facture traditionnelle et des chapitres composés par l'insertion d'articles. Cette thèse comprend donc l'insertion intégrale de deux articles qui composent le contenu des chapitres 2 et 3 de ce document. Quelques modifications mineures ont été apportées aux articles principalement dans le but d'homogénéiser la terminologie et les symboles utilisés dans cette thèse. Ces modifications sont indiquées en avant-propos des chapitres 2 et 3. Deux articles publiés dans des actes de conférence sont aussi insérés en annexe. Ces deux articles sont insérés sans modification en raison de la nature préliminaire de ces travaux et pour éviter la confusion avec certains concepts traités différemment dans le corps de la thèse. Les références des articles insérés ainsi que leur statut de publication au moment de la publication de ce document se détaillent comme suit :

Chapitre 2

Dumais, S., et Konrad, J.-M. 2018. One-dimensional large-strain thaw consolidation using nonlinear effective stress – void ratio – hydraulic conductivity relationships. Canadian Geotechnical Journal, 55(3): 414–426. doi:10.1139/cgj-2017-0221. (Soumis le 18 avril 2017, accepté le 3 août 2017, publié sur le Web le 15 août 2017)

Chapitre 3

Dumais, S., et Konrad, J.-M. 2019. Large-Strain Nonlinear Thaw Consolidation Analysis of the Inuvik Warm-Oil Experimental Pipeline Buried in Permafrost. Journal of Cold Regions Engineering, 33(1): 04018014. doi:10.1061/(ASCE)CR.1943-5495.0000179. (Soumis le 27 avril 2018, accepté le 24 août 2018, publié sur le Web le 22 décembre 2018)

Annexe A

Dumais, S., et Konrad, J.-M. 2015. Laying the foundations for the development of an extension to the theory of thaw consolidation. In Cold Regions Engineering 2015 : Developing and Maintaining Resilient Infrastructure. Salt Lake City, USA. pp. 78–89. doi:10.1061/9780784479315.008.

Annexe B

Dumais, S., et Konrad, J.-M. 2016. Compressibility and hydraulic conductivity of thawed fine-grained permafrost. In 11th International Symposium on Cold Regions Development: Energy Development in Cold Regions. Incheon, Korea.

L'article intitulé *One-dimensional large-strain thaw consolidation using nonlinear effective stress – void ratio – hydraulic conductivity relationships* publié par la Revue canadienne de géotechnique a été primé en tant que « Choix du rédacteur en chef ». Cette distinction « met en vedette des articles d'actualité et de calibre particulièrement élevé » qui ont été choisis par les rédacteurs en chef de la Revue canadienne de géotechnique. (Canadian Science Publishing 2019) Les articles recevant cette mention figurent sur la page d'accueil du site internet de la Revue canadienne de géotechnique.

L'article intitulé *Large-Strain Nonlinear Thaw Consolidation Analysis of the Inuvik Warm-Oil Experimental Pipeline Buried in Permafrost* publié par le *Journal of Cold Regions Engineering* de l'ASCE a été sélectionné comme « Choix du rédacteur en chef ». Grâce à cette distinction, l'article a figuré sur la page d'accueil du site internet du *Journal of Cold Regions Engineering*.

Les articles ont été insérés intégralement en anglais, la langue d'origine de leur publication. Il est à noter que le corps des chapitres 4 et 5 sont aussi rédigés en anglais pour assurer l'uniformité de ce document. Le reste de la thèse est rédigé en français. Notamment, les chapitres 2 à 5 sont complétés de discussions complémentaires rédigées en français afin d'assurer la transition entre les chapitres.

L'auteur de cette thèse de doctorat est le premier auteur de tous les articles mentionnés ci-haut. Sa contribution scientifique aux articles comprend les tâches suivantes: la définition des objectifs spécifiques de la recherche, la revue de littérature, la collecte de données provenant de la littérature, la formulation des concepts mathématiques, l'implémentation numérique des modèles, la réalisation des simulations numériques, l'analyse et l'interprétation des résultats, la rédaction des articles, la production des figures et des graphiques, et la communication avec les revues scientifiques.

Un seul coauteur a contribué à tous les articles mentionnés ci-haut : Professeur Jean-Marie Konrad, directeur de recherche de l'auteur de cette thèse de doctorat. Sa contribution scientifique aux articles comprend les tâches suivantes : la définition des objectifs principaux de la recherche, la supervision générale des travaux de recherche, la révision critique des articles avant leur soumission et durant le processus de révision, la révision linguistique et la révision de la terminologie scientifique, et le perfectionnement des analyses et de l'interprétation des résultats en collaboration avec l'auteur de cette thèse.

Pour les deux articles publiés, la contribution de quatre réviseurs anonymes ainsi que celle des rédacteurs en chef, des corédacteurs et des éditeurs de la Revue canadienne de géotechnique et du *Journal of Cold Regions Engineering* doivent aussi être soulignés. Ils ont émis de nombreux commentaires qui ont permis d'améliorer la qualité et la compréhension générale des articles.

Introduction

Contexte

Le pergélisol s'étend sur environ le quart de la superficie terrestre mondiale et la moitié de la superficie terrestre du Canada (French 2017). Au Canada, plusieurs villages et communautés se retrouvent en zone de pergélisol continu et discontinu, principalement au Yukon, aux Territoires du Nord-Ouest, au Nunavut, au Nunavik et dans le nord du Manitoba (TAC 2010). De plus, l'arctique renferme d'importantes quantités de ressources naturelles telles que des ressources minérales, pétrolières et gazières. Selon le United States Geological Survey, jusqu'à 22 % de l'ensemble des ressources mondiales de pétroles et de gaz naturel pourraient se trouver en régions arctiques (Committee on appropriations 2009).

Le développement socio-économique, l'amélioration de la qualité de vie des communautés et l'exploitation des ressources naturelles nécessitent la construction d'infrastructures diverses. Les infrastructures de transports telles que les routes, les pistes d'atterrissage et les chemins de fer permettent d'avoir accès à ces endroits éloignés. Les bâtiments permettent d'abriter les personnes, les biens et les activités des communautés.

Or, le régime thermique du pergélisol est inévitablement affecté par la construction d'infrastructures. Une dégradation thermique peut être causée, entre autres choses, par le retrait de la végétation (Linell 1973), par la modification des propriétés géothermiques des sols naturels, par la mise en place d'une couche de sol minéral à la surface du sol naturel pour la construction de remblais, par la modification des réseaux d'écoulement de l'eau de surface et de l'eau souterraine (de Grandpré et coll. 2012) et par l'accumulation préférentielle de neige (O'Neil et Burn 2017). Ces facteurs favorisent l'absorption de chaleur de chaleur dans le sol durant la période de dégel et/ou réduisent l'extraction de chaleur du sol durant la période de gel.

Cette dégradation thermique peut mener à la fonte des couches supérieures du pergélisol et entrainer des problèmes de tassements de fonte et d'instabilités. L'importance des problèmes rencontrés dépend de nombreux facteurs tels que la teneur en glace du sol gelé, la sensibilité au dégel du pergélisol et les propriétés du sol dégelé. Pour les infrastructures de transports, la fonte du pergélisol se manifeste sous la forme de rotation des épaulements des remblais

routiers, de fissures longitudinales et de tassements différentiels (Doré et Zubeck 2008). Les bâtiments sont particulièrement touchés par les tassements de fonte importants et les tassements différentiels. Les instabilités de pentes lors du dégel peuvent aussi être problématiques lorsque celles-ci surviennent à proximité d'infrastructures. Les dommages environnementaux liés à la dégradation du pergélisol sont aussi substantiels notamment en raison de l'écoulement de sédiments fins provenant du pergélisol riche en glace au sein des cours d'eau et de la perturbation des délicats écosystèmes en milieux de pergélisol (TAC 2010).

Pour les raisons décrites ci-haut, la conception d'infrastructures sur pergélisol présente un défi d'ingénierie majeur. Les changements climatiques contribuent aussi à aggraver les problématiques liées à la dégradation thermique du pergélisol. Ainsi, la pérennité de l'état des infrastructures existantes peut être compromise. L'ampleur des problèmes dépend des méthodes et des outils de conception utilisés qui sont souvent inadaptés au contexte particulier du pergélisol (Doré et Zubeck 2008). Les outils d'ingénierie adaptés à la pratique de la géotechnique du pergélisol sont donc nécessaires afin d'assurer une conception sécuritaire et durable des infrastructures construites sur pergélisol et pour l'évaluation des infrastructures existantes.

Problématique

On considère maintenant le phénomène de consolidation au dégel. Pour ce faire, on considère un sol saturé à grains fins initialement gelé dont la température à la surface du sol augmente au-dessus de 0 °C. Le front de dégel pénètre alors dans le sol à un taux qui dépend de la température à la surface et des propriétés géothermiques du sol. Au front de dégel, un volume d'eau provenant de la fonte de la glace initialement contenue dans le sol est libéré. Le sol gelé se trouvant sous le front de dégel forme alors une barrière imperméable. Le domaine où se trouve le sol dégelé est défini entre la surface et le front de dégel. Le sol dégelé est soumis à une contrainte composée du poids propre du sol et de la surcharge à la surface du sol. L'eau de fonte au front de dégel est donc soumise à des pressions interstitielles. Si ces pressions interstitielles excèdent les pressions hydrostatiques, l'eau s'écoule alors vers la surface. Il se produit alors un processus de consolidation. Des tassements de fonte résultent de l'expulsion de l'eau de fonte hors du sol et du déplacement des particules de sol. Le drainage de l'eau

peut être entravé par le sol dégelé se trouvant au-dessus du front de dégel. Il peut donc y avoir déséquilibre entre le taux de génération et le taux de dissipation des pressions interstitielles et des pressions interstitielles excédentaires subsistent dans le sol. Si les conditions thermiques en surface changent de sorte que la pénétration du front de dégel se stabilise, les pressions interstitielles excédentaires peuvent se dissiper. Un tassement de fonte supplémentaire se produit dans cette phase post-dégel.

Une théorie ou un modèle de consolidation au dégel permet de modéliser le phénomène physique se produisant lors du dégel d'un sol. Un premier objectif d'une théorie de consolidation au dégel est d'obtenir la vitesse de pénétration du dégel dans le sol ainsi que la position du front de dégel ce qui permet d'évaluer le taux de génération des pressions interstitielles et le domaine de consolidation. À partir de ces paramètres, les pressions interstitielles excédentaires dans le sol sont calculées afin de déterminer leur évolution ainsi que l'évolution du tassement de fonte en fonction du temps. Une théorie de consolidation cherche aussi à calculer les tassements de fonte à la fin du dégel et dans la phase post-dégel.

Une théorie ou un modèle de consolidation au dégel est constitué de deux composantes : une composante thermique et une composante hydromécanique. Une théorie ou un modèle de consolidation au dégel est le résultat du couplage entre ces deux composantes. Pour la composante hydromécanique, on utilise typiquement une théorie de consolidation des sols dans le domaine de la géotechnique.

Plusieurs théories et modèles de consolidation au dégel ont été formulés (Tsytovich et coll. 1965, Morgenstern and Nixon 1971, Sykes et coll. 1974, Foriero et Ladanyi 1995, Qi et coll. 2013). Ces théories et modèles utilisent différentes composantes et adoptent différentes stratégies de couplage. Morgenstern et Nixon (1971) ont proposé la première théorie complète de consolidation au dégel en adoptant la configuration proposée par Tsytovich et coll. (1965) et en formulant correctement les conditions hydromécaniques au front de dégel. Il s'agit encore aujourd'hui d'une théorie communément utilisée dans la pratique en raison de sa simplicité et des solutions analytiques pratiques proposées. Cette théorie peut donc être utilisée à titre comparatif pour le développement d'une extension à la théorie de consolidation au dégel.

La formulation de la théorie de Morgenstern et Nixon (1971) repose sur certaines hypothèses simplificatrices pouvant avoir un impact important sur le calcul de la consolidation au dégel. Notamment, la théorie de consolidation de Terzaghi est utilisée comme la composante hydromécanique. Or, la théorie de Terzaghi est une théorie de consolidation à petites déformations. Les grandes déformations résultant de la fonte de sols riches en glace ne peuvent être prises en compte dans l'analyse. En effet, le niveau de la surface du sol est toujours fixé à son élévation initiale. Dans une théorie de consolidation au dégel, les conditions limites de drainage libre et de température sont typiquement imposées à la surface. En ne considérant pas les grandes déformations, on néglige l'impact important du déplacement de la surface du sol lors de la consolidation, et donc, du déplacement des conditions limites sur le taux de pénétration du front de dégel et sur le taux de dissipation des pressions interstitielles.

Aussi, la solution de Neumann est utilisée comme composante thermique de la théorie de Morgenstern et Nixon (1971). Le taux de pénétration au dégel est donc d'abord obtenu à partir de cette solution analytique. Le taux de pénétration au dégel est ensuite utilisé pour l'évaluation du processus hydromécanique lors du dégel. Il s'agit donc d'une approche non couplée qui ne considère pas les interactions entre le processus de thermique du dégel et le processus hydromécanique de la consolidation.

Enfin, les propriétés de sol utilisées dans la théorie de Morgenstern et Nixon (1971) sont constantes tout au long de l'analyse. Cette approche ne permet pas de considérer l'évolution des propriétés thermiques et hydromécaniques du sol lors du dégel. Les sols riches en glace sont particulièrement problématiques, car leur teneur en eau change de manière importante tout au cours du processus de consolidation au dégel.

Il est important de noter que les hypothèses simplificatrices précédemment énoncées ont dû être adoptées en raison du contexte technologique existant lors du développement de la théorie de Morgenstern et Nixon (1971). En effet, la puissance des outils de calcul disponibles à l'époque était limitée. Il aurait donc été complexe d'obtenir des solutions pour la consolidation au dégel sans simplifier la formulation théorique. La formulation simplifiée a d'ailleurs permis d'obtenir des solutions analytiques ce qui explique en grande partie l'adoption générale de la théorie dans la pratique.

Remarquant certaines lacunes à la formation de la théorie de consolidation au dégel à petites déformations, certains chercheurs ont offert d'importantes contributions afin d'améliorer la théorie de consolidation au dégel. Sykes et coll. (1974) ont d'abord proposé un modèle prenant en compte le déplacement de la surface du sol lors du processus de consolidation au dégel en intégrant des équations de transfert de chaleur comme composante thermique. Foriero et Ladanyi (1995) ont utilisé la théorie de consolidation de Gibson à grandes déformations pour la modélisation de la consolidation au dégel. Qi et coll. (2013) ont récemment revisité les travaux de Sykes et coll. (1974) en améliorant la formulation thermique et en implémentant le modèle au logiciel FLAC3D communément utilisé dans la pratique de la géotechnique. Bien que ces travaux offrent d'intéressantes pistes de solutions, aucun modèle proposé ne parvient à améliorer l'ensemble des lacunes notables de la théorie de Morgenstern et Nixon (1971) qui demeure donc la plus pratique. De plus, les modèles de Sykes et coll. (1974) et de Qi et coll. (2013) sont basés sur la théorie de consolidation de Biot qui est une théorie à petites déformations. Donc, ils ne sont théoriquement pas adaptés à la modélisation de la consolidation au dégel à grandes déformations. Le modèle de Foriero et Ladanyi (1995) quant à lui ne comporte pas de composante thermique comme telle et la formulation de la condition limite à la frontière mobile au front de dégel n'est pas formulée en cohérence avec la formulation généralement acceptée de la théorie de Morgenstern et Nixon (1971).

Enfin, malgré les nombreux modèles de consolidation au dégel disponibles, très peu de recherches se sont intéressées directement à la caractérisation complète des propriétés hydromécaniques des sols à grains fins utilisées pour la modélisation de la consolidation au dégel. Ainsi, les propriétés de sol utilisées pour la consolidation au dégel sont typiquement définies telles que proposées par les théories de consolidation des sols non gelés.

Les propriétés des sols dégelés à grains fins ont été principalement étudiées en ce qui concerne l'effet des cycles de gel et de dégel (Chamberlain et Gow 1979, Chamberlain et Blouin 1977, Chamberlain et coll. 1990, Konrad et Samson 2000a, 2000b, Konrad 2010). Dans ces études, les échantillons de sol non gelé sont soumis à des cycles de gel et de dégel en utilisant différentes conditions thermiques et différents cheminements de contraintes. Les propriétés du sol dégelé et consolidé sont alors analysées en comparaison aux propriétés du

sol non gelé en termes des changements de conductivité hydraulique et des changements d'indice des vides. Le cheminement particulier des contraintes est rarement défini en termes des changements d'état du sol lors du gel et du dégel. Ces recherches offrent des informations intéressantes quant à la façon dont la structure du sol est affectée par le gel. Cependant, les relations qui en résultent ne peuvent être utilisées directement pour la modélisation de la consolidation au dégel, car l'état initial du sol gelé n'est souvent pas caractérisé. Ceci est particulièrement problématique pour le pergélisol pour lequel l'état du sol gelé est utilisé comme principal intrant à l'analyse de consolidation au dégel.

Cette discussion souligne l'importance de poursuivre les travaux de recherches sur la consolidation au dégel autant en point de vue de la modélisation du phénomène que de la caractérisation des propriétés des sols lors du dégel. Le développement d'une extension à la théorie de consolidation au dégel pouvant tenir en compte des grandes déformations et de l'évolution des propriétés lors du processus de consolidation au dégel est rendu possible grâce à l'accessibilité croissante des outils de calcul numérique puissants. L'utilisation de ces outils dans la pratique de la géotechnique s'est d'ailleurs largement démocratisée. De plus, le développement d'un modèle de consolidation au dégel numérique plus complet peut bénéficier de l'amélioration de la caractérisation des propriétés des sols lors du dégel. Les travaux présentés dans cette thèse constituent une extension à la théorie de consolidation au dégel existante et s'inscrivent donc à la suite des travaux antérieurs sur le sujet.

Objectifs de la recherche

La Figure I.1 résume les objectifs de la recherche ainsi que la structure de la thèse. L'objectif principal de la recherche est de **développer une méthode complète d'ingénierie pour la modélisation de la consolidation au dégel.** L'objectif principal se subdivise en objectifs spécifiques qui se regroupent en deux axes concomitants.

Les objectifs spécifiques de l'axe 1 qui porte sur la modélisation numérique de la consolidation au dégel sont de :

1.1. **Développer un modèle numérique de consolidation au dégel à grandes déformations avec relations $\sigma'_v - e - k_v$ non linéaires;**

   a. **Développement du modèle;**

       b. **Validation du modèle;**

1.2. Déterminer les implications pratiques des grandes déformations et de la non-linéarité des relations $\sigma'_v - e - k_v$ sur la modélisation de la consolidation au dégel.

Les objectifs spécifiques de l'axe 2 qui porte sur les propriétés des sols lors du dégel sont de :

1.1. Développer un modèle conceptuel pour la consolidation au dégel en termes des relations $\sigma'_v - e - k_v$ des sols à grains fins;

1.2. Développer une méthode empirique pour la prédiction des caractéristiques des relations $\sigma'_v - e - k_v$ des sols à grains fins.
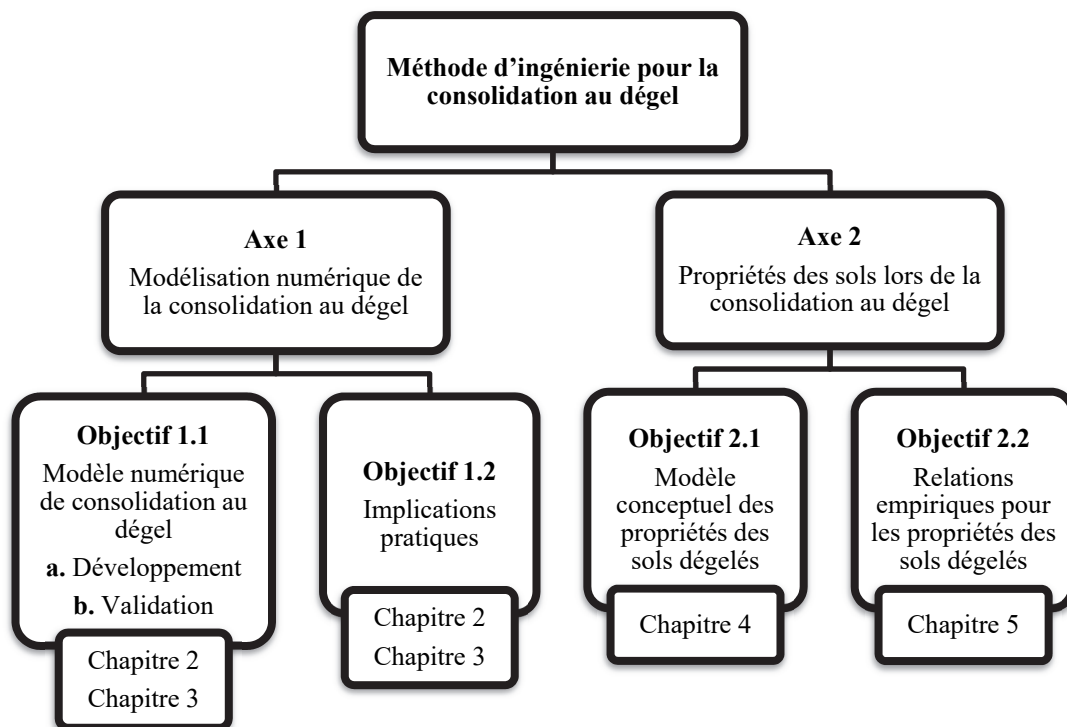
Figure I.1 : Résumé des objectifs de la recherche et structure de la thèse

Plan de la thèse

Ce document est composé de cinq chapitres principaux. Le chapitre 1 présente une revue de littérature. Les chapitres 2 et 3 portent sur la modélisation numérique de la consolidation au dégel et couvrent donc l'axe 1 de la recherche. Les chapitres 4 et 5 portent sur les propriétés des sols dégelés et couvrent donc l'axe 2 de la recherche.

Le chapitre 1 dresse un état de connaissance sur la modélisation de la consolidation au dégel afin de préciser la problématique traitée dans cette thèse. Cette revue de littérature permet de complémenter les mises en contexte et les états de connaissance inclus aux chapitres 2 à 5. Les modèles et théories de consolidation au dégel sont présentés suivant l'ordre chronologique de leur parution. Les différentes composantes et les approches de modélisation des différentes théories ainsi que les améliorations et extensions qu'elles ont apportées à l'évaluation de la consolidation au dégel sont présentées. Une description des propriétés des sols dégelés utilisée par ces modèles est aussi incluse.

Comme mentionné dans l'avant-propos, les chapitres 2 et 3 comportent l'insertion d'articles. La structure de ces chapitres est donc semblable. Un avant-propos rédigé en français présente les informations essentielles des articles. Les articles insérés constituent le corps des chapitres. Le corps des chapitres est donc rédigé en anglais. Enfin, une discussion complémentaire est présentée afin de faire la transition entre les chapitres, mais aussi de discuter de certains aspects du contenu des articles. Cette discussion est rédigée en français. La majeure partie de la discussion de cette thèse se trouve donc en après-propos des chapitres 2 à 5. Il est important de noter que la même structure est adoptée pour les chapitres 4 et 5 que pour les chapitres 2 et 3 afin d'homogénéiser les quatre chapitres principaux de la thèse. Le corps des chapitres 4 et 5 est donc aussi rédigé en anglais bien qu'il ne s'agisse pas d'un article publié ou soumis au moment de la publication de cette thèse. La structure générale d'un article scientifique traditionnel est aussi utilisée aux chapitres 4 et 5.

Le chapitre 2 présente un modèle numérique de consolidation au dégel à grandes déformations utilisant des relations $\sigma'_v - e - k_v$ non linéaires. La théorie de consolidation à grandes déformations de Gibson est utilisée comme composante hydromécanique. Des équations de transferts de chaleur simples sont utilisées pour la composante thermique. Ces deux composantes sont complètement couplées au sein d'un modèle à coordonnées Lagrangiennes. L'utilisation de coordonnées Lagrangiennes permet de considérer aisément les grandes déformations. La dérivation de l'ensemble des équations mathématiques soutenant le modèle de consolidation au dégel est présentée. Un exemple d'application du modèle pour un essai de laboratoire de consolidation au dégel est présenté. Les résultats obtenus sont comparés avec ceux obtenus avec la théorie de consolidation au dégel de

Morgenstern et Nixon (1971). La différence fondamentale entre les conceptions théoriques de la profondeur du dégel entre les deux théories est soulignée. L'impact des grandes déformations pour le calcul de la vitesse de pénétration du dégel sur les résultats obtenus est discuté.

Le chapitre 3 présente une application pratique du modèle de consolidation au dégel proposé. Le chapitre présente la marche à suivre pour utiliser le modèle pour un cas appliqué. Le pipeline expérimental d'Inuvik construit sur un pergélisol riche en glace est utilisé à titre d'exemple. La caractérisation des propriétés du sol au dégel à partir d'essai de laboratoire est présentée. L'objectif principal de ce chapitre est de présenter les implications pratiques du modèle non linéaire à grandes déformations. Ainsi, les résultats thermiques (taux de pénétration au dégel) et les résultats hydromécaniques (tassements de fonte, évolution des tassements et pressions interstitielles excédentaires) obtenus à l'aide du modèle sont comparés à ceux rapportés par Morgenstern et Nixon (1975) en utilisant leur théorie linéaire à petites déformations. Le chapitre permet aussi de valider le modèle numérique présenté au chapitre 2 en comparant les résultats de modélisation aux résultats obtenus sur le terrain.

Le chapitre 4 porte sur le modèle conceptuel pour la définition des propriétés des sols dégelés à grains fins utilisés pour l'évaluation de la consolidation au dégel. Les relations $\sigma'_v - e - k_v$ sont donc définies à partir de l'interprétation générale du comportement au dégel des sols. Le concept de contrainte résiduelle est intégré au modèle conceptuel. Le concept de la contrainte résiduelle est généralisé aux sols riches en glace en considérant la contrainte effective spécifique des éléments de sol plutôt que globalement. Des résultats d'essais de laboratoire réalisés pour définir les propriétés pour la consolidation au dégel provenant de la littérature sont analysés en fonction du modèle conceptuel proposé. Les relations définies par le modèle conceptuel peuvent être utilisées directement comme intrant pour le modèle numérique de consolidation au dégel présenté au chapitre 2.

Le chapitre 5 présente une méthode empirique afin d'obtenir les caractéristiques des relations $\sigma'_v - e - k_v$ pour les sols dégelés à grains fins à partir des propriétés d'index des sols. Un compendium de données provenant de la littérature est utilisé pour développer les relations empiriques. La méthode empirique proposée permet de définir les relations $\sigma'_v - e - k_v$ tel

que défini par le modèle conceptuel présenté au chapitre 4 et conformément au modèle numérique de consolidation au dégel présenté au chapitre 2.

Enfin, la conclusion résume et discute des principales contributions présentées dans cette thèse en plus de brosser le portrait des besoins additionnels de recherches concernant la consolidation au dégel par rapport aux travaux présentés dans cette thèse.

Chapitre 1   Consolidation au dégel

1.1   Introduction

L'évaluation du comportement lors du dégel constitue une considération essentielle pour l'étude géotechnique du pergélisol. Au dégel, la glace contenue dans le sol fond et le squelette du sol dégelé doit trouver un nouvel équilibre en réponse aux contraintes externes. La conséquence principale du dégel du pergélisol se manifeste sous la forme de tassements de fonte lorsque le squelette de sol dégelé ne peut contenir l'ensemble de l'eau de fonte.

L'évaluation des tassements de fonte est primordiale pour la conception d'infrastructures construites sur pergélisol pouvant affecter le régime thermique. Comme le contenu en glace du pergélisol est très variable, et ce même sur de très courtes distances, le dégel du pergélisol peut engendrer des tassements différentiels importants. Les tassements de fonte se manifestent aussi lors de la fonte des sols affectés par le gel saisonnier ou à la suite du gel artificiel en raison de la création de glace de ségrégation lors du gel.

Les conséquences du dégel ne se limitent pas aux tassements de fonte. Il peut y avoir génération de pressions interstitielles excédentaires si le drainage de l'eau de fonte est entravé en raison de la faible perméabilité du sol dégelé. Ces pressions interstitielles excédentaires peuvent être la source d'instabilité lors du dégel, notamment pour les pentes en dégel.

La caractérisation des propriétés des sols dégelés est au cœur de l'évaluation de la consolidation au dégel. Or, il s'agit d'un aspect qui a été très peu étudié directement en relation au processus de dégel des sols. Ainsi, la plupart des approches d'évaluation de consolidation au dégel font usage des propriétés des sols telles que définies par les théories de consolidation traditionnelles. Pourtant, il est généralement reconnu que les propriétés des sols à grains fins sont affectées par le gel (Chamberlain et Gow 1979 et Konrad et Samson 2000a).

1.2   Consolidation au dégel

La modélisation du processus de consolidation au dégel vise à évaluer les tassements de fonte, l'évolution de ces tassements en fonction du temps ainsi que les pressions interstitielles excédentaires. Le processus de consolidation au dégel résulte de l'effet combiné du dégel et

de la consolidation. Une composante thermique et une composante hydromécanique sont donc utilisées pour la modélisation de la consolidation au dégel.

Les premières études cherchant à modéliser le processus de consolidation au dégel sont menées par des chercheurs de l'URSS au milieu des années 60. Au début des années 70, des efforts de recherches au Canada ont permis d'apporter des améliorations importantes aux théories initialement proposées. Périodiquement, des recherches se sont penchées sur l'amélioration de certains aspects des modèles proposés. La théorie de la consolidation au dégel a donc évolué au cours des années grâce à une suite de contributions. Il est donc approprié de présenter les différents modèles et théories de consolidation au dégel des sols sur lesquels s'appuient les travaux présentés dans cette thèse en ordre chronologique.

1.2.1 Tsytovich et coll. 1965

Tsytovich et coll. (1965) proposent une première théorie ayant pour objectif de calculer l'évolution des tassements de fonte et des pressions interstitielles lors du dégel. Ils posent ainsi les bases de la théorie unidimensionnelle de consolidation au dégel qui seront utilisées par plusieurs par la suite. On considère un sol gelé dont la température à la surface augmente instantanément au-dessus de 0°C. En se basant sur des observations expérimentales, ils posent l'hypothèse que le front de dégel se déplace alors à un taux constant défini par :

Équation 1-1 $X(t) = \alpha \sqrt{t}$

où X est la profondeur de dégel et α est le taux de pénétration du dégel.

Le paramètre α est alors déterminé expérimentalement. Afin de généraliser l'utilisation de la théorie, Tsytovich et coll. (1965) soulignent la nécessité de trouver une solution analytique pour déterminer le paramètre α.

La consolidation du sol dégelé est modélisée en utilisant la théorie de consolidation des sols par filtration, principe de base de la théorie de Terzaghi, avec un domaine de consolidation à frontière mobile au front de dégel. Les contraintes effectives au sein du sol dégelé sont donc calculées selon :

Équation 1-2 $c_v \dfrac{\partial^2 \sigma_v'}{\partial x^2} = \dfrac{\partial \sigma_v'}{\partial t}$

où c_v est le coefficient de consolidation et σ_v' est la contrainte effective.

La méthode de détermination du coefficient de consolidation pour les sols dégelés n'est pas spécifiée par Tsytovich et coll. (1965).

L'Équation 1-1 constitue la composante thermique de la théorie; l'Équation 1-2 est la composante hydromécanique. Le domaine de consolidation est défini entre la surface du sol et le front de dégel qui se déplace en fonction du temps. La frontière au front de dégel est considérée comme étant imperméable. Les conditions limites au front de dégel sont formulées en se basant sur le principe que l'eau interstitielle ne reprend pas l'ensemble des contraintes appliquées lors du dégel. Ces conditions limites sont formulées en fonction de paramètres expérimentaux. Elles ne sont donc pas généralisables pour l'évaluation de la consolidation au dégel hors d'un contexte expérimental. Une solution analytique à la théorie proposée est développée pour le calcul de l'évolution des tassements de fonte et des pressions interstitielles. Les tassements dus au changement de phase lors de la fonte de la glace sont ajoutés à la suite de l'évaluation des tassements de consolidation.

Tsytovich et coll. (1965) introduisent aussi pour la première fois le paramètre adimensionnel $\frac{\alpha}{2\sqrt{c_v}}$. Ce paramètre sera grandement utile aux développements des théories de consolidation au dégel par la suite. Selon la formulation de la théorie de Tsytovich et coll. (1965), ce paramètre est constant tout au long du processus de dégel pour un sol donné soumis à une température constante à la surface. Ils utilisent donc ce paramètre pour représenter des résultats de calcul généralisés.

1.2.2 Zaretskii 1968

Zaretskii (1968) cherche à généraliser la théorie proposée par Tsytovich et coll. (1965). Les conditions limites au front de dégel sont donc reformulées en assumant que le changement de teneur en eau du sol lorsque le front de dégel pénètre d'une profondeur donnée pour un certain pas de temps est égal à la quantité d'eau qui traverse le front de dégel durant ce pas de temps. Cependant, ces conditions limites sont erronées car Zaretskii (1968) considère que le changement de teneur en eau d'un élément de sol est égal à sa déformation volumique (Morgenstern et Nixon 1971). Encore une fois, des solutions analytiques sont

développées pour le calcul des tassements et du degré de consolidation. La définition du ratio $\frac{\alpha}{2\sqrt{c_v}}$ est aussi précisée comme étant le ratio entre le taux de dégel et le taux de l'expulsion de la phase liquide au sein de la couche dégelée.

1.2.3 Morgenstern et Nixon 1971

Morgenstern et Nixon (1971) reprennent la définition du problème de consolidation au dégel proposé par Tsytovich et coll. (1965). La configuration unidimensionnelle de la consolidation au dégel est illustrée à la Figure 1.1. Morgenstern et Nixon (1971) utilisent aussi l'Équation 1-1 comme composante thermique. Pour la composante hydromécanique, ils utilisent l'équation de Terzaghi formulée en fonction des pressions interstitielles u pour une contrainte appliquée qui ne varie pas dans le temps :

Équation 1-3 $\quad c_v \frac{\partial^2 u}{\partial z^2} = \frac{\partial u}{\partial t}$.
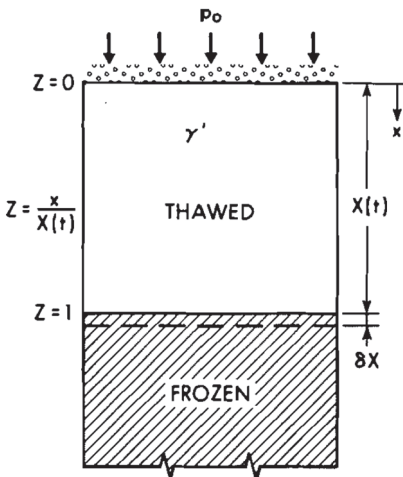
Figure 1.1 : Consolidation au dégel unidimensionnelle (d'après Morgenstern et Nixon 1971)

La contribution principale de Morgenstern et Nixon (1971) au développement de la théorie de consolidation au dégel est la formulation des conditions limites exactes au front de dégel. Les conditions limites sont formulées à partir du principe que l'écoulement d'eau au front de dégel est dû à la présence d'un gradient de pressions interstitielles. Cet écoulement qui provoque l'expulsion d'eau interstitielle hors du squelette de sol est lié à la déformation

volumique du sol. Pour les sols compressibles, les déformations volumiques sont liées à la variation de la contrainte effective. Les conditions limites au front de dégel sont donc données par :

$$\textit{Équation 1-4} \quad P_0 + \gamma'X - u - \sigma_0' = \frac{c_v\frac{\partial u}{\partial x}}{\frac{dX}{dt}}$$

où P_0 est la charge appliquée en surface, γ' est le poids volumique déjaugé et σ_0' est la contrainte résiduelle.

Morgenstern et Nixon (1971) dérivent alors une solution analytique au problème de la consolidation au dégel unidimensionnelle des sols similaire à celle formulée par Tsytovich et coll. (1965) et Zaretskii (1968). Cette solution est maintenant exacte en raison de la formulation des conditions limites au front de dégel utilisée.

Morgenstern et Nixon (1971) ont consacré le nom de ratio de consolidation au dégel (*thaw consolidation ratio*) et le symbole R au paramètre adimensionnel $\frac{\alpha}{2\sqrt{c_v}}$. Ils ont aussi introduit deux variables adimensionnelles pour leur permettre de produire une série d'abaques de calcul et de solutions sous forme d'équations:

$$\textit{Équation 1-5} \quad z = \frac{x}{X(t)}$$

et

$$\textit{Équation 1-6} \quad W_r = \frac{\gamma'X(t)}{P_0}.$$

Les deux abaques de calculs principaux développés par Morgenstern et Nixon (1971) sont présentés à la Figure 1.2 et à la Figure 1.3. Ces abaques permettent d'obtenir le profil de pressions interstitielles excédentaires pour différentes valeurs du ratio de consolidation au dégel R.
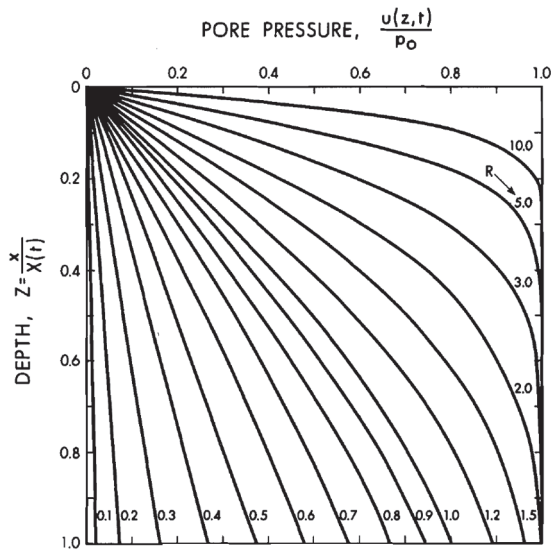
FIG. 2. Excess pore pressures; $W_r = 0$ (weightless material).

Figure 1.2 : Abaque des pressions interstitielles excédentaires en négligeant le poids propre du sol (Morgenstern et Nixon 1971)
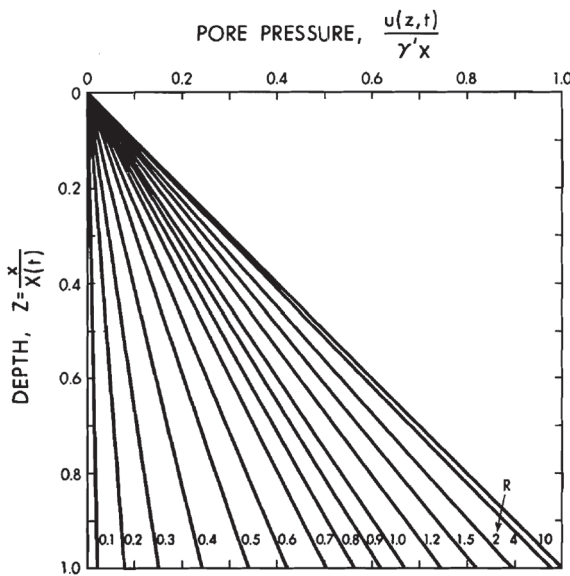
FIG. 3. Excess pore pressures; $W_r = \infty$ (no applied load).

Figure 1.3 : Abaque des pressions interstitielles excédentaires sans charge appliquée (Morgenstern et Nixon 1971)

Morgenstern et Nixon (1971) ont aussi développé un abaque pour obtenir le degré de consolidation au sein de la couche dégelée (Figure 1.4).
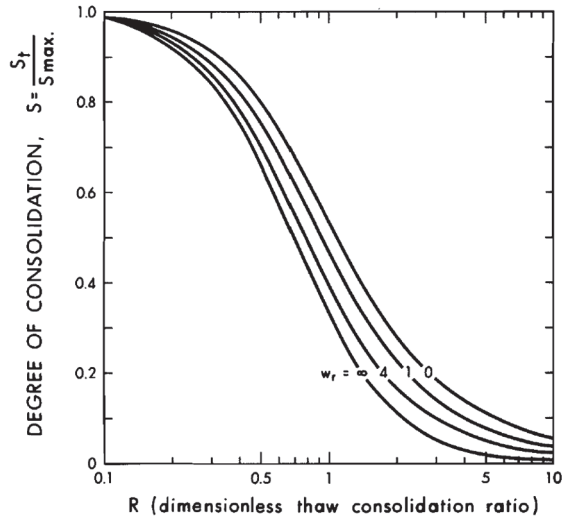
FIG. 5. Variation of S with R, $0 \leqslant W_r \leqslant \infty$.

Figure 1.4 : Abaque du degré de consolidation (Morgenstern et Nixon 1971)

Comme leurs prédécesseurs, Morgenstern et Nixon (1971) n'abordent pas initialement la méthode de détermination du coefficient de consolidation c_v pour les sols dégelés ni celle du taux de pénétration au dégel α.

L'élégance et l'efficacité des abaques et des solutions proposées par Morgenstern et Nixon (1971) ont grandement contribué à l'adoption générale de cette théorie dans les domaines de la pratique de la géotechnique et de la recherche sur le pergélisol. La théorie a été l'objet de plusieurs études subséquentes pour en valider l'exactitude et pour proposer des extensions pratiques.

1.2.4 Extensions à la théorie de Morgenstern et Nixon

L'aspect thermique du processus de consolidation au dégel a été étudié par Nixon et McRoberts (1973) qui ont évalué les différentes solutions analytiques disponibles pour obtenir le taux de pénétration au dégel α. La solution de Neumann et la solution de Stefan sont notamment jugées appropriées à l'évaluation de la consolidation au dégel. La solution de Stefan est décrite comme suit :

Équation 1-7 $X(t) = \sqrt{\frac{2k_u T_s}{L_s}} \sqrt{t}$

où k_u est la conductivité thermique du sol dégelé, T_s est la température en surface et L_s est la chaleur latente du sol.

Nixon et McRoberts (1973) ont notamment développé un abaque graphique pour la solution du Neumann (Figure 1.5). Les paramètres introduits à la Figure 1.5 se définissent ainsi : T_g est la température du sol, k_f est la conductivité thermique du sol gelé, κ_u et κ_f sont les diffusivités du sol dégelé et gelé et c_u est la capacité thermique volumétrique du sol dégelé.
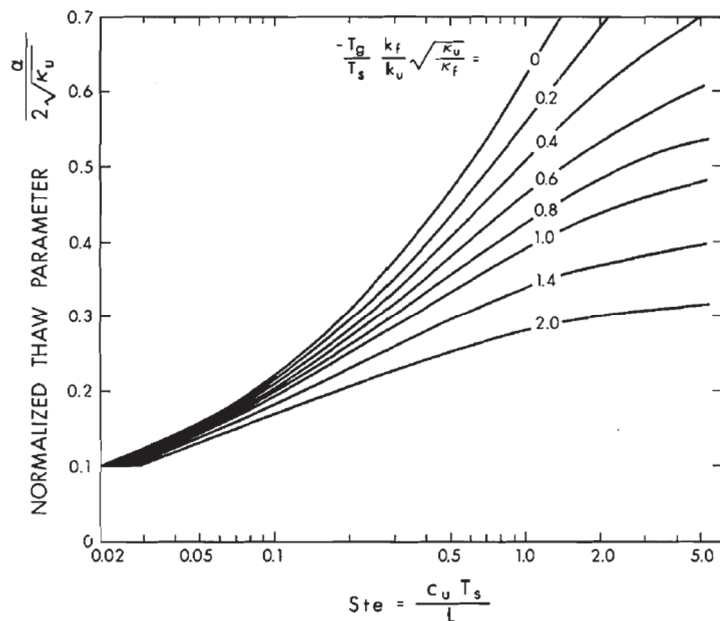
Figure 1.5 : Abaque pour la solution de Neumann (Nixon et McRoberts 1973)

Par la suite, Nixon et Morgenstern (1973b) développent une série d'extension pratique à la théorie initiale. Notamment, une définition plus générale de la pénétration du dégel est adoptée selon laquelle:

Équation 1-8 $X(t) = Bt^n$

où B et n sont des coefficients fonction des propriétés thermiques du sol, de la température de sol et de la température en surface.

Nixon (1973b) propose des solutions pour les systèmes multicouches communs en milieux de pergélisol. Il propose notamment un abaque pour le calcul des pressions interstitielles à la base d'une couche de sol sous laquelle se trouve une couche de glace (Figure 1.6). Les paramètres introduits à la Figure 1.6 se définissent ainsi : K est la perméabilité du sol dégelé, γ_i est le poids volumique de la glace et T_f est le point de fusion du sol.
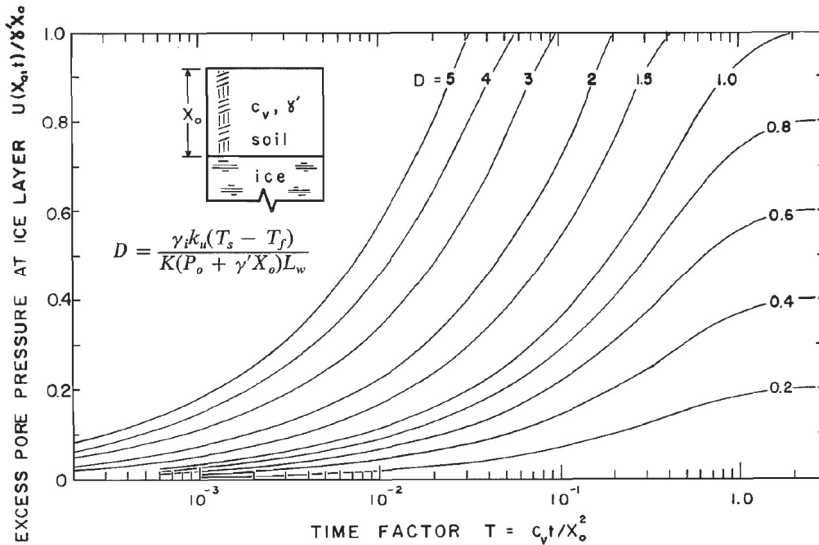
Figure 1.6 : Pressions interstitielles à l'interface entre le sol et la glace (Nixon 1973b)

La théorie de Morgenstern et Nixon (1971) et ses extensions sont validées grâce à une série d'articles portant sur des essais de laboratoire de consolidation au dégel pour des sols à grains fins remaniés (Morgenstern et Smith 1973), des pergélisols intacts (Nixon et Morgenstern 1974) et sur l'étude de cas du pipeline expérimental d'Inuvik (Morgenstern et Nixon 1975).

1.2.5 Sykes et coll. 1974

Sykes et coll. (1974) proposent de modéliser la consolidation au dégel à l'aide de la méthode des éléments finis. Ils cherchent à inclure à la théorie de consolidation au dégel certains aspects négligés par leurs prédécesseurs. Alors que les modèles précédents considèrent seulement les échanges de chaleur par conduction, Sykes et coll. (1974) considèrent aussi les échanges de chaleur dus à la convection forcée et à la radiation. La convection forcée est le résultat de l'écoulement de l'eau lors de la consolidation. La modification la plus importante apportée à la théorie de consolidation au dégel est de considérer le mouvement de la surface

du sol dans l'analyse. En effet, lors du processus de consolidation au dégel, la position de la surface du sol change en raison des tassements de fonte. La position de la surface joue un rôle primordial dans l'évaluation de la consolidation au dégel car il s'agit de l'endroit où certaines conditions limites sont imposées, notamment, les conditions thermiques et la condition de drainage libre. En considérant le mouvement de la surface, on considère donc aussi le déplacement de ces conditions limites lors du processus de consolidation au dégel. Enfin, ils notent l'importance d'inclure la variation des propriétés du sol lors du processus de dégel.

Pour développer leur modèle par éléments finis, Sykes et al. (1974) utilisent la théorie de consolidation de Biot. Cette théorie est une généralisation tridimensionnelle de la théorie de Terzaghi. Cette théorie est jumelée à des équations de transfert de chaleur des échanges de chaleur par conduction et par convection. L'analyse théorique du pipeline expérimental d'Inuvik démontre que le mouvement de la surface du sol et que les échanges de chaleur par convection ont un impact notable sur la pénétration du dégel et sur le tassement à la surface (Figure 1.7).
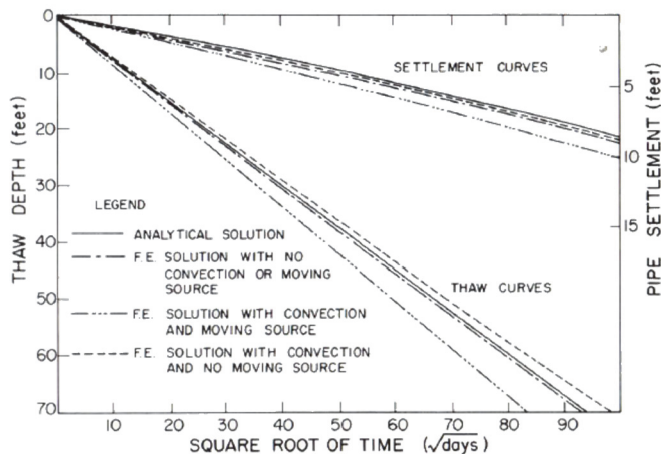
Figure 1.7 : Comparaison des analyses pour la pénétration du dégel et les tassements (Sykes et coll. 1974)

Malgré la pertinence indéniable des modifications proposées pour améliorer la théorie de consolidation au dégel, la validité du modèle proposé est remise en question en raison de l'utilisation de la théorie de Biot (Edgar 2015). La théorie de Biot est une théorie de consolidation à petites déformations ce qui limite la possibilité d'implémentation au sein d'un

modèle par éléments finis permettant les grandes déformations. La théorie de Biot n'est donc pas directement applicable aux sols lors du dégel si on considère le mouvement de la surface du sol. De plus, les conditions limites au front de dégel ne sont pas énoncées clairement (Edgar 2015). Enfin, les tassements dus à l'expulsion de l'eau en excès ne sont pas pris en compte ce qui limite grandement la plage d'applicabilité du modèle alors que ces tassements dominent le comportement au dégel des sols riches en glace.

1.2.6 Foriero et Ladanyi 1995

Foriero et Ladanyi (1995) notent aussi l'importance de considérer le mouvement de la surface du sol et le changement des propriétés hydromécaniques lors du processus de consolidation au dégel. Ils proposent donc un modèle de consolidation au dégel à grandes déformations. La simplicité de l'énoncé du problème de Morgenstern et Nixon (1971) est conservée. La composante thermique est donc prise en charge par une solution analytique simple. Cependant, la théorie de consolidation à grandes déformations de Gibson est utilisée pour remplacer la théorie de Terzaghi. La théorie de Gibson est en fait une généralisation de la théorie de Terzaghi. La différence principale est que la variable d'état utilisée est l'indice des vides plutôt que les pressions interstitielles. Ce changement permet d'implémenter la théorie au sein d'un système de coordonnées lagrangiennes qui s'adapte aux tassements lors du processus de consolidation au dégel en fonction des changements d'indice des vides. De plus, les propriétés hydromécaniques peuvent être définies en fonction de l'indice des vides pour permettre leur variation au cours du processus de consolidation au dégel.

La formulation de la théorie de Gibson utilisée par Foriero et Ladanyi (1995) est :

Équation 1-9 $\quad -\frac{1}{g}\frac{\partial e}{\partial t} + \frac{\partial^2 e}{\partial z^2} + \lambda(\gamma_s - \gamma_w)\frac{\partial e}{\partial z} = 0$

où e est l'indice des vides, g et λ sont des coefficients qui sont fonction du sol, γ_s et γ_w sont les poids volumiques des solides et de l'eau.

Cependant, les conditions limites au front de dégel sont formulées comme une condition imperméable alors que le processus se produisant au front de dégel correctement formulé par Morgenstern et Nixon (1971) n'est pas pris en compte. De plus, la solution analytique utilisée pour calculer la pénétration du dégel n'est pas couplée à la composante hydromécanique.

L'impact du mouvement de la surface du sol sur la pénétration du dégel ne peut donc être considéré que si on connait l'évolution des tassements de fonte à la surface avant l'analyse ce qui est seulement possible pour faire des analyses rétrospectives.

1.2.7 Qi et coll. 2013

Plus récemment, Qi et coll. (2013) ont revisité la théorie de Sykes et al. (1974) afin d'en améliorer la composante thermique utilisée. Les changements des propriétés géothermiques sont donc définis en fonction des changements de phase et de la teneur en eau pour améliorer la précision du calcul de la pénétration du dégel. Les limitations mentionnées ci-haut concernant l'utilisation de la théorie de consolidation de Biot demeurent problématiques pour l'évaluation de la consolidation au dégel des sols riches en glace.

1.3 Propriétés hydromécaniques des sols dégelés utilisées pour la modélisation de la consolidation au dégel

Les propriétés hydromécaniques des sols dégelés sont l'intrant principal des modèles de consolidation au dégel. Ces propriétés sont généralement définies par une relation contrainte-déformation et par la conductivité hydraulique du sol. La précision d'une évaluation de consolidation au dégel dépend grandement de la caractérisation des propriétés hydromécaniques utilisées.

La définition des propriétés hydromécaniques utilisée pour la modélisation du dégel varie selon les différents modèles de consolidation au dégel. Cependant, la plupart des modèles utilisent les théories de consolidation et les définitions des propriétés hydromécaniques telles que définies pour les sols non gelés. Le cheminement d'état particulier que subit le sol lors du dégel n'est donc pas toujours pris en compte pour la modélisation de la consolidation au dégel bien qu'il soit généralement reconnu que le comportement des sols dégelés diffère de celui des sols non gelés.

Les modèles qui reposent sur l'utilisation de la théorie de consolidation à petites déformations de Terzaghi utilisent le coefficient de consolidation comme paramètre hydromécanique. Le coefficient de consolidation est défini par :

Équation 1-10 $c_v = -\dfrac{(1+e_f) \cdot k_v}{\gamma_w \cdot \frac{de}{d\sigma_v'}}$

où e_f est l'indice des vides du sol gelé et k_v est la conductivité hydraulique du sol.

Une valeur constante du coefficient de consolidation est typiquement utilisée pour la modélisation se la consolidation au dégel suivant l'hypothèse selon laquelle les changements d'indice des vides lors de la consolidation sont suffisamment petits pour que la conductivité hydraulique et le ratio $de/d\sigma_v'$ ne varient pas significativement. Or, cette hypothèse est applicable qu'aux sols présentant de faibles déformations au dégel.

Nixon (1973) note l'incompatibilité de l'approche de consolidation à petites déformations avec la modélisation du dégel des sols riches en glace. Il considère alors différentes définitions de la relation entre l'indice des vides et la contrainte effective (Figure 1.8). Il calcule notamment les pressions interstitielles excédentaires obtenues pour l'analyse d'un sol incompressible et les compare aux résultats obtenus avec la théorie linéaire (Figure 1.9). Il note que le comportement non linéaire typique d'un sol riche en glace se trouve entre ces deux relations.
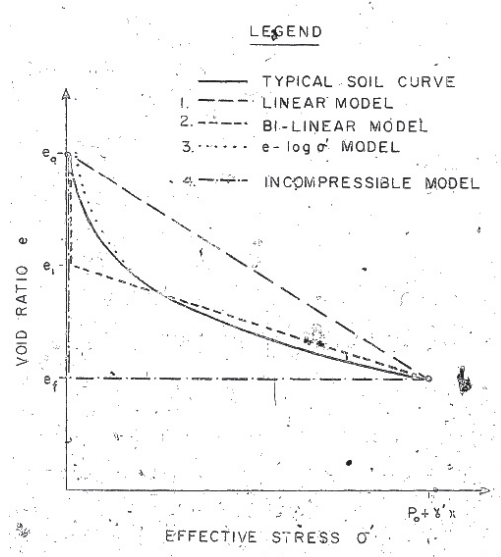
Figure 1.8 : Différentes relations entre l'indice des vides et la contrainte effective (Nixon 1973)
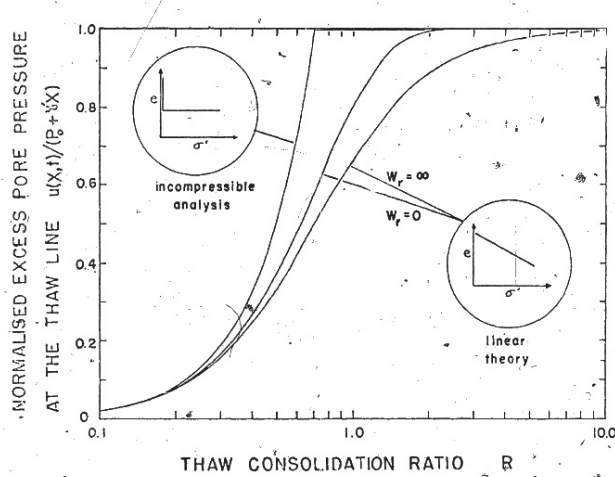
Fig. 5.10 Pore Pressures from Incompressible Analysis

Figure 1.9 : Pressions interstitielles pour l'analyse d'un sol incompressible (Nixon 1973)

La non-linéarité de la relation entre la contrainte effective et l'indice des vides est étudiée par Nixon et Morgenstern (1973b). Ils notent que la théorie de consolidation de Terzaghi considère que la relation entre la contrainte effective et l'indice des vides est linéaire. Cependant, pour les changements d'indice des vides importants lors de la consolidation, comme lors de la consolidation au dégel de sols riches en glace, la relation typique entre la contrainte effective et l'indice des vides est plutôt non linéaire (Figure 1.10).
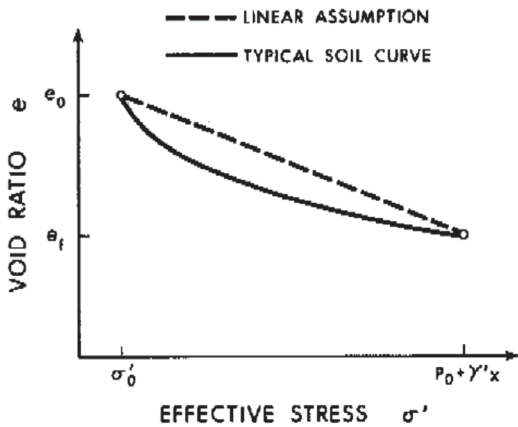
Figure 1.10 : Relation contrainte effective - indice des vides des sols dégelés (Nixon et Morgenstern 1973b)

L'hypothèse d'une relation linéaire a un impact sur la génération de pressions interstitielles excédentaires en raison du gradient entre l'indice des vides et la contrainte effective qui est utilisé pour le calcul du taux de consolidation du sol dégelé. Nixon et Morgenstern (1973b)

proposent donc d'utiliser le ratio P_0/σ_0' comme mesure de l'augmentation de contrainte effective dans le sol pour caractériser la non-linéarité. La contrainte résiduelle σ_0' est la contrainte effective dans le sol en conditions de dégel non drainées, c'est-à-dire la contrainte effective initiale dans le sol lors du dégel. Nixon et Morgenstern (1973b) développent donc un abaque de calcul qui prend en compte la non-linéarité de la relation σ_v' - e (Figure 1.11).
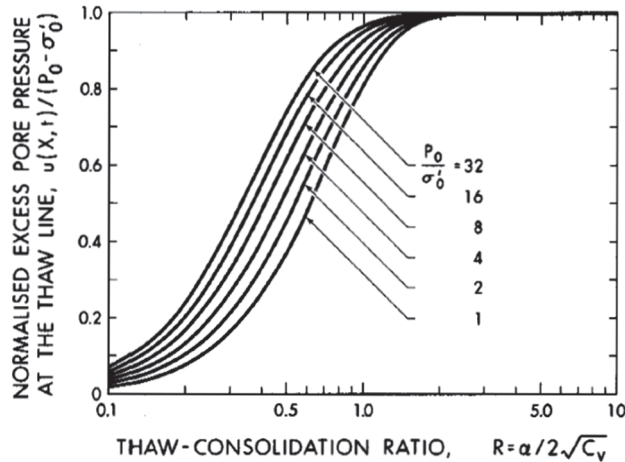
Figure 1.11 : Pressions interstitielles au front de dégel pour la théorie non linéaire (Nixon et Morgenstern 1973b)

1.3.1 La contrainte résiduelle

Selon Nixon (1973), la caractérisation de la non-linéarité de la relation contrainte effective – indice des vides peut être basée sur la contrainte résiduelle σ_0'. La contrainte résiduelle est définie comme la contrainte effective dans le skeleton de sol dégelé en conditions non drainées (Nixon et Morgenstern 1973a). La contrainte effective est illustrée à la Figure 1.12. Un sol est normalement consolidé au Point A sous une contrainte appliquée P_0. Il est alors gelé en conditions non drainées. Le soulèvement au dégel pour atteindre le Point B se limite donc au changement de phase de l'eau vers la glace. Lors du gel, l'eau se trouvant dans les macropores gèle en premier. L'eau adsorbée et l'eau capillaire des micropores sont alors en contact avec la glace remplissant les macropores. Selon les lois de la thermodynamique, l'eau non gelée est alors dans un état de succion. Cette succion lors du gel mène à la surconsolidation des éléments de sol qui atteignent le point D. Le sol gelé est donc constitué d'éléments de sol surconsolidés et de glace discrète. Lors du dégel en condition non drainée, les éléments de sol absorbent l'eau de fonte pour rejoindre le point E. La contrainte effective

dans le sol est alors la contrainte résiduelle. Lorsque le drainage est permis, le sol qui se trouve toujours sous une contrainte appliquée P_0 se consolide au point C. On note donc un tassement au dégel net du point A au point C lors du dégel. La contrainte résiduelle caractérise la contrainte dans le squelette de sol lors du dégel.
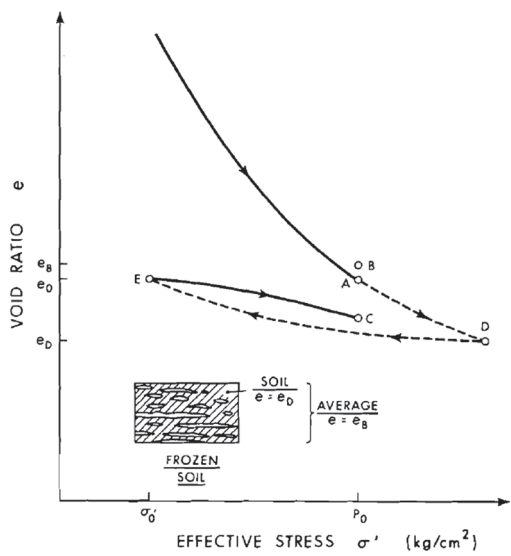
Figure 1.12 : Contrainte effective d'un sol soumis à un cycle de gel et de dégel (Nixon et Morgenstern 1973a)

Chapitre 2   One-Dimensional Large-Strain Thaw Consolidation Using Nonlinear Effective Stress – Void Ratio – Hydraulic Conductivity Relationships

Avant-propos

Auteurs et affiliation

Simon Dumais et Jean-Marie Konrad

Département de génie civil et de génie des eaux, Université Laval.

Titre français

Consolidation unidimensionnelle à grandes déformations lors du dégel avec relations non-linéaires contrainte effective – indices des vides – conductivité hydraulique

Modifications apportées à l'article publié

L'article publié est reproduit intégralement. Quelques modifications mineures ont été apportées en ce qui a trait à la nomenclature et aux symboles utilisés pour la définition des propriétés des sols dégelés afin d'homogénéiser l'ensemble de la thèse.

2.1   Résumé français

Un modèle unidimensionnel de consolidation au dégel est formulé en combinant les théories de consolidation à grandes déformations et de transfert de chaleur. Le modèle inclut les transferts de chaleur dus à la conduction, au changement de phase et à l'advection. Le comportement hydromécanique est modélisé selon la théorie de consolidation à grandes

déformations. Les équations sont couplées dans un domaine à frontières mobiles formulé en coordonnées Lagrangiennes. Les grandes déformations sont permises et l'évolution des propriétés du sol est caractérisée par des relations contrainte effective – indice des vides – conductivité hydraulique non linéaires. Les conditions initiales et les conditions limites sont présentées avec une attention particulière portée au développement des conditions limites mobiles au front de dégel en termes de la consolidation à grandes déformations. Le modèle proposé est appliqué à un exemple théorique du dégel d'un échantillon de sol à grains fins et les résultats sont comparés à ceux obtenus avec la théorie de consolidation au dégel à petites déformations. Les résultats de modélisation sont présentés en fonction du profil de température, de la pénétration du dégel, du tassement, de l'indice des vides et des pressions interstitielles excédentaires.

2.2   Abstract

A one-dimensional model for the consolidation of thawing soils is formulated in terms of large-strain consolidation and heat-transfer equations. The model integrates heat transfer due to conduction, phase change, and advection. The hydromechanical behaviour is modelled by large-strain consolidation theory. The equations are coupled in a moving boundary scheme developed in Lagrangian coordinates. Finite strains are allowed and nonlinear effective stress – void ratio – hydraulic conductivity relationships are proposed to characterize the thawing soil properties. Initial conditions and boundary conditions are presented with special consideration for the moving boundary condition at the thaw front developed in terms of large-strain consolidation. The proposed model is applied and compared with small-strain thaw consolidation theory in a theoretical working example of a thawing fine-grained soil sample. The modelling results are presented in terms of temperature, thaw penetration, settlements, void ratio, and excess pore-water pressures.

2.3   Introduction

The assessment of instabilities related to thawing soils is paramount for the sustainable design of infrastructure built on permafrost. There is thus a substantial incentive for developing a comprehensive engineering theory to predict the magnitude and rate of settlement as well as the magnitude of the pore-water pressures generated upon thawing of a frozen soil.

There is general agreement that modelling this complex thermo-hydro-mechanical process involves coupling heat transfer with consolidation theory. The first complete thaw consolidation theory was proposed by Morgenstern and Nixon (1971); it was formulated in terms of conventional small-strain consolidation theory, which may not be applicable to ice-rich soils undergoing large thaw strains due to the imposed limitation of small strains and the use of linear soil properties. A solution for thaw consolidation with a nonlinear void ratio – effective stress relationship was presented by Nixon and Morgenstern (1973a) indicating that the pore-water pressure at the thaw front increases with increasing degree of non-linearity. This solution was nevertheless derived in a small-strain configuration. Subsequently, Foriero and Ladanyi (1995) modelled thaw consolidation using large-strain consolidation theory, which allows for finite strains and accounts for the variation of the hydraulic conductivity and compressibility during consolidation.

Nevertheless, the aforementioned studies reduced thaw consolidation to an uncoupled moving boundary consolidation problem. The rate of thaw penetration was evaluated by a closed-form solution to heat conduction for simple boundary conditions prior to any assessment of consolidation. The displacement of the surface thermal boundary condition as settlement proceeds was ignored, which led to an underestimation of the rate of thaw penetration (Sykes et al. 1974). For complex thermal boundary conditions, the rate of thaw penetration can be determined more rigorously from the temperature profile calculated using the heat-transfer equation including conduction, phase change, and advection implemented in a moving boundary modelling scheme (Sykes et al. 1974).

To comply with the intricate coupled nature of the problem at hand, this paper presents the development and application of a theory of generalized coupled thaw consolidation for saturated soils. The formulation retains the simplicity of the problem statement of one-dimensional thaw consolidation while gaining the generality of large-strain consolidation and heat-transfer theories. Nonlinear effective stress – void ratio – hydraulic conductivity relationships are used for the characterization of the hydromechanical behaviour of the soil upon thawing. The theory is numerically implemented in a moving boundaries finite-element model formulated in Lagrangian coordinates. Finally, the model is applied to the theoretical case of thawing fine-grained soil in a working example. Model results are compared with the

analytical solution to the problem of small-strain thaw consolidation derived by Morgenstern and Nixon (1971) to highlight the main implications inherent to the large-strain configuration adopted in this study.

2.4 Problem Statement

Changes in the thermal conditions at the surface of a semi-infinite mass of frozen soil may initiate thawing. Thaw penetration then proceeds at a rate controlled mainly by the surface thermal conditions and by the thermal properties of the soil. Water released at the thaw front from the melting of ice contained in the ground is subjected to a pore-water pressure gradient generated from the combination of thawed soil self-weight and applied load. Consequently, water in excess of the amount that can be absorbed by the soil skeleton under existing stress conditions flows towards the surface. The length of the drainage path is initially infinitely small and consolidation of the upper thawed layers of the soil is almost instantaneous. This leads to the creation of a thawed soil layer with reduced permeability impeding the drainage of water subsequently generated at the thaw front, and excess pore-water pressures may be generated if drainage is insufficient. In addition to the deformations due to phase change from ice to water, thaw settlement proceeds by seepage of the excess melt water. In thaw consolidation theory, the frozen soil can be considered impermeable and incompressible as water flow and deformations in the thawed layer are significantly larger than in the frozen region.

It should also be noted that the rate of thaw penetration is affected by the consolidation process. As settlement proceeds, surface thermal boundary conditions move towards the thaw front accelerating the rate of thaw penetration. Also, the soil thermal properties, which are largely controlled by the volumetric fractions of ice, water, and soil particles, are affected by the void ratio changes upon consolidation. Furthermore, seepage of water towards the surface upon consolidation generates heat transfer by advection (Nixon 1975, Sykes et al. 1974).

Consequently, the interaction between consolidation and heat transfer needs to be considered in the assessment of thaw consolidation. Accordingly, the coupled large-strain thaw consolidation model proposed hereafter circumvents the shortcomings of previously proposed theories by considering consolidation and heat transfer concurrently within a

unified modelling domain. This is facilitated by using the void ratio as a state variable as it can be used as a proxy as the variable that governs most physical processes involved in thaw consolidation. The modelling domain, also defined in terms of void ratio, is thus capable of efficiently handling soil deformations and multiple moving boundaries, such as surface settlement and advancing thaw front.

2.4.1 Modelling Domain

A schematic representation of one-dimensional large-strain thaw consolidation is presented in Figure 2.1 in Lagrangian coordinates (a, which represents depth). The modelling domain is divided into two regions: the thawed region and the frozen region. Heat transfer is effectively modelled over the full height of the soil column while consolidation modelling is limited to the thawed region as the frozen region is assumed to be impermeable and incompressible.

The heat-transfer domain is defined in Lagrangian coordinates between an upper boundary at the surface of the ground $a = 0$ and a lower boundary set at an arbitrary depth $a = H_i$. At the initial state $t = 0$, the soil temperature is below the freezing point of the soil, T_f. Thawing is initiated by changing thermal boundary conditions at the surface, which is commonly modelled as a step increase in surface temperature. The lower thermal boundary conditions at $a = H_0$ can be defined by a geothermal flux. During thaw consolidation at any given time $t > 0$, the freeze–thaw interface is located at thaw depth $a = Z(t)$. Heat-transfer continuity is ensured between the thawed and frozen regions at $a = Z(t)$.

The consolidation domain is defined between a free-draining upper boundary at the surface of the ground $a = 0$, where a uniformly distributed load P_0 is applied, and a moving impervious lower boundary at $a = Z(t)$. Settlement $s(a, t)$ is defined as a function of depth and time. During thaw consolidation, the position of the upper boundary at $a = 0$ for consolidation and heat transfer is thus given by the surface settlement denoted $s(0, t)$.
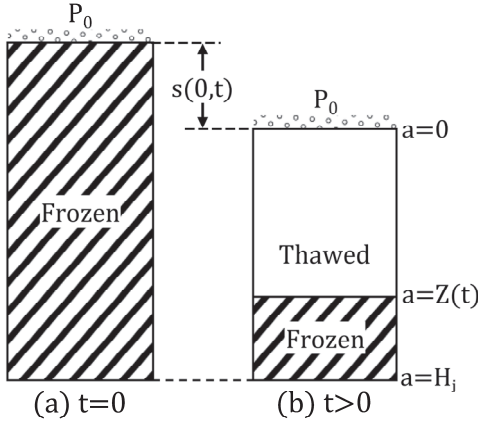
Figure 2.1 : One-dimensional large-strain thaw consolidation in Lagrangian coordinates: (a) t = 0 and (b) t > 0

2.4.2 Coordinate Systems

Before proceeding to the mathematical development of the thaw consolidation model, it is convenient to properly differentiate the two coordinate systems used in the current study. The following description is adapted from Gibson et al. (1981) for the case of the consolidation of thawing soils. One-dimensional consolidation within the thawed soil layer is presented in Figure 2.2 in terms of Lagrangian and convective coordinates. The configuration presented in Lagrangian coordinates in Figure 2.2a is analogous to the state before consolidation of the thawed soil occurs. The bottom boundary taken as the datum plane is at the thaw front $a = Z(t)$ and the upper boundary is at the soil surface $a = 0$. An element of soil $A_0B_0C_0D_0$ is located at the Lagrangian coordinate position a and has a thickness ∂a. At any given time $t > 0$ during consolidation, the state of the thawed soil layer can be represented by the convective coordinates configuration shown in Figure 2.2b. The element of soil, now bound by $ABCD$, is located at the convective coordinate position ξ and has a thickness $\partial\xi$. The datum plane remains at the thaw front, which is expressed in convective coordinates as $\xi = Z(t)$. In the current study, thaw depth $Z(t)$ is always expressed with respect to the initial position of the ground surface; the height of the thawed layer at any given time $t > 0$ is thus given by

Equation 2-1 $\quad H(t) = Z(t) - s(0, t).$
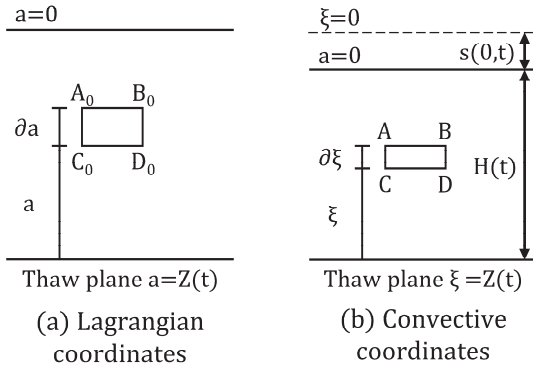
Figure 2.2 : Coordinate systems for consolidation of thawing soil (adapted from Gibson et al. (1981)): (a) Lagrangian coordinates and (b) convective coordinates

The upper boundary moves with surface settlements $s(0, t)$. The convective coordinate position of the upper boundary located at the surface of the ground $a = 0$ is thus always given by

Equation 2-2 $\quad \xi(0, t) = s(0, t)$.

This definition can be extended for any depth such that convective coordinates ξ are related to Lagrangian coordinates a and to settlement $s(a, t)$ by

Equation 2-3 $\quad \xi = a + s(a, t)$.

The schematic representation of the change in void ratio during thaw consolidation presented in Figure 2.3 illustrates that the conversion between Lagrangian coordinates and convective coordinates is given by

Equation 2-4 $\quad \dfrac{\partial \xi}{\partial a} = \dfrac{1+e}{1+e_f}$.

where $e = e(a, t)$ is the void ratio profile at time t and $e_f = e(a, 0)$ is the initial void ratio profile of the frozen soil. Accordingly, Lagrangian coordinates can always be referenced back to the initial state characterized by the frozen void ratio.
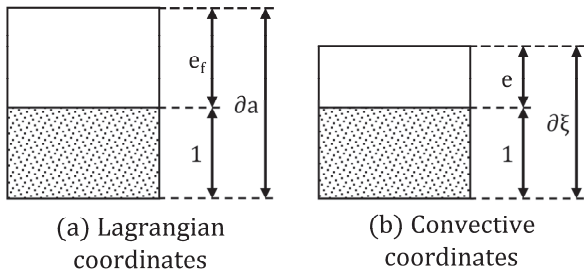
Figure 2.3 : Change in void ratio during thaw consolidation (adapted from Gibson et al. 1981):
(a) Lagrangian coordinates and (b) convective coordinates

Convective coordinates ξ move along with the material deformations. Consequently, they would be physically convenient for the description of large-strain consolidation as they constitute a lifelike portrayal of the problem (Gibson et al. 1981); however, the convective system is time dependent and is therefore numerically impractical. Indeed, the location of the thaw consolidation upper boundary is defined as a function of surface settlement $s(0, t)$, which is unknown prior to the assessment of consolidation. Convective coordinates will only be used in this study for the graphical representation of modelling results.

The main governing equations for thaw consolidation are derived hereafter in Lagrangian coordinates a, which relate all events to an initial configuration as a function of the void ratio (Gibson et al. 1981). As a result, boundaries can always be identified, and boundary conditions can seamlessly be implemented without knowing the exact location of the boundaries prior to the analysis. For example, the surface is always located at a Lagrangian position $a = 0$ as shown in Figure 2.2b while surface settlement $s(0, t)$ can still be fully accounted for numerically. Although Lagrangian coordinates and Eulerian coordinates commonly used in soil mechanics might appear to be the same, they differ in that Eulerian coordinates are fixed in space for all time.

2.5 Large-Strain Consolidation

The large-strain consolidation theory proposed by Gibson et al. (1967) and Gibson et al. (1981) is assumed to be valid within the thawed region of compressible saturated soil. Gibson's theory of consolidation is effectively a one-dimensional model of mass transfer based on the vertical equilibrium of soil mass and pore water. The simplest and most convenient form of the theory is derived in terms of void ratio. It is thus primarily oriented

towards the prediction of deformations from which other geotechnical quantities of interest such as excess pore-water pressures can be calculated.

2.5.1 General Equations for Large-Strain Consolidation

Under the assumption that soil particles and pore water are incompressible, large-strain consolidation of thawing saturated soils can be described by the following set of equations formulated in Lagrangian coordinates (Gibson et al. 1967, 1981, Xie and Leo 2004).

The vertical equilibrium of the soil mass is given by

Equation 2-5 $\dfrac{\partial \sigma_v}{\partial a} = \dfrac{(G_s + e)\gamma_w}{(1 + e_f)}$

where σ_v is the total vertical stress, G_s is the specific gravity of the solid particles, and γ_w is the unit weight of water.

Also, the equilibrium of pore water requires that

Equation 2-6 $\dfrac{\partial u}{\partial a} = \dfrac{\partial u_e}{\partial a} + \dfrac{(1 + e)\gamma_w}{(1 + e_f)}$

where u is the total pore-water pressure and u_e the excess pore-water pressure.

Darcy's law relates the relative velocity of the soil skeleton and pore water to the excess pore-water pressure gradient such that

Equation 2-7 $v_w - v_s = -\dfrac{k_v(e)(1 + e_f)}{\gamma_w e} \dfrac{\partial u_e}{\partial a}$

where v_w and v_s are the velocities of the pore water and soil particles relative to the datum plane and $k_v(e)$ the vertical hydraulic conductivity as a function of the void ratio.

Additionally, the continuity of pore-water flow requires that

Equation 2-8 $\dfrac{\partial}{\partial a}\left[\dfrac{e(v_w - v_s)}{1 + e}\right] = \dfrac{1}{1 + e_f} \dfrac{\partial e}{\partial t}.$

Equation 2-7 and Equation 2-8 can be combined to yield the following equation governing large-strain consolidation:

Equation 2-9 $\dfrac{1}{\gamma_w}\dfrac{\partial}{\partial a}\left[\dfrac{k_v(e)(1+e_f)}{1+e}\dfrac{\partial u_e}{\partial a}\right] = \dfrac{1}{1+e_f}\dfrac{\partial e}{\partial t}.$

Equation 2-9 is mathematically inconvenient as both excess pore-water pressures and void ratio are used as dependent variables. It can be reduced to an equation expressed solely in terms of void ratio by using the principle of effective stress given by

Equation 2-10 $\sigma_v = \sigma'_v + u$

where σ'_v is the vertical effective stress.

The derivative of Equation 2-10 with respect to depth is

Equation 2-11 $\dfrac{\partial \sigma_v}{\partial a} = \dfrac{\partial \sigma'_v}{\partial a} + \dfrac{\partial u}{\partial a}.$

Equation 2-5 and Equation 2-6 can be substituted into Equation 2-11 such that

Equation 2-12 $\dfrac{(G_s+e)\gamma_w}{(1+e_f)} = \dfrac{\partial \sigma'_v}{\partial a} + \dfrac{\partial u_e}{\partial a} + \dfrac{(1+e)\gamma_w}{(1+e_f)}.$

Accordingly, the excess pore-water pressure gradient is given by

Equation 2-13 $\dfrac{\partial u_e}{\partial a} = \dfrac{(G_s-1)\gamma_w}{(1+e_f)} - \dfrac{\partial \sigma'_v}{\partial a}.$

Equation 2-9 and Equation 2-13 can be combined to yield the following equation governing void ratio:

Equation 2-14 $\dfrac{d}{de}\left[\dfrac{k_v(e)(G_s-1)}{1+e}\right]\dfrac{\partial e}{\partial a} + \dfrac{1}{\gamma_w}\dfrac{\partial}{\partial a}\left[-\dfrac{k_v(e)(1+e_f)}{1+e}\dfrac{d\sigma'_v(e)}{de}\dfrac{\partial e}{\partial a}\right] = \dfrac{1}{1+e_f}\dfrac{\partial e}{\partial t}$

where the dependent variable e is spatially dependent such that $e = e(a,t)$ and $e_f = e(a,0)$, and $\sigma'_v(e)$ is the relationship between void ratio and effective stress.

Equation 2-14 is the main governing equation used in the model to describe the hydromechanical processes within the thawed region. It is developed under the assumption that the effective stress and hydraulic conductivity are related to the void ratio alone.

2.5.2 Evaluation of Geotechnical Parameters

By formulating the equation for consolidation in terms of void ratio, soil deformations are obtained directly from the modelling results. However, additional relations need to be developed for the evaluation of other geotechnical quantities of interest.

The settlement as a function of depth and time is given by

Equation 2-15 $s(a,t) = \int_a^{Z(t)} \frac{e_f - e}{1 + e_f} da.$

The settlement at the thaw front $a = Z(t)$ is obviously null because all points deeper than $Z(t)$ are in the frozen region. The settlement of the ground surface $a = 0$ is

Equation 2-16 $s(0,t) = \int_0^{Z(t)} \frac{e_f - e}{1 + e_f} da.$

The degree of consolidation as a function of depth and time is given by

Equation 2-17 $U(a,t) = \int_a^{Z(t)} \frac{e_f - e(a,t)}{e_f - e(a,\infty)} da.$

The degree of consolidation for the whole thawed layer is calculated with $a = 0$.

Thaw strain for the thawed layer is defined as a function of the thaw depth in Lagrangian coordinates as

Equation 2-18 $\delta(0,t) = \frac{s(0,t)}{Z(t)}.$

In addition to the deformations, assessment of thaw consolidation related instabilities requires the evaluation of the stress conditions in the ground.

The total vertical stress can be calculated by integrating Equation 2-5 such that

Equation 2-19 $\sigma_v = \sigma_v(a,t) = \sigma_v(0,t) + \int_0^a \frac{(G_s + e)\gamma_w}{1 + e_f} da$

where $\sigma_v(0,t)$ is total stress at the surface given by

Equation 2-20 $\sigma_v(0,t) = P_0(t) + \gamma_w H_w(0,t)$

where $H_w(0,t)$ is the height of water accumulating at the surface from consolidation. If the water seeping out of the soil skeleton during consolidation is drained away from the ground surface, $H_w(0,t)$ is equal to zero. If water accumulation is allowed, $H_w(0,t)$ is equal to surface settlement $s(0,t)$.

The total pore-water pressure is defined as

Equation 2-21 $u(a,t) = u_h(a,t) + u_e(a,t)$

where u_h is the hydrostatic pore-water pressure given by

Equation 2-22 $u_h(a,t) = \gamma_w(a + s(a,t) - s(0,t) + H_w(0,t))$.

Under the assumption that effective stress is a function of void ratio alone, the vertical effective stress profile is given by

Equation 2-23 $\sigma'_v(a,t) = \sigma'_v(e(a,t))$.

Based on the principle of effective stress presented in Equation 2-10, the excess pore-water pressure can be calculated from the combination of Equation 2-19 to Equation 2-23

Equation 2-24 $u_e(a,t) = P_0(t) + \int_0^a \frac{(G_s+e)\gamma_w}{1+e_f} da - \sigma'_v(e(a,t)) - \gamma_w(a + s(a,t) - s(0,t))$

2.5.3 Nonlinear Effective Stress – Void Ratio – Hydraulic Conductivity Relationships

Determination and characterization of the consolidation properties of thawing soils have rarely been discussed in previous thaw consolidation studies despite their paramount role in the development of a comprehensive theory of practical engineering relevance (Morgenstern and Nixon 1971, Sykes et al. 1974, Foriero and Ladanyi 1995). As shown in Equation 2-14, large-strain consolidation is primarily governed by void ratio dependent functions for effective stress and hydraulic conductivity. While those relationships have been studied thoroughly for unfrozen soils, the properties of thawing soils are drastically different thus warranting the ensuing analysis.

Figure 2.4 presents the effective stress – void ratio – hydraulic conductivity relationships for thawing soils in a unified semi-logarithmic workspace. To provide a physical interpretation

of thaw consolidation with regards to the soil properties, the theoretical case of a soil sample at a frozen void ratio e_f is now considered. If the sample is thawed in undrained conditions, the change in void ratio is solely due to the 9% volume contraction of ice to water. The frozen void ratio e_f is thus related to the initial thawed void ratio e_i^* such that

Equation 2-25 $e_i^* = \frac{e_f}{1.09}$.
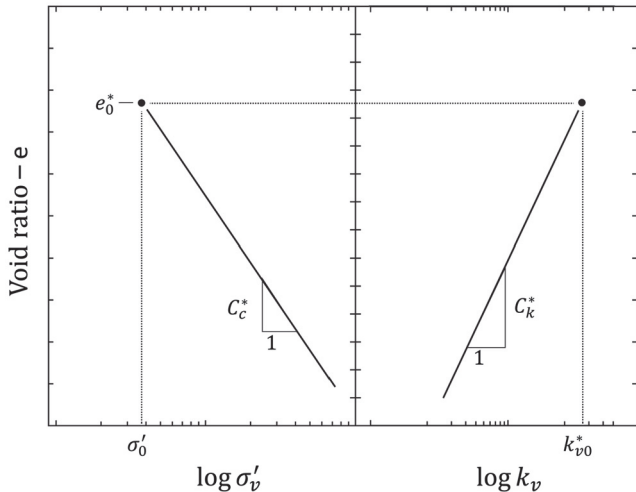
Figure 2.4 : Nonlinear effective stress – void ratio – hydraulic conductivity relationships for thawing soils (C_c^*, compression index of the thawed soil; C_k^*, hydraulic conductivity change index of the thawed soil)

If a constant external load P_0 is applied on the sample during undrained thawing, pore-water pressures can develop. The effective stress in the sample upon thawing is thus equal to the difference between the applied load and pore-water pressure. The effective stress that is sustained by the soil skeleton in undrained conditions is called the residual stress (Nixon and Morgenstern 1973a). At the residual stress, the void ratio of the thawed soil is the thawed void ratio e_0^*. The thawed void ratio e_0^* characterizes the amount of water that the soil skeleton can hold upon thawing. For ice-poor soils, the soil skeleton can absorb all the melt water such that $e_i^* = e_0^*$. If the applied load is equal to the residual stress, no excess pore-water pressures develop upon thawing. For applied loads larger than the residual stress, excess pore-water pressures develop, and consolidation occurs if drainage is allowed. Void ratio changes during consolidation are then governed by the effective stress – void ratio relationship of the thawed soil.

It is generally accepted that the change in void ratio with effective stress for thawing fine-grained soils is nonlinear over the range of stresses of practical interest (Konrad 2010, Konrad and Samson 2000a, Nixon and Morgenstern 1973a, 1973b). Indeed, some small limited loading is required to induce substantial thaw settlement for soils with high frozen void ratio. However, expulsion of additional pore water leading to further settlement is only achieved at significantly higher stresses. For thawed fine-grained soils, experimental evidence (Konrad 2010, Konrad and Samson 2000a) demonstrates that this behaviour can be defined by a semi-logarithmic relationship given by

Equation 2-26 $(e - e_0^*) = -C_c^* \, log \left(\frac{\sigma_v'(e)}{\sigma_0'} \right)$

where C_c^* is the compression index of the thawed soil.

In addition to the effective stress – void ratio relationship, consolidation of thawing soils is regulated by the hydraulic conductivity of the soil. Studies have demonstrated that the variation of hydraulic conductivity with void ratio can be described by a semi-logarithmic relationship characterized by a slope parameter C_k^* called the hydraulic conductivity change index of the thawed soil (Konrad 2010, Konrad and Samson 2000a). The void ratio – hydraulic conductivity relationship for thawed fine-grained soils is given by

Equation 2-27 $(e - e_0^*) = C_k^* \, log \left(\frac{k_v(e)}{k_{v0}^*} \right).$

The initial state of the thawed soil is fully defined by the combination of the residual stress σ_0', the thawed void ratio e_0^*, and the initial hydraulic conductivity k_{v0}^*. From the initial state of the thawed soil, the hydromechanical behaviour during thaw consolidation is governed by the stress increment, which is the difference between the applied effective stress P_0 and the residual stress σ_0'. Morgenstern and Nixon (1971) indicated that the residual stress of soils with high initial void ratio could be assumed to be equal to zero for first-order estimates. However, this approach overlooks the non-linearity of the effective stress – void ratio relationship and the interdependence between the effective stress – void ratio – hydraulic conductivity relationships over the particular state path followed by the thawing soil.

2.5.4 Initial Conditions and Boundary Conditions for Consolidation

The initial conditions for consolidation are simply described by the initial void ratio profile of the frozen soil

Equation 2-28 $e(a, 0) = e_f(a).$

Although this definition may appear trivial, calculation of settlements and excess pore-water pressures is contingent on a precise description of the frozen void ratio profile as it is used extensively in the formulation of large-strain consolidation equations and in the characterization of the soil properties upon thawing.

Modelling one-dimensional consolidation of thawing soils typically involves two boundary conditions: a free-draining boundary at the ground surface and a moving impervious boundary at the thaw front. Although handling of these boundary conditions is relatively simple in classical consolidation theory developed in terms of pore-water pressures, their implementation into a large-strain consolidation scheme where the free-draining boundary at the ground surface is a moving boundary is more complex because of the formulation in terms of void ratio and of the movement of the lower boundary at the thaw front.

At the free-draining boundary, no excess pore-water pressure is sustained. From Equation 2-26, the condition at the ground surface $a = 0$ in terms of excess pore-water pressure is thus given by

Equation 2-29 $u_e(0, t) = P_0(t) - \sigma_v'\big(e(0, t)\big) = 0.$

Taking advantage of the effective stress – void ratio relationship defined in Equation 2-24, Equation 2-29 can be rearranged such that the boundary condition at $a = 0$ in terms of void ratio is given by

Equation 2-30 $e(0, t) = e_0^* - C_c^* \log\left(\frac{P_0(t)}{\sigma_0'}\right).$

The conditions at the thaw front were first formulated by Morgenstern and Nixon (1971). The derivation of the lower boundary conditions is reformulated here in terms of large-strain consolidation. Also, volume changes due to phase change from ice to water, which were never explicitly integrated in any thaw consolidation theory, are directly included into the

following development at no additional computation costs due to the formulation in terms of void ratio.

As described in the one-dimensional problem statement, water released at the thaw front flows towards the surface due to the pore-water pressure gradient to which it is subjected. According to Darcy's law, the volumetric discharge of water at the thaw front is given by

Equation 2-31 $\Delta V = -\dfrac{k_v(e)(1+e_f)}{\gamma_w e} \dfrac{\partial u_e}{\partial a} A\Delta t$

where A is the cross section of the soil element and Δt is the time increment.

Consequently, the volumetric strain due to water discharge of a layer of thickness ΔZ is

Equation 2-32 $\dfrac{\Delta V}{V} = \dfrac{\Delta V}{A\Delta Z} = -\dfrac{k_v(e)(1+e_f)}{\gamma_w e} \dfrac{\partial u_e}{\partial a} \dfrac{1}{\frac{\Delta Z}{\Delta t}}.$

The additional volumetric strain due to phase change of ice to water is given by

Equation 2-33 $\dfrac{\Delta V}{V} = -\dfrac{e_i^* - e_f}{1+e_f}.$

As per the principle of compressibility, the total volume change is related to a corresponding change in effective stress such that

Equation 2-34 $\dfrac{\Delta V}{V} = -m_v \Delta\sigma_v' = \dfrac{\Delta e}{\Delta\sigma_v'} \dfrac{\Delta\sigma_v'}{1+e_f}$

where m_v is the coefficient of volume change.

If volumetric strain from water discharge and phase change are accommodated by a change in effective stress, the combination of Equation 2-32 to Equation 2-34 yields

Equation 2-35 $-\dfrac{k_v(e)(1+e_f)}{\gamma_w e} \dfrac{\partial u_e}{\partial a} \dfrac{1}{\frac{\Delta Z}{\Delta t}} - \dfrac{e_i^* - e_f}{1+e_f} = \dfrac{\Delta e}{\Delta\sigma_v'} \dfrac{\Delta\sigma_v'}{1+e_f}.$

By considering volume changes due to phase change and consolidation separately, Equation 2-35 becomes

Equation 2-36 $\dfrac{\Delta e}{\Delta\sigma_v'} \dfrac{\Delta\sigma_v'}{1+e_f} = \dfrac{e_i^* - e_f}{\sigma_0' - \sigma_v'(e_f)} \dfrac{\sigma_0' - \sigma_v'(e_f)}{1+e_f} + \dfrac{e - e_i^*}{\sigma_v'(e) - \sigma_0'} \dfrac{\sigma_v'(e) - \sigma_0'}{1+e_f}.$

For infinitely small time-steps, the contribution of phase change can be removed from both sides of Equation 2-36 such that

Equation 2-37 $\quad -\frac{k_v(e)(1+e_f)}{\gamma_w e}\frac{\partial u_e}{\partial a}\frac{1}{\frac{dZ(t)}{dt}} = \frac{1}{\frac{d\sigma'_v(e)}{de}}\frac{(\sigma'_v(e)-\sigma'_0)}{1+e_f}.$

By replacing the excess pore-water pressure gradient in Equation 2-37 by Equation 2-13, the conditions at the thaw front in terms of void ratio are given by

Equation 2-38 $\quad \frac{d\sigma'(e)}{de}\frac{\partial e}{\partial a} = \frac{(G_s-1)\gamma_w}{1+e_f} + \frac{dZ(t)}{dt}\frac{\gamma_w e}{k_v(e)(1+e_f)}\frac{1}{\frac{d\sigma'_v(e)}{de}}\frac{\sigma'_v(e)-\sigma'_0}{1+e_f}.$

2.6 Heat Transfer

As shown in the previous section, the consolidation of thawing soils is geometrically controlled by the thaw depth. However, reducing the assessment of heat transfer to the calculation of the rate of thaw penetration offers very little coupling possibilities between the consolidation and heat-transfer components. For more complex analysis, the heat-transfer component of thaw consolidation needs to be implemented within the moving boundary scheme previously defined by large-strain consolidation theory. Initiation and progression of thaw penetration should thus be calculated using the equation of heat transfer that includes phase change, conduction, and advection.

2.6.1 General Equations for Heat Transfer

The one-dimensional convection–conduction heat-transfer equation in Lagrangian coordinates is

Equation 2-39 $\quad \left(C - L\rho_i \frac{\partial\theta_i}{\partial T}\right)\frac{\partial T}{\partial t} - \frac{\partial}{\partial a}\left[\lambda\frac{(1+e_f)^2}{(1+e)^2}\frac{\partial T}{\partial a}\right] + c_w\rho_w v_a\frac{1+e_f}{1+e}\frac{\partial T}{\partial a} = 0$

where C is the volumetric heat capacity of the soil, L is the latent heat of fusion of water per unit mass, ρ_i and ρ_w are the density of ice and water, respectively, θ_i is the volumetric ice fraction, T is the temperature in Kelvin, λ is the thermal conductivity of the soil, c_w is the heat capacity of water by mass, and v_a is the water flow velocity in the direction of a.

The relative water flow velocity in the direction of a, calculated by combining Equation 2-7 and Equation 2-13, is given by

Equation 2-40 $v_a = -\dfrac{k_v(e)(1+e_f)}{\gamma_w e}\left(\dfrac{(G_s-1)\gamma_w}{(1+e_f)} - \dfrac{d\sigma'_v(e)}{de}\dfrac{\partial e}{\partial a}\right).$

2.6.2 Soil Thermal Properties

The geothermal properties introduced in Equation 2-39 are mainly dependent on the relative contribution of the soil components that are readily obtained from the void ratio.

The volumetric fraction of the soil particles is given by

Equation 2-41 $\theta_s = \dfrac{1}{1+e}$

while the volumetric fraction of the voids is given by

Equation 2-42 $\theta_v = \dfrac{e}{1+e}.$

In a saturated soil, the voids are entirely filled with either ice, water or a mix of both such that

Equation 2-43 $\theta_v = \theta_w + \theta_i = \dfrac{e}{1+e}$

where θ_w and θ_i are the volumetric fractions of liquid water and ice, respectively.

The volumetric fraction of liquid water is given by

Equation 2-44 $\theta_w = \begin{cases} \dfrac{e}{1+e}, & T>T_f \\ \theta_u, & T\le T_f \end{cases}$

where θ_u is the unfrozen water content and T_f is the freezing point.

The relationship between unfrozen water content and temperature, also called the phase composition curve, is often represented using a power function such that

Equation 2-45 $w_u = \alpha_u(T_f - T)^{\beta_u}$

where w_u is the unfrozen water content by mass, α_u and β_u are coefficients characteristic of the soil. Typical values for α_u and β_u can be found in the literature (Nixon 1991) or determined experimentally. The volumetric fraction of unfrozen water is

Equation 2-46 $\theta_u = \alpha_u(T_f - T)^{\beta_u}\dfrac{G_s}{1+e}.$

From the volumetric contribution of each of the soil components, the volumetric heat capacity of the soil is given by

Equation 2-47 $C = \rho_w c_w \theta_w + \rho_s c_s \theta_s + \rho_i c_i \theta_i$

where ρ is the density and c the heat capacity by mass with subscripts w, s, and i denoting liquid water, solids, and ice, respectively.

Finally, the generalized model proposed by Côté and Konrad (2005) states that the thermal conductivity of a saturated soil is given by

Equation 2-48 $\lambda = \lambda_s^{\theta_s} \times 2.24^{\theta_i} \times 0.6^{\theta_w}$

where λ_s is the thermal conductivity of solid particles.

2.6.3 Initial Conditions and Boundary Conditions for Heat Transfer

The initial conditions for heat transfer are typically given by the temperature profile of the frozen soil:

Equation 2-49 $T_0 = T(a, 0) \le T_f$.

For the simplest case of thaw consolidation, thawing is initiated by a step increase in temperature at the surface given by boundary conditions:

Equation 2-50 $T_s = T(0, t) > T_f$.

The surface temperature T_s may vary with time given that it remains strictly above the freezing point T_f because the proposed model does not integrate the effect of freeze-back.

For simple analysis, the lower boundary conditions at $a = H_i$ may be given as a function of temperature

Equation 2-51 $T_{H_i} = T(H_i, t)$

or as a function of heat flux

Equation 2-52 $q_{H_i} = q(H_i, t)$.

To reproduce field conditions, the heat flux q_{H_i} may be defined by the geothermal heat flux such that

Equation 2-53 $q_g(H_i) = -k_g G$

where k_g is the thermal conductivity of the soil below H_i and G is the geothermal gradient defined in permafrost by the temperature gradient with depth below the depth of zero annual amplitude.

A major benefit of the current model is its ability to handle any type of thermal boundary conditions that may be required for more complex analysis. For example, a combination of boundary conditions can be used to simulate the energy balance at the surface of a natural ground. However, it should be noted that the model is limited to monotonic top-down thawing. Accordingly, boundary conditions at the top should not initiate freeze-back and lower boundary conditions should not initiate thawing of the soil from the bottom.

2.7 Coupling

A thaw consolidation model is established by coupling the consolidation and heat-transfer components. Most aspects of the interaction between the two components have already been explicitly or implicitly introduced in previous sections. Still, the coupling scheme is best defined by sequentially describing the contributions of each component to the overall model. It should be noted that all contributions occur simultaneously as each time step is solved in an iterative process over the unified modelling domain.

The consolidation component is used to define the coordinate system of the modelling domain and the position of the boundaries from the calculation of the void ratio at all time steps. The modelling domain is kept physically coherent as the Lagrangian coordinates are normalized at each time step as a function of the initial void ratio and current void ratio profiles. Accordingly, the boundary conditions at the surface, namely the heat source causing thawing of the frozen soil and the free-draining boundary for consolidation, are always physically coherent with surface settlements. Additionally, the void ratio is used in the calculation of the soil's geothermal properties. The consolidation component is also

analogous to a mass transfer model that provides the pore-water flow velocity for calculation of the advective heat transfer.

The heat-transfer component contributes to the model by defining the position of the interface between the thawed and frozen regions where the lower boundary for consolidation is located. The depth where the temperature is equal to the freezing point T_f is calculated at each time step and the lower boundary for consolidation is moved accordingly. The rate of thaw penetration is equal to the rate of displacement of the thaw depth during each time step. The movement of the boundary is mathematically accommodated by the formulation of the impervious boundary condition at the thaw front in Equation 2-38.

2.7.1 Numerical Implementation

The proposed model can be implemented using any numerical calculation tool capable of solving nonlinear partial differential equations systems for multiple coupled components and moving boundaries. While several commercial and free software solutions are capable of such feats, COMSOL Multiphysics version 5.2a (COMSOL 2016) was used for the current study. The model is implemented using a combination of two "coefficient form PDE mathematics interfaces" with a "fully coupled direct MUMPS time-dependent solver". The one-dimensional geometry is formed of two "intervals" for the thawed and frozen regions. The consolidation component is first activated in the initially infinitely small thawed region to allow the top boundary conditions for consolidation to stabilize. The heat-transfer component is then initiated by the step increase in temperature at the surface, which triggers the movement of the interface between the thawed and frozen regions. The moving boundary is handled by a "deformed mesh" component of the type "deformed geometry" (dg). Both the thawed and frozen intervals are composed of very fine mesh elements to facilitate numerical stability of the deforming geometry. A "strict backward differentiation formula, BDF" time stepping is adopted. It is important to mention that none of the preprogramed physics modules offered in COMSOL was used to set up the model and that all the properties and equations were user-defined.

2.8 Working Example

The model developed herein is applied to a typical thaw consolidation laboratory problem. Athabasca clay is used in this example because all soil properties pertaining to the assessment of thaw consolidation were reported by Smith (1972). This example considers a 50 mm thick sample of Athabasca clay at an initial frozen void ratio e_f of 2.83 that corresponds to the initial thawed void ratio e_i^* of 2.60 for which the effective stress – void ratio – hydraulic conductivity relationships were determined by Smith (1972). The soil is considered ice-poor such that $e_i^* = e_0^*$. The sample is at an initial uniform temperature T_0 of –5 °C and thawing is initiated by increasing the temperature at the top of the sample T_s to 5 °C. The thermal boundary conditions at the bottom of the sample simulate a semi-infinite mass of frozen soil to reproduce the laboratory conditions used by Smith (1972). A constant load P_0 of 15 kPa is applied at the top of the sample. The thermal and loading conditions were specifically selected to yield a combination of thaw penetration and consolidation rates in the range of practical interest with regards to the properties of Athabasca clay.

2.8.1 Soil Properties

Athabasca clay is a clay of low plasticity with a clay content of 45%, a silt content of 54%, and a sand content of 1% (Smith 1972). The properties of Athabasca clay are similar to those of the lean silty clays commonly found in permafrost regions of northern Canada, which are characterized by high compressibility and low hydraulic conductivity (Morgenstern and Smith 1973). Athabasca clay has a specific gravity G_s of 2.65, a thermal conductivity of the solid particles λ_s of 2.1 W/m°C, and a volumetric heat capacity of the solid particles C_s of 712 MJ/m³°C (Smith 1972). Parameters α_u and β_u for the unfrozen water content are set equal to 9.0 and –0.45, respectively, in concordance with literature data for soils with a similar grain-size distribution curve (Andersland and Ladanyi 2004). The freezing point T_f is set at 0 °C (Smith 1972).

The effective stress – void ratio – hydraulic conductivity relationships of thawed Athabasca clay are shown in Figure 2.5. The relationships were experimentally determined by oedometric consolidation tests performed on thawed samples with applied loading ranging from 1.3 to 230 kPa (Smith 1972). The experimental curves are extrapolated to the initial thawed void ratio as indicated by the empty dots in Figure 2.5 to fully characterize both

48

relationships over the full range of void ratio changes expected upon thawing. The effective stress – void ratio relationship of thawed Athabasca clay is given by

Equation 2-54 $(e - 2.60) = -0.421 \, log \left(\frac{\sigma_v'(e)}{0.0028} \right)$

while the void ratio – hydraulic conductivity relationship of thawed Athabasca clay is given by

Equation 2-55 $(e - 2.60) = 0.305 \, log \left(\frac{k_v(e)}{8.1 \times 10^{-6} \, m/s} \right).$
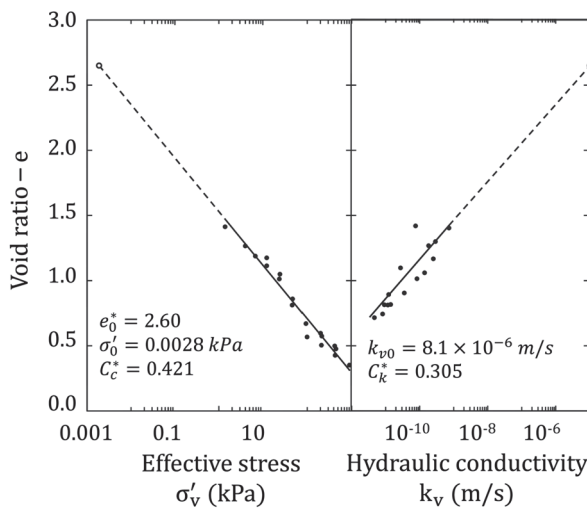
Figure 2.5 : Properties of thawed Athabasca clay (adapted from Smith (1972))

2.8.2 Numerical Modelling

The previously described strategy is used for the numerical implementation of the model in COMSOL Multiphysics version 5.2a (COMSOL 2016). The initial height of the thawed interval is one hundred times smaller than the sample height. The thawed interval is divided into 500 mesh elements and the frozen interval into 100 mesh elements. Several "probes" and "coefficient form PDE mathematics interfaces" are set up to facilitate post-processing of the simulation data by automating the calculation of settlements and stress state variables. Time stepping is automatically adapted by COMSOL during computing of the model. The conversion from Lagrangian coordinates to convective coordinates is computed during the simulation to allow for a physically coherent representation of the modelling results as a function of the actual geometry.

Thaw consolidation testing is typically designed to reproduce field conditions (Smith 1972). The boundary conditions at the bottom of the sample for the heat-transfer component should thus simulate thawing of a semi-infinite column of soil. This is achieved by increasing the modelling domain for heat transfer to five times the height of the frozen soil sample, which effectively creates a heat sink at the bottom of the modelled sample. Thaw penetration is automatically stopped when the maximum thaw depth that is equal to the frozen height of the sample is reached. The simulation then enters the post-thaw consolidation phase and an impervious boundary condition is automatically imposed at the bottom of the sample.

2.8.3 Typical Results

It is convenient to first examine the thermal component of thaw consolidation because of its importance in defining the rate of thaw penetration that regulates the rate at which pore-water pressures are generated at the thaw front. Figure 2.6 shows the model-predicted temperature profiles in the sample at times 0, 5, 25, 95, and 348 min. The y-axis represents depth in convective coordinates below the initial position of the top of the frozen sample. The constant initial temperature set equal to –5 °C is shown by the $t = 0$ min isochrone while it can be seen that the temperature at the top of the sample is set equal to 5 °C at $t > 0$. The temperature isochrones are characterized by a break at the 0 °C isotherm, which is typical of thawing soils due to the difference between the thermal properties of the frozen and thawed soil and because of latent heat. The downward progression of thaw depth Z(t) is defined by the intersection between the temperature isochrones and the 0 °C isotherm. At $t = 348$ min, the sample is fully thawed as thaw depth reaches the bottom of the sample and the post-thaw consolidation phase is initiated.
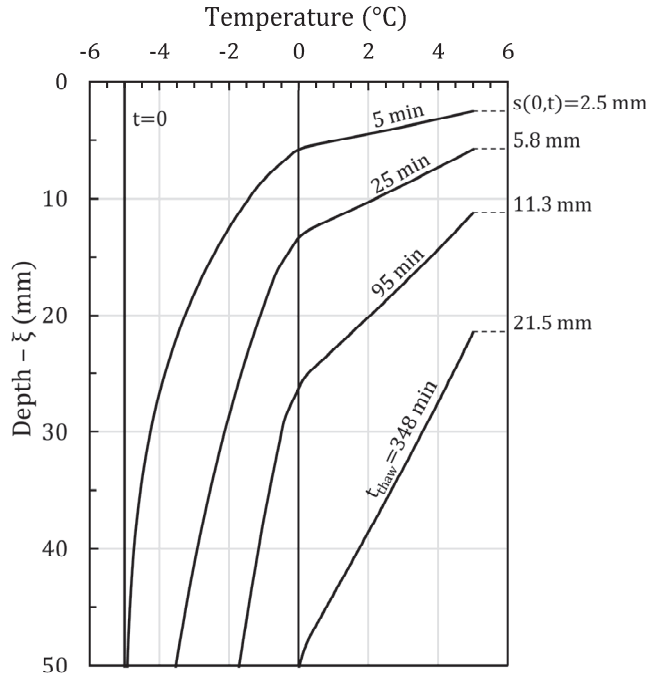
Figure 2.6 : Temperature isochrones during thaw consolidation phase

A simulation performed without the inclusion of the advection heat-transfer term indicated that heat transfer by advection causes a reduction of the thaw depth of less than 1% for the working example presented herein. This result confirms that heat transfer by advection due to seepage of water caused by consolidation is not significant in thaw consolidation (Nixon 1975). However, it should be mentioned that the advection term is added at no additional computational costs due to the formulation of the model in terms of void ratio. Also, the proposed formulation allows for the addition of an external hydraulic gradient that might have a more significant impact on thaw depth.

The position of the top of the sample corresponding to the progression of surface settlement $s(0,t)$ is indicated by dashed lines in Figure 2.6. Accordingly, the boundary conditions applied at the top of the sample in the proposed model move along with the soil deformations in concordance with the physical reality of the problem. In comparison, a small-strain thaw consolidation theory implemented in Eulerian coordinates (Morgenstern and Nixon 1971) always considers that the upper boundary conditions are applied at the initial position of the top of the sample at $\xi = 0$. In the example presented herein for ice-rich Athabasca clay undergoing large thaw strain, the model results indicate that the top of the sample when thaw depth reaches the bottom of the sample is 21.5 mm lower than its initial position. Small-strain

thaw consolidation theory would thus underestimate the rate of thaw penetration by not considering the movement of the 5 °C temperature boundary condition towards the thaw front.

Figure 2.7 shows model-predicted void ratio profiles in the thawed layer during the thaw consolidation and post-thaw consolidation phases. The alternate x-axis at the bottom represents the corresponding hydraulic conductivity of the soil. The constant initial void ratio of the frozen sample equal to 2.83 is not shown in Figure 2.7. At the free-draining boundary at the top of the sample, the void ratio that is given by Equation 2-54 for an applied load P_0 of 15 kPa is equal to 1.03. For all time steps, the void ratio profile is plotted between the top of the sample as a function of surface settlement and the bottom of the thawed layer, which is always equal to the thaw depth $Z(t)$.

The surface settlement is indicated for each time step in Figure 2.7. The model results indicate that most consolidation occurred during the thaw consolidation phase for the ice-rich Athabasca clay sample subjected to the specified thermal conditions. In the current example, the void ratio at the thaw front decreases as thaw consolidation proceeds, which indicates that the excess water is drained out of the soil skeleton faster than it is released at the thaw front. The hydromechanical behaviour during thaw consolidation is regulated by three main factors: the hydraulic conductivity of the thawed layer, the velocity of the thaw front, and the length of the drainage path, which is controlled by the compressibility of the soil. As anticipated, the hydraulic conductivity in the thawed layer decreases with time as shown in Figure 2.7. The rate of drainage of the excess water released at the thaw front is thus expected to decrease with time. However, the velocity of the thaw front $dZ(t)/dt$, which is a key parameter in Equation 2-38 in regulating the boundary conditions at the thaw front, also decreases with time, which means that the incremental thaw depth $dZ(t)$ for a constant time step dt is getting smaller. Consequently, the volume of water released at the thaw front decreases with time, which offsets the decreasing hydraulic conductivity of the thawed layer. Moreover, the length of the drainage path does not increase as much as it might be anticipated due to surface settlement, which also contributes to facilitating the drainage of the excess water.
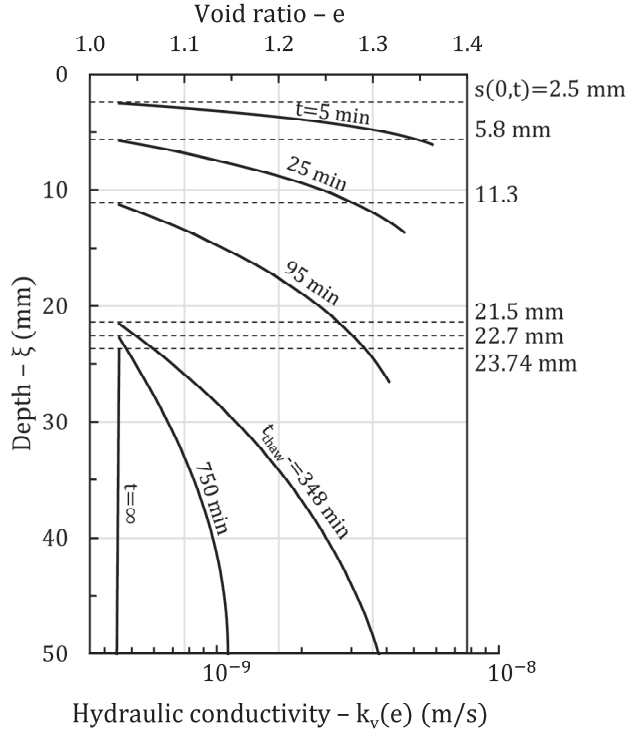
Figure 2.7 : Void ratio and hydraulic conductivity isochrones in thawed layer

2.8.4 Comparison with Small-Strain Thaw Consolidation Theory

This section presents a comparison between the proposed large-strain model and the small-strain thaw consolidation approach as proposed by Morgenstern and Nixon (1971). The large-strain and small-strain configurations for thaw consolidation are compared in Figure 2.8. In the large-strain configuration at time $t > 0$, thaw depth is equal to $Z(t)$ and the position of the surface is equal to $s(0, t)$ which is below the datum given by the initial position of the soil surface $\xi = 0$. After incremental time Δt, thaw depth and surface settlement both increases such that

Equation 2-56 $Z(t + \Delta t) > Z(t)$

and

Equation 2-57 $s(0, t + \Delta t) > s(0, t)$.

The increase in thaw depth over time step Δt in small-strain configuration is given by

Equation 2-58 $\Delta Z = Z(t + \Delta t) - Z(t)$.

In the small-strain configuration, the surface is always located at the datum given by the initial position of the soil surface $\xi = 0$ and the small-strain thaw depth is always given by the height of the thawed layer as defined in Equation 2-1 such that

Equation 2-59 $Z_z(t) = Z(t) - s(0,t)$

where Z_z is the small-strain thaw depth.

After incremental time Δt, the small-strain thaw depth is thus equal to

Equation 2-60 $Z_z(t + \Delta t) = Z(t + \Delta t) - s(0, t + \Delta t).$

The increase in small-strain thaw depth over time step Δt is thus given by

Equation 2-61 $\Delta Z_z = Z_z(t + \Delta t) - Z_z(t) = \big(Z(t + \Delta t) - s(0, t + \Delta t)\big) - \big(Z(t) - s(0,t)\big)$

which can be rearranged as

Equation 2-62 $\Delta Z_z = Z_z(t + \Delta t) - Z_z(t) = \big(Z(t + \Delta t) - Z(t)\big) - \big(s(0, t + \Delta t) - s(0,t)\big)$

By comparing Equation 2-58 and Equation 2-62, it can be seen that the incremental thaw depth is always smaller when calculated in the small-strain configuration given that the condition formulated in Equation 2-57 is satisfied. This effectively means that the small-strain approach underestimates the volume of water released at the thaw front, which may ultimately lead to an underestimation of the excess pore-water pressure at the thaw front. It should be mentioned that the length of the drainage path given by the height of the thawed layer is the same in both large- and small-strain configurations.

The difference between the large- and small-strain approaches can be efficiently analyzed using the modelling results from the previously discussed working example. Figure 2.9a presents the thaw depth and the surface settlement as a function of the square root of time. The small-strain thaw depth is always defined relative to the position of the surface. It is obtained by subtracting the surface settlement curve from the large-strain thaw depth curve. As the soil sample of the working example is subjected to very large thaw strain, the difference between the large- and small-strain thaw depths is most noticeable. The rates of

thaw penetration are thus considerably different. Nevertheless, the length of the drainage path is the same for both configurations.

Figure 2.9b presents the model computed excess pore-water pressure isochrones in the thawed layer at times 5, 95, and 348 min. Also plotted in this figure are the values obtained by using the analytical solution based on the thaw consolidation ratio proposed by Morgenstern and Nixon (1971). At each time step, the thaw depth is indicated by empty dots on the excess pore-water pressure isochrones and on the thaw penetration curves of Figure 2.9a. The position of the surface is indicated by full dots on the excess pore-water pressure isochrones and on the settlement curve of Figure 2.9a. For the small-strain configuration, the surface is always at $\xi = 0$ as seen in Figure 2.9a.
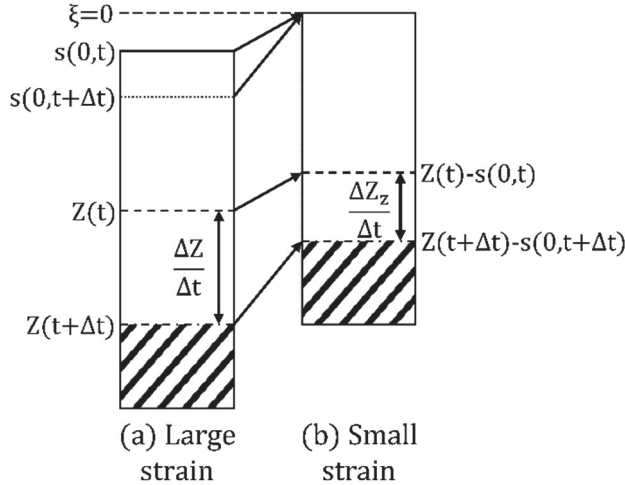
Figure 2.8 : Thaw consolidation in (a) large-strain and (b) small-strain configurations
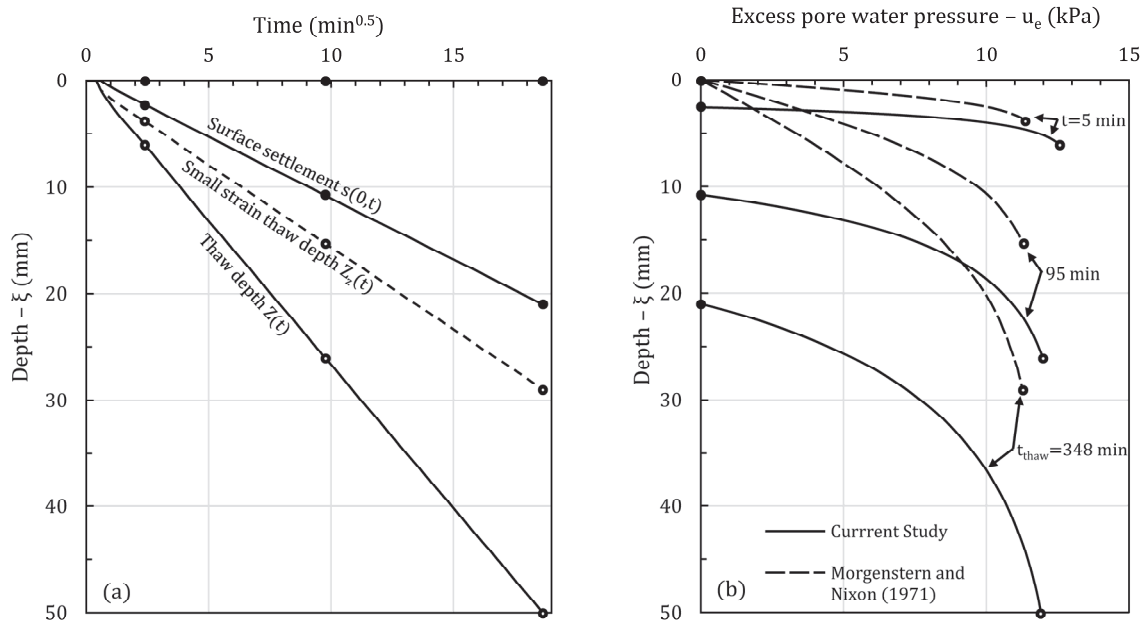
Figure 2.9 : (a) Thaw depth and surface settlement progression and (b) excess pore-water pressure isochrones in thawed layer

The thaw consolidation ratio that parameterizes the theoretical balance between the generation and the dissipation of pore-water pressure in Morgenstern and Nixon (1971) theory is defined as

Equation 2-63 $R = \dfrac{\alpha_T}{2\sqrt{c_v}}$

where α_T is the rate of thaw penetration and c_v is the coefficient of consolidation.

If thaw penetration is assumed to be proportional to the square root of time (Morgenstern and Smith 1973), the rate of thaw penetration can be calculated as

Equation 2-64 $\alpha_T = \dfrac{Z(t_{thaw}) - s(0, t_{thaw})}{\sqrt{t_{thaw}}}$

where $Z(t_{thaw}) - s(0, t_{thaw})$ represents the thaw depth relative to the position of the surface in the small-strain configuration and t_{thaw} is the time when the thaw depth reaches the bottom of the sample.

From Figure 2.9a, $Z(t_{thaw}) - s(0, t_{thaw}) = 0.05–0.0215$ m and $t_{thaw} = 348$ min, which yields a rate of thaw penetration α_T in the sample equal to 0.00153 m/min$^{1/2}$.

By assuming that the consolidation of thin thawing soil samples is controlled by the conditions at the surface, the coefficient of consolidation can be calculated by

Equation 2-65 $c_v = \dfrac{k(e(P_0))}{\dfrac{C_c^*}{P_0\,ln(10)}\dfrac{1}{1+e_f}\gamma_w}$

Using the effective stress – void ratio – hydraulic conductivity relationships of thawed Athabasca clay defined by Equation 2-54 and Equation 2-55, the coefficient of consolidation for $P_0 = 15$ kPa is thus equal to 1.24×10^{-8} m²/s.

The thaw consolidation ratio for this example is thus equal to 0.89. The analytical solution derived by Morgenstern and Nixon (1971) for $R = 0.89$ gives a normalized maximum excess pore-water pressure at the thaw front of 0.75 that is equal to a value of 11.2 kPa for an applied load of 15 kPa. The excess pore-water pressure profile in the thawed layer plotted in Figure 2.9b is obtained from the graphical solution developed by Morgenstern and Nixon (1971).

Figure 2.9b efficiently illustrates the fundamental difference between the large-strain and the small-strain configurations. The magnitude and the shape of the excess pore-pressure isochrones predicted by both approaches are similar. However, without a direct assessment of soil deformations, excess pore-water pressures are predicted outside of the soil sample by the small-strain thaw consolidation theory. This is also typically observed when comparing small- and large-strain consolidation theories (Gibson et al. 1981). Furthermore, thaw consolidation theory presents an added level of complexity inherent to the moving thaw depth.

Figure 2.10 presents the excess pore-water pressure isochrones in the thawed layer in large-strain configuration. The small strain results were adapted to the large-strain configuration by plotting the excess pore-water pressure isochrones from the top of the sample as a function of the settlement computed by the proposed model to provide a visually improved comparison between the proposed model and the small-strain approach.
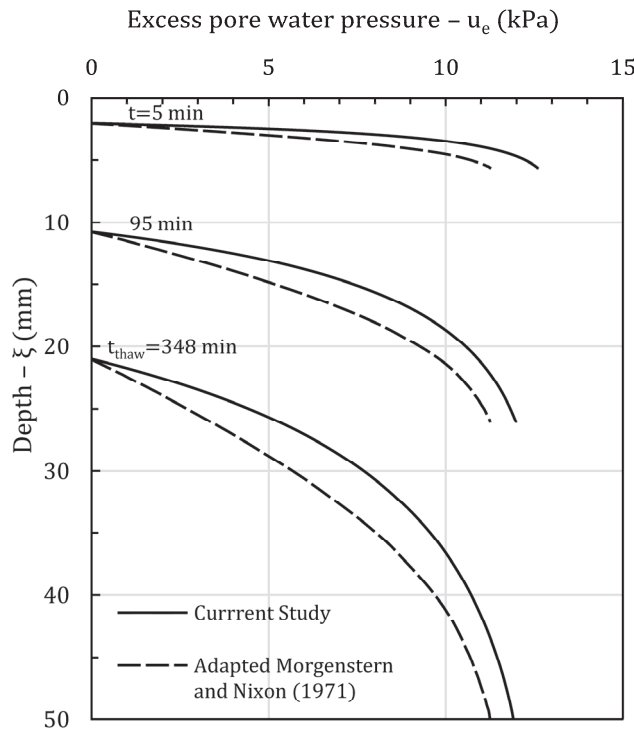
Figure 2.10 : Excess pore-water pressures in thawed layer in large-strain configuration

Figure 2.10 shows that the excess pore-water pressures at the thaw front computed by the proposed model are slightly larger than the ones predicted by small-strain theory. This is mainly due to the large-strain configuration that allows for a physically coherent assessment of the thaw penetration rate. In a small-strain configuration, the thaw depth is defined relative to the position of the surface. As the displacement of the surface is not accounted for in small-strain consolidation, the small-strain thaw penetration rate is thus always smaller than the actual thaw penetration rate. This divergence is expected to increase with increasing thaw strain. It is acknowledged that the large-strain thaw penetration rate can be used in Morgenstern and Nixon (1971) theory. However, this is only possible if surface settlements are known prior to the analysis as Morgenstern and Nixon (1971) theory does not provide a direct assessment of deformations. For example, the large-strain thaw penetration rate was used in the analysis of the experimental Inuvik warm-oil pipeline (Morgenstern and Nixon 1975).

Finally, the excess pore-water pressure profile predicted by Morgenstern and Nixon (1971) theory is constant with time. This is due to the thaw consolidation ratio approach that

considers a constant rate of thaw penetration α_T and a constant and uniform coefficient of consolidation c_v. However, the conditions at the thaw front are controlled by the velocity of the thaw front $dZ(t)/dt$ that decreases with time, whereas the rate of thaw penetration α_T is constant. Also, the hydraulic conductivity of the thawed layer varies with time as consolidation proceeds notwithstanding its spatial variation. The thaw consolidation ratio should also change during thaw consolidation.

2.9   Discussion

In addition to the advantages provided by the large-strain configuration discussed in the previous section, the model presented herein proposes two main improvements for the assessment of thaw consolidation: the implementation into a large-strain configuration of both the consolidation and the heat-transfer components and the characterization of the thawing soil properties by nonlinear effective stress – void ratio – hydraulic conductivity relationships.

The application of large-strain consolidation theory to thaw consolidation was first proposed by Foriero and Ladanyi (1995). However, the innovation of the proposed model lies in the direct integration of heat transfer into the coupled large-strain modelling scheme. The model is thus capable of considering the impact of surface settlements on the movement of the upper boundary conditions for consolidation and heat transfer concurrently. The working example demonstrated that for ice-rich soils undergoing large thaw strain this would affect the evaluation of thaw penetration and of the length of the drainage path even for simple thaw consolidation problems.

The model's most important contribution is, however, the comprehensive description of the thawed soil properties. The use of physically meaningful relationships relieves the ambiguity inherent of previous thaw consolidation theories that sometimes required subjective determination of the soil properties.

Nixon (1973) proposed that the coefficient of consolidation determined during the post-thaw consolidation phase could be used to evaluate the consolidation behaviour during the thaw consolidation phase. However, this assumption is based on Terzaghi's small-strain consolidation theory and on the evaluation of the stress state when thaw depth reaches the

bottom of a frozen soil (Nixon 1973). The post-thaw coefficient of consolidation is thus dependent on the specific loading condition and thaw penetration rate combination under which it is experimentally determined, and it is unclear how it can be generalized to various field conditions. In contrast, the void ratio dependent soil properties used in the proposed framework can effectively model both the thaw consolidation and post-thaw consolidation phases and their determination is independent of the experimental thermal conditions (Smith 1972). In practice, the added benefit is that the effective stress – void ratio – hydraulic conductivity relationships determined for a thawed soil can be used with any thaw penetration rate and applied loading combination anticipated in the field.

Furthermore, it is convenient to mention that the effective stress – void ratio – hydraulic conductivity relationships can be derived from limited testing. The properties of thawed Athabasca Clay presented in Figure 2.5 were determined from only three samples (Smith 1972). Only one sample would have been sufficient as the same thawed sample can be tested under multiple loads (Smith 1972). Limiting the number of samples is particularly beneficial in the case of permafrost soils as retrieving intact permafrost frozen core samples constitutes a significant challenge and a costly endeavour especially in remote areas. Likewise, the relationships could be established from remoulded permafrost samples (McRoberts and Morgenstern 1974). In contrast, the evaluation of the coefficient of consolidation under different conditions requires either multiple intact frozen samples (Nixon and Morgenstern 1974) or refreezing the thawed sample (Morgenstern and Smith 1973), which could affect the properties of the soil.

Finally, the Morgenstern and Nixon (1971) assessment of thaw consolidation is primarily based on the assumption that the coefficient of consolidation is constant and homogeneous in the thawed soil layer. Yet, determination of the proper coefficient of consolidation value applicable to thaw consolidation analysis is highly subjective due to the absence of a generalized characterization method. Morgenstern and Nixon (1975) defined the coefficient of consolidation from the ultimate average effective stress for the analysis of a pipeline built on permafrost. However, the ultimate effective stress state that is established only at the very end of the post-thaw consolidation phase may not be representative of the whole thaw consolidation process. Indeed, the void ratio isochrones presented in Figure 2.7 indicate that

the properties of the soil vary both as a function of depth and time. The spatial variation is expected to be even more significant in the field where the thickness of the thawed layer is much larger than in the laboratory. The proposed framework is supported by void ratio dependent constitutive relationships that ensure a continuous description of the soil properties. Therefore, no subjective assessment needs to be made prior to the analysis of thaw consolidation.

The nonlinear effective stress – void ratio – hydraulic conductivity relationships for thawed fine-grained soils are defined in the proposed framework as a function of the initial state of the thawed soil and of the slope parameters C_c^* and C_k^*. The characteristics of these parameters will be analyzed in detail in a subsequent paper. However, early evidence indicates that the residual stress and hydraulic conductivity values are intrinsic properties of the soil that otherwise depend only on the frozen void ratio (Smith 1972). They also appear to be independent of thermal and stress histories (Nixon and Morgenstern 1974). Furthermore, the slope parameters C_c^* and C_k^*, which change with initial thawed void ratio, can be predicted from the index properties of thawed soils (Dumais and Konrad 2016).

2.10 Conclusion

A framework for the evaluation of the consolidation of saturated thawing soils has been proposed based on a one-dimensional model formulated by coupling large-strain consolidation and heat transfer into a Lagrangian moving boundary scheme. The model considers nonlinear effective stress – void ratio – hydraulic conductivity relationships. The mathematical formulation of the critical impervious boundary conditions at the thaw front has been revised to integrate the non-linearity of the soil properties and the deformations due to phase change.

The model has been applied to the experimental case of a thawing ice-rich fine-grained soil sample, which showed that:

1. The movement of the heat source and the reduction of the length of the drainage path due to surface settlement is duly accounted for in the proposed large-strain configuration.

2. The hydromechanical behaviour is effectively modelled from nonlinear effective stress – void ratio – hydraulic conductivity relationships characterized from the initial thawed state of the soil by the residual stress and its hydraulic conductivity.

3. Both the thaw consolidation and post-thaw consolidation phases can be modelled successively using a consistent model configuration from the same set of effective stress – void ratio – hydraulic conductivity relationships.

A comparison with conventional small-strain thaw consolidation theory showed that:

1. Small-strain thaw consolidation theory has the potential to underestimate excess pore-water pressures in the thawed layer mainly due to the underestimation of the thaw penetration rate inherent to the small-strain configuration.

2. The large-strain configuration provides a more physically coherent representation of thaw consolidation.

3. The evolution and the interdependence of the soil parameters as thaw consolidation proceeds is handled seamlessly by the proposed model.

The practical implication of the proposed model is that the assessment of thaw consolidation is facilitated by the comprehensive and objective characterization of the properties of thawing soils. The effective stress – void ratio – hydraulic conductivity relationships can be determined experimentally and applied to a wide range of field conditions for the calculation of the thaw strain and excess pore-water pressures.

2.11 Acknowledgements

Discussion complémentaire

L'objectif principal de l'article inséré est de présenter le développement d'un modèle de consolidation au dégel à grandes déformations (axe 1 – objectif 1.1a de la thèse). Ainsi,

l'ensemble des équations, la stratégie de couplage et l'implémentation numérique du modèle sont présentées afin de démontrer l'utilisation du modèle pour l'évaluation de la consolidation. Quelques implications pratiques du modèle sont aussi discutées (axe 1 – objectif 1.2 de la thèse). Cependant, l'objectif 1.2 concernant les implications pratiques du modèle non linéaire à grandes déformations est majoritairement couvert par le chapitre 3.

Une des qualités de la formulation du modèle non linéaire à grandes déformations qui n'est pas abordé dans l'article est sa grande flexibilité. En effet, certains aspects du modèle peuvent être simplifiés ou complexifiés selon les problématiques étudiées. En fait, la base du modèle de consolidation au dégel est la composante hydromécanique et la définition du domaine de consolidation (géométrie de la couche de sol dégelée). Cette composante repose sur l'équation de Gibson (Equation 2-14), sur les conditions limites au front de dégel (Equation 2-24) et sur la définition de la position du front de dégel fournie par la composante thermique. Théoriquement, le reste des paramètres présentés peut facilement être modifié ou adapté autant au point de vue de la composante hydromécanique que de la composante thermique.

Tout d'abord, la composante hydromécanique du modèle intègre des relations pour la contrainte effective et pour la conductivité hydraulique qui sont fonction de l'indice des vides (section 2.4.3). La caractérisation particulière des propriétés de sols lors du dégel sera étudiée en détail au chapitre 4 et 5 (axe 2 – objectif 2.1 et 2.2 de la thèse). Les intrants du modèle numérique seront alors définis à partir d'une analyse plus complète (chapitre 4). En ce qui concerne le modèle de consolidation au dégel à grandes déformations présenté au chapitre 2, il est important de mentionner que l'équation de consolidation de Gibson utilisée comme composante hydromécanique offre une certaine flexibilité quant à la définition de relations $\sigma_v'(e)$ and $k_v(e)$. Ainsi, il est possible d'utiliser une définition différente de celle présentée à la section 2.4.3 ou une définition simplifiée des propriétés de sol. Ceci permet de modéliser les sols, dont les relations $\sigma_v'(e)$ and $k_v(e)$ ne seraient pas complètement caractérisées. Par exemple, une valeur unique et constante de la conductivité hydraulique peut être utilisée en complément d'une relation complète $\sigma_v'(e)$ s'il est impossible de définir une relation $k_v(e)$. Le chapitre 5 présente une méthode empirique permettant de définir les caractéristiques des relations $\sigma_v'(e)$ and $k_v(e)$ définies par un modèle conceptuel présenté au chapitre 4.

Ensuite, la composante thermique du modèle est prise en charge par une équation de transfert de chaleur et une définition des propriétés thermiques relativement simples. Ce choix a été fait dans le but de favoriser l'accessibilité du modèle pour les praticiens. Il existe des équations plus complexes de transfert de masse et d'énergie utilisant des propriétés plus complexes qui auraient pu être utilisées. Celles-ci auraient pu apporter un gain de précision pour le calcul des températures dans le sol. Cependant, ces approches font souvent appel à des propriétés thermiques plus complexes. Dans la pratique du génie, il n'est pas toujours possible de pouvoir caractériser en détail les propriétés thermiques des sols étudiés. Des données de la littérature ou des valeurs jugées adéquates par un ingénieur sont alors utilisées. Dans de tels cas, il est plus avisé d'utiliser des équations de transfert de chaleur plus simple afin de diminuer l'erreur associée avec le choix des intrants. L'augmentation de la complexité de la composante thermique entrainerait aussi une augmentation des coûts de calcul liés à l'utilisation du modèle.

L'utilisation de l'équation de consolidation de Gibson comme composante hydromécanique permet de considérer facilement les échanges de chaleur par advection dû à la consolidation. Il est important de noter qu'il s'agit seulement des échanges de chaleur dû à l'écoulement de l'eau provoqué par le gradient de pression interstitielle. Dans l'exemple présenté à la section 2.7, on note que les échanges de chaleur par advection dû à la consolidation sont négligeables. Bien qu'il s'agisse d'un seul exemple d'un sol ayant une conductivité hydraulique faible, cette conclusion est en accord avec celle proposée par Nixon (1975) selon laquelle les échanges de chaleur par advection dû à la consolidation sont négligeables. Cette conclusion est applicable à la plupart des gammes de valeur de coefficient de consolidation, de tassement de fonte et de taux de pénétration au dégel rencontrées dans la pratique de la géotechnique des régions froides (Nixon 1975).

Même si la composante thermique utilisée pour le modèle proposé est relativement simple, il s'agit tout de même d'une méthode plus complexe que les solutions analytiques utilisées par certaines théories de consolidation au dégel (ex. Morgenstern et Nixon 1971, Foriero et Ladanyi 1995). Il peut parfois être plus avantageux ou nécessaire d'utiliser une méthode plus simple soit pour réduire les coûts de calcul ou encore pour faire l'analyse rétrospective d'un problème dont on connait déjà le taux de pénétration au dégel. Il est possible d'implémenter

le modèle proposé en utilisant une solution analytique pour la profondeur de dégel. Pour ce faire, il suffit d'imposer la vitesse de pénétration du front de dégel à l'Equation 2-37 et de définir l'épaisseur du sol dégelé en fonction d'une solution analytique ou d'une équation connue. Il est d'ailleurs possible d'utiliser la solution de Stefan ou une des autres solutions étudiées par Nixon et McRoberts (1973) avec des propriétés thermiques variables en fonction de la composante de consolidation pour obtenir un modèle couplé. Cette approche simplifiée conserverait la plupart des avantages du modèle proposé pourvu que la pénétration du dégel soit définie en fonction de la position initiale de la surface pour bénéficier de l'analyse à grandes déformations (voir section 2.7.4).

Enfin, les avantages de la composante thermique utilisée sont de permettre un couplage complet avec la composante hydromécanique et une implémentation au sein du même domaine de consolidation en plus d'obtenir un profil de température complet au lieu d'avoir seulement la profondeur de dégel. Ainsi, cette formulation offre la possibilité de développer des extensions au modèle proposé qui pourraient faire usage de propriétés dépendantes de la température. Par exemple, on pourrait ajouter une composante de fluage pour le domaine de sol gelé ou une définition thermique des propriétés hydromécaniques pour modéliser le comportement de consolidation d'un sol partiellement gelé.

L'impact pratique des améliorations proposées par le modèle non linéaire à grandes déformations et une comparaison plus approfondie avec la théorie de consolidation linéaire à petites déformations sont présentés au chapitre 3. L'étude de cas du pipeline expérimental d'Inuvik (chapitre 3) présente une application pratique du modèle de consolidation au dégel non linéaire à grandes déformations afin d'illustrer l'implémentation du modèle pour des cas réels. Les avantages ainsi que les limitations du modèle pour la pratique du génie seront aussi discutés en discussion complémentaire du chapitre 3.

Aussi, le chapitre 3 sert de validation pour le modèle proposé (axe 1 – objectif 1.1b de la thèse). En effet, il s'agit d'un cas unique pour lequel les données complètes du processus de consolidation au dégel sont disponibles (profondeur de dégel, tassements de fonte, tassements à la surface et pressions interstitielles) et pour lequel les propriétés hydromécaniques non linéaires du sol ont été déterminées en laboratoire conformément aux définitions utilisées par le modèle. D'autres résultats d'essai de consolidation au dégel sont

aussi disponibles dans la littérature (Smith 1972 et Nixon 1973). Cependant, les propriétés hydromécaniques non linéaires complètes des sols étudiés ne sont pas disponibles. Ainsi, l'analyse de ces résultats nécessiterait de spécifier certaines propriétés fondamentales. L'analyse de la validité du modèle dépendrait alors du choix de ces paramètres. L'étude de cas du pipeline expérimental d'Inuvik est donc plus appropriée pour juger de la performance du modèle.

Chapitre 3 Large-Strain Nonlinear Thaw Consolidation Analysis of the Inuvik Warm-Oil Experimental Pipeline Buried in Permafrost

Avant-propos

Auteurs et affiliation

Simon Dumais et Jean-Marie Konrad

Département de génie civil et de génie des eaux, Université Laval.

Titre français

Analyse de la consolidation au dégel non linéaire à grandes déformations du pipeline expérimental d'Inuvik construit sur un pergélisol riche en glace

Modifications apportées à l'article publié

L'article publié est reproduit intégralement ici. Quelques modifications mineures ont été apportées en ce qui a trait à la nomenclature et aux symboles utilisés pour la définition des propriétés des sols dégelés afin d'homogénéiser l'ensemble de la thèse.

3.1 Résumé français

Le modèle de consolidation au dégel non linéaire à grandes déformations développé par Dumais et Konrad (2018) est utilisé pour l'analyse du pipeline expérimental d'Inuvik construit sur des fondations de pergélisol riche en glace. Les prédictions pour le taux de pénétration du dégel, les tassements de fonte, le taux de tassement et les pressions interstitielles maximales se comparent favorablement aux observations du terrain. Les

résultats de modélisation sont comparés avec les résultats obtenus par la théorie de consolidation de dégel linéaire à petites déformations formulée par Morgenstern et Nixon (1971). Le modèle non linéaire à grandes déformations offre une meilleure précision en raison de la configuration à grandes déformations utilisée pour la définition du taux de pénétration au dégel et de la caractérisation non linéaire des relations $\sigma_v' - e - k_v$. Le modèle non linéaire à grandes déformations améliore la formulation de la théorie unidimensionnelle de consolidation au dégel afin d'obtenir une évaluation physiquement réaliste grâce à l'introduction d'une frontière mobile à la surface et en considérant les changements des propriétés du sol lors de la consolidation.

3.2 Abstract

The large-strain nonlinear thaw consolidation model developed by Dumais and Konrad is used to analyze the Inuvik experimental warm-oil pipeline built on ice-rich permafrost foundations. Predictions for the thaw penetration rate, the final thaw settlements, the settlement rate, and the maximum excess pore water pressure compare favourably with the field observations. The modelling results are compared with the results obtained by the small strain linear thaw consolidation theory formulated by Morgenstern and Nixon. The Dumais and Konrad model offers a notable increase in accuracy given the large-strain configuration used for the definition of the thaw penetration rate and the nonlinear characterization of the $e - \sigma_v'$ and $e - k_v$ relationships. The Dumais and Konrad model improves on the formulation of one-dimensional thaw consolidation theory to yield a realistic assessment of thaw consolidation by the introduction of a second moving boundary at the surface and by considering the changes of soil properties as thaw consolidation proceeds. An important practical implication of the model is the ability to handle a complex initial frozen soil profile and its corresponding soil properties.

3.3 Introduction

Thaw penetration resulting from a drastic alteration of the thermal regime of permafrost may compromise the stability of infrastructure. Indeed, thawing of frozen soil can lead to excess pore water pressures and a loss of shear strength if drainage of the melt water is impeded. Furthermore, the subsidence associated with thawing permafrost and differential settlement

68

given uneven ground ice distribution and other heterogeneities can cause significant damage to infrastructure.

Thaw consolidation is especially problematic for infrastructure that generates heat because of the amount of energy that can be quickly transferred to the permafrost. Thies infrastructure includes buildings, oil and gas production wells, warm-oil pipelines, or any structure that can harness environmental energy sources such as paved road embankments via absorption of solar radiation. A warm-oil experimental pipeline was built in 1971 in Inuvik, Northwest Territories to investigate the effect of heated structures on permafrost. The sought-after combination of a fast-advancing thaw front in ice-rich permafrost was achieved by circulating oil in the pipeline at a temperature of 71°C and selecting a site with high ice content.

The theoretical stability of new and existing infrastructure built on degrading permafrost can be assessed using engineering thaw consolidation theories that provide predictions of ground temperatures, thaw settlements, and excess pore water pressures. Morgenstern and Nixon (1971) formulated the first complete thaw consolidation theory in terms of small strain linear consolidation theory and simple analytical heat transfer solutions. However, its applicability to ice-rich soils undergoing large thaw strains may be limited given the uncoupled small-strain formulation and the use of linear soil properties. Mainly, the small strain configuration entails that the movement of the surface as consolidation proceeds is neglected, leading to an underestimation of the thaw penetration rate and of the generation rate of pore water pressures (Sykes et al. 1974). To provide a more physically coherent assessment of thaw consolidation, Dumais and Konrad (2018) developed a fully coupled large-strain nonlinear model in which the position of the surface and the soil properties change as a function of deformations.

The main objective of this paper is to demonstrate the general applicability of the large-strain nonlinear model developed by Dumais and Konrad (2018) for heated structures built on permafrost by analyzing the Inuvik experimental pipeline. The accuracy of the model is evaluated by comparing the modelling results to the field experimental data. The modelling results are also compared with the results of the small strain linear thaw consolidation analysis of the pipeline presented by Morgenstern and Nixon (1975). The practical

implications of the Dumais and Konrad (2018) model are examined with respect to large-strain thaw consolidation and the non-linearity of soil properties. The objective of this paper is to present a general engineering analysis of thaw consolidation applicable to heated structures built on permafrost and not to propose a procedure specifically for the design of pipelines given that the experimental setup is not entirely representative of pipeline operations built on permafrost.

3.4 Large-Strain Thaw Consolidation Model

The one-dimensional large-strain thaw consolidation model developed by Dumais and Konrad (2018) is presented and is formulated in terms of large-strain consolidation theory and heat transfer equations.

The hydro-mechanical behaviour of the thawing soil is given by Gibson's large-strain consolidation equation governing the void ratio (Gibson et al. 1981, Dumais and Konrad 2018)

Equation 3-1 $\dfrac{d}{de}\left[\dfrac{k_v(e)(G_s-1)}{1+e}\right]\dfrac{\partial e}{\partial a} + \dfrac{1}{\gamma_w}\dfrac{\partial}{\partial a}\left[-\dfrac{k_v(e)(1+e_f)}{1+e}\dfrac{d\sigma'_v(e)}{de}\dfrac{\partial e}{\partial a}\right] = \dfrac{1}{1+e_f}\dfrac{\partial e}{\partial t}$

where e is the void ratio, e_f is the frozen void ratio, a is the depth in Lagrangian coordinates, G_s is the specific gravity of the solid particles, γ_w is the unit weight of water, and $k_v(e)$ and $\sigma'_v(e)$ are void ratio-dependent relationships for the vertical hydraulic conductivity and the vertical effective stress, respectively. In Equation 3-1, the void ratio e is spatially and time dependent such that $e = e(a, t)$ and $e_f = e(a, 0)$.

Based on the principle of the balance between the generation and the dissipation of pore water pressure on thawing (Morgenstern and Nixon 1971), the boundary condition at the impervious moving thaw front is given by

Equation 3-2 $\dfrac{d\sigma'(e)}{de}\dfrac{\partial e}{\partial a} = \dfrac{(G_s-1)\gamma_w}{1+e_f} + \dfrac{dZ(t)}{dt}\dfrac{\gamma_w e}{k_{vT}(e)(1+e_f)}\dfrac{1}{\frac{d\sigma'_v(e)}{de}}\dfrac{\sigma'_v(e)-\sigma'_v(e_0)}{1+e_f}$

where $Z(t)$ is the thaw depth relative to the initial position of the surface and σ'_0 is effective stress at the initial thawed void ratio $e_0 = e_f/1.09$.

The thaw depth corresponds to the depth at which the temperature equals the freezing point T_f. The temperature profile is calculated using the following one-dimensional convection-conduction heat transfer equation

Equation 3-3 $\left(C - L\rho_i \frac{\partial\theta_i}{\partial T}\right)\frac{\partial T}{\partial t} - \frac{\partial}{\partial a}\left[\lambda \frac{(1+e_f)^2}{(1+e)^2}\frac{\partial T}{\partial a}\right] + c_w\rho_w v_a \frac{1+e_f}{1+e}\frac{\partial T}{\partial a} = 0$

where C is the volumetric heat capacity of the soil, L is the latent heat of fusion of water per unit mass, ρ_i is the density of ice, ρ_w is the density of water, θ_i is the volumetric ice fraction, T is the temperature in Kelvin, λ is the thermal conductivity of the soil, c_w is the heat capacity of water by mass, and v_a is the water flow velocity in the direction of a.

The volumetric heat capacity of the soil is obtained from the volumetric fraction of each of the soil components such that

Equation 3-4 $C = \rho_w c_w \theta_w + \rho_s c_s \theta_s + \rho_i c_i \theta_i$

where θ is the volumetric fraction, ρ is the density, and c is the heat capacity by mass with subscripts w, s, and i denoting liquid water, solids, and ice, respectively.

The thermal conductivity of the saturated soil is calculated by the generalized model proposed by Côté and Konrad (2005) such that

Equation 3-5 $\lambda = \lambda_s^{\theta_s} \times 2.24^{\theta_i} \times 0.6^{\theta_w}$

where λ_s is the thermal conductivity of solid particles.

The relationship between unfrozen water content and temperature, also called the phase composition curve, can be represented using a power function such that

Equation 3-6 $\theta_u = \alpha_u(T_f - T)^{\beta_u}\frac{G_s}{1+e}$

where θ_u is the volumetric fraction of unfrozen water, α_u and β_u are coefficients characteristic of the soil, and T_f is the freezing point.

The large-strain thaw consolidation model is obtained by coupling Equation 3-1 and Equation 3-3 in a Lagrangian coordinate moving boundary modelling scheme. The Lagrangian

coordinate system adapts to soil deformation because it is defined as a function of the changes in the void ratio. Thus, the model is composed of two physically coherent moving boundaries: one at the thaw front and one at the surface. The effects of the movement of the boundary conditions located at the surface are fully accounted for. In comparison, the Morgenstern and Nixon (1971) theory is composed of a single moving boundary at the thaw front under the assumption that the movement of the surface from thaw consolidation can be neglected in the assessment of thaw consolidation.

In the Dumais and Konrad (2018) model, the void ratio is used as the coupling state variable such that the hydromechanical and thermal soil properties change as consolidation proceeds. The relationships between the void ratio and other geotechnical quantities of interests, such as the surface settlement and excess pore water pressures, are integrated into the model. In comparison, the Morgenstern and Nixon (1971) theory is based on the calculation of excess pore water pressures and constant soil properties determined before any assessment of thaw consolidation is used as input parameters.

Nevertheless, the principal quality of the Morgenstern and Nixon (1971) theory lies in its simplicity for the assessment of thaw consolidation. The simple formulation allowed for the development of analytical solutions and graphical calculation tools that are easy to use in engineering practice. Extensions to the theory were also formulated to complete the initial theory (Nixon 1973). A discussion of the theoretical formulations adopted by Morgenstern and Nixon (1971) can be found in Dumais and Konrad (2018). The use of the Morgenstern and Nixon (1971) theory for comparison with the Dumais and Konrad (2018) model is justified because of its general use in the literature.

3.5 Site Conditions and Experimental Setup

The Inuvik pipeline test site is located in the vicinity of the Mackenzie River Delta in continuous permafrost (Watson et al. 1973). The general stratigraphy at the site that is characteristic of the area is presented in Figure 3.1. The upper layer composed of organics and silt is underlain by a clear ice layer with compact silt inclusions, a thick silt layer with decreasing ice content with depth, and a dense till layer of gravel and sand with some fines (Watson et al. 1972).
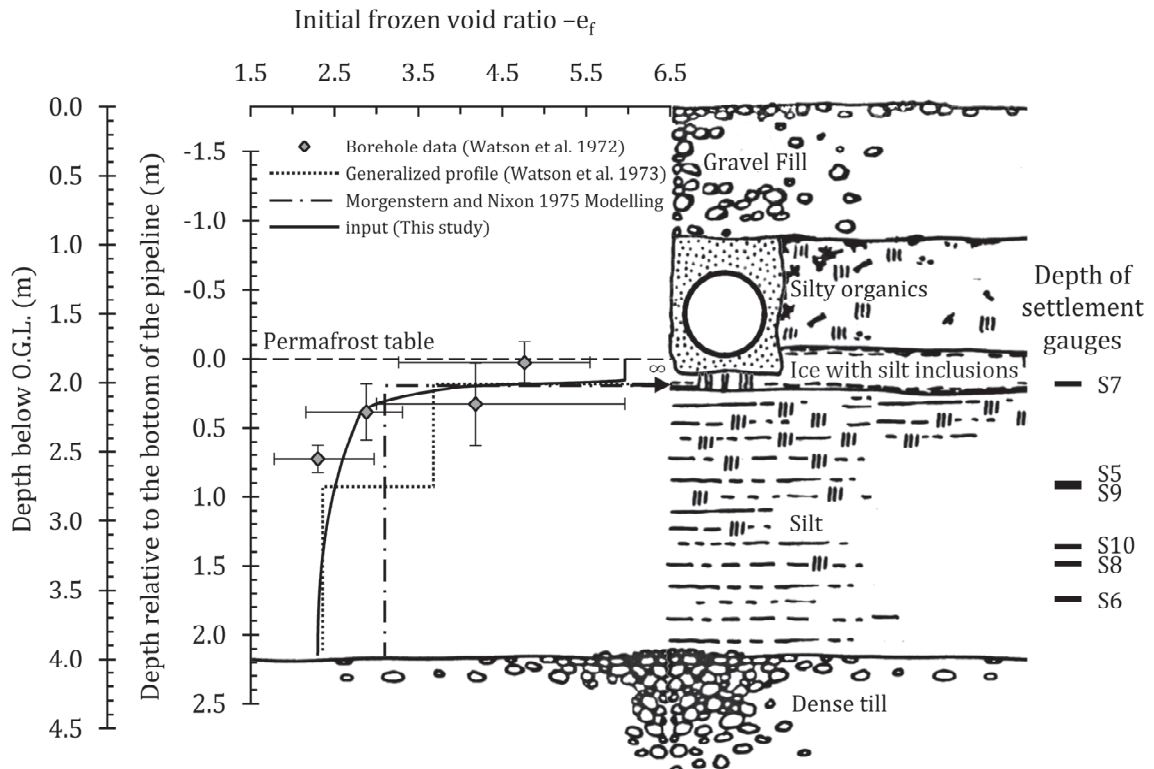
Figure 3.1 : Stratigraphy at Inuvik experimental pipeline site

An unused gravel pad next to existing pipeline research facilities was used for the thaw consolidation test section. A trench was dug in the gravel pad and the organic layer to install the 61-cm diameter pipeline directly on top of the ice-rich permafrost. The pipe was bedded on a thin sand layer, and sand was placed around and on top of the pipe in lieu of the organic layer. The gravel pad was then restored by filling up the trench with gravel fill material. In the current study, the depth datum $a = 0$ is located at the initial elevation of the bottom of the pipeline.

The instrumentation used to monitor the thaw consolidation field experiment included thermistors, settlement gauges, and piezometers installed at different depths near the central portion of the pipeline (Slusarchuk et al. 1973, Watson et al. 1973). The position of the settlement gauges located below the pipeline is shown in Figure 3.1. Settlement rods were also welded on top of the pipe at the east and west ends to monitor its settlement. A plan of the location of selected piezometers installed near the centre of the pipeline is presented in

Figure 3.2. Circulation of hot oil at a temperature of 71°C was initiated on July 22, 1971, which corresponds to the initial time $t = 0$ in the current study.
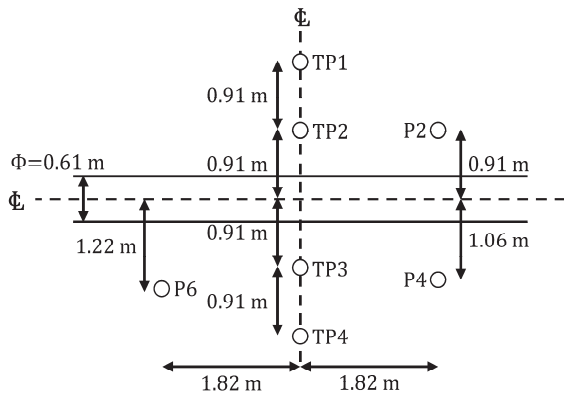
Figure 3.2 : Location of selected piezometers near the centre of the pipeline

Geotechnical investigation at the site included three boreholes to validate the general stratigraphy, to determine the ice content of the soil, and to retrieve samples for testing the properties of the permafrost. In Figure 3.1, the average frozen void ratio of the four frozen core samples obtained from the mineral soil is plotted as a function of the depth relative to the elevation of the interface between the gravel fill and the natural ground. Multiple specimens were prepared out of each core for laboratory testing. Horizontal error bars show the variability of the frozen void ratio of the laboratory specimens, and the vertical error bars show the total length of the large diameter cores.

In concordance with the analysis by Morgenstern and Nixon (1975), only the soil located between the pipeline and the top of the dense till layer is considered to undergo thaw consolidation. The soil located above and below is considered free draining when thawed. The soil above the elevation of the bottom of the pipeline is considered as a surcharge. The thin sand layer is not considered in the analysis, in line with the previous studies on the Inuvik experimental pipeline (Watson et al. 1973, Morgenstern and Nixon 1975).

The generalized soil profile below the pipeline proposed by Watson et al. (1972) is presented in Figure 3.1 in terms of the frozen void ratio and can be described as follows: a 0.15-m thick ice lens with traces of silt underlain by 0.76-m of ice with silt inclusions, and then 1.22-m of silt and ice, and finally a gravel till layer from a depth of 2.13 m. In their analysis, Morgenstern and Nixon (1975) considered a simplified stratigraphy consisting of a 0.19-m

thick pure ice layer underlain by a homogeneous soil layer with an average frozen void ratio of 3.1 to facilitate the application of the small strain linear thaw consolidation theory.

The Dumais and Konrad (2018) model is not limited in its ability to handle more complex initial conditions. Thus, a frozen void ratio profile more representative of field observations and of the geotechnical investigation can be used for the large-strain analysis. In contrast with previous studies, the 0.15-m thick ice-rich layer directly below the pipeline is considered to have a frozen void ratio of 5.96 rather than being pure ice. This value corresponds to the frozen void ratio of the most ice-rich specimen tested in the laboratory. This approach also allows for consideration of the compact silt inclusions observed in the ice layer (Watson et al. 1972). The underlying 1.98-m thick silt layer is characterized by a sharp decrease in ice content at the top and a subsequent gradual decrease until reaching the minimum frozen void ratio at the interface with the dense till layer. The minimum frozen void ratio is set at 2.30, which corresponds to the lowest void ratio core sample.

Figure 3.3 presents the progression of the 0°C isotherm along the longitudinal centreline of the pipeline. Heat transfer around a buried pipe is two-dimensional, as demonstrated by the bowl-shaped 0°C isotherms. Still, the magnitude of the pore water pressures is expected to be most significant directly below the pipe along its centreline. Because symmetry exists along this axis, a one-dimensional configuration is adopted to simplify the assessment of thaw consolidation below the pipeline (Morgenstern and Nixon 1975). The one-dimensional assumption is considered valid for the relatively flat portion of the 0°C isotherms on either side of the pipeline. Because instrumentation at the site was not installed directly below the pipeline, only the measurements of the instrumentation located within about 1 m on either side of the pipeline will be used in this study. For instance, the thaw front reaches piezometers TP2 and TP3 almost at the same time that the thaw penetration reaches the same depth along the centreline. However, a significant delay occurs before thaw penetration reaches TP1 and TP4, which are located further from the pipeline centreline.
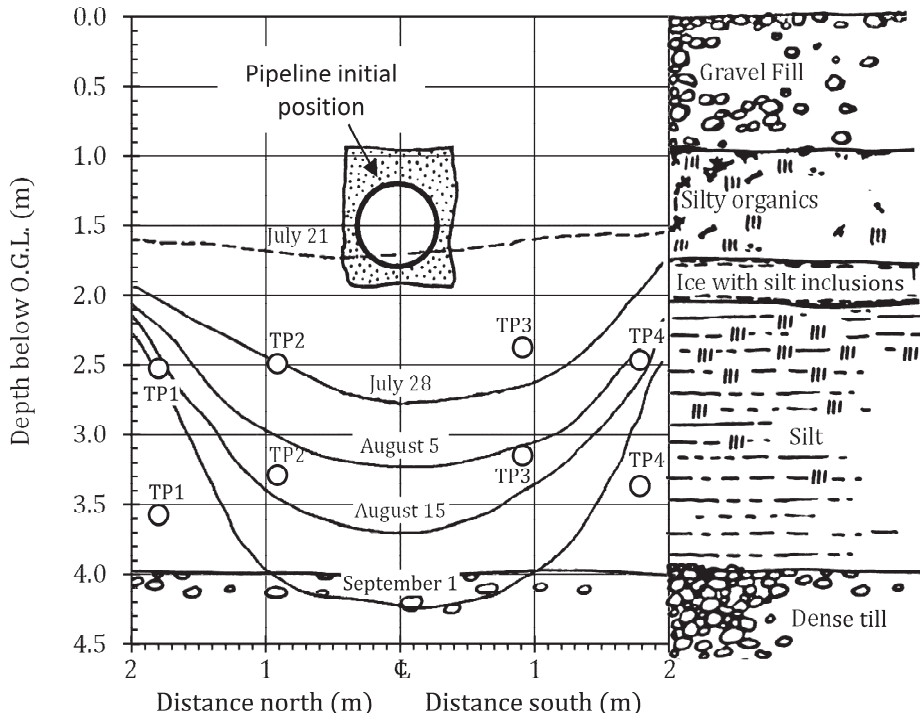
Figure 3.3 : Position of the 0°C isotherm along the centreline of the test section during the thaw consolidation test

3.6   Soil Properties

Inuvik silt is composed of 8% sand, 42% silt, and 40% clay. It has a liquid limit of 50.4%, a plastic limit of 32.3%, and a specific gravity of 2.67. The thick silt deposit contains little organic matter.

Experimental data on selected thaw settlement tests and the hydraulic conductivity of the thawed Inuvik silt k_v are presented in Figure 3.4. For each individual tested specimen, the experimental relationship between the void ratio and the effective stress is best characterized by a semilogarithmic linear relationship $e - \log \sigma'_v$. At lower effective stresses, an idealized $e - \sigma'_v$ relationship identified by a dotted line in Figure 3.4 can be defined from the physical interpretation of the behaviour of thawing ice-rich soils.
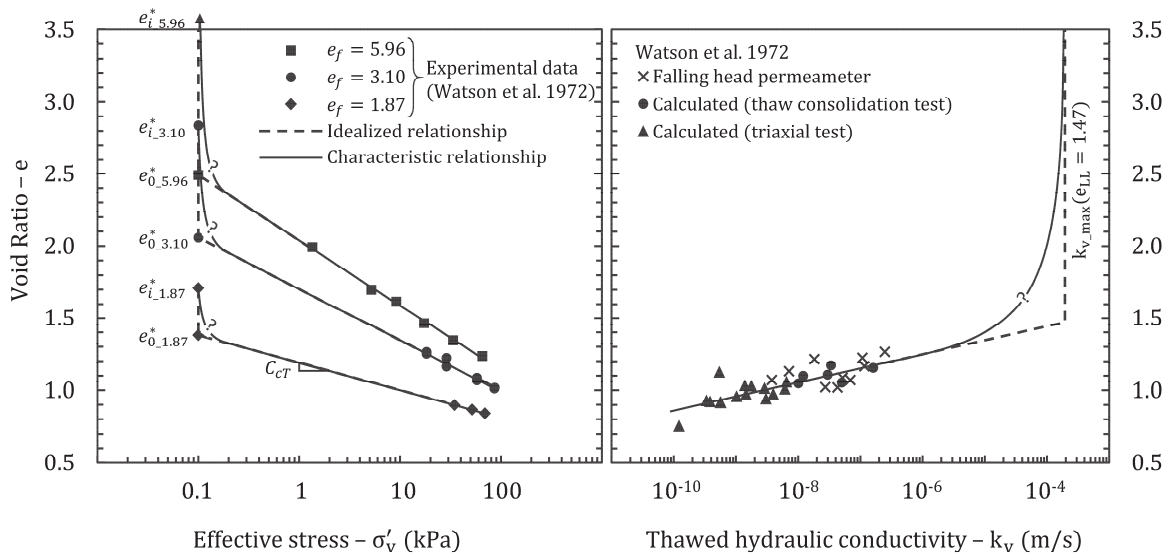
Figure 3.4 : Properties of thawed Inuvik silt for large-strain thaw consolidation analysis

On thawing, a volumetric change attributed to phase change causes the void ratio to decrease from the frozen void ratio e_f to the initial thawed void ratio e_i^* such that

Equation 3-7 $e_i^* = \dfrac{e_f}{1.09}$.

On thawing, any infinitesimal increase in effective stress will result in the expulsion of the water that the soil skeleton in its initial thawed state cannot hold. Consequently, the void ratio of the soil further decreases to the thawed void ratio e_0^*. The thawed void ratio e_0^* is defined at an effective stress σ_0' of 0.1 kPa on the extrapolated curve of the $e - \sigma_v'$ relationship defined experimentally. The arbitrary value of 0.1 kPa is chosen because it is large enough to have practical relevance, yet small enough to uphold the physical meaning of e_0^*. It can be considered that from e_0^* the consolidation behaviour is characterized by a semi-logarithmic linear relationship $e - \log \sigma_v'$, as shown in Figure 3.4 for the Inuvik silt. The complete idealized $e - \sigma_v'$ relationship for thawing ice-rich soils is defined by

Equation 3-8 $For\ e_i^* < e < e_0^*,$ $\sigma_v' = \sigma_0' = 0.1\ kPa,$

                                         $For\ e < e_0^*,$ $(e - e_0^*) = -C_c^* \log\left(\dfrac{\sigma_v'(e)}{\sigma_0' = 0.1\ kPa}\right).$

For compressible soils, changes in the void ratio should always be associated with effective stress variations such that the $de/d\sigma_v'$ gradient is never null. For physically coherent thaw consolidation modelling, it is necessary to define smoothed characteristic $e - \sigma_v'$

relationships such as those illustrated in Figure 3.4. The full lines marked by a question mark indicate that the illustrated characteristic relationships are approximations. Details of the parameterization of the characteristic relationships used in this study will be discussed in the numerical implementation section of this paper.

The experimental data presented in Figure 3.4 demonstrate the impact of the ice content on the compressibility behaviour of thawing soils. Parameters C_c^* and e_0^* are also plotted as a function of the frozen void ratio in Figure 3.5 and Figure 3.6, respectively. All the Inuvik silt specimens have similar index soil properties and differ only in terms of their initial ice content.

The laboratory results demonstrate that the thawed compression index C_c^*, which characterizes the compressibility of the Inuvik silt, decreases with a decreasing frozen void ratio. Therefore, an increase in effective stress will lead to a larger deformation for Inuvik silt with a higher initial ice content. In other words, more pressure is required to expel water out of the soil skeleton of the Inuvik silt with less ice initially.

This phenomenon can be explained by the changes in the fabric of thawed fine-grained soils. On thawing, fine-grained soils are characterized by an arrangement of macrostructure and microstructure (Konrad 2010). The macrostructure is formed of the coarser silt grains, whereas the microstructure is formed of packets of finer-grained particles (Konrad and Samson 2000a). The microstructure is characterized by a low porosity.
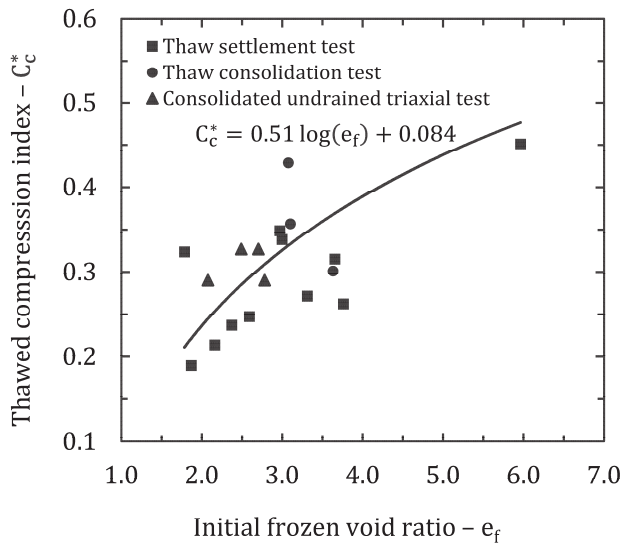
Figure 3.5 : Compressibility of thawed Inuvik silt
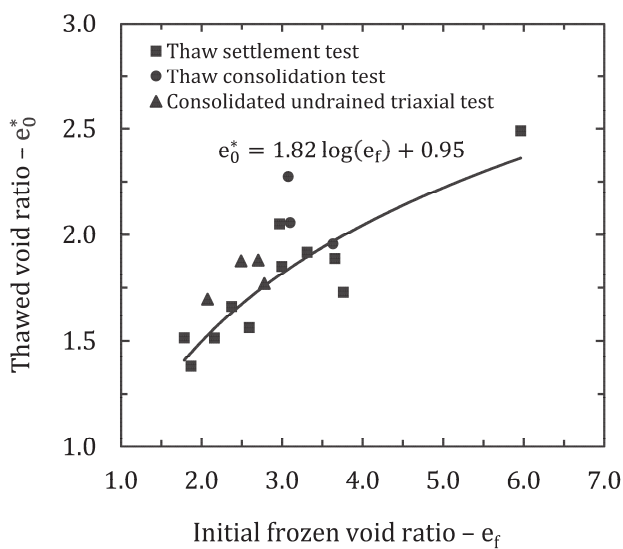
Figure 3.6 : Void ratio of thawed Inuvik silt at σ'ᵥ=0.1 kPa

On freezing, suction-induced freezing forces cause a destructuration of the soil's fabric, especially affecting the microstructure (Konrad 1988). The high ice content of a soil may be an indication that its structure is characterized by a macrostructure with little enduring microstructure. Because water located in the microstructure is more difficult to expel than water located in the macrostructure, ice-rich soils are more compressible on thawing. The relationship between the thawed compression index C_c^* of Inuvik silt and the frozen void ratio is given by

Equation 3-9 $C_c^* = 0.51 \log(e_f) + 0.084$

The structure of thawing soils also explains that the thawed void ratio e_0^* of Inuvik silt increases with an increasing frozen void ratio. Indeed, ice-rich Inuvik silt can hold a larger volume of water per volume of solids on thawing. In a soil dominated by its macrostructure, the arrangement of the solid particles is more uniform, leading to more effective contacts between the particles. Thus, the soil skeleton of the less structured thawing soil can sustain higher effective stresses when holding the same volume of water. The relationship between the thawed void ratio e_0^* of Inuvik silt and the frozen void ratio is given by

Equation 3-10 $e_0^* = 1.82 \log(e_f) + 0.95$

The experimental relationship between the void ratio and the hydraulic conductivity of thawed Inuvik silt presented in Figure 3.4 can also be characterized by a semilogarithmic relationship $e - \log k_v$. Multiple specimens with a wide range of frozen void ratio were tested, and the experimental data do not show any noticeable dependency of the $e - k_v$ relationship with the ice content, as was the case for the compressibility of the thawed soil samples. Thus, a unique $e - k_v$ relationship is adopted for modelling thaw consolidation of the thawed Inuvik silt.

The hydraulic conductivity of thawed Inuvik silt was only measured for samples consolidated at low void ratios. However, the $e - k_v$ relationship needs to be defined over the full range of thawed void ratios to model large-strain nonlinear thaw consolidation. The experimental curve can be extrapolated to a higher void ratio, which eventually leads to unrealistically high calculated hydraulic conductivity values. In the current study, the hydraulic conductivity of thawed Inuvik silt is assumed to reach a maximum void ratio value corresponding to the liquid limit, e_{LL}. This arbitrary threshold is believed to be realistic and high enough to allow unimpeded drainage of the excess water in loose thawing soils. In fact, the transition to higher hydraulic conductivity values at a high void ratio is believed to be smoother, as illustrated by the characteristic relationship in Figure 3.4. Given the lack of experimental data required to develop a more complex relationship, a simpler bilinear $e - k_v$ relationship as indicated by the dashed line in Figure 3.4 is adopted in this study such that:

Equation 3-11 $\qquad For\ e > e_{LL},\qquad k_v = 1.94 \times 10^{-4}\ m/s,$

$$For\ e < e_{LL}, \qquad (e - e_{LL}) = log\left(\frac{k_v(e)}{1.94 \times 10^{-4}\ m/s}\right).$$

As part of the geotechnical investigation, the thermal properties of Inuvik silt were measured in the laboratory (Watson et al. 1972, Smith 1985). The volumetric heat capacity and the thermal conductivity of the soil particles are 1.85 MJ/m³°C and 2.05 W/m°C, respectively (Watson et al. 1972). The coefficients α_u and β_u are 14.5 and 0.254, respectively (Smith 1985). The freezing point T_f is set at 0°C.

3.7 Numerical Implementation

The numerical implementation strategy of the large-strain thaw consolidation model detailed in Dumais and Konrad (2018) is adopted in the current study. The numerical modelling software COMSOL Multiphysics v5.3 is used for the numerical simulation. The model is implemented in Lagrangian coordinates such that the effects of soil deformations are fully accounted for as a function of void ratio variations (Dumais and Konrad 2018).

The modelling domain for the thermal component is defined from $a = 0$ m up to $a = 6$ m which comprises the ice lens with silt inclusions and the entire ice-rich silt layer, and extends 3.87 m into the dense till layer. The initial temperature of the soil is homogeneously set at $T_0 = -5°C$ (Slusarchuk et al. 1973). The thermal boundary conditions at the top are dictated by a Dirichlet boundary condition such that $T_s = 71°C$ (Morgenstern and Nixon 1975). The temperature of the oil in the experimental pipeline increased to 71°C almost instantaneously after initiation of the oil flow (Watson et al. 1972). To ensure numerical stability, the temperature at the top boundary is nonetheless ramped up from $T_0 = -5°C$ to $T_s = 71°C$ in 1 min, which is fast enough to reproduce field conditions. A zero-flux boundary condition is applied at the bottom of the thermal modelling domain at $a = 6$ m. The thermal properties are modelled as specified previously.

The consolidation modelling domain is defined between $a = 0$ and the position of the thaw front. Consolidation modelling is limited to the compressible layers: the ice lens with silt inclusions and the ice-rich silt layer. At $a = 0$, the conditions are controlled by the surcharge loading $P_0 = 17$ kPa of the materials above the bottom of the pipeline (Morgenstern and

Nixon 1975). The free-draining conditions at $a =0$ are defined by setting up the consolidated void ratio $e_s =1.30$ corresponding to the surcharge $P_0 =17$ kPa as a Dirichlet boundary condition. During the thaw consolidation phase, the position of the bottom boundary moves as a function of the position of the thaw front. The impervious boundary conditions at the bottom are defined in Equation 3-2. When the thaw front reaches the interface between the silt layer and the dense till layer, the consolidation component enters the post-thaw consolidation phase. Accordingly, the position of the bottom boundary is fixed at $a =2.13$ m, and the conditions at the bottom are switched to a free-draining boundary condition.

The initial conditions of the consolidation component are given by the frozen void ratio profile presented in Figure 3.1. The corresponding thawed compression index and thawed void ratio are calculated by Equation 3-9 and Equation 3-10 to parametrize the $e - \sigma'_v$ relationship as a function of the frozen void ratio. Smooth characteristic relationships as those illustrated in Figure 3.4 are formulated to ensure numerical stability. The linear formulation of the $e - \sigma'_v$ relationship is used for effective stresses higher than 0.2 kPa. For effective stress between 0.1 and 0.2 kPa, the relationship is adapted by gradually ramping up the compression index. The ramp function is adjusted such that the curve reaches the initial thawed void ratio e_0 at the effective stress value of 0.1 kPa. The hydraulic conductivity idealized relationship is implemented as is for the numerical simulation.

3.8   Modelling Results

The results of the Inuvik warm-oil pipeline experiment are presented in terms of pipeline settlement and thaw depth in Figure 3.7 and Figure 3.8. The dotted lines in Figure 3.7 and Figure 3.8b present the observed experimental results (Watson et al. 1972, 1973). The experimental settlement is presented for both the east and west ends of the pipeline. The modelling results obtained with the large-strain nonlinear Dumais and Konrad (2018) model are represented by full lines in Figure 3.7. The results obtained with the small strain linear Morgenstern and Nixon (1971) theory are represented by dashed lines in Figure 3.8. The small strain linear results are presented as computed in the analysis detailed by Morgenstern and Nixon (1975) except for the post-thaw settlements that are computed from the design chart presented by Nixon (1973). For all data sets, thaw consolidation proceeds from $t = 0$

until the thaw depth reach the dense till layer. The experiment then enters the post-thaw consolidation phase when indicated for the modelling results in Figure 3.7 and Figure 3.8b.
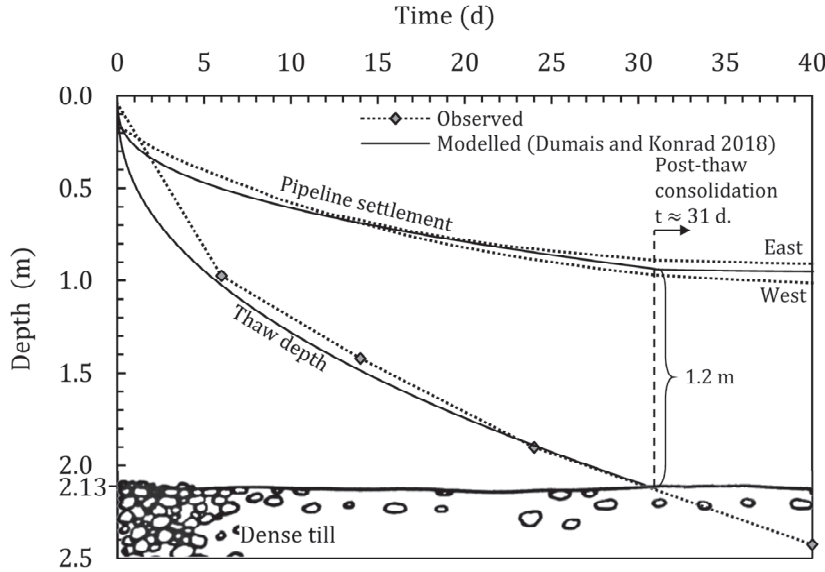
Figure 3.7 : Large-strain nonlinear thaw consolidation modelling results of the Inuvik pipeline
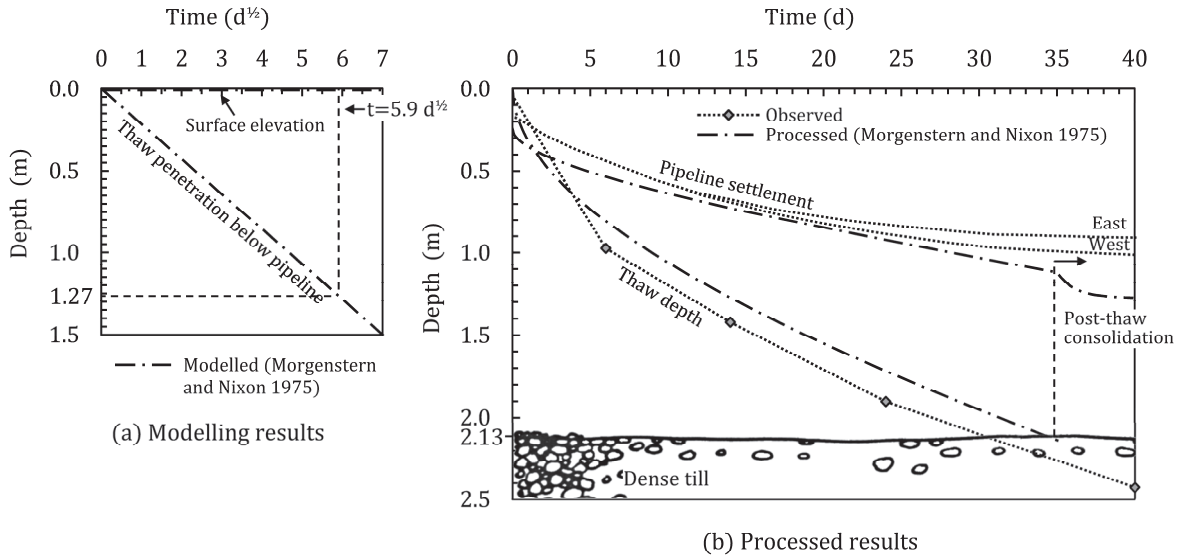
Figure 3.8 : Small strain linear thaw consolidation modelling results of the Inuvik pipeline: (a) modelling results; and (b) processed results

It should be noted that two modifications were applied to the experimental settlement curves presented in Figure 3.7 and Figure 3.8b. First, the settlement curves were shifted by six days to coincide with the settlement behaviour measured by the settlement gauges. Indeed, a significant unexpected delay occurs at the onset of the experiment before the settlements

given that the thawing of the ice-rich layer found just below the pipeline could be measured by the settlement rods attached to the pipeline, which may be caused by a combination of factors. Although the connections between the oil supply lines and the pipeline were designed such that they could be adjusted as the pipeline settles, there could still have been some structural inertia, especially at the very beginning of the experiment when the deformation rate is very important. Additionally, the pipeline was installed in a trench such that there might be ice present longitudinally beyond both ends of the pipeline. The presence of this could have slowed down the penetration rate to below the ends of the pipeline at the beginning of the experiment, which would explain the delayed settlement response. A second modification to the settlement curves was applied to subtract the settlements attributable to the 12.5% thaw strain observed during the post-thaw consolidation phase in the dense till layer that was not included in the thaw consolidation analysis (Watson et al. 1972). The general agreement between the corrected settlement curves and the results of both the large and small strains' thaw consolidation analysis supports the validity of the applied corrections.

A preliminary analysis of the modelling results presented in Figure 3.7 and Figure 3.8 offers interesting insights into the modelling strategies adopted by Dumais and Konrad (2018) and Morgenstern and Nixon (1971). In the coupled method proposed by Dumais and Konrad (2018), soil deformation is directly integrated into the model's formulation such that the locations at which the boundary conditions are applied are always in agreement with the physical locations of the boundaries. In that way, the modelled pipeline settlement and thaw depth curves presented in Figure 3.7 represent the physical configuration used for the numerical computation. This representation is most important when thaw settlement is significant for the thermal and drainage boundary conditions applied at the surface.

In contrast, the uncoupled Morgenstern and Nixon (1971) theory assumes that surface settlement can be neglected in the assessment of thaw consolidation. Thus, all quantities are calculated relative to a surface elevation of $a = 0$. Furthermore, the computation is sequential. First, the thaw penetration rate is calculated under the assumption that the elevation of the surface at which the heat source is located remains unchanged, as presented in Figure 3.8a. Then, the excess pore water pressures are computed as a function of the thaw penetration rate with the drainage surface located at $a = 0$, as shown in Figure 3.8a.

To obtain surface settlement and the actual thaw depth as presented in Figure 3.8b, the modelling results expressed in terms of excess pore water pressures must be processed. First, the degree of consolidation is obtained from the excess pore water pressures. Then, the surface settlement at time t is calculated from the degree of consolidation as a function of the total expected thaw settlement under the assumption that the $e - \sigma_v'$ relationship is linear. Finally, the thaw depth is obtained by combining thaw penetration and surface settlement.

The impact of this sequential linear approach will be discussed throughout this paper regarding the modelling results. Most notably, an important divergence exists between where the boundary conditions are effectively applied for computation as shown in Figure 3.8a and the physical locations of the boundaries as shown in Figure 3.8b. For example, the modelling configuration when the computed thaw front reaches the till layer at a depth of 2.13 m after about 35 days (5.9 days$^{0.5}$) is outlined in Figure 3.8a by a dashed line. At that time, the top boundary conditions for the calculation of the excess pore water pressures are still applied at $a = 0$, although the bottom of the pipeline is physically located 0.92-m lower than the initial position of the bottom of the pipeline. Concurrently, the bottom boundary conditions at the thaw front are applied at a depth of 1.3 m, whereas the thaw penetration is effectively 2.13 m. This incoherence between the modelling and physical configurations is duly addressed in the Dumais and Konrad (2018) model because the boundary conditions are always seamlessly applied at the physical locations of the boundaries computed by the model.

3.9   Analysis of Thermal Behaviour

Beginning the detailed analysis of the results by examining the thermal behaviour is logical because thaw penetration triggers the initiation of thaw consolidation. Most importantly, the thaw penetration rate controls the release rate of water at the thaw front and, consequently, the generation rate of pore water pressure.

For the large-strain assessment, the actual position of the thaw front as presented in Figure 3.7 is used directly in the numerical formulation. The volumetric water release rate is calculated from the advancement of thaw penetration over time $dZ(t)/dt$. In contrast, the small strain assessment presented in Figure 3.8a is based on the thaw penetration rate obtained from analytical solutions to the heat transfer problem in soils. These solutions

calculate the distance between the heat source and the thaw front rather than the actual depth of the thaw front.
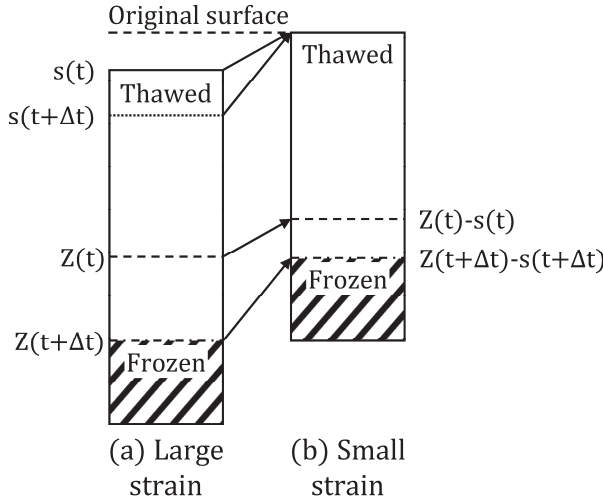
Figure 3.9 : Thaw consolidation in (a) large-strain; and (b) small strain configuration

The difference between the large-strain and the small strain approaches is schematized in Figure 3.9. The large-strain configuration presented in Figure 3.9a is a realistic representation of thaw consolidation. At time $t > 0$, the thaw front is at a depth $Z(t)$, and the surface is located at $s(t)$ given thaw settlement. Over an incremental time step Δt, both thaw penetration and thaw settlement increase such that the thaw front and the surface are now located at $Z(t + \Delta t)$ and $s(t + \Delta t)$, respectively.

In the small strain configuration presented in Figure 3.9b, surface settlement $s(t)$ is neglected. The thaw depth is given by the distance between the heat source located at the surface and the thaw front. In other words, the small strain configuration yields the rate at which the thaw front moves away from the surface rather than the rate at which the thaw front penetrates the ground. Thus, the small strain thaw depth is obtained by subtracting the surface settlement from the thaw depth. At time t and $t + \Delta t$, the thaw front is located at $Z(t) - s(t)$ and $Z(t) - s(t + \Delta t)$, respectively.

The physical implication of the small strain configuration is that the volume of water generated at the thaw front is underestimated because the contribution of the surface settlement to the thaw penetration rate is neglected. In contrast, the contribution of surface

settlement is fundamentally integrated into the large-strain approach such that the volume of water generated at the thaw front is physically coherent with the advancement rate of the thaw front. Note that the length of the drainage path given by the difference between the thaw depth and the surface elevation is not affected by the large and small strain configurations.

The impact of the different configurations for the calculation of the thaw penetration rate can be analyzed regarding the experimental pipeline results. The thaw penetration rate α is typically calculated as a function of the square root of time such that

Equation 3-12 $\alpha = \frac{z(t)}{\sqrt{t}}.$

Figure 3.7 shows that the thaw depth obtained from the Dumais and Konrad (2018) model very closely agrees with the field measurements throughout the experiment. The model results indicate that the thaw front reaches the till layer at a depth of 2.13 m in 31 days, which is approximately the time recorded experimentally. The thaw penetration rate obtained by the large-strain model is 0.383 m/d$^{0.5}$, which compares favourably with the experimental thaw penetration rate of 0.387 m/d$^{0.5}$. Thus, the modelled rate at which water is released at the thaw front is expected to concord with the field conditions.

In contrast, Figure 3.8a presents the thaw penetration as conceived in the small strain configuration in terms of the distance between the pipeline and the thaw front as a function of the square root of time. The solution developed by Nixon and McRoberts (1973) is used to compute thaw depth for the small strain assessment (Morgenstern and Nixon 1975). The thaw penetration rate in the small strain configuration is 0.215 m/d$^{0.5}$ (Morgenstern and Nixon 1975), which is significantly smaller than the experimental thaw rate. The important divergence is highlighted when comparing the thaw depth data presented in Figure 3.7 and Figure 3.8. From the initial configuration, thaw depth reaches the dense till layer at 2.13 m. However, when the thaw front reaches the dense till layer, pipeline settlement is 0.92 m and the distance between the thaw front and the pipeline is approximately 1.20 m. By omitting the contribution of surface settlement to thaw penetration, the small strain configuration considers that the thaw front penetrates the ground by 1.20 m to reach the dense till layer in approximately the same amount of time. The thaw penetration rate is underestimated, and an

important volume of water released at the thaw front is excluded from the Morgenstern and Nixon (1975) analysis.

It should be reiterated that the processed position of the thaw front for the small strain approach as presented in Figure 3.8b can only be computed subsequent to the thaw consolidation modelling for the Morgenstern and Nixon (1971) theory. This computation is achieved by combining the processed surface settlements and the distance between the heat source and the thaw front used as input in the analysis (Morgenstern and Nixon 1975). Therefore, the processed position of the thaw front presented in Figure 3.8b cannot be used to compute the pore water pressure generation rate.

3.10 Analysis of Hydromechanical Behaviour

Now that the thermal analysis has asserted the accuracy of the computed thaw penetration rate of the Dumais and Konrad (2018) model, we can proceed with the analysis of the hydromechanical behaviour of the Inuvik experimental pipeline. In the thaw consolidation analysis, the strongest practical interest is in the settlement rate and the excess pore water pressure quantities.

3.10.1 Settlement

In practice, engineers are first interested in predicting the total settlement that can be expected on completion of thaw consolidation. For the Inuvik pipeline, the total thaw strain is best analyzed from the settlement gauge measurements as the deformation can be isolated with precision for the soil located between two given gauges. In contrast, the total thaw settlement measured by the rods attached to the pipe is ultimately impacted by external factors, such as deformations in the till layer and freeze back.

Table 3.1 presents the thaw settlement of seven pairs of settlement gauges. The experimental values are compared with the results predicted by the Dumais and Konrad (2018) model as well as the Morgenstern and Nixon (1971) theory. The values inferred from laboratory thaw settlement testing and the generalized frozen void ratio profile presented in Figure 3.1 are also presented in Table 3.1 (Watson et al. 1973). The mean percentage error (MPE) is calculated for each predicted data set. A positive error means that the prediction is lower than the measured value. Thus, for the Dumais and Konrad (2018) model, the MPE of 2.1%

indicates a tendency to slightly underestimate the maximum thaw settlement. However, the predictions of the large-strain model are well within the range acceptable in engineering practice. In contrast, the MPE value of −24.1% suggests that the Morgenstern and Nixon (1971) theory significantly overestimates thaw settlement.

Table 3.1 : Thaw settlement at the end of thaw consolidation

Settlement gauges set	Observed (m)	This study (m)	Morgenstern and Nixon 1975 (m)	Watson et al. 1973 (m)
S7-S8	0.43	0.57	0.67	0.65
S5-S7	0.40	0.33	0.35	0.40
S6-S7	0.74	0.68	0.82	0.76
S5-S8	0.23	0.24	0.32	0.23
S6-S8	0.10	0.11	0.15	0.10
S5-S6	0.33	0.35	0.47	0.34
S9-S10	0.27	0.18	0.24	0.21
Mean percentage error	2.1 %	-24.1 %	-4.9 %	

Compared with the MPE value of −4.9% of the traditional thaw settlement testing approach, only the Dumais and Konrad (2018) model offers an increase in accuracy for the prediction of thaw settlements given its ability to handle a complex frozen void ratio profile and its corresponding soil properties. The thaw settlement results also suggest that the characterization of the $e - \sigma_v'$ relationship used in this study is valid for modelling consolidation of thawing ice-rich soils.

3.10.2 Rate of Settlement

For the analysis of infrastructure affected by thaw consolidation, the settlement rate is also of interest in determining the portion of the total thaw settlement occurring on thawing and the amount of additional settlements that may be expected during the post-thaw consolidation phase.

During the thaw consolidation phase, settlements are caused by the combination of consolidation and of volumetric changes attributable to phase change from pore ice to water. During the post-thaw consolidation phase, settlements are only the result of consolidation as the contribution of the phase change ends. The consolidation rate in thawing soils is regulated

by the rate at which water is drained out of the soil skeleton. Equation 3-1 can be rearranged to examine the factors that control the consolidation rate, as:

Equation 3-13 $\frac{1}{\gamma_w}\frac{\partial}{\partial a}\left[\frac{k_v(e)(1+e_f)}{1+e}\frac{\partial u_e}{\partial a}\right] = \frac{1}{1+e_f}\frac{\partial e}{\partial t}$

where the excess pore pressure gradient is defined as

Equation 3-14 $\frac{\partial u_e}{\partial a} = \frac{(G_s-1)\gamma_w}{(1+e_f)} - \frac{d\sigma'_v(e)}{de}\frac{\partial e}{\partial a}$

The void ratio change rate with time $\partial e/\partial t$ is controlled by the hydraulic conductivity of the thawed soil $k_v(e)$, which controls the rate at which water can be drained out of the soil skeleton and by the excess pore pressure gradient $\partial u_e/\partial a$ that characterizes the amount of stress to be transferred from the pore water to the soil skeleton. The second term of the right-hand side in Equation 3-14 indicates that for a given void ratio gradient $\partial e/\partial a$, the excess pore water pressure gradient decreases when the derivative of the effective stress with void ratio $d\sigma'_v(e)/de$ increases. Therefore, the $e - \sigma'_v$ relationship plays a significant role in regulating the consolidation rate. Indeed, the excess pore water pressure gradient generated on consolidation will be smaller in soils for which changes in void ratio de induce large changes in effective stress $d\sigma'_v(e)$. In other words, the consolidation rate is lower for less compressible soils.

Although the previous discussion may appear to be self-evident, it is critical to the understanding of the behaviour of thawing ice-rich soils not only in terms of the non-linearity of the properties but also in terms of the impact of the initial ice content. As seen in Figure 2.5, the compressibility of thawed Inuvik silt increases with initial ice content. Furthermore, Figure 3.4 and Figure 3.6 indicate that more ice-rich Inuvik silt is also associated with higher hydraulic conductivity on consolidation as the consolidated void ratio of thawed Inuvik silt increases with the initial ice content. The consolidation rate on thawing is expected to be higher near the pipeline where the most ice-rich Inuvik silt is located, given a high excess pore pressure gradient and high hydraulic conductivity, and decelerates with depth as the soil becomes less ice-rich.

The progression of the settlement with time during the thaw consolidation and post-thaw consolidation phases is presented in Figure 3.7 and Figure 3.8b. The pipeline settlement curve modelled by the large-strain model matches well the experimental curves and the anticipated thaw consolidation behaviour. Indeed, the settlement rate is initially high as the thaw front is rapidly advancing in the most ice-rich layers of soil. It gradually decreases as the thaw progression decelerates and reaches less ice-rich layers of soil. During the post-thaw consolidation phase, settlements proceed at a lower rate as the outstanding excess pore water pressure is expelled at a lower rate. In the case of the Inuvik pipeline, most deformations occur during the thaw consolidation phase, and settlements are limited in the post-thaw consolidation phase.

The small strain settlement curve shows some notable divergence with the experimental data. First, predicted settlements are overestimated throughout. Second, the small strain analysis predicts an acceleration of the settlement rate during the post-thaw consolidation phase, which is caused by the linearization of the $e - \sigma'_v$ relationship inherent to the Morgenstern and Nixon (1971) formulation.
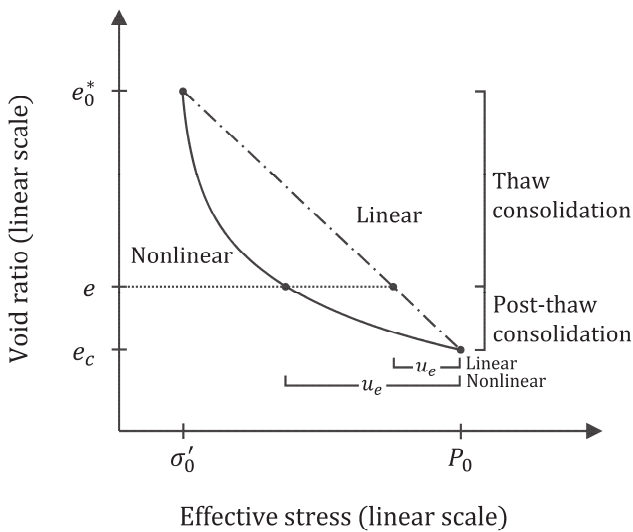
Figure 3.10 : Schematization of the $\sigma'_v - e$ relationship in thawing soils

Figure 3.10 shows a schematization of the difference between linear and nonlinear $e - \sigma'_v$ relationships for modelling thaw consolidation. The linear curve is an approximation used in small strain consolidation theory to facilitate resolution of the problem, whereas the nonlinear

relationship can be considered a more adequate characterization of soils undergoing consolidation (Nixon 1973).

In Figure 3.10, soil at a thawed void ratio e_0^* is submitted to a surcharge P_0. The void ratio e at the onset of the post-thaw consolidation phase is the same for both the linear and the nonlinear curves (Davis and Raymond 1965, Nixon 1973). The first notable disparity between the two curves is an important difference of excess pore water pressure at the void ratio value e, which is a generally recognized consequence of the linearization of the $e - \sigma_v'$ relationship (Davis and Raymond 1965, Nixon 1973).

Another noteworthy difference between the two curves is their slopes. The slope of the $e - \sigma_v'$ relationship characterizes the compressibility of a soil. More compressible soils that are associated with faster consolidation are characterized by steeper slopes. The linear approximation assumes that the relationship between e and σ_v' is defined by a constant linear slope. Although this approximation is valid for soils undergoing small void ratio changes, soils undergoing large void ratio changes present a change in compressibility, as discussed in the soil properties section of this paper.

This change is of utmost importance in thaw consolidation modelling because the consolidation of thawing soils is characterized by two distinct phases: the thaw consolidation phase and the post-thaw consolidation phase. As illustrated in Figure 3.10, the nonlinear curve is defined by a steep slope in the thaw consolidation phase and a notably gentler slope in the post-thaw consolidation phase. The consolidation rate is expected to be lower in the post-thaw consolidation phase. In contrast, the linear approximation considers a constant linear slope. When thaw penetration reaches a free-draining incompressible layer, as is the case in the Inuvik pipeline experiment, the consolidation rate for the linear approach increases drastically at the onset of post-thaw consolidation because the length of the drainage path is suddenly halved. The effect of linearization of the $e - \sigma_v'$ relationship is exemplified by the small-strain linear settlement curve presented in Figure 3.8b, in which the settlement rate is underestimated during the consolidation phase and overestimated during the post-thaw consolidation phase.

3.10.3 Pore Water Pressures

The results for the maximum excess pore water pressures for the Inuvik experimental pipeline are presented in Figure 3.11. The modelled curves represent the excess pore water pressure at the thaw front. The results of two additional simulations using Dumais and Konrad (2018) also plotted in Figure 3.11 were obtained by varying the hydraulic conductivity of the thawed Inuvik silt by half an order of magnitude to investigate the effect of the hydraulic conductivity on pore water pressures. The simulations cover a relatively narrow range of one order of magnitude, with the hydraulic conductivity of the thawed Inuvik silt defined by Equation 3-11 being the geometric mean of this range. The experimental values in Figure 3.11 represent the maximum excess pore water pressures measured at any time after thaw penetration had reached the tip of each piezometer. The accuracy of the field measurements is estimated at ± 3 kPa given the difficulty of measuring pore water pressures in thawing soils (Slusarchuk et al. 1973). The experimental points are plotted at the depth of the tip of the piezometers, which represents the depth at which the maximum pore water pressure is measured when the thaw front reaches the piezometers.
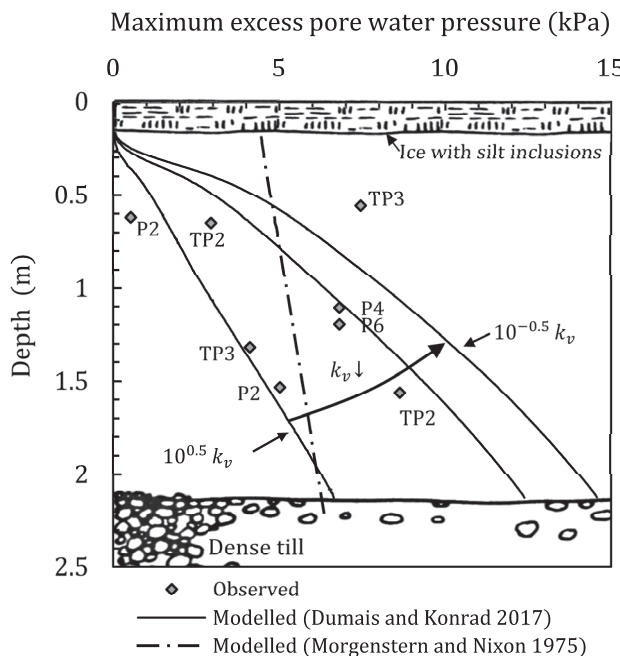
Figure 3.11 : Maximum excess pore water pressures at the thaw front

Figure 3.11 shows some scattering of the measured maximum pore water pressures. This can probably be attributed to the natural variation of geotechnical properties of the Inuvik silt at

the site, mainly the hydraulic conductivity. Most field measurements are located within the range of hydraulic conductivity defined by the simulation results, which demonstrates the ability of the model to assess the effect of the variability of the geotechnical properties at a specific site on thaw consolidation-related instabilities.

It can be noted that the observed pore water pressures are slightly lower than the modelled values when using the unique characteristic k_v relationship defined by Equation 3-11. This result may be due to the geometric effect discussed previously. Because heat transfer around a buried pipe is two-dimensional, the thaw penetration rate for which the piezometers are installed is slightly smaller than directly below the pipe along the centreline, as shown in Figure 3.3. Excess pore water pressures are expected to be most significant directly below the pipe, as predicted by the modelling results using Equation 3-11.

The experimental results can be compared with the modelling results in terms of the range covered by each data set. The experimental values range from a minimum value of 0.5 kPa at 0.62 m to a maximum value of 8.6 kPa at 1.56 m and are expected to be larger at a depth of 2.13 m. The Dumais and Konrad (2018) results cover the entire range of measured values because the highest maximum excess pore water pressure value computed by the large-strain nonlinear model is 12.5 kPa for thaw penetration that reaches the dense till layer when using the hydraulic conductivity value defined by Equation 3-11. In contrast, three measured values are lower and, most of all, four measured values are higher than the lowest—4.5 kPa—and highest—6.3 kPa—maximum excess pore water pressures computed using the small strain linear approach (Morgenstern and Nixon 1975).

The experimental data show a general trend for the maximum excess pore water pressures to increase with depth. Both modelling approaches show an increase in the maximum excess pore water pressure as thaw penetration deepens. For the Morgenstern and Nixon (1975) results, this increase is only caused by the increase of overburden stress. Indeed, the ratio between the maximum pore water pressure and the overburden stress is almost constant with depth (Morgenstern and Nixon 1975). Although overburden stress is also considered in the Dumais and Konrad (2018) model, the more important increase in the large-strain nonlinear modelled curves is mainly the result of the variation in the silt properties with depth. The

thaw front initially crosses the ice lens with silt inclusions without generating excess pore water pressures because the ice-rich silt directly below the pipeline is characterized by high compressibility and high hydraulic conductivity. As the thaw front reaches silt with less initial ice content, the excess pore water pressures increase from the reduced values of compressibility and hydraulic conductivity. With respect to the prediction of the maximum excess pore water pressures, the Dumais and Konrad (2018) model once again offers an increase in accuracy over the Morgenstern and Nixon (1971) theory.

3.11 Discussion

The practical relevance of the Dumais and Konrad (2018) model is now discussed. To begin with, the numerical implementation of the model is achieved at a nominal computational cost, which should not represent a barrier to the adoption of the model in practice. Indeed, the large-strain nonlinear model retains much of the simplicity of the one-dimensional formulation of the Morgenstern and Nixon (1971) theory, which facilitates numerical implementation. Nevertheless, the more robust formulation allows for consideration of more complex input parameters. In the case of the Inuvik experimental pipeline, this consideration leads to an increase in the accuracy of the predictions for all computed geotechnical quantities of interest. First, the model's ability to handle a complex frozen void ratio profile leads to an overall more accurate representation of the conditions identified during the geotechnical investigations. However, the capability to seamlessly implement the nonlinear $e - \sigma_v'$ and $e - k_v$ relationships and the dependency of the characteristics of the $e - \sigma_v'$ relationship on the frozen void ratio contribute most to more accurate predictions. Most of all, this capability allows for the objective use of all thaw consolidation, thaw settlement, and hydraulic conductivity testing results available for the Inuvik silt in the thaw consolidation analysis.

Outlining that all input data used in this study were also available to previous researchers is important. However, only the Dumais and Konrad (2018) model can take advantage of the entirety of the soil properties obtained in the comprehensive laboratory and site investigation. In contrast, Morgenstern and Nixon (1975) were effectively limited to considering a single arbitrarily selected frozen void ratio value in their analysis. All input soil properties and computed geotechnical quantities depended on this assumption. For example, a single

hydraulic conductivity value and a single point on one $e - \sigma_v'$ experimental curve was used to obtain the coefficient of consolidation of the Inuvik silt.

Oftentimes, not as much data are available in practice for design than for the analysis of the Inuvik experimental pipeline. The Dumais and Konrad (2018) method may seem impractical in that regard. However, the increased accuracy of the assessment of thaw consolidation achieved by the proposed model by utilizing more complex input data can be valuable. The additional costs associated with measuring the soil properties may be offset by the cost savings associated with more accurate predictions for thaw settlement and excess pore water pressures. The model can also be used with simpler input data. For example, the thaw settlement analysis can be achieved using only the $e - \sigma_v'$ relationship if data for hydraulic conductivity are not available. Furthermore, Dumais and Konrad (2016) have shown that some properties of thawing fine-grained soils can be derived from the index properties of the thawed soils. The development of empirical relationships to obtain all of the properties of thawing fine-grained soils required for the assessment of thaw consolidation will be the aim of a forthcoming paper.

The study of the Inuvik experimental pipeline shows that the simplified Morgenstern and Nixon (1975) theory may lead to errors in the prediction of thaw settlement and excess pore water pressures. In the case of the Inuvik experimental pipeline, the thaw settlement may be of greatest interest in terms of engineering design. In that regard, the 24.1% mean percentage error of the Morgenstern and Nixon (1975) results may be accurate enough for a simple engineering assessment considering the important magnitude of the final thaw settlement. However, excess pore water pressures may be relevant in other thaw consolidation-related problems, such as unstable thawing slopes, in which cases the important error of the Morgenstern and Nixon (1975) excess pore water pressure predictions may lead to unsafe design.

That is not to say that the validity of the Morgenstern and Nixon (1971) theory is being questioned, but that it should be applied cautiously in the context of large-strain nonlinear thaw consolidation. Applicability of the Morgenstern and Nixon (1971) theory and of the

Dumais and Konrad (2018) model should be evaluated with regard to the limitations discussed in this paper for any engineering assessment of thaw consolidation.

3.12 Conclusion

The thaw consolidation behaviour of the Inuvik warm-oil experimental pipeline has been analyzed with the large-strain nonlinear model formulated by Dumais and Konrad (2018). This model retains the simplicity of the one-dimensional thaw consolidation theory but gains in efficiency by the introduction of a second moving boundary at the surface and the consideration of more complex input parameters.

The following conclusions arise from the analysis of the Inuvik pipeline.

1.   The large-strain configuration adopted by the Dumais and Konrad (2018) model provides an accurate prediction of thaw penetration. In contrast, the small strain configuration of the Morgenstern and Nixon (1971) theory that neglects the movement of the surface can lead to an important underestimation of the volume of water released at the thaw front.

2.   For the Inuvik pipeline experiment, the Dumais and Konrad (2018) model offers an improvement in the prediction of thaw settlements over the Morgenstern and Nixon (1971) theory and the traditional thaw settlement laboratory testing approach given the improved characterization of the $e - \sigma'_v$ relationships and the ability to use a complex frozen void ratio profile as modelling input.

3.   The progression of the settlement predicted by the Dumais and Konrad (2018) model matches the experimental data in both the thaw consolidation and post-thaw consolidation phases given the nonlinear $e - \sigma'_v$ relationships used as modelling input. The linear approximation used in the Morgenstern and Nixon (1971) theory leads to an underestimation of the settlement rate in the thaw consolidation phase and an overestimation in the post-thaw consolidation phase.

4.   All aforementioned elements contribute to a safe and robust prediction of the maximum excess pore water pressures in the thawing Inuvik silt by the Dumais and Konrad (2018) model.

An important practical implication of the Dumais and Konrad (2018) model is that the increase in accuracy is achieved by using more effective input data that were also available to previous researchers. The Dumais and Konrad (2018) model can be recommended with confidence for modelling thaw consolidation based on its strong theoretical formulation and its overall performance demonstrated when applied to the case of the Inuvik experimental pipeline.

3.13 Acknowledgments

Discussion complémentaire

Le chapitre 3 permet de répondre aux objectifs 1.1b (validation du modèle) et 1.2 (implications pratiques) de l'axe 1 de la thèse.

Le chapitre 3 a pour objectif partiel d'évaluer la validité du modèle non linéaire à grandes déformations développé au chapitre 2. Bien que l'application du modèle à une seule étude de cas ne représente pas une validation exhaustive, la précision des résultats apporte une certaine confiance quant à son utilisation. Le cas du pipeline d'Inuvik représente une occasion unique de valider le modèle, car il existe très peu de cas ou d'essais de consolidation au dégel aussi bien documenté pour lesquels les propriétés de sol sont complètement disponibles. Deux autres études expérimentales de consolidation au dégel auraient pu offrir des occasions intéressantes de validation du modèle (Morgenstern et Smith 1973, Nixon et Morgenstern 1974). Cependant, les propriétés des sols dégelés ne sont pas complètement caractérisées afin de permettre l'évaluation de la consolidation au dégel non linéaire. La validation du modèle à partir de ces données aurait donc nécessité de faire certaines estimations des propriétés et la validation aurait donc porté autant sur le modèle que sur la méthode d'estimation des propriétés. La caractérisation des propriétés des sols dégelés est discutée au chapitre 4 et une méthode de détermination empirique des relations $\sigma'_v - e - k_v$ des sols dégelés est présentée

au chapitre 5. L'utilisation de ces relations empiriques pour la validation du modèle à partir des données expérimentales de Morgenstern et Smith (1973) et de Nixon et Morgenstern (1974) aurait aussi constitué un processus de validation pour lequel deux composantes auraient été évaluées simultanément.

Deux implications théoriques du modèle non linéaire à grandes déformations sont présentées dans l'article. La section 3.8 reprend la discussion initiée au chapitre 2 quant à l'impact de considérer le tassement de la surface sur la définition de la vitesse de pénétration au dégel. Pour le cas du pipeline d'Inuvik, il est intéressant de pouvoir comparer les positions du front de dégel calculées par les approches à petites déformations et à grandes déformations avec la position réelle du front de dégel. La Figure 3.7 démontre que la pénétration du dégel est modélisée adéquatement par le modèle non linéaire à grandes déformations. La Figure 3.8a présente la pénétration du dégel utilisée pour le calcul des pressions interstitielles par la théorie de Morgenstern et Nixon. On constate que la profondeur de dégel telle que définie dans la théorie de consolidation au dégel à petites déformations est calculée en fonction de la position de la surface. Ainsi, le taux de pénétration au dégel utilisé pour le calcul des pressions interstitielles au front de dégel est défini à partir de la distance entre le front de dégel et la surface. Le tassement de la surface est donc soustrait à la profondeur réelle de pénétration du dégel qui doit être définie en fonction de la position initiale du sol.

Ensuite, la non-linéarité de la relation $\sigma_v' - e$ est discutée par rapport à la modélisation de la consolidation lors du dégel et durant la phase post-dégel à la section 3.9.2. Le taux de dissipation des pressions interstitielles lors de la consolidation dépend du gradient entre la contrainte effective et l'indice des vides. Ainsi, en considérant une relation linéaire (Figure 3.10) le taux de dissipation des pressions interstitielles lors de la phase post-dégel est surestimé. Aussi, la Figure 3.10 montre que les pressions interstitielles excédentaires pour une relation linéaire et une relation non linéaire sont différentes à un même indice des vides. Ainsi, pour les sols qui sont caractérisés par une relation $\sigma_v' - e$ non linéaire, le degré de consolidation défini en fonction des pressions interstitielles excédentaires n'est pas le même que le degré de consolidation défini en fonction des tassements. Les solutions analytiques de la théorie de Morgenstern et Nixon (1971) pour le degré de consolidation en fonction du tassement doivent donc être utilisées avec prudence, car elles ont été développées à partir des

pressions interstitielles excédentaires en suivant l'hypothèse de la théorie de Terzaghi d'un sol linéaire.

Un avantage important du modèle de consolidation au dégel non linéaire à grandes déformations est de réduire considérablement la subjectivité quant à l'analyse de la consolidation au dégel. Tout d'abord, les intrants du modèle non linéaire à grandes déformations peuvent être définis tels que déterminés par l'évaluation des conditions de terrain. Notamment, le profil d'indice des vides initial est implémenté à partir des données des forages et les relations $\sigma_v' - e - k_v$ telles que mesurées en laboratoire. En comparaison, la théorie de Morgenstern et Nixon utilise un coefficient de consolidation unique et homogène pour toute l'analyse. Ainsi, il est nécessaire de définir une valeur d'indice des vides initial unique et homogène pour calculer une valeur du coefficient de consolidation et à partir de laquelle la déformation au dégel et le tassement de fonte sont obtenus. De plus, les résultats obtenus avec le modèle non linéaire à grandes déformations n'ont pas à être modifiés de manière subjective. Toutes les quantités géotechniques d'intérêt peuvent être obtenues à l'aide des relations présentées au chapitre 2. En comparaison, les résultats de l'analyse de la théorie de Morgenstern et Nixon doivent être modifiés afin de représenter les conditions physiques réelles observées. Ces modifications sont décrites à la fin de la section 3.9 et à la Figure 3.8.

Comme mentionné dans l'article à la section 3.10, la validité de la théorie de Morgenstern et Nixon n'est pas remise en question. Cependant, il est recommandé de faire preuve de prudence quant à son utilisation lorsque les déformations sont très importantes et que les changements d'indice des vides sont suffisamment importants de telle sorte que la non-linéarité des propriétés des sols au dégel a un impact sur les résultats de calcul. Il est complexe de déterminer la plage de validité de la théorie linéaire à petites déformations. C'est pourquoi on peut faire appel au jugement de l'ingénieur géotechnicien afin de déterminer si la théorie de Morgenstern et Nixon est applicable ou s'il serait préférable de faire appel au modèle non linéaire à grandes déformations.

La théorie de Morgenstern et Nixon est très fonctionnelle en raison de sa simplicité, de l'élégance des solutions analytiques développées et des outils de calcul rapides à utiliser.

Dans tous les cas, la théorie de Morgenstern et Nixon peut donc être utilisée pour une évaluation préliminaire de la consolidation au dégel. Si les résultats démontrent qu'on a un problème non linéaire et/ou à grandes déformations, l'ingénieur a alors comme choix d'appliquer des corrections ou un facteur de sécurité aux valeurs obtenues à la lumière des observations émises au chapitre 2 et 3 quant à l'impact de la non-linéarité et des grandes déformations sur la consolidation au dégel. L'ingénieur a aussi le choix d'utiliser le modèle non linéaire à grandes déformations pour réaliser une analyse plus précise.

Certaines conditions peuvent justifier l'utilisation du modèle non linéaire à grandes déformations. Si le profil initial de teneur en glace du sol est complexe et que la profondeur de dégel est importante, comme c'est le cas pour le pipeline expérimental d'Inuvik, l'utilisation du modèle non linéaire à grandes déformations est très avantageuse, car il diminue la quantité de choix subjectifs que l'ingénieur doit faire quant aux intrants utilisés. Si les propriétés du sol sont bien connues, comme c'est le cas pour le pipeline expérimental d'Inuvik, les coûts de calcul ne sont pas prohibitifs à l'utilisation du modèle non linéaire à grandes déformations. En effet, les coûts associés à la détermination des propriétés du pergélisol sont alors largement supérieurs ce qui justifie l'utilisation d'une analyse plus complexe. Il est important de noter que le chapitre 5 présente des relations empiriques qui permettent de déterminer les relations $\sigma'_v - e - k_v$ des sols dégelés.

Dans tous les cas, certains coûts sont associés à la première utilisation du modèle non linéaire à grandes déformations au sein d'une organisation en raison de l'implémentation numérique initiale et de l'achat d'un outil de calcul numérique. L'utilisation d'un ordinateur de calcul est recommandée et l'achat d'un logiciel de calcul tel que COMSOL est aussi nécessaire. Cependant, l'utilisation du modèle est très facile et rapide suite à l'implémentation initiale. Tel que mentionné dans la discussion complémentaire au chapitre 2, il est aussi possible de simplifier la composante thermique du modèle afin de grandement réduire les coûts de calcul. Cette approche peut être particulièrement intéressante pour l'étude d'infrastructures linéaires. La conception de ce type d'infrastructure peut nécessiter d'effectuer un très grand nombre de modélisations. Les coûts associés à l'implémentation initiale peuvent alors être compensés par les économies réalisées par l'augmentation de la précision des résultats sur chacune des sections évaluées.

Dans ce chapitre, les résultats de modélisation du pipeline d'Inuvik du modèle de consolidation non linéaire à grandes déformations introduit au chapitre 2 sont comparés seulement avec ceux obtenus avec la théorie de Morgenstern et Nixon alors ils auraient aussi pu être comparés à ceux obtenus avec d'autres modèles de consolidation au dégel existants (Sykes et coll. 1974, Foriero et Ladanyi 1995, Qi et coll. 2013). Le but premier de cette comparaison n'est pas de démontrer que l'approche proposée est supérieure à une autre, mais plutôt de démontrer les différences fondamentales entre les deux approches donc l'impact de la non-linéarité et l'impact des grandes déformations sur le processus de consolidation au dégel. De plus, il existe des lacunes dans le fondement théorique des autres modèles de consolidation au dégel existants comme discuté au chapitre 1. Ainsi, il aurait été ardu d'offrir une comparaison objective avec ces modèles, car il aurait fallu discerner l'impact des lacunes théoriques sur les résultats obtenus. Le choix de comparer les résultats seulement avec la théorie de Morgenstern et Nixon reflète l'état des connaissances et l'état de la pratique actuels en ce qui concerne la consolidation au dégel.

Choix des paramètres de modélisation

Les choix concernant certains paramètres de modélisation sont maintenant discutés. Tout d'abord, des conditions de drainage libre sont utilisées comme conditions limites à l'interface entre le silt et le till lorsque le front de dégel atteint le till et que le till est dégelé. L'analyse des résultats expérimentaux indique que le front de dégel forme une cuvette lorsque le dégel pénètre dans la couche de till. Ainsi, on ne peut s'attendre à avoir un écoulement d'eau vers le bas de la couche de till comme le suggèrent des conditions de drainage libre. Cependant, on assume que la conductivité hydraulique du till est largement supérieure à celle du silt dégelé. Ainsi, il y a une redistribution de l'eau de fonte à l'interface entre ces deux couches du silt vers le till. Il y a donc dissipation des pressions interstitielles à l'interface ce qui justifie l'utilisation d'une condition de drainage libre. De plus, les données de terrain indiquent que la génération de pressions interstitielles dans la couche de till est minime ce qui appuie l'approche utilisée pour la modélisation.

Ensuite, le profil d'indice des vides initial est définie entre les deux valeurs d'indice des vides extrêmes des échantillons. Cette approche a été adoptée afin de ne modéliser le silt qu'à l'intérieur de la gamme de valeur d'indice des vides dont les propriétés sont disponibles. Le

profil d'indice des vides initial modéliser est ainsi représentatif des conditions de sol alors qu'il est défini entre ces deux valeurs extrêmes.

Chapitre 4 Conceptual Model for Thaw Consolidation of Fine-Grained Soils

Avant-propos

Titre français

Modèle conceptuel pour la consolidation au dégel des sols à grains fins

4.1 Résumé français

Un modèle conceptuel pour la consolidation au dégel des sols à grains fins est proposé. Le développement du modèle se base sur la définition générale de la consolidation à grandes déformations et sur le comportement général des sols lors du dégel. La contrainte résiduelle et la courbe de contrainte résiduelle sont utilisées comme des éléments centraux du modèle. Le concept de la contrainte effective est généralisé aux sols riches en glace en spécifiant que la contrainte résiduelle est la contrainte effective au sein des éléments de sol lors du dégel plutôt que la contrainte effective du sol global. La courbe de contrainte résiduelle qui donne la relation entre la contrainte résiduelle et l'indice des vides du sol dégelé est considérée comme étant une propriété intrinsèque du sol. Le modèle conceptuel est formulé en fonction des relations $\sigma_v' - e - k_v$. Les déformations des sols pauvres en glace sont décrites par une relation semi-logarithmique linéaire entre la contrainte effective et l'indice des vides. La pente de la relation $\log \sigma_v' - e$ est donnée par l'indice de compression du sol dégelé. Pour les sols riches en glace, une relation bilinéaire $\log \sigma_v' - e$ est adoptée. Premièrement, le drainage de l'eau de fonte en excès se produit sans compression du squelette de sol. Ensuite, l'eau est expulsée en raison de la compression du squelette du sol de manière équivalente à un sol pauvre en glace. La relation $e - k_v$ des sols dégelés à grains fins est définie par une relation semi-logarithmique linéaire avec une pente définie par l'indice de changement de la conductivité hydraulique du sol dégelé. Le modèle conceptuel proposé peut être utilisé pour définir les propriétés utilisées comme intrant pour la modélisation numérique de la consolidation au dégel.

4.2 Abstract

A conceptual model for thaw consolidation of fine-grained soils is proposed. The development of the model is based on the general definition of large-strain consolidation and

on the general behaviour of soils upon thawing. The residual stress and the residual stress curve are used as a backbone to the conceptual model. The concept of the residual stress is generalized to ice-rich soils by specifying that the residual stress is the effective stress within the soil elements upon thawing rather than the effective stress in the bulk soil. The residual stress curve which gives the relationship between the thawed void ratio and the residual stress is considered as an intrinsic soil property. The conceptual model is formulated in terms of $\sigma_v' - e - k_v$ relationships. The volume change behaviour of ice-poor soils is described by a semi-logarithmic linear $\sigma_v' - e$ relationship. The slope of the $\log \sigma_v' - e$ relationship is given by the compression index of the thawed soil. For ice-rich soils, a bilinear $\log \sigma_v' - e$ relationship is adopted. First, drainage of the excess water occurs with no compression of the soil skeleton. Then, water is drained out of the soil upon compression of the soil skeleton in an ice-poor equivalent manner. The $e - k_v$ relationship of thawed fine-grained soils is defined by a semi-logarithmic linear curve with a slope defined by the hydraulic conductivity change index of the thawed soil. The proposed conceptual model can be used to define the properties used as input for the numerical modelling of thaw consolidation.

4.3   Introduction

Several thaw consolidation models have been formulated to evaluate the evolution of thaw settlements and of excess pore water pressures developing upon thawing of a frozen soil (Zaretskii 1968, Morgenstern and Nixon 1971, Foriero and Ladanyi 1995, Qi et al. 2013, Dumais and Konrad 2018). Yet, limited attention has been given to the characterization of the hydro-mechanical properties for the specific state path experienced by thawing soils. The engineering assessment of consolidation upon thawing usually requires two governing parameters: the hydraulic conductivity of the thawed soil and the relationship between volume change and applied stress.

Specifically, previous studies have demonstrated the importance of:

1) the stress conditions at the onset of thawing (Nixon and Morgenstern 1973a);

2) the relationship between the effective stress and the void ratio of the thawed soil (Nixon and Morgenstern 1973b, Dumais and Konrad 2018, 2019);

3) and the relationship between the void ratio and the hydraulic conductivity of the thawed soil (Dumais and Konrad 2018, 2019).

It is thus warranted to carry out a comprehensive investigation of the properties of thawed fine-grained soils and their implementation in an engineering approach for thaw consolidation.

The objective of this paper is to present a conceptual model for thaw consolidation in terms of the relationships between the effective stress, the void ratio and the hydraulic conductivity of thawed fine-grained soils. The development of the model is based on the theoretical analysis of large-strain consolidation and on the general behaviour of thawing soils. The concept of the residual stress previously defined for ice-poor soils is generalized for ice-rich soils such that it can be used as the backbone of the conceptual model. Thaw consolidation experimental results from the literature are interpreted using the model with a special attention for the interpretation of ice-rich soils. The use of the conceptual model for the determination of the properties used as input in engineering practice for the assessment of thaw settlement is discussed. Finally, the conceptual model interpretation of freeze-thaw cycling experimental results is presented.

4.4 Background

4.4.1 General Definition of the Consolidation Properties of Thawing Soils

In order to provide a general definition of the relationships which characterize the hydraulic conductivity and the volume change behaviour of thawing soils, one can use the following equation which describes large-strain consolidation (Gibson et al. 1981, Dumais and Konrad 2018):

$$\textit{Equation 4-1} \qquad \frac{d}{de}\left[\frac{k_v(e)(G_s-1)}{1+e}\right]\frac{\partial e}{\partial a} + \frac{1}{\gamma_w}\frac{\partial}{\partial a}\left[-\frac{k_v(e)(1+e_f)}{1+e}\frac{d\sigma_v'(e)}{de}\frac{\partial e}{\partial a}\right] = \frac{1}{1+e_f}\frac{\partial e}{\partial t}$$

where e is the void ratio of thawing soil, e_f is the frozen void ratio, a is depth in Lagrangian coordinates, G_s is the specific gravity of the solid particles, γ_w is the unit weight of water, k_v is the vertical hydraulic conductivity of the thawed soil and σ_v' is the vertical effective stress.

As seen in Equation 4-1, the consolidation of thawing soils is governed by the relationships between the effective stress and the void ratio, $\sigma'_v(e)$; and between the hydraulic conductivity and the void ratio, $k_v(e)$. It is convenient to use the void ratio as the state variable in concordance with the formulation of Equation 4-1 to allow for consideration of the changes of the soil properties as consolidation proceeds and soil deformations occur (Dumais and Konrad 2018).

It should be noted that the coefficient of consolidation has also been widely used for thaw consolidation modelling (Zaretskii 1968, Morgenstern and Nixon 1971). The coefficient of consolidation for thawed soils is defined as:

Equation 4-2 $\quad c_v = -\dfrac{(1+e_f) \cdot k_v}{\gamma_w \cdot \frac{de}{d\sigma'_v}}.$

As seen in Equation 4-2, the coefficient of consolidation combines the hydraulic conductivity, k_v, and the compressibility, *de/dσv'*, in a single coefficient. A constant coefficient of consolidation is typically used for thaw consolidation modelling such that changes in soil properties are not accounted for (Morgenstern and Nixon 1971, Morgenstern and Smith 1973, Dumais and Konrad 2018). Furthermore, a unique value of the coefficient of consolidation is used for modelling both the thaw consolidation and the post-thaw consolidation phases based on the assumption that the relationship between the effective stress and the void ratio is linear (Nixon 1973). An analysis of the Inuvik experimental pipeline demonstrated that this assumption may not be applicable to soils undergoing large thaw strain (Dumais and Konrad 2019).

Moreover, it is convenient to adopt separate generalized functions $\sigma'_v(e)$ and $k_v(e)$ which allows for a more flexible and accurate definition of the behaviour of thawing soils. Advantageously, the stand-alone $\sigma'_v(e)$ relationship can be used for more accurate calculation of the thaw settlement (Dumais and Konrad 2019) which is not always possible when the relationship between the effective stress and the void ratio is an integral part of the coefficient of consolidation.

We are thus seeking to propose a conceptual model for the determination of the $\sigma'_v(e)$ and $k_v(e)$ relationships for thawing fine-grained soils.

4.4.2 Description of the Behaviour of Thawing Soils

The physical processes occurring upon freezing and thawing of a fine-grained soil are now analyzed. Although the conceptual model developed herein aims at characterizing only the behaviour upon thawing, the analysis of the mechanisms acting on the soil upon freezing is key to gain insights into the factors controlling the state path of the soil upon thawing. Mostly, this theoretical example will allow to define the stress conditions existing in the soil skeleton at the onset of thawing in terms of the concept of the residual stress σ_0' introduced by Morgenstern and Nixon (1971). Figure 4.1 presents schematic representations of the state paths of soils subjected to (a) closed-system freezing and thaw consolidation; and (b) open-system freezing and thaw consolidation.

4.4.2.1 Closed-System Freezing

Figure 4.1a presents the theoretical behaviour of a soil subjected to closed-system freeze-thaw cycling. An unfrozen consolidated soil is located at point A at a known stress P_0 on the virgin compression line of the unfrozen soil. A constant external stress P_0 is applied on the soil throughout freezing and thawing. The soil is frozen in closed-system conditions, i.e., there is no access to external water upon freezing. During freezing, an increasing portion of the pores is filled with ice as temperature decreases. The unfrozen water in the soil is then in contact with ice such that it is in a state of suction according to the laws of thermodynamics. The soil elements are thus locally subjected to an effective stress greater than the external stress P_0 which leads to further consolidation as represented by the path from point A to point B.

Since the total volume of water in the soil remains unchanged in closed-system freezing, discrete ice features form in between the overconsolidated soil elements. An overall increase in volume to point A_f upon freezing is attributable to the volumetric expansion of water to ice during phase change.

(a) CLOSED-SYSTEM FREEZING ; $e_f = 1.09 e_A$
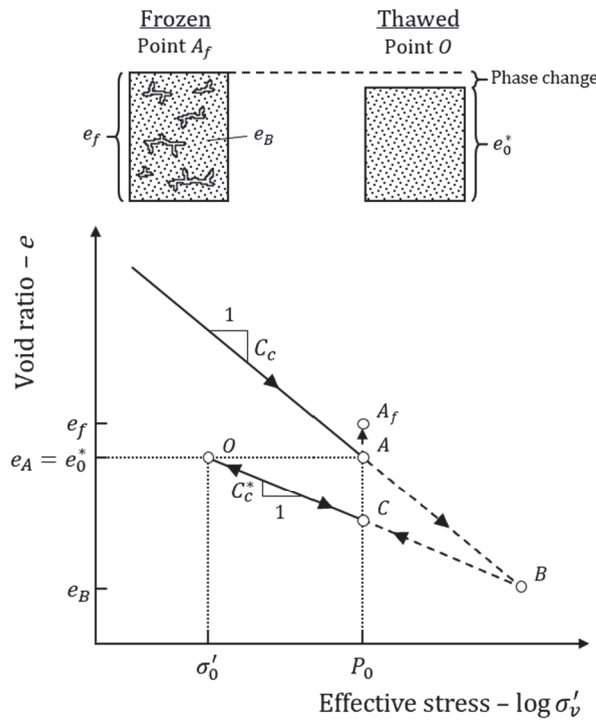
(b) OPEN-SYSTEM FREEZING ; $e_f > 1.09 e_A$
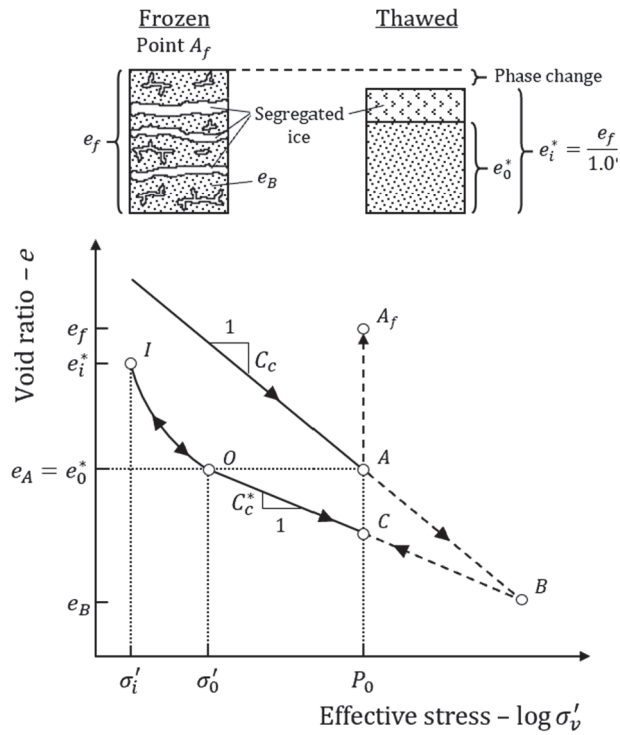
Figure 4.1 : Freezing and thaw consolidation of fine-grained soils

The soil is now thawed in undrained conditions. The overconsolidated soil elements swell as the melt water from the discrete ice features is absorbed. Swelling of the soil elements is defined along the state path from point B to point O. If the soil elements can absorb all the available melt water, the soil thawed in undrained conditions swells to point O. The effective stress in the soil skeleton at point O is called the residual stress σ_0'. If drainage is permitted, the soil which is still subjected to an external stress P_0, consolidates along the compression curve defined between point O and point C.

Globally, the entire process of closed-system freezing followed by thaw consolidation under a constant external stress P_0 is characterized by a bulk void ratio increase from point A to point A_f upon freezing followed by a bulk void ratio decrease from point A_f to point C upon thawing. Conversely, the state path followed by the soil elements at a local scale is described by overconsolidation from point A to point B upon freezing followed by swelling upon thawing to point O and consolidation to point C. Ultimately, it is the state path followed by the soil elements that controls the thaw consolidation behaviour and the bulk void ratio decrease upon thawing.

4.4.2.2 Open-System Freezing

Figure 4.1b presents the theoretical behaviour of a soil subjected to open-system freeze-thaw cycling. An unfrozen consolidated soil located at point A at a known stress P_0 on the virgin compression line of the unfrozen soil is again considered. The soil is now frozen with access to external water. As described previously, the unfrozen water in the soil is in a state of suction as temperature decreases since it is in contact with the ice gradually filling the pores of the soil. Since drainage is now allowed, water is drawn to the freezing front under the action of the suction forces which leads to the formation of segregated ice in the form of ice lenses. Consequently, the soil elements found in between the ice lenses are effectively in closed-system conditions as the ice lenses act as impermeable barriers. As temperature continues to decrease, the soil elements in between the ice lenses are locally subjected to an effective stress greater than the external stress P_0 which leads to further consolidation as represented by the path from point A to point B.

In open-system freezing, the access to external water leads to ice segregation. The increase in volume to point A_f upon freezing thus exceeds the volumetric expansion resulting from the freezing of the pore water initially present in the unfrozen soil.

The soil is now thawed in undrained conditions. The overconsolidated soil elements first absorb the free melt water available locally, i.e., the melt water from the discrete ice features created as a result of overconsolidation. Swelling of the soil elements is then defined along the state path from point B to point O. However, there is water in excess of the amount that the soil skeleton can absorb at the residual stress σ_0' due to ice segregation upon freezing. When thawed in undrained conditions, the excess melt water from the ice lenses is distributed among the bulk sample which reaches point I upon thawing. The effective stress in the bulk soil at point I, σ_i', can be infinitely small if the soil contains much excess water. If drainage is later permitted, the soil which is still subjected to an external stress P_0 consolidates to point C.

The state path followed by a soil with excess melt water thawed in drained conditions is best characterized in terms of the behaviour of the overconsolidated soil elements as illustrated in Figure 4.2. In effect, it is the overconsolidated soil elements that controls the thaw consolidation behaviour. The soil elements are only able to absorb a finite volume of melt water as they swell to point O. The effective stress sustained by the soil skeleton at point O is the residual stress σ_0'. When a frozen soil is thawed in drained conditions under a load $P_0 > \sigma_0'$, the melt water in excess is not absorbed by the soil skeleton. Upon thawing, the excess water is thus drained out of the bulk soil without compression of the soil skeleton. The effective stress in the soil elements upon drainage of the excess water remains at the residual stress. When the soil is free of all excess water, additional compression occurs as water is expelled out of the soil skeleton for $\sigma_v' > \sigma_0'$.
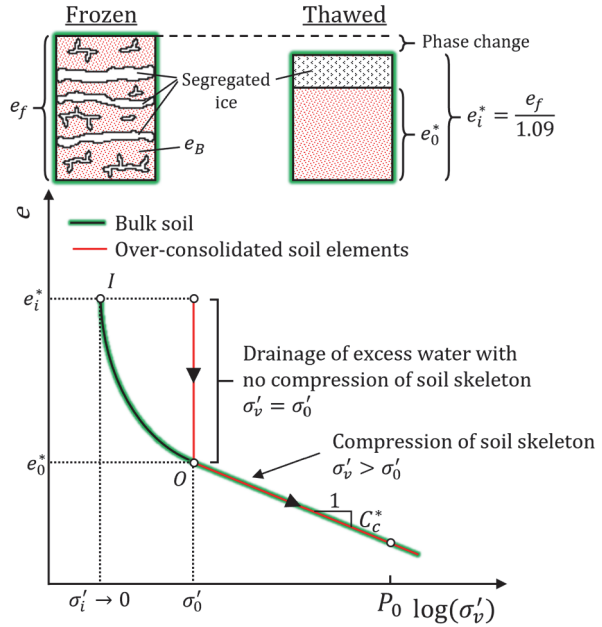
Figure 4.2 : Thaw consolidation of fine-grained soils with excess water

The objective of this chapter is to characterize the state path followed by the soil upon thawing. For the soil illustrated in Figure 4.1a, the state path of interest must be defined from point O to point C. For the soil illustrated in Figure 4.1b and Figure 4.2, the state path of interest must be defined from point I to point O and to point C.

4.4.3 Thaw Consolidation Terminology

Some of the terminology used in this paper is now presented. The residual stress σ_0' is defined as the effective stress that the soil skeleton can sustain when thawed in undrained conditions. In order to generalize the concept of the residual stress to soils with excess water, it is important to emphasize that the effective stress within the soil elements is considered for defining the residual stress rather than the effective stress of the bulk soil. This distinction is shown in Figure 4.2. While the overall effective stress in the bulk soil, σ_i', may approach zero, the effective stress in the soil elements, σ_0', remains significant. This definition is in theoretical agreement with the definition of the residual stress given by Nixon and Morgenstern (1973a). However, it is noted that some of the practical interpretations of the residual stress made by Nixon and Morgenstern (1973a) may not conform to the definition adopted herein. Mostly, Nixon and Morgenstern (1973a) measure the effective stress of the

bulk soil to determine the residual stress of a soil. This will be discussed in detail in the next sub-section of this chapter.

The state of the soil at the residual stress is called the thawed state (point O in Figure 4.1a and Figure 4.1b). At the thawed state, the amount of water that the soil skeleton can hold in its pores is characterized by the thawed void ratio e_0^*. Superscript * is used throughout this paper to indicate the properties of the thawed soil in contrast with the properties of the unfrozen soil.

The state of the soil thawed in undrained conditions is generally called the initial thawed state (point O in Figure 4.1a and point I in Figure 4.1b). At the initial thawed state, the amount of water in the bulk soil is characterized by the initial thawed void ratio e_i^*. In its frozen state, the void ratio of the soil is the frozen void ratio e_f (point A_f in Figure 4.1a and Figure 4.1b). Volume changes from the frozen state to the initial thawed state are only due to phase change from ice to water. In saturated soils, the initial thawed void ratio e_i^* is thus related to the frozen void ratio e_f as:

Equation 4-3 $e_i^* = \frac{e_f}{1.09}$.

For soils that do not contain melt water in excess of the amount that the soil skeleton can hold at the residual stress, the initial thawed state is the same as the thawed state (point O in Figure 4.1a), i.e., $e_0^* = e_i^*$. However, the initial thawed state of a soil with excess melt water (point I in Figure 4.1b and Figure 4.2) differs from its thawed state (point O in Figure 4.1b and Figure 4.2), i.e., $e_i^* > e_0^*$.

Soils with no excess melt water are referred to as ice-poor soils. The typical behaviour of an ice-poor soil upon thawing is illustrated in Figure 4.1a. Conversely, soils with excess melt water are referred to as ice-rich soils. The typical behaviour of an ice-rich soil upon thawing is illustrated in Figure 4.1b and Figure 4.2. Herein, ice-poor and ice-rich soils are differentiated by their respective behaviour upon thawing rather than in terms of the presence of discrete ice features. Ice-poor soils may contain discrete ice features resulting from the overconsolidation of the soil elements (Nixon and Morgenstern 1973a).

4.4.4 Residual Stress

The concept of the residual stress introduced in the previous sections can now be examined in more detail. The most complete theoretical and laboratory study of the residual stress to date was undertaken by Nixon and Morgenstern (1973a). The concept of the residual stress was later successfully applied as a basis for the development of a framework to predict the hydraulic conductivity changes of fine-grained soils upon freeze-thaw cycling (Konrad and Samson 2000a). More recently, the general applicability of the residual stress for thaw consolidation modelling and its practical relevance were reasserted by Dumais and Konrad (2018 and 2019).

To determine the factors controlling the effective stress conditions in the soil skeleton upon thawing, Nixon and Morgenstern (1973a) measured the residual stress of three different fine-grained soils over a range of initial ice contents. The residual stress is measured by allowing frozen samples to thaw in undrained conditions in a modified oedometer cell. The load applied on the sample during thawing is continuously adjusted such that no excess pore water pressures develop in the sample. Upon completion of thawing, the excess pore water pressure is null, and the load applied on the sample gives the value of the residual stress. The void ratio at the residual stress, the thawed void ratio, is determined for each test. The relationship between the residual stress and the thawed void ratio for a given soil can be determined by testing samples with different initial ice contents. Furthermore, thawed samples can be consolidated and refrozen in the oedometer cell to subsequently measure the residual stress of samples of the same soil subjected to different stress and thermal histories.

As mentioned previously, the effective stress measured by the experimental method used by Nixon and Morgenstern (1973a) is the effective stress in the bulk sample rather than the effective stress within the soil elements. According to the generalized definition of the residual stress adopted herein, this method is only applicable for ice-poor soils. Experimental determination of the residual stress of ice-rich soils would require the measurement of the effective stress at a local scale within the soil elements which is experimentally impractical. This must be taken into account for the interpretation of the experimental results reported by Nixon and Morgenstern (1973a). The determination of the residual stress of ice-rich soils from thaw consolidation test data will be discussed later in this chapter.

Figure 4.3 presents the relationships between the residual stress and the thawed void ratio for undisturbed and refrozen Norman Wells silt, reconstituted Athabasca clay and reconstituted Mountain River clay. The most notable difference between the three investigated soils is the approach used to determine the residual stress of soils with different initial ice content. Indeed, samples of the three soils were subjected to different thermal and stress histories. For the Athabasca clay, two remoulded samples were subjected to freeze-thaw cycling under different loading conditions. The residual stress was measured for each thawing sequence. For specimen A4, the load was increased after each thawing sequence before refreezing and thawing. For specimen A6, the freezing and thawing cycles were undertaken under a constant applied load for all tests. For the Mountain River clay, two remoulded samples were subjected to different consolidation and freeze-thaw cycling sequences. For both samples, the applied load was increased before each subsequent freezing sequence. For the Normal Wells silt, the residual stress of four undisturbed frozen permafrost samples was measured. The visible discrete ice contents of the samples varied from 5 to 10%. The samples were then consolidated under incremental loading and subjected to one freeze-thaw cycle to measure the residual stress of the refrozen soil.

As noted earlier, the effective stress measured upon thawing in undrained conditions by Nixon and Morgenstern (1973a) is the effective stress within the bulk sample. According to the generalized definition of the residual stress adopted herein, this value is only equal to the residual stress for ice-poor soils. For ice-rich soils, the effective stress of the bulk sample upon thawing in undrained conditions is expected to be infinitely small (Nixon and Morgenstern 1973a). Since the effective stress values presented in Figure 4.3 are large enough to be measured, it can be assumed that the residual stress as generally defined for ice-rich and ice-poor soils was measured. In fact, the effective stress of two tested samples were too small to be measured (Nixon and Morgenstern 1973a). One was an Athabasca clay sample with a high frozen void ratio. Most notably, the other was an undisturbed permafrost Norman Wells silt sample with a visible ice content of 25 %. This sample can thus be considered ice-rich. In comparison, the other undisturbed permafrost Norman Wells silt samples can be considered ice-poor even though they contained 5 to 10 % of visible ice. This confirms the hypothesis introduced previously, according to which ice-poor soils may

contain appreciable discrete ice features. The distinction between ice-poor and ice-rich soils should thus not be made in terms of the visible ice content.

4.4.4.1 Residual Stress Curve
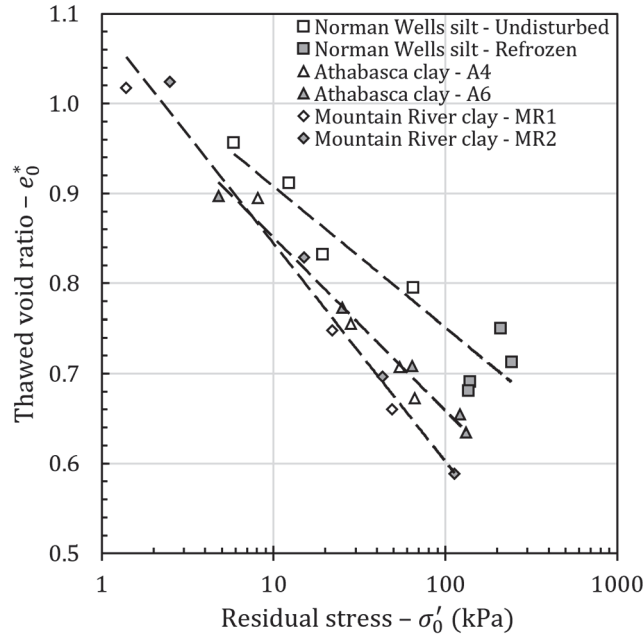
Figure 4.3 : Residual stress curves of undisturbed and refrozen Norman Wells silt, reconstituted Athabasca Clay and reconstituted Mountain River Clay (data from Nixon and Morgenstern 1973a)

Figure 4.3 shows that the relationship between the thawed void ratio and the residual stress for each of the three investigated soils is given by a unique semi-logarithmic curve (Nixon and Morgenstern 1973a). This relationship is called the residual stress curve. The results presented in Figure 4.3 suggest that the residual stress curve is unique for a given soil composition. Based on the limited experimental evidence available in the literature, it appears that the residual stress curve is independent of the thermal and stress histories (Nixon and Morgenstern 1973a). In the current study, the residual stress curve is thus considered an intrinsic property of a soil. For thaw consolidation analysis, the residual stress curve gives the initial conditions for the compressibility behaviour in terms of the thawed void ratio e_0^* and of the residual stress σ_0'. The practical implication of considering the residual stress curve as an intrinsic property is that the residual stress can be obtained for any thawed void ratio value if the residual stress curve of the soil is known. The factors controlling the characteristics of the residual stress curve will be analyzed in Chapter 5 of this thesis. The

link between the residual stress curve and the residual stress of ice-rich and ice-poor soils will also be discussed in Chapter 5.

4.5 Conceptual Model for Thaw Consolidation

A conceptual model for thaw consolidation of fine-grained soils formulated in terms of $\sigma_v' - e - k_v$ relationships can be proposed based on the description of the general behaviour upon thawing hitherto described. Figure 4.4 presents the proposed conceptual model. The void ratio – hydraulic conductivity relationship of thawed soils is introduced in Figure 4.4 in complement to the effective stress – void ratio relationship already discussed. The conceptual model adopts distinct compatible definitions for ice-rich and ice-poor soils.
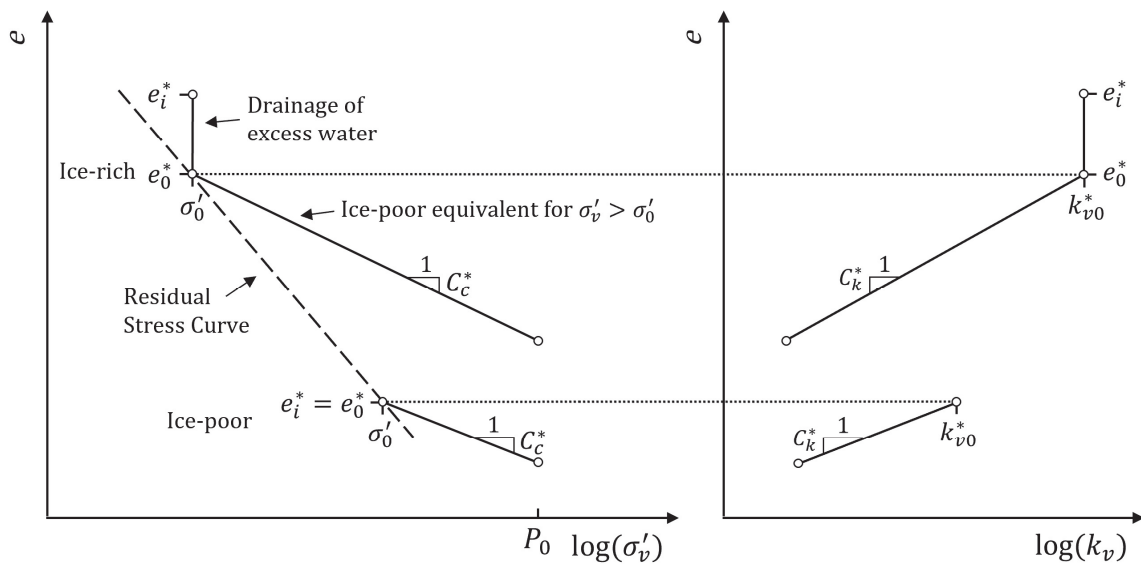
Figure 4.4 : Conceptual model for thaw consolidation of fine-grained soils

The residual stress curve is used as the backbone for the conceptual model based on the principle that it is an intrinsic soil property. The residual stress curve is represented as a dashed line in Figure 4.4 to emphasize that it does not represent a state path followed by the soil. Rather, it gives the initial conditions for the compressibility behaviour in terms of the relationship between the thawed void ratio e_0^* and the residual stress σ_0'.

The conceptual model describes the $\sigma_v' - e - k_v$ relationships after phase change has occurred. For the development of the conceptual model, it is assumed that phase change occurs

instantly. The relationships are thus described from the initial thawed void ratio e_i^* which is directly related to the frozen void ratio e_f according to Equation 4-3.

For ice-poor soils, the initial void ratio e_i^* is equal to the thawed void ratio e_0^*. Upon thawing, the soil is thus located on the residual stress curve at the residual stress σ_0'. The hydraulic conductivity of the soil at the thawed void ratio is the initial hydraulic conductivity of the thawed soil k_{v0}^*.

It is generally accepted that the $\sigma_v' - e$ relationship of thawed fine-grained soils is nonlinear over the range of stresses of practical interest. The $\sigma_v' - e$ relationship for stresses higher than the residual stress can be described by a semi-logarithmic linear relationship with a slope given by the compression index of the thawed soil C_c^* (Konrad 2010, Konrad and Samson 2000a). The $\sigma_v' - e$ relationship of ice-poor soils for $\sigma_v' > \sigma_0'$ is mathematically given by:

Equation 4-4 $(e - e_0^*) = -C_c^* log\left(\frac{\sigma_v'(e)}{\sigma_0'}\right).$

Changes in void ratio induce changes in the hydraulic conductivity of the thawed soil. From the initial hydraulic conductivity of the thawed soil k_{v0}^*, changes in hydraulic conductivity can be described by a single semi-logarithmic linear relationship with a slope given by the hydraulic conductivity change index of the thawed soil C_k^* (Konrad and Samson 2000a). The $e - k_v$ relationship is given by:

Equation 4-5 $(e - e_0^*) = C_k^* log\left(\frac{k_v(e)}{k_{v0}^*}\right).$

For ice-rich soils, the initial void ratio e_i^* is larger than the thawed void ratio e_0^* due to the excess melt water. As described previously, the thaw consolidation behavior of ice-rich soils is governed by the overconsolidated soil elements. Upon thawing, excess water drains out of the bulk soil with no compression of the soil skeleton. The effective stress remains equal to the residual stress in the soil elements. After drainage of the excess water, the soil reaches the residual stress curve. Additional void ratio reduction is achieved through compression of the soil skeleton for applied stresses higher than the residual stress. The $\sigma_v' - e$ relationship is then said to be ice-poor equivalent such that it can be described by Equation 4-5. The complete $\sigma_v' - e$ relationship of ice-rich soils is given by:

Equation 4-6 $for\ e_i^* < e < e_0^*$ $\sigma_v'(e) = \sigma_0'$,

$$for\ \sigma_v'(e) \geq \sigma_0' \qquad (e - e_0^*) = -C_c^* \log\left(\frac{\sigma_v'(e)}{\sigma_0'}\right).$$

The bulk vertical hydraulic conductivity of the soil during drainage of the excess water is controlled by the soil elements. Since the soil elements are then at the residual stress, the hydraulic conductivity of the soil elements is equal to the initial hydraulic conductivity of the thawed soil k_{v0}^*. Between e_i^* to e_0^*, the hydraulic conductivity of the bulk soil remains at k_{v0}^*. For void ratio values lower than e_0^*, the ice-poor equivalent $e - k_v$ relationship is adopted. The complete $e - k_v$ relationship of ice-rich soils is thus given by:

Equation 4-7 $for\ e_i^* < e < e_0^*$ $k_v(e) = k_{v0}^*$,

$$for\ e < e_0^* \qquad (e - e_0^*) = C_k^* \log\left(\frac{k_v(e)}{k_{v0}^*}\right).$$

4.6   Typical Experimental σ'ᵥ – e – kᵥ Relationships

The proposed conceptual model for thaw consolidation of fine-grained soils is now applied to experimental thaw consolidation data from the literature. Selected experimental relationships are analyzed to describe the characteristics of the $\sigma_v' - e - k_v$ relationships.

4.6.1 Ice-Poor Soils

The $\sigma_v' - e - k_v$ relationships of selected ice-poor soils are presented in Figure 4.5. The relationships are defined over a range of effective stress larger than the residual stress, $\sigma_v' > \sigma_0'$. The experimental data points are represented by full symbols. Empty symbols represent the thawed state as interpreted by the conceptual model. The residual stress and the initial hydraulic conductivity are obtained from the experimental relationship at the thawed void ratio. Since the soils presented in Figure 4.5 are ice-poor, the thawed void ratio is equal to the initial void ratio.

The behaviour of the soils presented in Figure 4.5 agrees with the theoretical behaviour described by the conceptual model. The $\sigma_v' - e$ and the $e - k_v$ relationships are both appropriately characterized by semi-logarithmic linear relationships with the initial conditions given at the residual stress. The soils presented in Figure 4.5 have different compositions such that their complete residual stress curve is not determined.
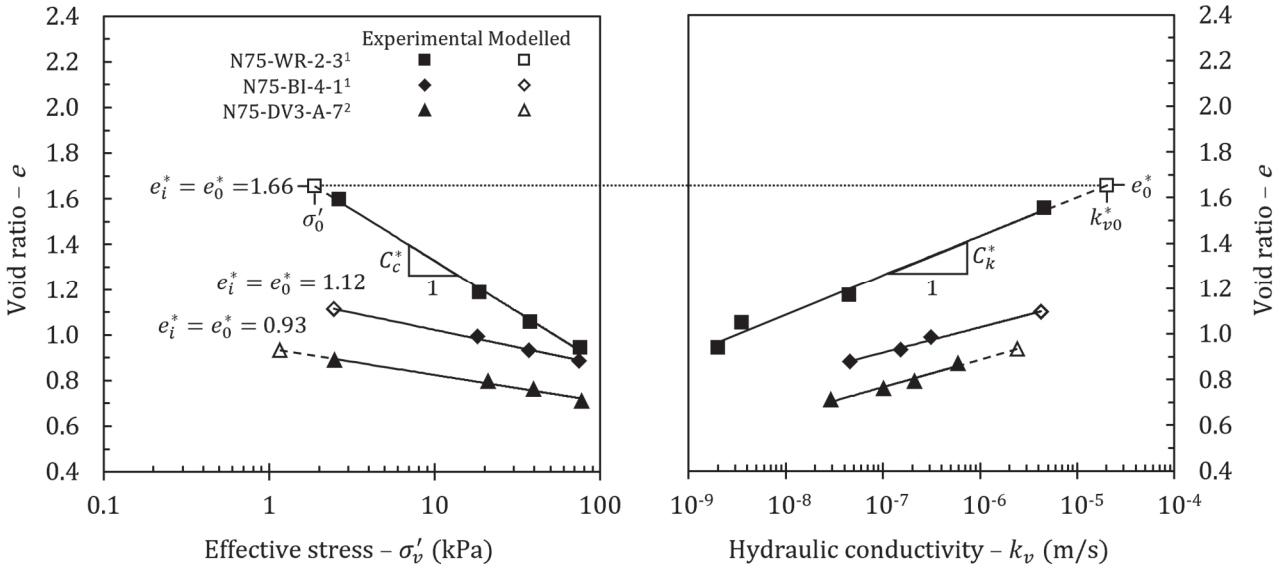
Figure 4.5 : Properties of selected thawed ice-poor fine-grained soils for σ'ᵥ > σ'₀ (NESCL 1977a[1] and 1977b[2])

4.6.2 Ice-Rich Soils

The analysis of the experimental relationships of ice-rich soils is generally more complex than for ice-poor soils. Since the thawed void ratio of ice-rich soils is not equal to the initial thawed void ratio, the value of the residual stress may not be given directly by the experimental $\sigma'_v - e$ as it is the case for ice-poor soils. As discussed earlier, the residual stress of the soil elements of ice-rich soils can also not be measured directly by the experimental methods described by Nixon and Morgenstern (1973a). In order to define the $\sigma'_v - e - k_v$ relationships as defined by the proposed conceptual model, the value of the residual stress must be determined. Two approaches are now being discussed to define the complete $\sigma'_v - e - k_v$ relationships of ice-rich soils from experimental thaw consolidation data.

The first approach to define the modelled $\sigma'_v - e - k_v$ relationships of ice-rich soils is schematized in Figure 4.6 and exemplified in Figure 4.7. In this approach, the experimental relationships are completed by selecting the value of residual stress from which the thawed void ratio and the initial hydraulic conductivity can be obtained.

120
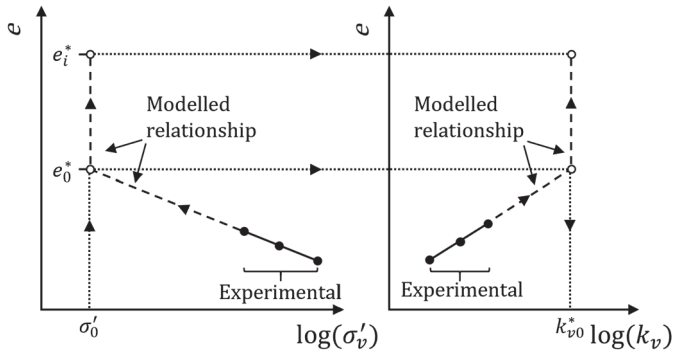
Figure 4.6 : Modelled relationships for ice-rich soils with a selected residual stress value
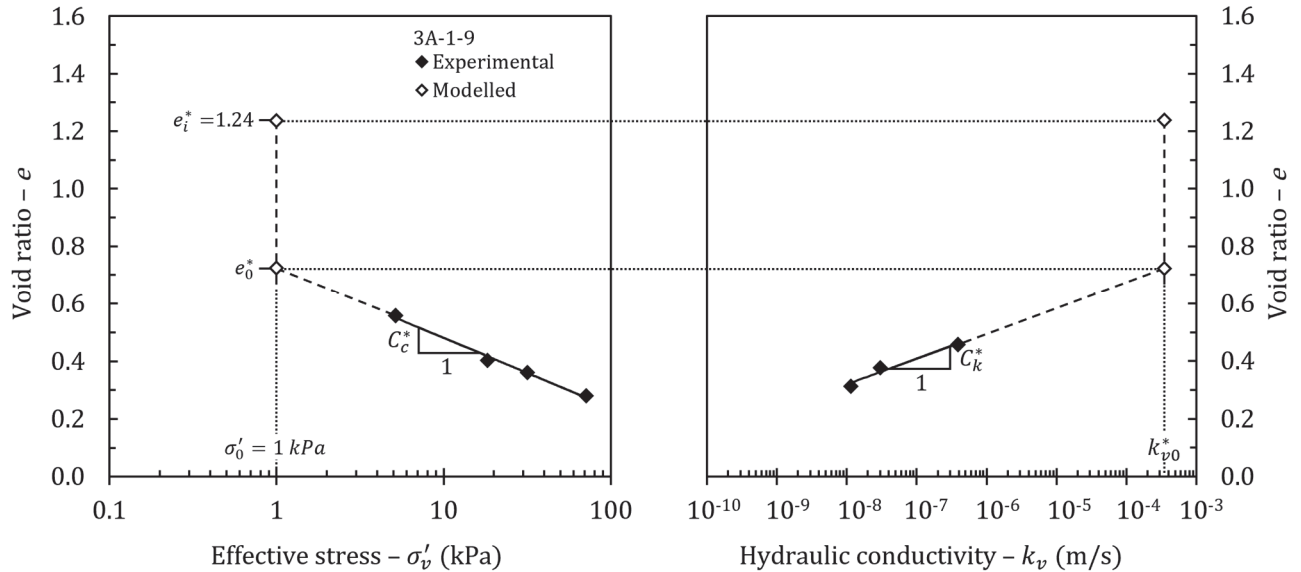
Figure 4.7 : Properties of a thawed ice-rich fine-grained soils with a selected residual stress value (NESCL 1976) (see Figure 4.6)

At first glance, the experimental $\sigma'_v - e$ relationship of Sample 3A-1-9 represented in Figure 4.7 as a solid line appears similar to the $\sigma'_v - e$ relationships of ice-poor soils presented in Figure 4.5. Indeed, the $\sigma'_v - e$ experimental curve is characterized by a semi-logarithmic linear relationship. The difference is that it is possible to obtain the residual stress of the soils in Figure 4.5 directly from the experimental curves at the initial thawed void ratio. On the other hand, the residual stress that would be obtained at the initial thawed void ratio from the extrapolation of the experimental curve of Sample 3A-1-9 would be infinitely small. This indicates that the soil in question is ice-rich and that the experimental curve shown in Figure 4.7 is within the ice-poor equivalent portion of the relationship.

121

In these cases, the experimental data does not give clear indication of the value of the residual stress. To complete the conceptual model $\sigma'_v - e - k_v$ relationships, it is thus proposed to select a realistic value for the residual stress. This value should be large enough to have practical relevance, yet small enough to uphold the physical meaning of the residual stress and of the thawed void ratio. For example, a value of 1 kPa was selected for sample 3A-1-9. The choice can be guided by the experimental $\sigma'_v - e - k_v$ relationships such that the thawed void ratio and the initial hydraulic conductivity remain meaningful and realistic. This method has also been successfully applied for the modelling of the ice-rich Inuvik silt found at the site of the warm oil experimental pipeline (Dumais and Konrad 2019). The residual stress for the Inuvik silt was then set at a value of 0.1 kPa.

The second approach to define the modelled $\sigma'_v - e - k_v$ relationships of ice-rich soils from experimental data is schematized in Figure 4.8 and exemplified in Figure 4.9. In this approach, the values of the residual stress and of the thawed void ratio is inferred from the experimental $\sigma'_v - e$ curve.

This approach is based on the analysis of the behaviour of the bulk ice-rich soil illustrated in Figure 4.1b and in Figure 4.2. Upon thawing, the overconsolidated soil elements first swell to the thawed void ratio at the residual stress by absorbing the melt water from the ice features resulting from the overconsolidation of the soil elements. Swelling of the soil elements is then defined by a linear relationship between e and $\log \sigma'_v$ (between point B and point O in Figure 4.1b). If thawed under an applied load smaller than the residual stress, the soil elements are not able to absorb the excess melt water which is then redistributed within the bulk sample resulting in a rapid increase of the bulk void ratio. The relationship between e and $\log \sigma'_v$ is then no longer linear (between point O and point I in Figure 4.1b). However, it is the behaviour of the overconsolidated soil elements which ultimately governs the thaw consolidation behaviour as discussed previously in relation to Figure 4.2. Figure 4.8 shows that the point at which the $\log \sigma'_v - e$ relationship transitioned from linear to nonlinear marks the value of the residual stress and of the thawed void ratio. The residual stress can thus be inferred from the experimental relationship if there is a nonlinear portion as shown in Figure 4.9 for sample N75-DV51-B-10. The accuracy of this approach depends on the quality of the

experimental σ'_v – e relationship. The demarcation between the nonlinear and linear portions will be easier to identify as the number of data point increases.
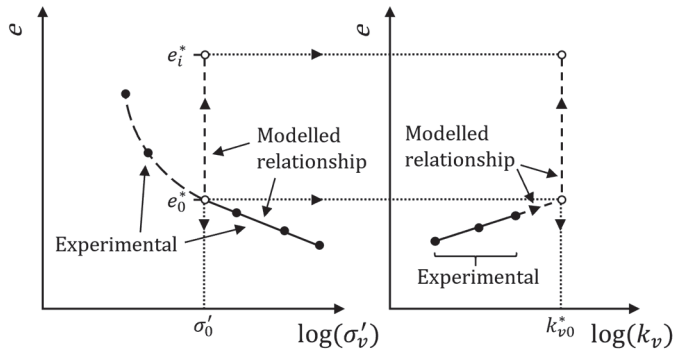
Figure 4.8 : Modelled relationships for ice-rich soils with a residual stress value inferred from the experimental data
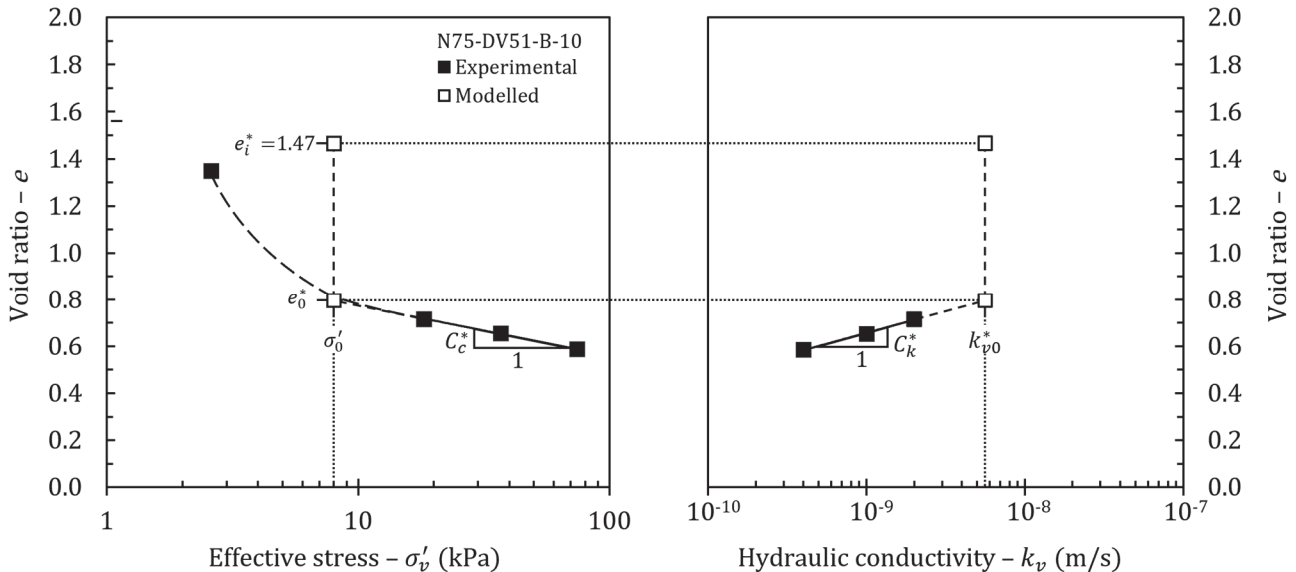
Figure 4.9 : Properties of a thawed ice-rich fine-grained soil with a residual stress value inferred from the experimental data (NESCL 1977b) (see Figure 4.8)

It should be noted that both approaches just presented for the definition of the modelled relationships may lead to the determination of residual stress values which differ from the actual residual stress. These approaches are generally valid if the modelled relationships are used for numerical modelling of thaw consolidation in engineering practice (Dumais and Konrad 2019). However, a previous discussion highlighted that the residual stress is an intrinsic property of thawed soils and that it holds physical significance. For more comprehensive analysis of the behaviour of thawing soils, it is thus recommended to

determine the actual value of the residual stress. The residual stress can be determined from the residual stress curve specific to a given soil (Nixon and Morgenstern 1973a). Measured residual stress data are also scarcely available in the literature (Nixon and Morgenstern 1973a, Nixon and Morgenstern 1974). Empirical relationships derived from a compendium of data from the literature to predict the residual stress and the thawed void ratio of ice-rich and ice-poor soils are presented in Chapter 5 of this thesis. The factors controlling the thaw consolidation properties of fine-grained soils will also be discussed to provide guidance in the application of the two approaches proposed to determine the residual stress from experimental data.

4.7   Numerical Modelling of Thaw Consolidation

The main practical application of the conceptual model is to define the properties of fine-grained soils required for the assessment of thaw consolidation in engineering practice. Dumais and Konrad (2018) formulated a large-strain nonlinear thaw consolidation numerical model in which the $\sigma_v' - e - k_v$ relationships derived from the conceptual model can be implemented. The mathematical integration and the numerical implementation of the $\sigma_v' - e - k_v$ relationships have been comprehensively described by Dumais and Konrad (2018 and 2019). Modelling results for a simple theoretical thaw consolidation test have been compared with the results obtained by the Morgenstern and Nixon (1971) thaw consolidation theory which uses the coefficient of consolidation as the main soil parameter rather than complete $\sigma_v' - e - k_v$ relationships (Dumais and Konrad 2018).

The main advantage of using the $\sigma_v' - e - k_v$ relationships as defined by the conceptual model is to provide a more lifelike assessment of thaw consolidation since the soil properties change as a function of the void ratio as consolidation proceeds (Dumais and Konrad 2018, 2019). This is particularly important for soils undergoing large thaw strains such as ice-rich soils and for soils with highly nonlinear properties in order to avoid underestimating the excess pore water pressures generated upon thawing (Dumais and Konrad 2019).

For ice-poor soils, the methodology described by Dumais and Konrad (2018) can be applied as is for thaw consolidation modelling. However, the idealized $\sigma_v' - e$ relationships for ice-rich soils defined by the conceptual model needs to be adapted for the numerical modelling

of thaw consolidation (Dumais and Konrad 2019). In the conceptual model, it is considered that the residual stress is constant between the initial thawed void ratio and the thawed void ratio. However, changes in the void ratio of compressible soils are always associated with effective stress variations such that the $\frac{\partial e}{\partial \sigma'_v}$ gradient in Equation 4-1 and Equation 4-2 is never null. For physically coherent thaw consolidation modelling, the $\sigma'_v - e$ relationship can be smoothed to maintain a finite value for the $\frac{\partial e}{\partial \sigma'_v}$ gradient. An example of the parametrisation of the smoothed $\sigma'_v - e$ relationship and its numerical implementation approach is detailed in the case study of the Inuvik pipeline (Dumais and Konrad 2019).

4.8 Interpretation of Freeze-Thaw Cycling

The proposed conceptual model is now applied to the analysis of the state paths upon thawing of a soil subjected to subsequent freezing and thaw consolidation cycles (Figure 4.10). The experimental data are taken from a study conducted on Athabasca clay by Smith (1972). The following discussion will focus on the thawing behaviour as it is assumed that the freezing mechanism described in the background section of this paper applies here. The state paths are interpreted in terms of the parameters of the conceptual model. In Figure 4.10, the full symbols represent the experimental data, while the open symbols represent the interpretation of the conceptual model. The residual stress curve and the virgin compression curve of Athabasca clay shown in Figure 4.10 were determined experimentally (Nixon and Morgenstern 1973a).

An unfrozen sample of Athabasca clay is first consolidated from a slurry under an applied load of 8.8 kPa to reach O_1; the applied load is then increased to 17 kPa and the soil consolidates along the virgin compression curve to O_2. Consolidation and thaw consolidation are represented by solid lines in Figure 4.10. For each consolidation or thaw consolidation sequence, the hydraulic conductivity can be obtained from the experimental coefficient of consolidation. For the consolidation sequence from O_1 to O_2, this value is denoted as $O_{\overline{12}}$. The full $e - k_v$ relationship was not determined. Still, a segment of an illustrative $e - k_v$ relationship is shown in Figure 4.10 to illustrate that the hydraulic conductivity is expected to vary with the void ratio.
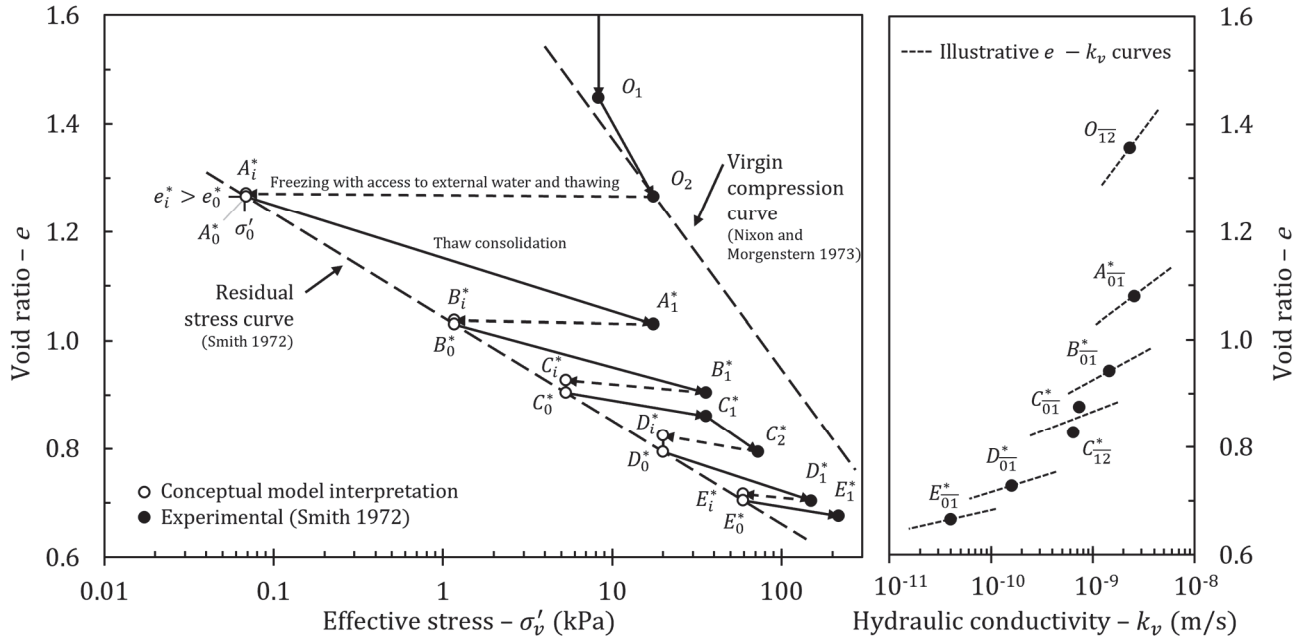
Figure 4.10 : Thaw consolidation state paths of a soil sample subjected to freeze-thaw cycling (data from Smith 1972)

The soil at O_2 is then frozen with access to external water under an applied load of 17 kPa. Frost heave slightly exceeds the expansion attributed to phase change alone due to ice segregation. Phase change is not represented in Figure 4.10. A thaw consolidation test is then carried in drained conditions under a constant applied load of 17 kPa such that the soil settles to the consolidated thawed point A_1^*. Superscript * is used to denote the soil in its thawed state.

It is the interpretation of the state path followed by the soil upon thawing which is of interest here. In Figure 4.10, the thaw consolidation state path is represented by a full line. The effect of the mechanisms acting upon the soil skeleton during freezing is not represented but it is assumed that the soil elements are overconsolidated along the virgin compression curve due to suction forces. Upon thawing, the soil elements swell to the thawed void ratio e_0^*. The residual stress in the soil elements is defined by the residual stress curve at point A_0^*. The soil contains some excess water. The initial thawed void ratio e_i^* at point A_i^* is thus slightly larger than e_0^*. Drainage of the excess water occurs with no compression of the soil skeleton while the effective stress within the soil elements is equal to the residual stress. The applied load upon thawing is larger than the residual stress such that thaw consolidation proceeds to the

126

consolidated thawed point A_1^*. The $\sigma_v' - e$ relationship used for modelling thaw consolidation would be defined by the curve from A_i^* to A_0^* on to A_1^*. The average hydraulic conductivity of the thawed soil for thaw consolidation sequence A is defined at $A_{\overline{01}}^*$.

The subsequent freezing and thawing cycle is denoted as sequence B. Sequence B differs from sequence A as the load applied on the sample is increased to 36 kPa after freezing prior to thawing. The sample is thus frozen and thawed under different loads. Once again, frost heave slightly exceeds the expansion attributed to phase change alone due to ice segregation. Thaw consolidation for sequence B is similar to the one described for sequence A. The bulk sample is at point B_i^* in its initial thawed state after phase change; drainage of the excess water occurs such that the soil settles at point B_0^* on the residual stress curve in its thawed state; and thaw consolidation proceeds due to consolidation of the thawed soil; skeleton to reach point B_1^*.

The third freezing and thawing cycle is denoted as sequence C. Frost heave due to ice segregation is more important at the onset of sequence C. Points C_i^* and C_0^* are easily differentiated and drainage of the excess water upon thawing is more significant. In this sequence, the applied load is kept constant at 36 kPa for freezing and thawing. However, the thawed sample is subsequently consolidated from C_1^* to C_2^* under an incremental load of 73 kPa to obtain a more complete $\sigma_v' - e$ relationship. A second hydraulic conductivity value $C_{\overline{12}}^*$ is also obtained. It is considered that a single $e - k_v$ relationship defines the hydraulic conductivity change behaviour during thaw consolidation sequence C.

Two additional freezing and thawing cycles (sequences D and E) are presented in Figure 4.10. The behaviour upon thawing is consistent with the behaviour described for previous sequences.

Figure 4.10 demonstrates an important aspect of the proposed conceptual model: the residual stress curve is an intrinsic property of the soil such that it always characterizes the state of the soil elements upon thawing. Indeed, freezing always resets the soil on the residual stress curve upon thawing. The conceptual model thus offers the ability to model thaw consolidation by defining a complete $\sigma_v' - e$ relationship from the residual stress curve. The

conceptual approach proposed to define the thawed state and the ensuing state path from the residual stress curve is supported by experimental evidence that showed state paths initiated at measured residual stress values (Nixon and Morgenstern 1973a). These experimental stress paths were not conceptually associated with the residual stress curve. The proposed conceptual model thus introduces the use of the residual stress curve for the definition of the state path upon thawing. Generalization of the residual stress concept to ice-rich soils further warrant general applicability of the residual stress curve as demonstrated in Figure 4.10. Finally, the conceptual model associates the $\sigma_v' - e$ relationship with the $e - k_v$ relationship for comprehensive thaw consolidation modelling.

4.9 Conclusion

A conceptual model for thaw consolidation of fine-grained soils has been proposed. It is formulated in terms of $\sigma_v' - e - k_v$ relationships. The model is developed from the analysis of the typical behaviour of thawing soils. The concept of the residual stress is generalized to ice-poor and ice-rich soils by specifying that the residual stress is the effective stress within the soil elements. The residual stress curve which gives the relationship between the thawed void ratio and the residual stress is considered as an intrinsic soil property. It is integrated in the conceptual model as the backbone which defines the initial conditions at the thawed state.

The conceptual model defines the $\sigma_v' - e - k_v$ relationships of thawed fine-grained soils. The volume change behaviour of ice-poor soils is described by a semi-logarithmic linear $\sigma_v' - e$ relationship. For ice-poor soils, the slope of the $\log \sigma_v' - e$ relationship is given by the compression index of the thawed soil. For ice-rich soils, the soil skeleton cannot hold the total volume of melt water at the residual stress. The volume change behaviour of ice-rich soils upon thawing is governed by the overconsolidated soil elements. A bilinear $\sigma_v' - e$ relationship is adopted. First, drainage of the excess water occurs with no compression of the soil skeleton. Then, water is drained out of the soil upon compression of the soil skeleton in an ice-poor equivalent manner. The $e - k_v$ relationship of thawed fine-grained soils is defined by a semi-logarithmic linear curve with a slope defined by the hydraulic conductivity change index of the thawed soil. For ice-rich soils, the hydraulic conductivity upon drainage of the excess water is controlled by the hydraulic conductivity of the overconsolidated soil elements.

The main application of the conceptual model is to characterize the properties used as input for the assessment of thaw consolidation in engineering practice. In that regards, the model innovates by integrating the residual stress curve as part of the definition of the $\sigma'_v - e - k_v$ relationships. This allows for a complete definition of the properties from the thawed state. Furthermore, the capability of the soil to absorb the melt water is defined in terms of the thawed state at the residual stress. The distinction between the behaviour of ice-poor and ice-rich soils is thus defined as a function of the physical properties of the soil skeleton. The $\sigma'_v - e - k_v$ relationships defined by the conceptual model can be used directly as input for the large-strain nonlinear thaw consolidation numerical model formulated by Dumais and Konrad (2018).

Chapter 5 of this thesis seeks to determine the factors controlling the characteristics of the $\sigma'_v - e - k_v$ relationships introduced in this chapter. The development of empirical relationships for the prediction of the characteristics from the index properties of fine-grained thawed soils are presented. This aims at facilitating the use of the proposed conceptual model in engineering practice as determining the properties from intact permafrost samples poses significant challenges in terms of logistics and costs.

Discussion complémentaire

L'objectif du chapitre 4 est de présenter le développement d'un modèle conceptuel pour la consolidation au dégel en termes des relations $\sigma'_v - e - k_v$ des sols dégelés à grains fins (axe 2 – objectif 2.1 de la thèse). Le but est donc de définir correctement les intrants utilisés lors de la modélisation numérique de la consolidation au dégel principalement en ce qui concerne l'utilisation du modèle non linéaire à grandes déformations développé au chapitre 2.

Il est primordial de rappeler que le modèle proposé s'applique principalement à la modélisation de la consolidation au dégel, et donc, à la phase de dégel. On cherche particulièrement à modéliser le comportement du pergélisol lors du dégel. Néanmoins, l'analyse des propriétés des sols dégelés est initiée à partir de la description du comportement de sols soumis à des cycles de gel et de dégel. Bien que cette approche permette de comprendre le comportement général lors du dégel, il existe une différence fondamentale

quant à l'évaluation du dégel du pergélisol et des sols soumis à des cycles de gel-dégel. En effet, l'état non gelé du pergélisol est généralement inconnu ou très difficile à caractériser avec précision. On utilise donc l'état gelé du sol tel que déterminé sur le terrain comme intrant à toutes évaluations géotechniques. En comparaison, l'état non gelé précédant le gel peut être utilisé comme intrant aux analyses dans les cas de cycles de gel-dégel. C'est pourquoi la plupart des études portant sur les effets du gel et du dégel comparent les propriétés des sols dans leur état non gelé aux propriétés des sols dans leur état dégelé. Ainsi, certaines analyses proposées par ces études sont abordées brièvement dans le corps du chapitre 4 sans être davantage développées. Celles-ci peuvent maintenant faire l'objet d'une discussion complémentaire. Ce n'est pas dire que le modèle conceptuel proposé ne pourrait pas éventuellement permettre d'améliorer l'analyse des phénomènes de gel, mais que les travaux présentés dans cette thèse se concentrent principalement sur le comportement au dégel.

Succion lors du gel

Tout d'abord, le comportement lors du dégel est grandement décrit en lien avec la surconsolidation des éléments de sols lors du gel. La surconsolidation du sol lors du gel est attribuée aux forces qui se développent lorsque l'eau non gelée se trouve dans un état de succion. La succion lors du gel est liée à la température de gel (Konrad et Samson 2000a). De la succion se développe aussi longtemps que l'abaissement de température produit une augmentation de la teneur en glace dans les pores et une diminution de la teneur en eau non-gelée. La Figure 4.11 montre la courbe de teneur en eau non gelée en fonction de la température (d'après Konrad et Samson 2000a). Sous une certaine température T_{min}, l'abaissement de température dans le sol produit une diminution négligeable de la teneur en eau non gelée. Ainsi, la pression de surconsolidation maximale lors du gel est atteinte à cette température (Konrad et Samson 2000b). Si la température lors du gel se trouve entre la température au point de congélation et la température minimale T_{min}, la pression de surconsolidation est moindre.
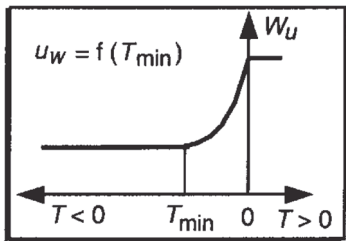
Figure 4.11 : Courbe de teneur en eau non gelée (Konrad et Samson 2000a)

Konrad et Samson (2000a) proposent de calculer la pression de surconsolidation en utilisant l'équation de Clausius-Clapeyron qui décrit la relation entre la pression interstitielle de l'eau non gelée, la pression interstitielle de la glace dans les pores et la température pour un sol partiellement gelé :

Équation 4-8 $u_{pw} \approx \frac{L(T-T_0)}{V_w T_0} + \frac{V_i}{V_w} P_i$

où u_{pw} est la succion, P_i est la pression de la glace, V_w et V_i sont les volumes spécifiques de l'eau et de la glace, L est la chaleur latente de fusion de l'eau, T_0 est la température de congélation de l'eau et T est la température.

Konrad et Samson (2000a) assument que la pression appliquée durant le gel égale la pression interstitielle de la glace dans les pores et que la pression de succion est exprimée par :

Équation 4-9 $u_{pw}(kPa) = 1250(T - T_0) + 1,09\sigma'_v \ (kPa),$

avec $T = T_{min}$ si la température durant le gel est inférieure à T_{min}.

La pression de surconsolidation est alors égale à pression de succion. Il est donc possible d'obtenir l'indice des vides des éléments de sols surconsolidés à partir de la courbe de compression vierge du sol non gelé. Cette approche peut être utilisée lorsque la courbe de compression vierge du sol non gelé est connue ce qui est rarement le cas pour un pergélisol.

Konrad et Samson (2000a) notent que la pression de surconsolidation est effective dans la phase argileuse des mélanges silt-argile. En effet, les sols à grains fins peuvent être définis comme étant un mélange de particules fines plus ou moins grossières. L'argile et le silt forment une macrostructure et une microstructure. La microstructure est formée de particules plus fines dont la teneur en eau-non gelée est plus élevée. C'est donc au sein de la

microstructure que les forces de succion se développent principalement. Le chapitre 5 présente une discussion sur l'impact de la macrostructure et de la microstructure sur les propriétés des sols dégelés.

Chamberlain (1981) a aussi cherché à définir la pression de surconsolidation lors du gel. La pression de surconsolidation due au gel est alors mesurée en laboratoire pour un nombre limité d'essais de gel et de dégel. La contrainte de surconsolidation est conceptuellement comparée à la pression de préconsolidation des sols non gelés. Chamberlain (1981) propose donc d'appliquer la méthode empirique de Casagrande utilisée pour déterminer la pression de préconsolidation pour trouver la contrainte de surconsolidation des sols dégelés. À la différence de l'approche proposée par Konrad et Samson (2000a), c'est la courbe de compression vierge globale du sol qui est utilisée au lieu de la courbe de compression vierge de la phase argileuse. Encore une fois, la courbe de compression vierge du sol non gelé doit être connue pour appliquer cette méthode, ce qui n'est pas toujours possible pour les pergélisols.

Drainage de l'eau de fonte en excès

La Figure 4.1b montre le comportement d'un sol riche en glace alors que le dégel se produit dans des conditions non drainées. On mentionne alors que l'eau de fonte en excès est redistribuée au sein du sol qui gonfle jusqu'à des conditions de contraintes effectives presque nulles. La Figure 4.2 montre plutôt le comportement d'un sol riche en glace pour lequel le dégel se produit dans des conditions drainées alors que le sol est soumis à une charge plus élevée que la contrainte résiduelle. Dans ce cas, l'eau de fonte en excès est drainée hors du squelette de sol sans affecter la contrainte effective dans les éléments de sol surconsolidés. En fait, il peut se produire une absorption partielle de la glace en excès par les éléments de sol surconsolidés accompagnée du drainage d'une partie de l'eau de fonte en excès. Le comportement global du sol se situe alors entre le drainage complet (Figure 4.2) et l'absorption complète (Figure 4.1b). Le comportement au dégel d'un sol avec des lentilles de glace dépend alors de plusieurs facteurs et principalement de l'épaisseur des lentilles de glace, de la distance entre les lentilles de glace, du taux de dégel, de la perméabilité globale du sol, de la surconsolidation des éléments de sol et de la contrainte externe appliquée. L'objectif de cette thèse est de modéliser le comportement global du sol lors du dégel, le

comportement local des lentilles de glace n'est donc pas étudié en détail. Chacun des éléments énumérés ci-haut pourrait faire l'objet d'une analyse expérimentale ou d'une analyse par modélisation numérique.

Il est important de souligner que la discussion précédente s'applique pour une configuration unidimensionnelle du dégel. Comme au chapitre 2, on considère un sol initialement gelé dont le front de dégel pénètre de la surface vers le bas. Le sol dégelé se trouve donc entre une frontière permettant le drainage à la surface et une frontière imperméable au front de dégel. Le drainage de l'eau de fonte, autant l'eau en excès que l'eau expulsée hors du squelette de sol, se produit de manière unidimensionnelle vers la surface. En réalité, le drainage de l'eau en excès lors de la dégradation thermique du pergélisol se produit par des chemins d'écoulement différents de ceux considérés par cette configuration unidimensionnelle. Les lentilles de glace épaisses forment un horizon par lequel l'écoulement se produit lors du dégel. Il y a alors peu d'interaction avec les éléments de sol se trouvant au-dessus et au-dessous de la lentille. Il y a plutôt création d'une surface où la contrainte effective est nulle localement. Dans ce cas, c'est le comportement de cette zone critique qui contrôle la stabilité plutôt que le comportement global du sol. Il en est de même pour de nombreux cas alors que la fonte d'éléments de glace entraine la création de chemin d'écoulement préférentiel pour l'eau de fonte.

Propriétés des sols du chapitre 2 et 3

Les relations $\sigma_v' - e - k_v$ utilisées pour la modélisation numérique de la consolidation au dégel au chapitre 2 et 3 peuvent maintenant être analysées à la lumière du modèle conceptuel développé au chapitre 4.

Au chapitre 2, la Figure 2.4 montre une définition des relations $\sigma_v' - e - k_v$ des sols dégelés à grains fins compatible avec la caractérisation des propriétés des sols pauvres en glace adoptée au sein du modèle conceptuel. La Figure 2.5 montre les courbes $\sigma_v' - e - k_v$ expérimentales pour l'échantillon d'argile d'Athabasca utilisé en exemple au chapitre 2. Cet échantillon possède un indice des vides initial du sol dégelé e_i^* est assez élevé. De plus, la contrainte résiduelle obtenue grâce à l'interpolation de la courbe expérimentale est très petite bien que sa valeur demeure physiquement réaliste. L'échantillon d'argile d'Athabasca utilisé

pour l'exemple est donc probablement légèrement riche en glace et pourrait contenir de la glace en excès. Comme la courbe expérimentale $\log \sigma'_v - e$ ne permet pas de différencier une portion linéaire et non linéaire, il aurait fallu poser une valeur pour la contrainte résiduelle. Le but de l'exemple présenté au chapitre 2 était de montrer l'impact théorique des grandes déformations et de la non-linéarité en comparaison au modèle linéaire à petites déformations de Morgenstern et Nixon (1971). L'adoption de relations $\sigma'_v - e - k_v$ d'un sol pauvre en glace est alors justifiée par les besoins de l'exemple.

Au chapitre 3, la définition des propriétés des sols riches en glace est adoptée pour la modélisation du silt d'Inuvik. Comme un des objectifs du chapitre est de valider le modèle numérique de consolidation au dégel non linéaire à grandes déformations, l'utilisation de la définition adéquate des relations $\sigma'_v - e - k_v$ est importante. La Figure 3.4 montre les propriétés adoptées pour la consolidation au dégel. La valeur de la contrainte résiduelle a été posée à 0,1 kPa pour le silt d'Inuvik peu importe la teneur en glace initiale. Cette approche suggère que les éléments de sols surconsolidés se comportent de manière similaire, peu importe la teneur en glace en excès. La relation entre la teneur en glace initiale et les caractéristiques des relations $\sigma'_v - e - k_v$, notamment la contrainte résiduelle, sera analysée au chapitre 5. Pour la modélisation du silt d'Inuvik, le fait de choisir une valeur de contrainte résiduelle constante et uniforme favorise grandement la stabilité numérique.

Chapitre 5   Empirical Framework for the Determination of the σ'$_v$ – e – k$_v$ Relationships of Thawed Fine-Grained Soils for Engineering Applications

Avant-propos

Titre français

Méthode empirique pour la caractérisation des relations $\sigma_v' - e - k_v$ des sols à grain fins pour des applications d'ingénierie

5.1   Résumé français

Les caractéristiques des relations $\sigma_v' - e - k_v$ des sols dégelés à grains fins sont étudiées grâce à l'analyse d'un compendium de données de la littérature. Un total de 209 échantillons de sol couvrant une grande plage de propriétés mécaniques et physiques sont inclus dans l'analyse. Les caractéristiques étudiées sont définies conformément à la définition proposée par le modèle conceptuel pour la consolidation au dégel des sols à grains fins présenté précédemment. En se basant sur l'analyse du comportement général des sols à grains fins lors du dégel, des relations empiriques sont développées pour l'indice de compression du sol dégelé, pour la contrainte résiduelle, pour l'indice de changement de la conductivité hydraulique du sol dégelé et pour la conductivité hydraulique initiale du sol dégelé. La limite de liquidité, la teneur en particules argileuses et la taille médiane des grains de la fraction fine sont utilisées comme paramètres de prédiction. La taille médiane des grains de la fraction fine offre la plus grande précision pour la caractérisation des relations $\sigma_v' - e - k_v$. Une méthode par étapes utilisant les relations empiriques développées est présentée avec un exemple d'application de cette méthode. La méthode peut être utilisée en entier pour définir les relations $\sigma_v' - e - k_v$ ou en partie pour compléter des relations incomplètes.

5.2   Abstract

The characteristics of the $\sigma_v' - e - k_v$ relationships of thawed fine-grained soils are investigated through the analysis of a compendium of literature data. A number of 209 soil samples covering a wide range of mechanical and physical properties are included in the

analysis. The investigated characteristics are defined in agreement with the definition formulated by the previously introduced conceptual model for thaw consolidation of fine-grained soils. Based on the general interpretation of the behaviour of thawing soils, empirical relationships are developed for the compression index of the thawed soil, the residual stress, the hydraulic conductivity change index of the thawed soil and the initial hydraulic conductivity of the thawed soil. The liquid limit, the clay content and the median grain size of the fine fraction are used as predictive parameters. The median grain size of the fine fraction offers the greatest precision for the determination of the characteristics of the $\sigma_v' - e - k_v$ relationships. A step-by-step method based on the empirical relationships is presented along with a working example illustrating the use of the method. The method may be used as a whole to completely define the $\sigma_v' - e - k_v$ relationships or in parts to supplement incomplete relationships.

5.3   Introduction

The input parameters for modelling thaw consolidation of permafrost are the hydraulic conductivity of the thawed soil and the relationship between volume change and applied stress. Proper determination of the consolidation properties of thawed soils is paramount for accurate assessment of thaw consolidation in engineering practice. A conceptual model for thaw consolidation of fine-grained soils was introduced in chapter 4 to define the properties needed for thaw consolidation modelling in terms of $\sigma_v' - e - k_v$ relationships.

Intact permafrost samples are generally required to determine the $\sigma_v' - e - k_v$ relationships experimentally. These samples need to remain frozen while they are taken from the field to the laboratory. This poses a significant logistical challenge and can be very costly due to the general remoteness of permafrost areas. This is in addition to the challenges of drilling in permafrost to retrieve intact samples. Furthermore, the experimental evaluation of complete $\sigma_v' - e - k_v$ relationships is time-consuming. The use of empirical relationships and data from the literature is common in permafrost engineering practice to limit the cost associated with laboratory testing of intact samples. However, the empirical relationships available for thaw consolidation are mainly limited to the evaluation of thaw settlements.

The objective of this chapter is to develop an empirical framework for the determination of the $\sigma'_v - e - k_v$ relationships of fine-grained thawed soils for engineering applications. The framework is developed in terms of the characteristics of the $\sigma'_v - e - k_v$ relationships defined in chapter 4. A compendium of thaw consolidation test results from the literature supports the development of the empirical framework. The general behaviour of thawed fine-grained is analyzed in order to determine the factors controlling the thaw consolidation properties. Empirical relationships are then formulated from the analysis of the compendium of literature data. A step-by-step method for the determination of the $\sigma'_v - e - k_v$ relationships with a working example is presented.

5.4 Characteristics of the σ'ᵥ – e – kᵥ Relationships

Figure 5.1 presents the conceptual model for thaw consolidation of fine-grained soils introduced in chapter 4. The model defines the properties of thawed fine-grained soils in terms of $\sigma'_v - e - k_v$ relationships. The volume change behaviour of ice-poor soils is described by a semi-logarithmic linear $\sigma'_v - e$ relationship. For ice-rich soils which contain melt water in excess of the amount that the soil skeleton can absorb upon thawing, a bilinear $\sigma'_v - e$ relationship is adopted. First, drainage of the excess water occurs with no compression of the soil skeleton. Then, water is drained out of the soil upon compression of the soil skeleton in an ice-poor equivalent manner. The $e - k_v$ relationship of thawed fine-grained soils is defined by a semi-logarithmic linear curve.
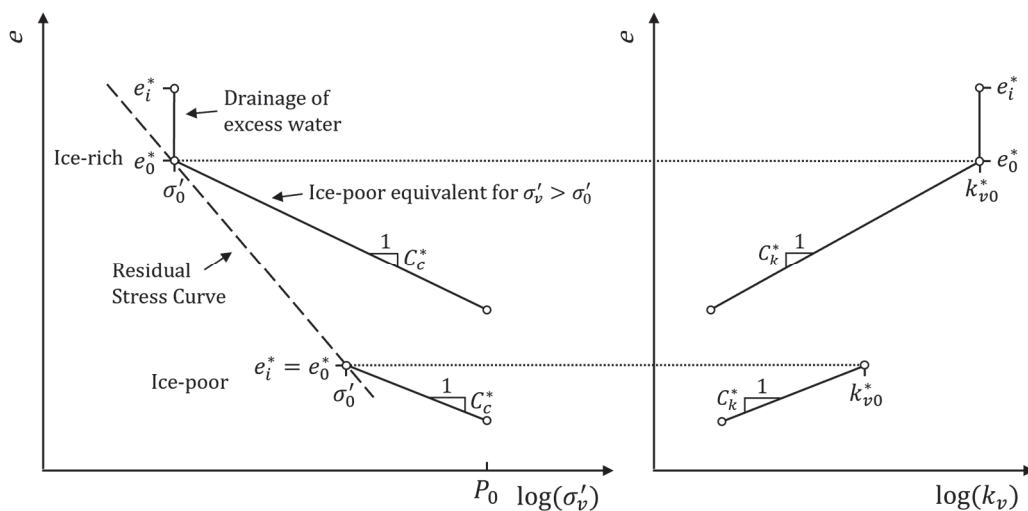
Figure 5.1 : Conceptual model for thaw consolidation of fine-grained soils

Table 5.1 : Characteristics of the $\sigma'_v - e - k_v$ relationships of thawed fine-grained soils

Symbol	Characteristic
e_f	Frozen void ratio
e_i^*	Initial thawed void ratio
e_0^*	Thawed void ratio
C_c^*	Compression index of the thawed soil
σ'_0	Residual stress
C_k^*	Hydraulic conductivity change index of the thawed soil
k_{v0}^*	Initial hydraulic conductivity at the thawed void ratio

The characteristics of the $\sigma'_v - e - k_v$ relationships are summarized in Table 5.1. The void ratio of the soil in its frozen state is the frozen void ratio e_f. The void ratio of the soil thawed in undrained conditions is the initial thawed void ratio e_i^*. The volumetric changes between the frozen void ratio and the initial thawed void ratio are only attributable to phase change such that they are related by:

Equation 5-1 $\quad e_i^* = \dfrac{e_f}{1.09}$.

The residual stress σ'_0 is defined as the effective stress that the soil skeleton can sustain when thawed in undrained conditions. It is thus the effective stress within the soil elements upon thawing. The residual stress is thoroughly studied in chapter 4. The thawed void ratio e_0^* is the void ratio of the soil elements at the residual stress. For ice-poor soils, the thawed void ratio is equal to the initial thawed void ratio. For ice-rich soils, the initial thawed void ratio is larger than the thawed void ratio due to the presence of excess melt water. The compression index of the thawed soil C_c^* is the slope of the $\log \sigma'_v - e$ curve. The initial hydraulic conductivity of the thawed soil k_{v0}^* is the hydraulic conductivity at the thawed void ratio, i.e., the hydraulic conductivity of the soil elements at the residual stress. The hydraulic conductivity change index of the thawed soil C_k^* is the slope of the $\log k_v - e$ curve.

5.5 Description of Investigated Soils

The study of the properties of thawed fine-grained soils presented in this chapter is based on the analysis of a compendium of data from the literature. The analysis is limited to non-

organic fine-grained saturated soils. A total of 201 permafrost soil specimens are considered in the current investigation: 2 are from the vicinity of the Qinghai-Tibet Highway (Yao et al. 2016); 6 are from the site of the Iqaluit airport (Mathon-Dufour and Allard 2015); 10 are from Nunavik (L'Hérault et al. 2012, L'Hérault et al. 2015); 165 are from the Mackenzie Valley in North-Western Canada (Northern Engineering Services Company Limited 1975, 1976, 1977a, 1977b, 1977c, 1977d,); and 18 are from the site of the experimental warm-oil pipeline near Inuvik (Watson et al. 1972). In addition, 8 remoulded soils subjected to freeze-thaw cycling are also considered in this study (Konrad 2010, Morgenstern and Smith 1973, McRoberts and Morgenstern 1974).

The raw laboratory data of each individual soil specimen was analyzed in order to establish the relationships between the effective stress, the void ratio and the hydraulic conductivity. The analysis was performed as a function of the characteristics of the $\sigma_v' - e - k_v$ relationships introduced in chapter 4 and presented in section 5.3. The soils were categorized as ice-poor and ice-rich soils in terms of the definition given in section 4.3 such that 117 specimens are ice-poor and 92 specimens are ice-rich. The methodology used to determine the characteristics of the $\sigma_v' - e - k_v$ relationships is exemplified in section 4.5.1 for ice-poor soil specimens and in section 4.5.2 for ice-rich soil specimens. The relationship between the effective stress and the void ratio was determined for 205 soil specimens, while the relationship between the hydraulic conductivity and the void ratio was determined for 91 soil specimens. The investigated soils cover a wide range of mechanical and physical properties such that general applicability of the analysis can be assumed. Index properties of the investigated soils are presented in Figure 5.2 in the form of histograms.

It should be noted that some thaw settlement data found in the literature could not be considered in the current analysis. The report by Luscher and Afifi (1973) is one notably well-cited study not included in the analysis. Some literature data were excluded because it was not possible to establish complete relationships between the effective stress and the void ratio and/or between the void ratio and the hydraulic conductivity. Indeed, many thaw settlement test results are reported as the thaw settlement at a specific applied load such that the complete relationship between the void ratio and the effective stress cannot be established.
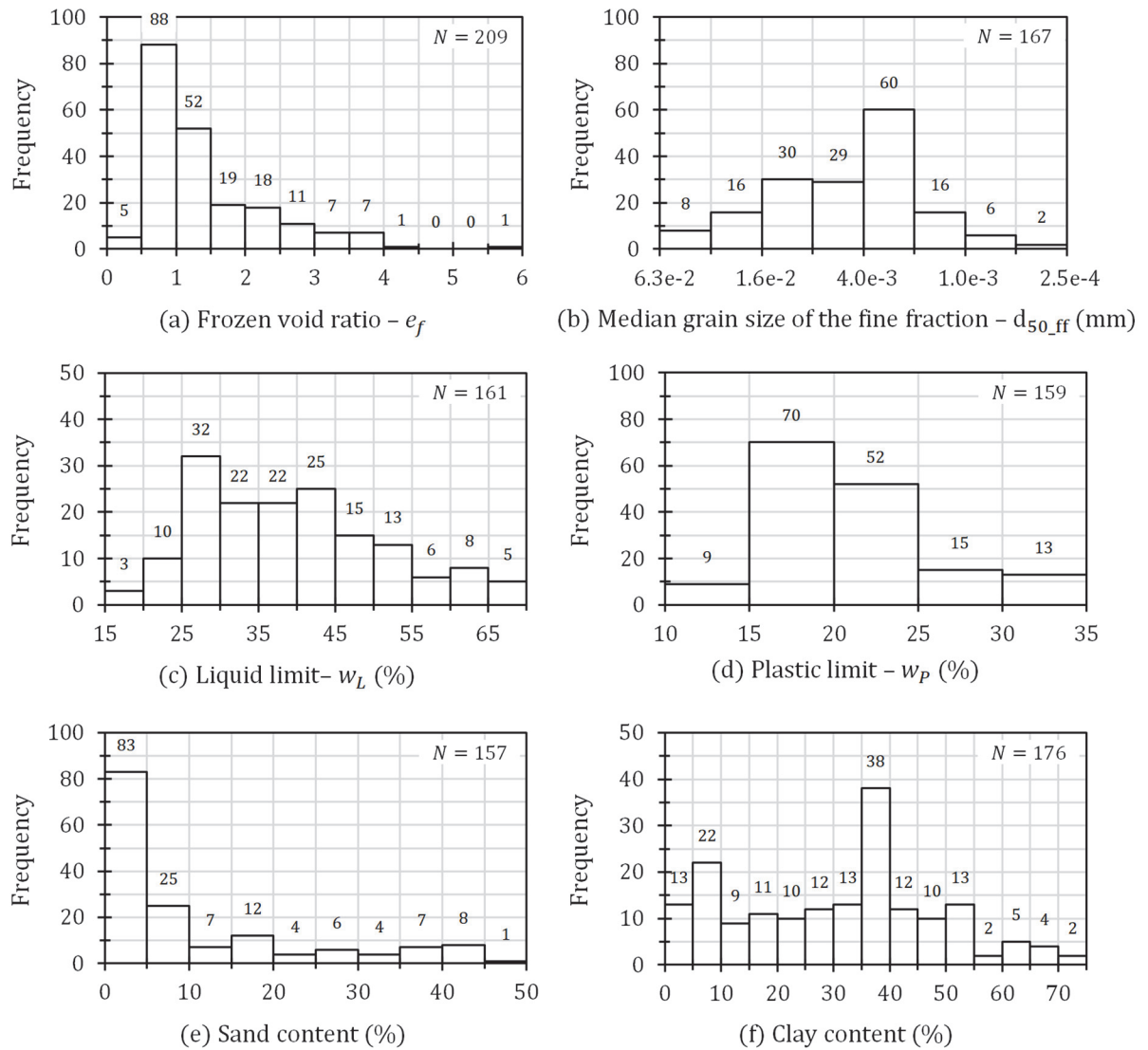
Figure 5.2 : Frequency histograms of some index properties of all investigated soils

5.6   General Interpretation of the Properties of Thawing Soils

The hydraulic conductivity and the volume change properties of fine-grained soils upon thawing are controlled by the soil composition and by the soil fabric. Fine-grained soils can be conceptualized as mixtures of silt and clay particles. The soil composition and the soil fabric of thawed fine-grained soils can be discussed in terms of the behaviour of the silt and clay phases (Chamberlain and Gow 1979, Konrad 1989). Fine-grained soils are characterized by their macro-pores and micro-pores distribution. The macro-pore space is mainly controlled by the coarser silt particles which control the packing. The micro-pore distribution within the soil skeleton is controlled by the clay-size particles and the clay minerals.

An appreciation of the mechanisms acting on the soil skeleton upon freezing is essential to explain the behaviour of fine-grained soil upon thawing. Closed-system freezing with no access to external water is first considered. This process is also schematized in Figure 4.1a which can be used as reference for the current discussion. As temperature decreases, the ice first forms in the macro-pores. Unfrozen water is then found in the micro-pores in the form of free water and adsorbed water films around the clay minerals. Temperature continues to decrease leading to the formation of additional ice in the pores which eventually starts to penetrate in the micro-pores. The unfrozen free capillary water and the adsorbed water is then in contact with ice such that it is in a state of suction according to the laws of thermodynamics. This causes a reduction of the amount of capillary water and of adsorbed water. The clay-size particles and clay minerals are then subjected to suction forces which induce a structural rearrangement in the pores leading to overconsolidation. The suction forces are mainly effective within the micro-pores.

Upon thawing, the soil particles do not move back to their original position. However, the overconsolidated soil elements within the micro-pores can absorb the free melt water. This leads to swelling of the overconsolidated clay elements. For the sake of simplicity, the state path followed upon thaw consolidation is defined by the swelling curve of the soil upon thawing as shown in Figure 4.1a. In other words, the swelling behaviour of the clay-silt mixture determines the volume change behaviour upon thawing. Swelling is mainly effective within the micro-pores. Since the micro-pores distribution is controlled by the clay-size particles and the clay minerals, the volume change behaviour upon thawing is expected to be a function of the clay content in the soil, i.e., a function of the soil composition.

The hydraulic conductivity of thawed fine-grained soils can also be analyzed in terms of the mechanisms acting on the soil skeleton upon freezing and thawing. Generally, it is the finer clay particles which control the hydraulic conductivity. In unfrozen soils, the clay-size particles form an organized structure. The suction forces cause a structural rearrangement of the clay-size particles upon freezing. This causes the clay packets to collapse into a denser and more dispersed structure. Upon thawing, the collapsed clay packets occupy less void space than in the unfrozen soil. The hydraulic conductivity of thawed soils is thus higher than the hydraulic conductivity of the soil prior to freezing. Regarding the soil composition, soils

141

with higher clay content have a lower hydraulic conductivity than soils composed predominantly of coarser silt particles.

As previously mentioned, the behaviour of the soil upon thawing is controlled by the fabric of the soil. The fabric of the soil is defined as the arrangements of the particles and the association between the particles. For the same soil composition, the particles of fine-grained soils may be arranged in different manners which affects the volume change behaviour and the hydraulic conductivity. For thawed fine-grained soils, the fabric of the soil can be discussed in terms of the initial ice content, and primarily with regard to the difference in behaviour between ice-poor and ice-rich soils. For the sake of the discussion, ice-poor soils are considered to be the result of closed-system freezing (see Figure 4.1a); and ice-rich soils are considered to be the result of open-system freezing (see Figure 4.1b). The main difference between ice-poor and ice-rich soils is the formation of segregated ice in the form of ice lenses in ice-rich soils. Two idealized clay-slit mixtures are now considered: one is ice-poor, and one is ice-rich. As previously stated in section 4.3.2, it is assumed that the suction forces acting in the micro-pores are similar in closed-system and open-system freezing. In other words, the arrangements of the particles in the micro-pores after freezing are comparable whether there is a presence of segregated ice or not. Yet, there is a difference in the fabric of thawed ice-poor and ice-rich fine-grained soils which can be attributed to the presence of excess ice upon thawing.

Upon thawing of an ice-poor soil, the overconsolidated soil elements absorb the free melt water found in the macro-pores. When thawed under an applied load higher than the residual stress, some of the melt water is simultaneously drained out due to the compression of the soil skeleton (see Figure 4.1a). The space in the macro-pores is thus reduced due to the concurrent drainage of water into the overconsolidated soil elements and outside the soil skeleton. In other words, the macrostructure of ice-poor soils mostly collapses upon thawing.

Upon thawing of an ice-rich soil, there are different operating seepage mechanisms. As the ice-rich soil thaws, the melt water in excess is draining out of the soil skeleton with no compression of the soil skeleton (see Figure 4.2). Unidimensional vertical consolidation is assumed such that the excess melt water seeps through the macro-pores of the thawing soil to reach the surface of the soil. Meanwhile, the overconsolidated soil elements are thawing

and absorbing free melt water. In contrast with ice-poor soils, the water absorbed by the overconsolidated soil elements from the macro-pores is replenished by the continuous seepage of excess melt water. The macrostructure is sustained by the pressure head within the macro-pores. As all the excess water is drained out of the bulk soil, consolidation of the soil occurs such that some of the macrostructure collapses. Still, the fabric of thawed fine-grained soils can maintain more macro-pore space due to the seepage of excess water upon thawing.

5.7 Parameters Controlling the Properties of Thawed Fine-Grained Soils

The previous discussion highlighted the importance of the soil composition and of the soil fabric in governing the properties of thawed fine-grained soils. We are now seeking for index properties indicative of the composition and fabric of thawed fine-grained soils to support the development of empirical relationships for the characteristics of the $\sigma'_v - e - k_v$ relationships.

First, the liquid limit can be used in continuity with several studies which have successfully developed empirical relationships for the compressibility of fine-grained soils from the liquid limit (Azzouz et al. 1976).

Second, the soil composition of fine-grained soils can be characterized by the clay content. As discussed in the previous section, the behaviour of thawed clay-silt mixtures is largely controlled by the content of clay-size particles which are most affected by freezing.

Third, the median grain size of the fine fraction, d_{50_ff}, can also be used to characterize the soil composition of fine-grained soils. Clay particles may differ in size depending on their origin and mineralogy. The size of clay particles is known to affect the consolidation properties of fine-grained soils. The median grain size of the fine fraction is used to give an indication of the mineralogy of the clay phase. The median grain size of the fine fraction is thus believed to be a more indicative parameter of the soil composition than the clay content. The median grain size of the fine fraction has been used successfully to develop empirical relationships for the frost susceptibility, a property highly correlated with the hydraulic conductivity of the soil (Konrad 1999). Figure 5.3 presents the correlation between the clay

content and the median grain size of the fine fraction for the investigated soils. As expected, the median grain size of the fine fraction decreases as the clay content increases. However, there is some variation which indicates the investigated soils may contain different sizes of clay particles.
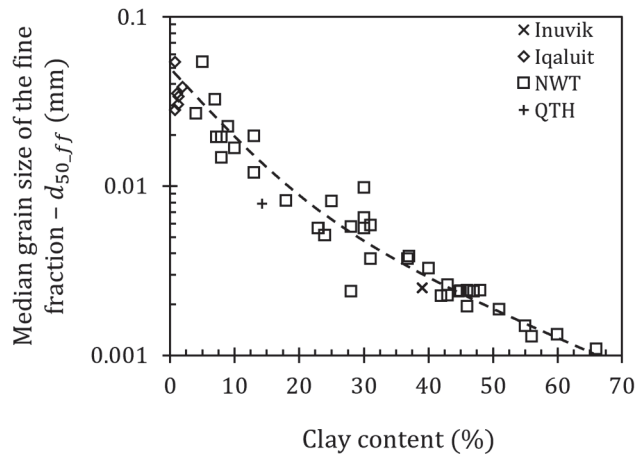
Figure 5.3 : Relationship between the median grain size of the fine fraction and the clay content of investigated soils

Finally, the initial void ratio is a parameter often used to develop empirical relationships for the compressibility of fine-grained soils (Azzouz et al. 1976). In unfrozen soil, the initial void ratio is used as a proxy to characterize the impact of the soil fabric and the soil composition on the compressibility. The initial thawed void ratio can thus be used as an index property to develop empirical relationships. It is convenient to use the initial thawed void ratio as it is directly related to the frozen void ratio by Equation 5-1. Furthermore, the void ratio is used as the state variable in the conceptual model presented in chapter 4 and in the numerical model presented in chapter 2. Like unfrozen soils, the use of the thawed void ratio may be redundant with the use of the liquid limit, the clay content or the median grain size of the fine fraction for ice-poor soils. However, using the initial thawed void ratio in addition to the liquid limit, the clay content or the median grain size of the fine fraction may be valuable for ice-rich soils to characterize the impact of the excess ice discussed in section 5.5.

5.8 Empirical Relationships for the Properties of Thawed Fine-Grained Soils

The compendium of literature data is now used to develop empirical relationships to determine the characteristics of the $\sigma_v' - e - k_v$ relationships. The liquid limit, the clay content, the median grain size of the fine fraction and the initial thawed void ratio are used as index properties.

5.8.1 Compression Index of the Thawed Soil

Figure 5.4 presents relationships between the initial void ratio and the compression index of the thawed soil. In Figure 5.4a, a relationship is presented for ice-poor soils for which the initial void ratio is equal to the thawed void ratio. For the analyzed data set, the use of a predictive parameter in addition to the thawed void ratio is not leading to any significant increase in the precision of the empirical relationship. A unique relationship in terms of the thawed void ratio is thus adopted for ice-poor soils. In unfrozen fine-grained soils, the regression analysis based on the combination of the initial void ratio and an additional independent variable also present insignificant increases in accuracy over regression analysis based on the initial void ratio alone (Azzouz et al. 1976). In these cases, the initial void ratio can be used as a proxy for the characterization of both the soil fabric and the soil composition. As expected, Figure 5.4a shows that the compression index of thawed ice-poor soils increases with the thawed void ratio.

For ice-rich soils, the effect of the excess ice on the macrostructure has been discussed in section 5.5. It is thus warranted to use an additional predictive parameter to establish empirical relationships. In Figure 5.4b, relationships between the initial thawed void ratio and the compression index of the thawed soil are presented as a function of the median grain size of the fine fraction. The data points are presented in terms of a range of median grain size of the fine fraction value from which relationships for the average value of the range are developed. The relationship for ice-poor soils is reproduced in Figure 5.4b. Once again, the compression index of thawed soils increases with the initial thawed void ratio. Also, Figure 5.4b shows that the compression index of thawed soils increases as the size of the soil particles decreases.
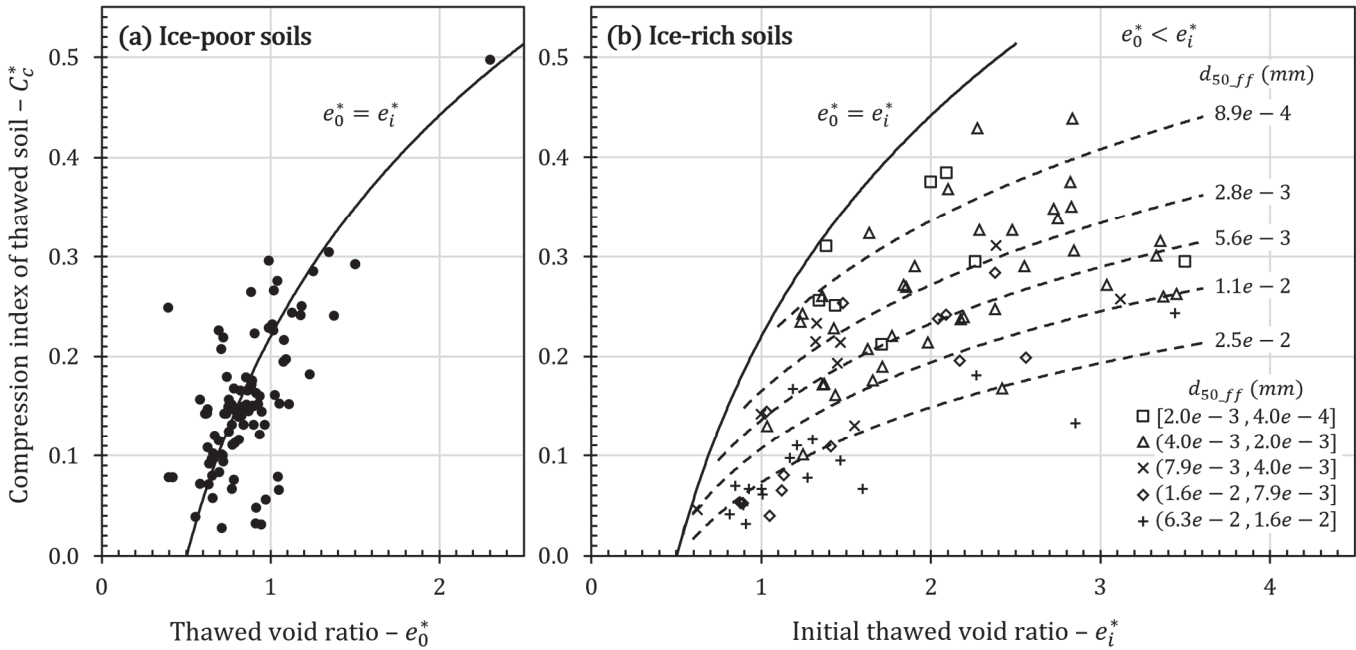
Figure 5.4 : Compression index of (a) ice-poor and (b) ice-rich thawed fine-grained soils

For the sake of illustration, the data point of an individual range of value is presented in Figure 5.5. In Figure 5.5, the ice-poor and ice-rich values alike are presented for soils with a median grain size of the fine fraction varying from 4e-3 to 2e-3 mm. The variability of the data with the predictive relationship for ice-rich soils appears to be significant. However, it should be mentioned that the illustrated predictive relationship is for the average median grain size of the fine fraction value while the data point spread over a range of value. The accuracy of the predictive relationships is best appreciated in terms of the predictive errors presented in Table 5.2 rather than visually from the graphical representation of the relationships.
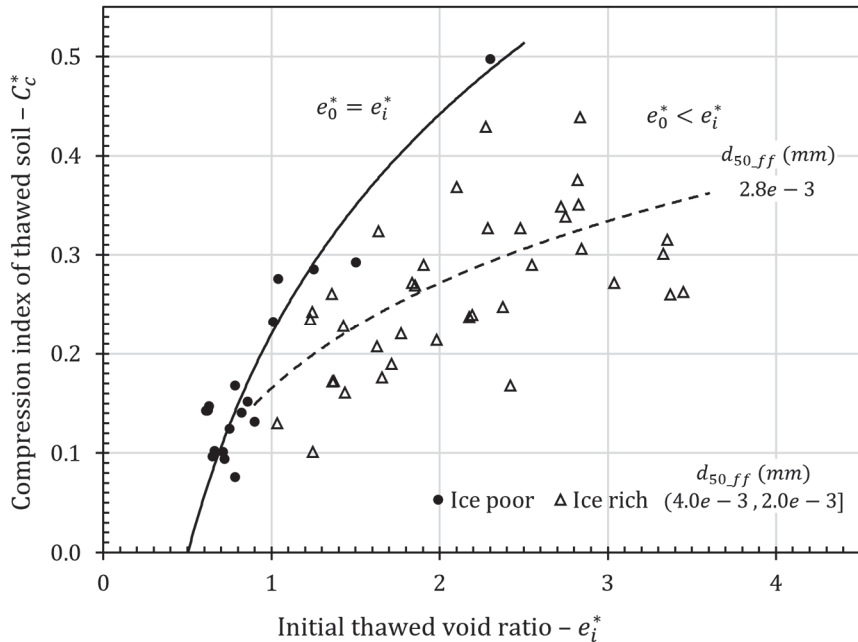
Figure 5.5 : Compression index of thawed fine-grained soils with a median grain size of the fine fraction between 4e-3 and 2e-3 mm

Table 5.2 presents the predictive relationships for the compression index of the thawed soil for ice-poor and ice-rich soils in terms of different index properties. The best-fit relationships for ice-poor soils and for the median grain size of the fine fraction presented in Table 5.2 correspond exactly to the graphical relationships presented in Figure 5.4. Relationships developed in terms of the liquid limit and the clay content are presented in addition to the relationship developed in terms of the median grain size of the fine fraction. For each relationship, the mean absolute error (MAE) is indicated to show the accuracy of the relationship. Given the general variability of geotechnical properties, the mean absolute error values obtained for all relationships for the compression index of the thawed soil is very satisfactory. For ice-rich soils, the median grain size of the fine fraction appears to be the best predictive parameter as the mean absolute error of the relationship is lowest.

Table 5.2 : Predictive relationships for the compression index of the thawed soil

	$e_0^* = e_i^*$	MAE	$e_0^* < e_i^*$	MAE
w_L (%)			$C_c^* = (0.0081w_L - 0.019)\log e_i^* + (0.0033w_L + 0.037)$	0.059
clay% (%)	$C_c^* = 0.74\log e_0^* - 0.22$	0.040	$C_c^* = (0.0051clay\% - 0.18)\log e_i^* + (0.0015clay\% + 0.096)$	0.052
d_{50_ff} (mm)			$C_c^* = (-0.11\log d_{50ff} + 0.080)\log e_i^* + (-0.097\log d_{50ff} - 0.082)$	0.043

5.8.2 Residual Stress

Figure 5.6 presents relationships between the thawed void ratio of ice-poor soils and the residual stress in terms of the median grain size of the fine fraction. While it was possible to determine the compression index of thawed ice-poor fine-grained soils from the thawed void ratio alone, the residual stress varies significantly as a function of the soil composition. As expected, the residual stress increases as the thawed void ratio decreases. Also, the residual stress at a constant thawed void ratio increases as the size of the soil particles decreases.
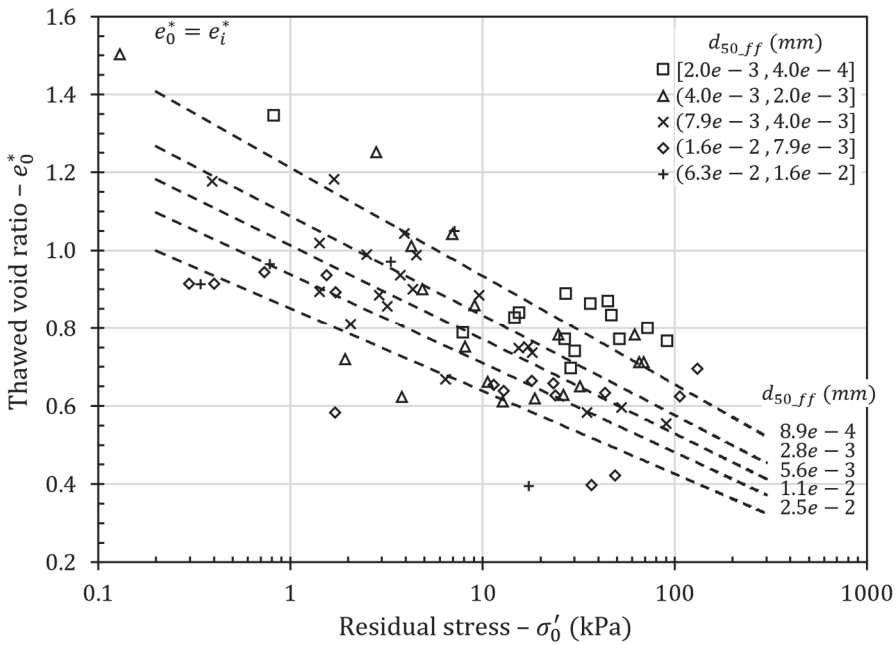
Figure 5.6 : Residual stress of thawed fine-grained soils

Table 5.3 presents the predictive relationships for the residual stress in terms of different index properties. Once again, the median grain size of the fine fraction appears to be the best predictive parameter as the mean absolute error of the relationship is lowest. The mean absolute error value of less than half an order of magnitude is very satisfactory.

148

Table 5.3 : Predictive relationships for the residual stress

	$e_0^* = e_i^*$	MAE
w_L (%)	$\sigma_0' = \exp[(e_0^* - 0.014 w_L - 0.42)/(-0.0014 w_L - 0.012)]$	$10^{0.903}$
$clay\%$ (%)	$\sigma_0' = \exp[(e_0^* - 0.0049 clay\% - 0.82)/(-0.00063 clay\% - 0.060)]$	$10^{0.659}$
d_{50_ff} (mm)	$\sigma_0' = \exp[(e_0^* + 0.25 \log d_{50\_ff} - 0.45)/(0.020 \log d_{50\_ff} - 0.060)]$	$10^{0.492}$

5.8.3 Hydraulic Conductivity Change Index of the Thawed Soil

Figure 5.7 presents relationships between the initial void ratio and the hydraulic conductivity change index of the thawed soil. The same approach as described for the compression index of the thawed soil is adopted here. In Figure 5.7a, a relationship is presented for ice-poor soils. Once again, a unique relationship in terms of the thawed void ratio is adopted for ice-poor soils. Figure 5.7a shows that the hydraulic conductivity change index of thawed ice-poor soils increases with the thawed void ratio.
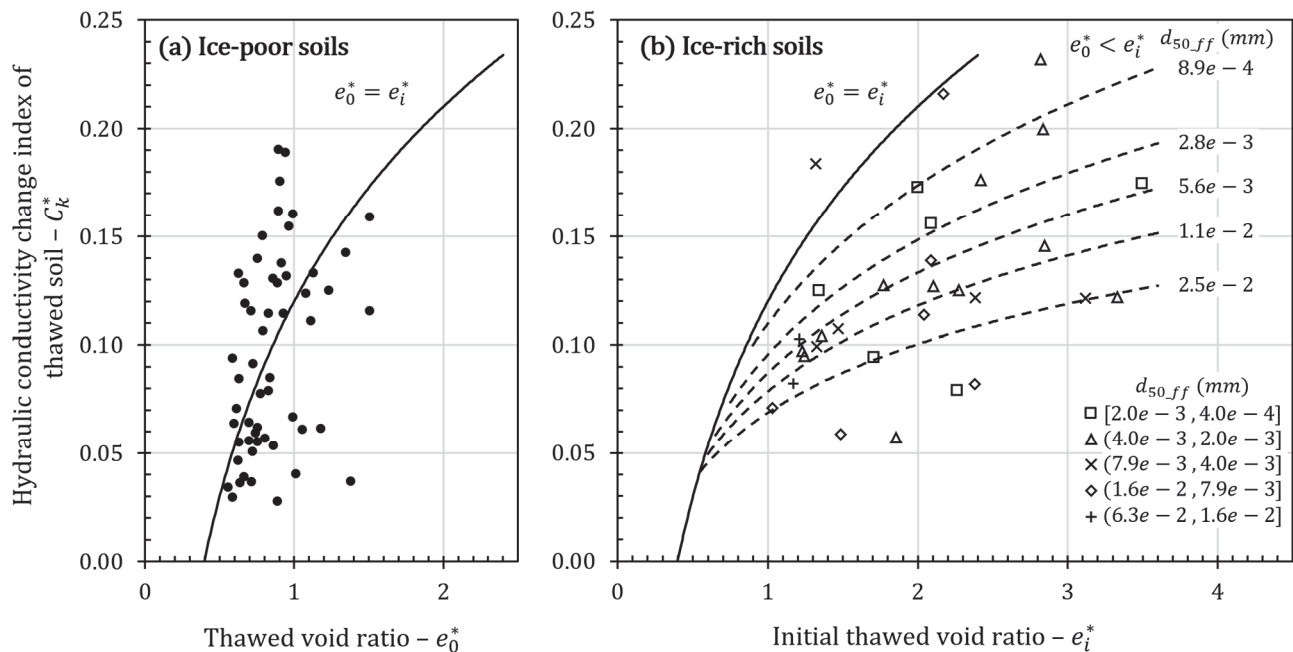
Figure 5.7 : Hydraulic conductivity change index of (a) ice-poor and (b) ice-rich thawed fine-grained soils

For ice-rich soils, Figure 5.7b presents the relationships between the initial thawed void ratio and the hydraulic conductivity change index of the thawed soil as a function of the median grain size of the fine fraction. The relationship for ice-poor soils is reproduced in Figure 5.7b. Once again, the hydraulic conductivity change index of thawed soils increases with the initial

thawed void ratio. Also, Figure 5.7b shows that the hydraulic conductivity change index of thawed soils increases as the size of the soil particles decreases.

Table 5.4 presents the predictive relationships for the hydraulic conductivity change index of thawed soils in terms of different index properties. Once again, the mean absolute error values are within an acceptable range. For the hydraulic conductivity change index of thawed soils, the clay content appears to be marginally more precise than the median grain size of the fine fraction.

Table 5.4 : Predictive relationships for the hydraulic conductivity change index of thawed soils

	$e_0^* = e_i^*$	MAE	$e_0^* < e_i^*$	MAE
w_L (%)			$C_k^* = (0.0035w_L - 0.018)\log e_i^* + (0.0019w_L + 0.021)$	0.045
$clay\%$ (%)	$C_k^* = 0.30\log e_0^* + 0.12$	0.036	$C_k^* = (0.0018clay\% - 0.099)\log e_i^* + (0.00070clay\% + 0.067)$	0.034
d_{50_ff} (mm)			$C_k^* = (-0.074\log d_{50ff} - 0.014)\log e_i^* + (-0.028\log d_{50ff} + 0.024)$	0.036

5.8.4 Initial Hydraulic Conductivity of the Thawed Soil

Figure 5.8 presents relationships between the thawed void ratio of ice-poor soils and the initial hydraulic conductivity in terms of the median grain size of the fine fraction. As expected, the initial hydraulic conductivity increases both as the thawed void ratio increases and as the size of the particles increases.
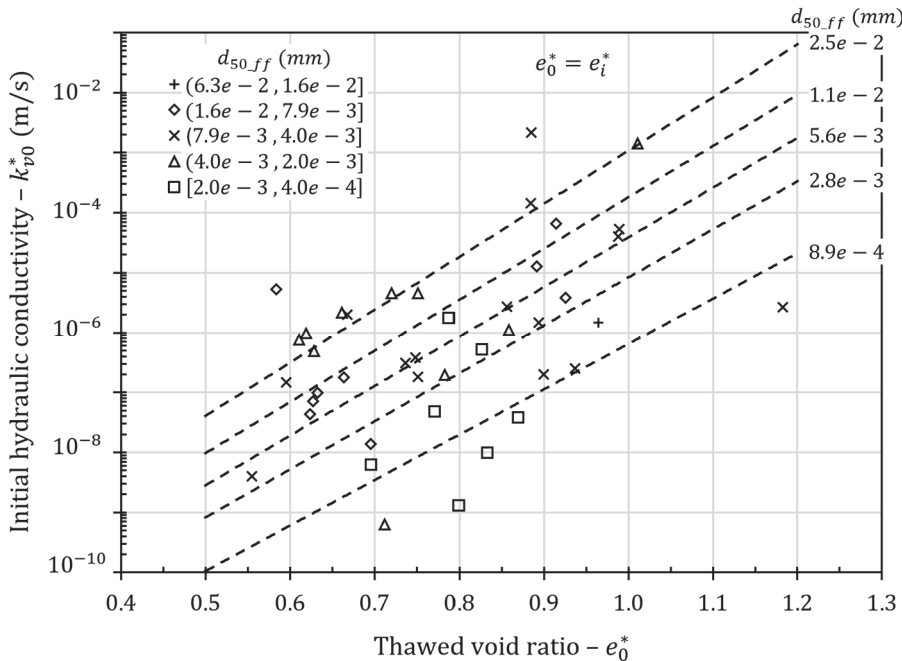
Figure 5.8 : Initial hydraulic conductivity of thawed fine-grained soils

Table 5.5 presents the predictive relationships for the initial hydraulic conductivity in terms of different index properties. The mean absolute error values of each of the three considered parameters are over one order of magnitude. However, the relationships can be considered accurate given the general variability of the hydraulic conductivity of fine-grained soils.

Table 5.5 : Predictive relationships for the initial hydraulic conductivity of thawed soils

	$e_0^* = e_i^*$	MAE
w_L (%)	$k_{v0}^* = 1.3 \times 10^{-8} \exp\left[-0.25 w_L + (0.08 w_L + 12.85) e_0^*\right]$	$10^{1.164}$
$clay\%$(%)	$k_{v0}^* = 1.1 \times 10^{-12} \exp\left[-0.077 clay\% + (-0.050 clay\% + 20.5) e_0^*\right]$	$10^{1.082}$
d_{50_ff} (mm)	$k_{v0}^* = 2.2 \times 10^{-10} \exp\left[3.1 \log d_{50ff} + (2.02 \log d_{50ff} + 23.6) e_0^*\right]$	$10^{1.064}$

5.9 Method for the Determination of the σ'ᵥ – e – kᵥ Relationships

A simple step-by-step method is now proposed to define the $\sigma_v' - e - k_v$ relationships from the empirical relationships presented in section 5.7. In this section, the particular case of ice-rich soils is first discussed with regard to the behaviour defined by the conceptual model developed in chapter 4. Then, the step-by-step method is presented. The section concludes with a working example of the method.

5.9.1 A Note on Ice-Rich Soils

The definition of the $\sigma_v' - e - k_v$ relationships for ice-rich soils must now be discussed in order to explain the use of the empirical relationships to frozen soils with excess ice. The importance of the transition from the ice-rich state to the ice-poor equivalent state should be emphasized in terms of the link between the initial thawed void ratio and the thawed void ratio.

As shown in Figure 5.1 and more precisely in Figure 4.2, thaw consolidation of an ice-rich soil is first characterized by the drainage of the excess water out of the bulk soil. Once the soil does not contain any more excess melt water, the behaviour is said to be ice-poor equivalent. This means that once the soil is at the thawed void ratio, the effective stress within the soil is equal to the residual stress and the compression of the soil skeleton is governed by a semi-logarithmic linear relationship between the void ratio and the effective stress.

As discussed in section 5.3, the excess ice contained in ice-rich soils contributes to the preservation of macro-pore space in the thawed soil. The macro-pore space is expected to

influence the compression behaviour of the ice-poor equivalent soil. In other words, there should exist a link between the initial void ratio of an ice-rich soil, its thawed void ratio and its compression index. The relationship between the initial void ratio of ice-rich soils and the compression index is shown in Figure 5.4. As the initial void ratio increases, the compression index increases due to the increasing macro-pore space in the thawed soil.
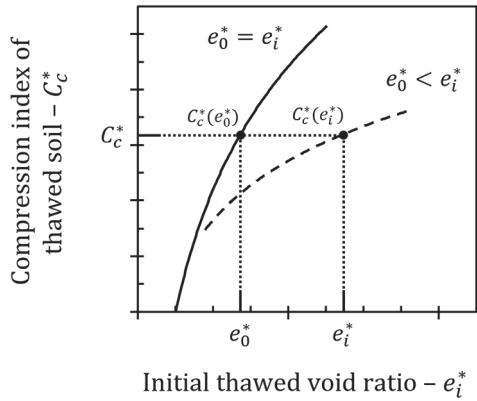
Figure 5.9 : Determination of the ice-poor equivalent thawed void ratio for ice-rich soils from the compression index of the thawed soil

Figure 5.9 presents a schematic representation of the method proposed to determine the ice-poor equivalent thawed void ratio for ice-rich soils. The thawed void ratio of the ice-poor equivalent soil can be found by using the empirical relationship between the compression index of the thawed soil and the thawed void ratio presented in Figure 5.4a. The compression index of the thawed ice-rich soil is first determined from the initial thawed void ratio. Then, the thawed void ratio of the ice-poor soil with the same compression index value is determined. The value hence determined can be used as the thawed void ratio of the ice-rich soil.

5.9.2 Step-by-Step Method

The step-by-step method for the determination of the $\sigma'_v - e - k_v$ relationships is presented in Table 5.6. It is based on the empirical relationships presented in section 5.7. It can be used as a whole to define the $\sigma'_v - e - k_v$ relationships of a soil or in part to complete relationships for which some parameters are already known. The inputs required to use the method are the frozen void ratio, one of the three index properties used in the empirical relationships (the

liquid limit, the clay content or the median grain size of the fine fraction) and an assessment of whether the soil is ice-poor or ice-rich.

Table 5.6 : Method for the determination of the $\sigma'_v - e - k_v$ relationships of thawed fine-grained soils

---

1 – Determine the initial thawed void ratio
From the frozen void ratio e_f

$$e_i^* = \frac{e_f}{1.09}$$

---

2 – Determine the compression index of the thawed soil
(a) For ice-poor soils from the thawed void ratio $e_0^* = e_i^*$

$$C_c^* = 0.74 \log e_0^* + 0.22$$

(b) For ice-rich soils from the initial void ratio e_i^*

w_L (%)	$C_c^* = (0.0081 w_L - 0.019) \log e_i^* + (0.0033 w_L + 0.037)$
$clay\%$ (%)	$C_c^* = (0.0051 clay\% - 0.18) \log e_i^* + (0.0015 clay\% + 0.096)$
d_{50_ff} (mm)	$C_c^* = (-0.11 \log d_{50ff} + 0.080) \log e_i^* + (-0.097 \log d_{50ff} - 0.082)$

---

3 – Determine the thawed void ratio of the ice-poor equivalent soil (for ice-rich soils only)
From the compression index of the thawed soils C_c^*

$$e_0^* = 10^{\frac{C_c^* - 0.22}{0.74}}$$

---

4 – Determine the residual stress
From the thawed void ratio e_0^*

w_L (%)	$\sigma_0' = \exp[(e_0^* - 0.014 w_L - 0.42)/(-0.0014 w_L - 0.012)]$
$clay\%$ (%)	$\sigma_0' = \exp[(e_0^* - 0.0049 clay\% - 0.82)/(-0.00063 clay\% - 0.060)]$
d_{50_ff} (mm)	$\sigma_0' = \exp[(e_0^* + 0.25 \log d_{50\_ff} - 0.45)/(0.02 \log d_{50ff} - 0.060)]$

---

5 – Determine the hydraulic conductivity change index of the thawed soil
(a) For ice-poor soils from the thawed void ratio $e_0^* = e_i^*$

$$C_k^* = 0.30 \log e_0^* + 0.12$$

(b) For ice-rich soils from the initial void ratio e_i^*

w_L (%)	$C_k^* = (0.0035 w_L - 0.018) \log e_i^* + (0.0019 w_L + 0.021)$
$clay\%$ (%)	$C_k^* = (0.0018 clay\% - 0.099) \log e_i^* + (0.00070 clay\% + 0.067)$
d_{50_ff} (mm)	$C_k^* = (-0.074 \log d_{50ff} - 0.014) \log e_i^* + (-0.028 \log d_{50ff} + 0.024)$

---

6 – Determine the initial hydraulic conductivity of the thawed soil
From the thawed void ratio e_0^*

w_L (%)	$k_{v0}^* = 1.3 \times 10^{-8} \exp[-0.25 w_L + (0.08 w_L + 12.85) e_0^*]$
$clay\%$ (%)	$k_{v0}^* = 1.1 \times 10^{-12} \exp[-0.077 clay\% + (-0.050 clay\% + 20.5) e_0^*]$
d_{50_ff} (mm)	$k_{v0}^* = 2.2 \times 10^{-10} \exp[3.1 \log d_{50ff} + (2.02 \log d_{50ff} + 23.6) e_0^*]$

5.9.3 Working Example

A working example is now presented to illustrate the use of the step-by-step method for the determination of the $\sigma'_v - e - k_v$ relationships of a thawed fine-grained soil. The figures presented in section 5.7 are used in this example as an alternative to the equations presented in Table 5.6 since the median grain size of the fine fraction is used as the predictive parameter. In this example, an ice-rich silty clay with a frozen void ratio of 2.0 and a median grain size of the fine fraction of 2.8e-3 mm is considered. Application of the step-by-step method is presented in Table 5.7. Figure 5.14 presents the complete $\sigma'_v - e - k_v$ relationships of the soil.

Table 5.7 : Working example of the method for the determination of the $\sigma'_v - e - k_v$ relationships of an ice-rich silty clay with e_f=2.0 and d_{50_ff}=2.8e-3 mm

---

1 – Determine the initial thawed void ratio from the frozen void ratio $e_f = 2.0$

$$e_i^* = \frac{e_f}{1.09} = \frac{2.0}{1.09} = 1.83$$

---

2 – Determine the compression index of the thawed soil (see Figure 5.10)
    (b) For ice-rich soils from the initial void ratio $e_i^* = 1.83$ with $d_{50\_ff} = 2.8e - 3\ mm$

$C_c^* = 0.26$

---

3 – Determine the thawed void ratio of the ice-poor equivalent soil (see Figure 5.10)
    For $C_c^* = 0.26$

$e_0^* = 1.13$

---

4 – Determine the residual stress (see Figure 5.11)
    For $e_0^* = 1.13$ with $d_{50\_ff} = 2.8e - 3\ mm$

$\sigma'_0 = 0.66\ kPa$

---

5 – Determine the hydraulic conductivity change index of the thawed soil (see Figure 5.12)
    (b) For ice-rich soils from the initial void ratio $e_i^* = 1.83$ with $d_{50\_ff} = 2.8e - 3\ mm$

$C_k^* = 0.14$

---

6 – Determine the initial hydraulic conductivity of the thawed soil (see Figure 5.13)
    For $e_0^* = 1.13$ with $d_{50\_ff} = 2.8e - 3\ mm$

$k_{v0}^* = 9.9e - 5\ m/s$
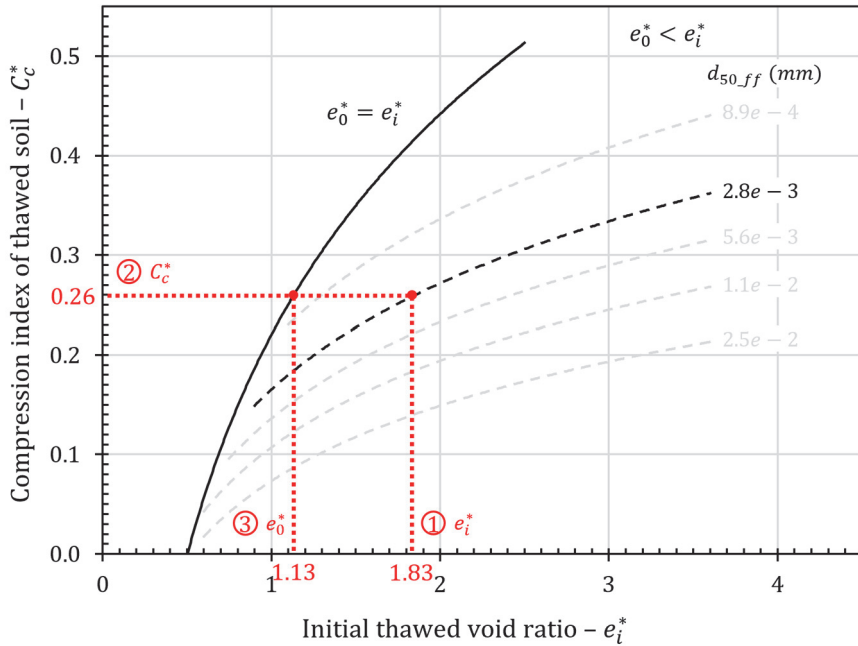
Figure 5.10 : Determination of the compression index and the thawed void ratio of an ice-rich silty clay with e_f=2.0 and d_{50_ff}=2.8e-3 mm (see Table 5.7 steps 1,2 and 3)
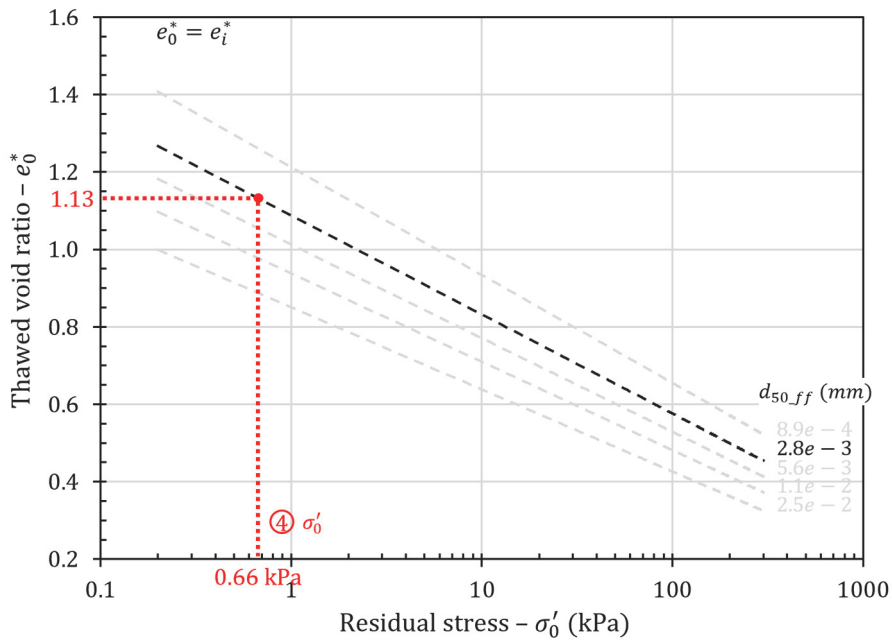
Figure 5.11 : Determination of the residual stress of an ice-rich silty clay with e_f=2.0 and d_{50_ff}=2.8e-3 mm (see Table 5.7 steps 4)
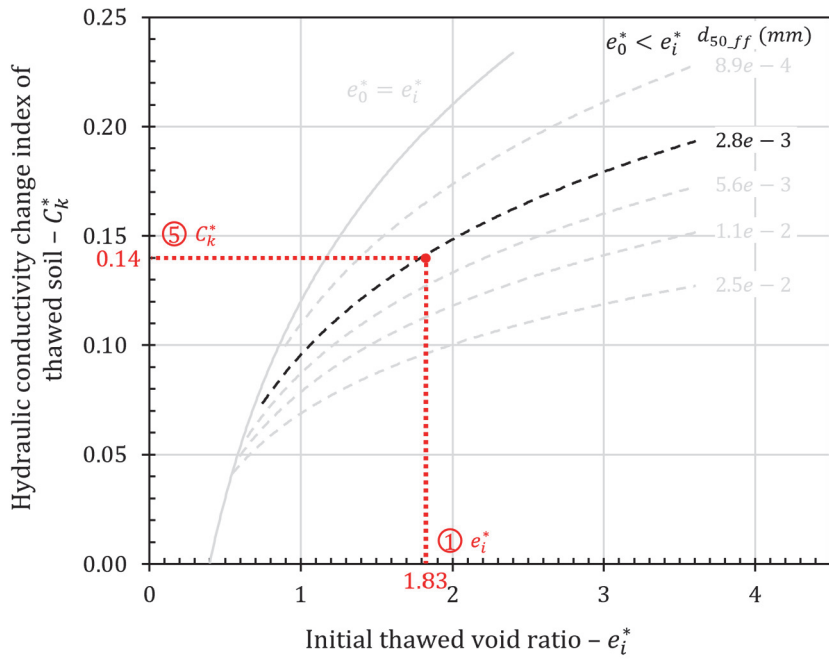
Figure 5.12 : Determination of the hydraulic conductivity change index of an ice-rich silty clay with
e_f=2.0 and d_{50_ff}=2.8e-3 mm (see Table 5.7 steps 5)
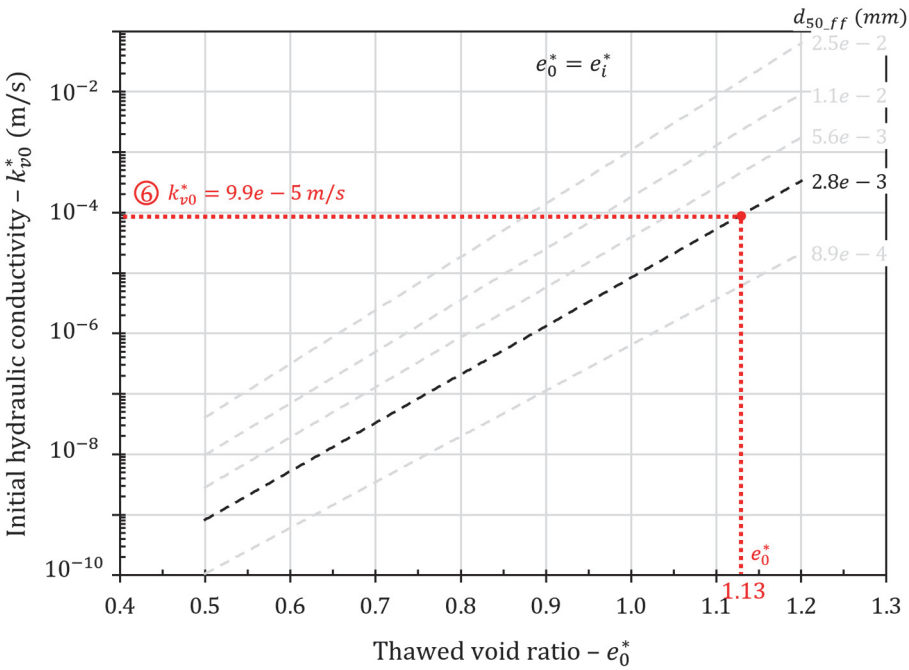
Figure 5.13 : Determination of the initial hydraulic conductivity of an ice-rich silty clay with e_f=2.0
and d_{50_ff}=2.8e-3 mm (see Table 5.7 steps 5)
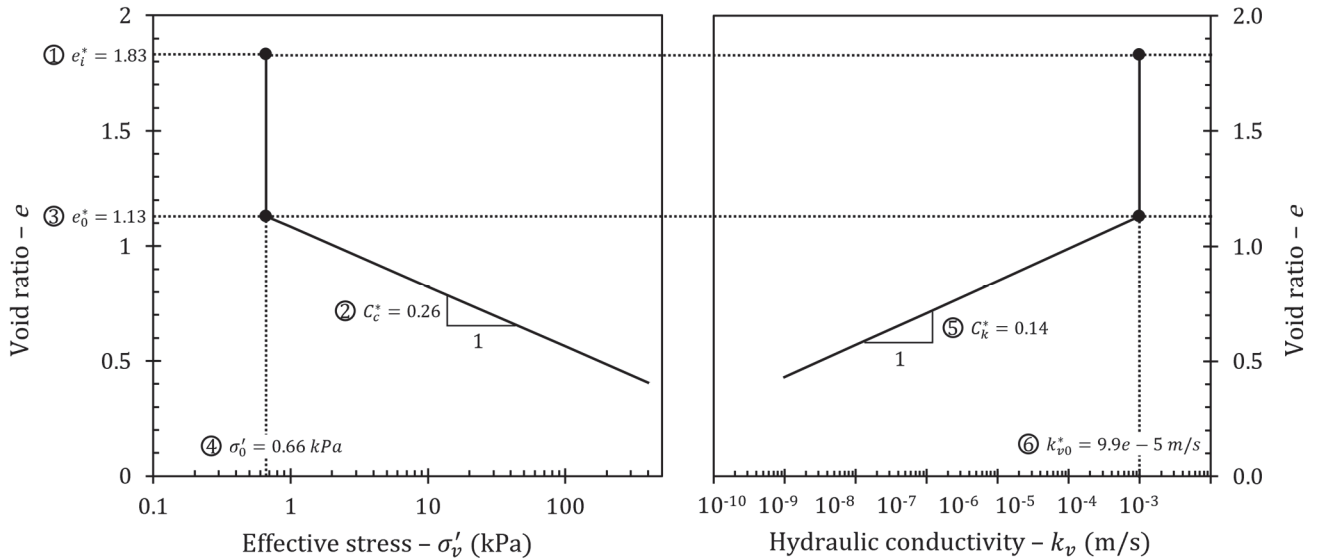
Figure 5.14 : The $\sigma'_v - e - k_v$ relationships of an ice-rich silty clay with e_f=2.0 and d_{50_ff}=2.8e-3 mm

5.10 Conclusion

Empirical relationships for the determination of the characteristics of the $\sigma'_v - e - k_v$ relationships of thawed fine-grained soils have been proposed. For ice-poor soils, the compression index of the thawed soil and the hydraulic conductivity change index of the thawed soil are functions of the thawed void ratio. For ice-rich soils, these two characteristics are functions of the initial thawed void ratio and of index properties which characterizes the soil composition and the soil fabric. The liquid limit, the clay content and the median grain size of the fine fraction are used as predictive parameters with the median grain size of the fine fraction yielding the greatest precision. The thawed void ratio of ice-rich soils can be obtained from the ice-poor equivalent soil with the same compression index. The residual stress and the initial hydraulic conductivity are functions of the thawed void ratio and of index properties. A step-by-step method based on the empirical relationships is proposed to define completely the $\sigma'_v - e - k_v$ relationships of thawed fine-grained soils or to supplement incomplete relationships.

The proposed empirical relationships are defined in agreement with the definition of the $\sigma'_v - e - k_v$ relationships of thawed fine-grained soils formulated by the conceptual model formulated in chapter 4. Hence, they can be used to define the input parameters required for the numerical modelling of thaw consolidation with the model formulated in chapter 2.

Discussion complémentaire

L'objectif du chapitre 5 est de présenter le développement de relations empiriques pour la caractérisation des relations $\sigma'_v - e - k_v$ des sols dégelés à grains fins (axe 2 – objectif 2.2 de la thèse). Ce développement est fait en fonction du modèle conceptuel présenté au chapitre 4. Le but est donc de permettre de définir les intrants pour la modélisation numérique de la consolidation au dégel grâce au modèle non linéaire à grandes déformations développé au chapitre 2.

Un article intitulé « Compressibility and hydraulic conductivity of thawed fine-grained permafrost » ayant été publié dans les actes du « 11th International Symposium on Cold Regions Development » en 2016 se trouve en annexe. Il s'agit d'un travail préliminaire concernant l'étude des propriétés des sols lors du dégel. Bien que l'analyse présentée dans cet article soit assez différente de celle présentée au chapitre 5, il s'agit tout de même d'un travail intéressant surtout au point de vue de l'identification des paramètres de sol pouvant être utilisés pour prédire les caractéristiques des relations $\sigma'_v - e - k_v$.

Tel que discuté en introduction du chapitre, la caractérisation des relations $\sigma'_v - e - k_v$ des sols dégelés à grains fins peut représenter un obstacle majeur à l'utilisation du modèle non linéaire à grandes déformations présenté au chapitre 2. En effet, des coûts importants sont associés aux campagnes de forage et aux essais de laboratoire nécessaires à la détermination de ces propriétés ce qui représente une contrainte importante pour les ingénieurs dans la pratique. Les relations empiriques développées au chapitre 5 permettent d'utiliser le modèle lorsque la caractérisation en laboratoire des relations $\sigma'_v - e - k_v$ n'est pas possible ou n'est pas accessible techniquement ou financièrement.

Bien que l'utilisation de relations empiriques dans la pratique du génie puisse représenter une certaine économie de coût par rapport à la réalisation de forages, d'essais in situ et d'essais de laboratoire, il est important de noter que l'incertitude associée à l'utilisation de relations empiriques peut aussi entrainer une augmentation de coût, car la conception nécessite alors un facteur de sécurité supplémentaire. Selon le type d'ouvrages considérés, il peut s'avérer moins coûteux de réaliser une conception basée sur des paramètres de sols définis précisément en laboratoire plutôt que sur les relations empiriques présentées ayant un certain

degré d'incertitude. Pour les infrastructures dont la tolérance aux conséquences de la consolidation au dégel est faible, il vaudrait mieux privilégier une approche plus complète d'évaluation des propriétés de sol alors que les relations empiriques peuvent être utilisées directement pour les infrastructures ayant une tolérance élevée aux conséquences de la consolidation au dégel. Enfin, il est important de noter que la méthode empirique proposée requiert de connaître la valeur d'indice des vides initial du sol dégelé. Cette valeur est typiquement obtenue à partir d'un échantillon de sol intact. Dans certains cas, les coûts additionnels engendrés par la réalisation d'essai de laboratoire sur un échantillon déjà prélevé ne sont pas excessifs par rapport au gain de précision obtenue. Cependant, l'utilisation des relations empiriques devient particulièrement intéressante pour compléter et pour valider les caractéristiques de propriétés déterminer en laboratoire.

La précision des relations empiriques est très satisfaisante. Il faut tenir en compte qu'une partie de l'incertitude liée à ces relations provient de la variabilité générale des propriétés géotechniques ainsi que de l'incertitude des mesures en laboratoire. Ce dernier point est particulièrement applicable à la détermination de la conductivité hydraulique des sols dégelés. Ainsi, il est normal d'obtenir une erreur plus importante pour la prédiction de la conductivité hydraulique. Néanmoins, les relations empiriques ont été développées à partir de l'analyse du comportement au dégel des sols aussi bien au niveau du modèle conceptuel que de la définition des caractéristiques. Ainsi, les relations proposées possèdent une signification physique et elles n'ont pas été développées simplement à partir de paramètres pour lesquels on obtiendrait une meilleure précision.

Une application potentielle des relations empiriques proposées serait le développement d'outils de calcul graphiques pour l'évaluation de la consolidation au dégel. En effet, ces relations pourraient être utilisées en combinaison avec le modèle numérique présenté au chapitre 2 afin de réaliser une analyse paramétrique. Des outils de calcul graphiques pourraient être développés pour les quantités d'intérêt (ex. : pressions interstitielles excédentaires et tassements de fonte) à partir des propriétés d'indice. Ces outils de calcul permettraient de faciliter l'utilisation du modèle pour des évaluations préliminaires alors qu'il n'est pas possible de développer de solutions analytiques pour le modèle numérique présenté au chapitre 2.

À la section 5.8.1, une méthode de détermination de l'indice des vides dégelé e_0^* à partir de l'indice de compression du sol dégelé C_c^* est présentée. Cette méthode est appuyée par le développement théorique du modèle conceptuel présenté au chapitre 4. On pose l'hypothèse qu'un sol riche en glace se comporte de manière équivalente à un sol pauvre en glace à la suite du drainage de l'eau en excès. Ainsi, il doit exister un sol pauvre en glace ayant un indice des vides dégelé e_0^* ayant le même indice de compression que le sol riche en glace. Les relations empiriques permettent d'obtenir l'indice de compression du sol riche en glace à partir de l'indice des vides initial du sol dégelé e_i^* et l'indice de compression du sol pauvre en glace à partir de l'indice des vides du sol dégelé e_0^*. L'indice de compression du sol riche en glace permet donc d'obtenir l'indice des vides du sol dégelé e_0^* d'un sol pauvre en glace équivalent. Il est aussi possible d'appliquer cette méthode avec l'indice de changement de conductivité hydraulique du sol dégelé C_k^*. De la même manière, l'indice de changement de conductivité hydraulique du sol riche en glace est obtenu à partir de l'indice des vides initial du sol dégelé e_i^* et l'indice des vides dégelé du sol pauvre en glace équivalent est obtenu à partir de cet indice de changement de la conductivité hydraulique. Il est tout de même recommandé d'utiliser l'indice de compression du sol dégelé pour déterminer l'indice des vides du sol dégelé, car la précision des relations empiriques pour ce paramètre est meilleure que pour l'indice de changement de la conductivité hydraulique. Pour l'exemple présenté à la section 5.8.3, on obtiendrait une valeur d'indice des vides du sol dégelé de 1,18 à partir de la valeur de l'indice de changement de la conductivité hydraulique de 0,14 plutôt que la valeur de 1,13 obtenue avec l'indice de compression.

Le grand nombre de données et de caractéristiques analysé pour le développement des relations empiriques permet aussi d'étudier certaines particularités des propriétés des sols dégelés à grains fins. Une analyse intéressante à réaliser est de vérifier si les sols dégelés à grains fins respectent les conditions de validité de la théorie de consolidation linéaire à petites déformations de Terzaghi. Cette théorie est utilisée comme composante hydromécanique de la théorie de consolidation au dégel de Morgenstern et Nixon (1971). L'analyse présentée à la Figure 5.15 s'applique donc aussi à cette théorie de consolidation au dégel.
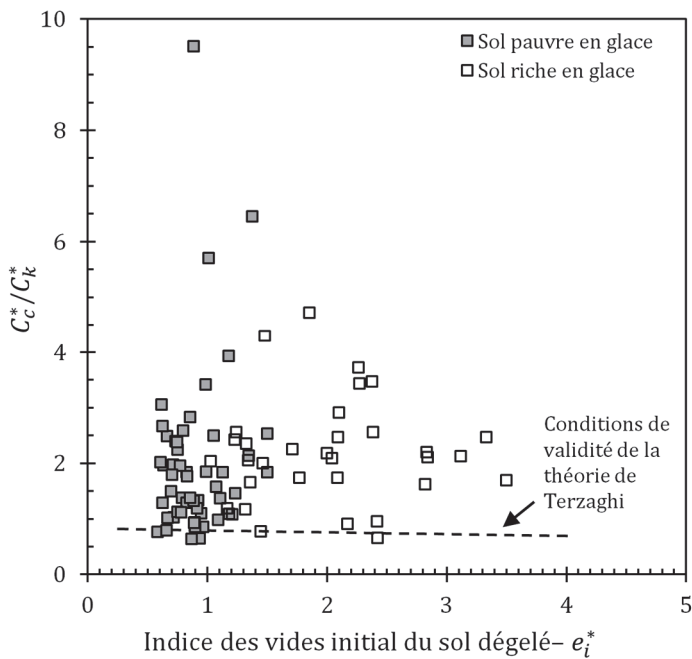
Figure 5.15 : Évaluation de la validité de la théorie de Terzaghi pour les sols dégelés à grains fins

La théorie de Terzaghi assume que le coefficient de consolidation du sol est constant lors de la consolidation. Deux conditions peuvent permettre de remplir les conditions de validité de cette hypothèse. Premièrement, les conditions sont respectées si le changement d'indice des vides lors de la consolidation est très faible. Or, c'est rarement le cas des pergélisols lors du dégel, du moins, dans le cas des sols problématiques au dégel. Deuxièmement, les conditions de validité sont remplies si un certain rapport est respecté entre le changement de conductivité hydraulique en fonction de l'indice des vides et le changement d'indice des vides en fonction de la contrainte effective. Ce rapport peut être caractérisé par le ratio entre l'indice de compression et l'indice de changement de la conductivité hydraulique en fonction de l'indice des vides initial du sol. Ce ratio qui a été établis par Tavenas et coll. (1983) est présenté à la Figure 5.15. La Figure 5.15 présente aussi le ratio C_c^*/C_k^* en fonction de l'indice des vides initial du sol dégelé pour l'ensemble des sols étudiés au chapitre 5. Pour respecter les conditions de validité de la théorie de Terzaghi quant au comportement linéaire des sols lors de la consolidation, le sol doit se trouver sur la courbe pointillée. On constate que très peu de sols respectent ces conditions. Ainsi, la théorie de Terzaghi et par extension la théorie de consolidation au dégel de Morgenstern et Nixon sont théoriquement rarement applicables aux sols dégelés. Certaines corrections à la théorie de consolidation au dégel de Morgenstern

et Nixon ont été proposées pour améliorer la modélisation des sols non linéaires (Nixon 1973). Cependant, celles-ci sont formulées en fonction de la contrainte résiduelle et ne corrigent pas l'ensemble du comportement non linéaire, notamment en ce qui concerne la variation de conductivité hydraulique.

Conclusion

Résumé et conclusions

Cette thèse présente le développement d'une méthode d'ingénierie complète pour la modélisation de la consolidation au dégel. Les travaux se divisent en deux axes de recherche concomitants. L'axe 1 porte sur le développement d'un modèle numérique pour la consolidation au dégel non linéaire à grandes déformations. L'axe 2 porte sur la définition des propriétés hydromécaniques des sols dégelés utilisées comme intrants au modèle numérique de consolidation au dégel.

Les chapitres 2 et 3 de cette thèse présentent les travaux relatifs à l'axe 1. Les équations décrivant le phénomène unidimensionnel de consolidation au dégel ainsi que leur implémentation au sein d'un modèle numérique sont présentées. La théorie de consolidation à grandes déformations de Gibson est utilisée comme composante hydromécanique du modèle. La théorie de Gibson est une généralisation de la théorie de consolidation par filtration. La théorie est formulée en fonction des changements d'indice des vides. Il est donc possible de considérer les déformations du sol ainsi que la variation des propriétés hydromécaniques du sol lors de la consolidation. Des équations simples de transfert de chaleur par conduction et advection sont utilisées comme composante thermique du modèle. Les deux composantes sont couplées au sein d'un domaine de consolidation défini en fonction de coordonnées lagrangiennes. Les coordonnées lagrangiennes permettent de considérer entièrement les déformations du sol, et donc, le déplacement de la position des conditions limites. Le domaine de consolidation au dégel est défini entre la surface du sol et le front de dégel. Dans les faits, l'utilisation des coordonnées lagrangiennes permet l'introduction d'une frontière mobile à la surface. Le modèle de consolidation au dégel est donc un modèle à deux frontières mobiles : une à la surface et une au front de dégel. À la surface, des conditions limites de drainage libre et les conditions thermiques provoquant le dégel du sol initialement gelé sont imposées. Le sol gelé est considéré comme étant imperméable et indéformable. Au front de dégel, les conditions limites d'une frontière imperméable sont donc imposées. Les conditions limites au front de dégel sont formulées en revisitant les conditions formulées pour le développement du modèle de consolidation au dégel à petites déformations de Morgenstern et Nixon pour le contexte à grandes

déformations. Les déformations dues au changement de phase sont aussi intégrées aux conditions limites au front de dégel. La composante hydromécanique du modèle de consolidation au dégel à grandes déformations proposé utilise des relations non linéaires entre la contrainte effective, l'indice des vides et la conductivité hydraulique. L'indice des vides est utilisé comme variable d'état conformément à l'équation de Gibson.

Au chapitre 2, le modèle numérique de consolidation au dégel non linéaire à grandes déformations est appliqué au cas théorique d'un échantillon de sol lors d'un essai de consolidation au dégel. Cet exemple théorique permet de démontrer les aspects suivants du modèle :

1. Le déplacement de la frontière à la surface du sol est pris en compte par le modèle. Ainsi, le déplacement des conditions limites imposées à la surface est considéré.

    a. Le déplacement de la source de chaleur vers le front de dégel provoque une accélération de la pénétration du dégel.

    b. Le déplacement de la surface de drainage libre vers le front de dégel provoque une réduction de la hauteur de drainage par rapport à une configuration à petites déformations.

2. Les phases de consolidation au dégel et de consolidation post-dégel sont modélisées successivement par le modèle à partir de la même configuration de modélisation. Surtout, les deux phases sont modélisées en utilisant les mêmes relations non linéaires entre la contrainte effective, l'indice des vides et la conductivité hydraulique.

3. La configuration à grandes déformations offre une représentation physiquement cohérente de la consolidation au dégel.

4. L'évolution et l'interdépendance des propriétés hydromécaniques et thermiques du sol sont dument prises en charge par le modèle.

Les résultats théoriques obtenus pour l'exemple présenté au chapitre 2 sont comparés aux résultats obtenus avec la théorie linéaire à petites déformations de Morgenstern et Nixon. La principale différence soulignée par cette comparaison entre les deux approches se situe au

niveau de la définition de la profondeur de dégel. Pour une configuration à petites déformations, la profondeur de dégel est calculée en tout temps par rapport à la position actuelle de la surface. Pour une configuration à grandes déformations, la profondeur de dégel est calculée par rapport à la position initiale de la surface. Lorsque les déformations au dégel sont importantes, le taux de pénétration au dégel est donc sous-estimé par la configuration à petites déformations. Ainsi, la théorie de consolidation au dégel à petites déformations peut sous-estimer les pressions interstitielles excédentaires dans la couche de sol dégelé.

Au chapitre 3, le modèle de consolidation au dégel non linéaire à grandes déformations est utilisé pour modéliser le cas du pipeline expérimental d'Inuvik. Cette étude de cas permet de faire une validation du modèle, de déterminer ses implications pratiques et de faire une comparaison avec les résultats obtenus avec la théorie de Morgenstern et Nixon.

En ce qui concerne la validation du modèle, les résultats obtenus par le modèle de consolidation au dégel non linéaire à grandes déformations pour la profondeur de dégel, pour l'évolution des tassements de fonte, pour les tassements de fonte totaux et pour les pressions interstitielles excédentaires maximales se comparent favorablement aux valeurs mesurées sur le terrain. Ils offrent aussi une amélioration de la précision de prédiction par rapport aux résultats de modélisation obtenus avec la théorie de consolidation au dégel linéaire à petites déformations. Notamment :

1. La différence conceptuelle de la configuration de la profondeur de dégel pour l'approche à petites déformations et pour l'approche à grandes déformations est encore une fois abordée. Les résultats de modélisation démontrent qu'en négligeant le mouvement de la surface le taux de pénétration du dégel est sous-estimé. La configuration adoptée par l'approche à grandes déformations offre une prédiction précise du taux de pénétration au dégel qui concorde avec les valeurs mesurées sur le terrain.

2. Pour le pipeline d'Inuvik, la prédiction des tassements de fonte du modèle non linéaire à grandes déformations est plus précise que la prédiction du modèle linéaire à petites déformations. Deux aspects du modèle non linéaire à grandes déformations expliquent ce gain de précision : l'utilisation de relations $\sigma'_v - e$

permettant de mieux caractériser les propriétés du sol et la capacité du modèle à considérer un profile d'indice des vides initial plus complexe. En effet, le modèle linéaire à petites déformations est limité à utiliser un indice des vides initial constant et homogène alors que le modèle non linéaire à grandes déformations peut considérer un profil complexe plus représentatif des conditions de terrain.

3. L'évolution des tassements modélisée par le modèle non linéaire à grandes déformations correspond aux mesures in situ, autant durant la phase de dégel que lors de la phase post-dégel. La caractérisation non linéaire des relations $\sigma'_v - e$ contribue grandement au gain de précision. En effet, l'approximation linéaire utilisée par la théorie à petites déformations mène à une sous-estimation du taux de consolidation durant le dégel et à une surestimation du taux de consolidation durant la phase post-dégel.

4. Tous ces éléments contribuent à une prédiction plus sécuritaire et robuste des pressions interstitielles excédentaires maximales par le modèle non linéaire à grandes déformations.

Les chapitres 4 et 3 de cette thèse présentent les travaux relatifs à l'axe 2. Au chapitre 4, un modèle conceptuel pour les propriétés des sols dégelés à grains fins est proposé. L'objectif du modèle conceptuel est de définir les paramètres hydromécaniques utilisés comme intrants au modèle numérique de consolidation au dégel non linéaire à grandes déformations. Les caractéristiques des relations $\sigma'_v - e - k_v$ des sols dégelés à grains fins sont donc définis.

Le concept de la contrainte résiduelle est généralisé aux sols riches en glace en spécifiant que la contrainte résiduelle correspond à la contrainte effective au sein du squelette de sol plutôt que la contrainte effective du sol global. Ainsi, la distinction entre les sols pauvres en glace et les sols riches en glace peut être définis en fonction de la contrainte résiduelle. Lors du dégel en conditions drainées sous un charge appliquée égale à la contrainte résiduelle, les sols pauvres en glace peuvent absorber toute l'eau de fonte. Pour les sols riches en glace, il y a de l'eau de font en excès du volume que le squelette de sol peut absorber.

Les relations $\sigma'_v - e - k_v$ des sols dégelés à grains fins sont alors définis. Pour un sol pauvre en glace, la relation entre la contrainte et les déformations est définie par une relation $\sigma'_v - e$ linéaire semi-logarithmique. La pente de la relation $\log \sigma'_v - e$ est donnée par l'indice de compression du sol dégelé. Pour les sols riches en glace, l'eau de fonte en excès est d'abord drainée hors du squelette de sol sans engendrer de compression du squelette de sol. Suite au drainage de l'eau en excès le sol se comporte comme un sol pauvre en glace. Une relation bilinéaire semi-logarithmique est donc adoptée pour les sols riches en glace. D'abord, le drainage de l'eau en excès se produit à contrainte effective constante à la contrainte résiduelle. Ensuite, une relation $\sigma'_v - e$ linéaire semi-logarithmique équivalente à celle des sols pauvres en glace est adoptée. La relation $e - k_v$ des sols dégelés à grains fins est définie par une relation linéaire semi-logarithmique avec une pente définie par l'indice de changement de la conductivité hydraulique du sol dégelé. Pour les sols riches en glace, le drainage de l'eau en excès est contrôlé par les éléments de sols surconsolidés. Les conditions initiales du sol à la contrainte résiduelle sont données par l'indice des vides du sol dégelé et par la conductivité hydraulique initiale du sol dégelé.

En continuité au chapitre 4, le chapitre 5 propose une méthode empirique pour déterminer les caractéristiques des relations $\sigma'_v - e - k_v$ des sols dégelés à grains fins. Il s'agit d'une contribution importante afin de favoriser l'adoption du modèle numérique, car la détermination des propriétés des pergélisols représente un défi logistique important. La composition et la structure des sols gouvernent le comportement au dégel des sols à grains fins. Ces propriétés sont caractérisées par la macrostructure et la microstructure résultant de l'interaction entre les particules silteuses plus grossières et les particules argileuses plus fines. Le gel et le dégel affectent les caractéristiques de la macrostructure et la microstructure des sols dégelés à grains fins. La teneur en glace des sols riches en glace a aussi un impact sur la macrostructure des sols dégelé alors que l'écoulement de l'eau de fonte en excès favorise le maintien de l'espace dans les macro-pores. Pour développer des relations empiriques, des paramètres d'index sont identifiés pour caractériser les propriétés des sols dégelés. La limite de liquidité, la teneur en particules argileuses et la taille médiane des grains de la fraction fine sont les trois paramètres sélectionnés pour développer les relations empiriques. De plus, l'indice des vides du sol dégelé et l'indice des vides initial du sol dégelé sont utilisés comme paramètre d'état pour les sols pauvres en glace et les sols riches en glace respectivement.

Pour les sols pauvres en glace, l'indice de compression du sol dégelé et l'indice de changement de la conductivité hydraulique du sol dégelé sont fonction de l'indice des vides du sol dégelé. Pour les sols riches en glace, ces indices sont fonction de l'indice des vides initial du sol dégelé et des paramètres d'indice énumérés précédemment. L'indice des vides du sol dégelé pour les sols riches en glace est obtenu à partir du sol pauvre en glace équivalent ayant le même indice de compression du sol dégelé que celui du sol riche en glace. La contrainte résiduelle et la conductivité hydraulique initiale du sol dégelé sont fonction de l'indice des vides du sol dégelé et des paramètres d'indice énumérés précédemment. Généralement, les relations développées à partir de la taille médiane des grains de la fraction fine offrent une meilleure précision que celles développées à partir de la limite de liquidité ou de la teneur en particules argileuses.

Implications pratiques

L'adoption des modèles présentés dans cette thèse dans la pratique de la géotechnique a été une considération importante tout au long de leur développement. Ainsi, les travaux ont été menés avec un esprit pratique. Les coûts de calcul associés à l'utilisation du modèle numérique de consolidation au dégel non linéaire à grandes déformations ne sont pas prohibitifs à son utilisation dans la pratique de la géotechnique des régions froides. De plus, le modèle conceptuel et la méthode empiriques proposés pour déterminer les propriétés des sols nécessaires à la modélisation de la consolidation au dégel non linéaire à grandes déformations rendent accessible l'utilisation du modèle numérique. Enfin, l'étude de cas du pipeline d'Inuvik a permis de démontrer que la principale contribution du modèle numérique repose dans sa capacité à utiliser efficacement et objectivement les intrants connus afin d'augmenter considérablement la précision des calculs.

Néanmoins, il est convenu que l'utilisation d'un modèle numérique relativement complexe n'est pas nécessairement adaptée à certaines études géotechniques. Dans ces cas, les travaux présentés dans cette thèse présentent certaines conclusions qu'il faut prendre en compte :

1. Pour la modélisation de la consolidation au dégel, la profondeur de dégel doit être calculée en fonction de la position initiale du sol afin d'obtenir le taux de déplacement du front de dégel relativement à la configuration initiale. Le taux de pénétration au

dégel calculé en fonction de la distance entre le front de dégel et la surface du sol dans les théories et modèles à petites déformations entrainent une surestimation de la vitesse du front de dégel.

2. Les pressions interstitielles excédentaires peuvent être sous-estimées si le taux de pénétration au dégel dans une configuration à petites déformations est utilisé.

3. L'utilisation d'une relation $\sigma_v' - e$ linéaire pour la modélisation de la consolidation au dégel mène à une sous-estimation du taux de consolidation lors de la phase de dégel et à une surestimation du taux de consolidation lors de la phase post-dégel.

4. Les propriétés des sols dégelés à grains fins peuvent être déterminées empiriquement en fonction de relations $\sigma_v' - e - k_v$ non linéaires à partir de l'indice des vides initial du sol dégelé et de propriétés d'indice.

Travaux futurs

Plusieurs travaux de recherche permettraient de poursuivre l'étude de la consolidation au dégel non linéaire à grandes déformations, notamment pour favoriser son utilisation dans la pratique :

1. Réaliser des études paramétriques comparatives entre le modèle non linéaire à grandes déformations et la théorie linéaire à petites déformations pour déterminer les domaines d'applicabilité de chacune des approches, c'est-à-dire, déterminer les limites pour lesquelles il est valide d'assumer que les propriétés des sols dégelés peuvent être modélisées par des relations linéaires et pour lesquelles il est valide d'assumer que l'impact des déformations est négligeable.

2. Utiliser le modèle non linéaire à grandes déformations pour réaliser des études paramétriques à partir des caractéristiques des propriétés $\sigma_v' - e - k_v$ définies par le modèle conceptuel pour soutenir le développement d'outils de calcul simples à utiliser dans la pratique. Des outils de calcul en fonction des propriétés d'indice et des relations empiriques du chapitre peuvent aussi être développés.

3. Réaliser des études en laboratoire concernant la contrainte résiduelle pour déterminer les caractéristiques de la courbe de contrainte résiduelle afin de valider l'hypothèse selon laquelle il s'agit d'une propriété intrinsèque du sol.

4. À partir des relations empiriques du chapitre 5, développer des abaques de calcul pour le tassement de fonte causé par l'expulsion de l'eau en excès des sols riches en glace. Ces relations pourraient permettre d'expliquer une partie de la grande variabilité des relations empiriques du tassement de fonte retrouvées dans la littérature en fonction des propriétés d'indice.

Bibliographie

Andersland, O.B., and Ladanyi, B. 2004. Frozen ground engineering. John Wiley & Sons, Hoboken, N.J.

Canadian Science Publishing. 2019. Disponible à partir de http://www.nrcresearchpress.com/journal/cgj.

Chamberlain, E., Iskandar, I., et Hunsickert, S.E. 1990. Effect of freeze-thaw cycles on the permeability and macrostructure of soils. In Proceedings of the International Symposium on Frozen Soil Impacts on Agricultural, Range, and Forest Lands. Spokane, Wash. pp. 145–155.

Chamberlain, E.J. 1981. Overconsolidation effects of ground freezing. Engineering geology, 18(1–4): 97–110.

Chamberlain, E.J., et Blouin, S.E. 1977. Freeze-thaw enhancement of the drainage and consolidation of fine-grained dredged material in confined disposal areas. Technical Report D-77-16, Foundations and Materials Research Branch, U.S. Army Cold Regions Research and Engineering Laboratory, Hanover, N.H.

Chamberlain, E.J., et Gow, A.J. 1979. Effect of freezing and thawing on the permeability and structure of soils. Engineering Geology, 13(1–4): 73–92.

Committee on appropriations. 2009. Strategic Importance of the Arctic in U.S. Policy. United States Senate.

COMSOL Multiphysics® v. 5.2a. 2016. COMSOL, Stockholm, Suède.

Côté, J., et Konrad, J.-M. 2005. A generalized thermal conductivity model for soils and construction materials. Canadian Geotechnical Journal, 42(2): 443–458.

Crory, F.E. 1973. Settlement associated with the thawing of permafrost. North American Contribution to the Second International Conference on Permafrost. National Academy of Sciences, Yakustk, U.S.S.R. pp. 599–607.

Davis, E.H., et Raymond, G.P. 1965. A non-linear theory of consolidation. Geotechnique, 15(2): 161–173.

Doré, G., et Zubeck, H. 2008. Cold Regions Pavement Engineering. McGraw-Hill Education, Reston, VA : New York.

Dumais, S., et Konrad, J.-M. 2015. Laying the foundations for the development of an extension to the theory of thaw consolidation. In Cold Regions Engineering 2015 : Developing and Maintaining Resilient Infrastructure. Salt Lake City, USA. pp. 78–89.

Dumais, S., et Konrad, J.-M. 2016. Compressibility and hydraulic conductivity of thawed fine-grained permafrost. In 11th International Symposium on Cold Regions Development: Energy Development in Cold Regions. Incheon, Corée.

Dumais, S., et Konrad, J.-M. 2018. One-dimensional large-strain thaw consolidation using nonlinear effective stress – void ratio – hydraulic conductivity relationships. Canadian Geotechnical Journal, 55(3): 414–426.

Dumais, S., et Konrad, J.-M. 2019. Large-Strain Nonlinear Thaw Consolidation Analysis of the Inuvik Warm-Oil Experimental Pipeline Buried in Permafrost. Journal of Cold Regions Engineering, 33(1): 04018014.

Foriero, A., et Ladanyi, B. 1995. FEM assessment of large-strain thaw consolidation. Journal of Geotechnical Engineering, 121(2): 126–138.

French, H.M. 2017. The Periglacial Environment. 4e édition. Wiley-Blackwell, Hoboken, NJ.

Gibson, R.E., England, G.L., et Hussey, M.J.L. 1967. The Theory of One-Dimensional Consolidation of Saturated Clays. Géotechnique, 17(3): 261–273.

Gibson, R.E., Schiffman, R.L., et Cargill, K.W. 1981. The theory of one-dimensional consolidation of saturated clays. II. Finite nonlinear consolidation of thick homogeneous layers. Canadian geotechnical journal, 18(2): 280–293.

de Grandpré, I., Fortier, D., et Stephani, E. 2012. Degradation of permafrost beneath a road embankment enhanced by heat advected in groundwater1This article is one of a series of papers published in this CJES Special Issue on the theme of Fundamental and applied research on permafrost in Canada. Canadian Journal of Earth Sciences, 49(8): 953–962.

Hanna, A.J., Saunders, R.J., Lem, G.N., et Carlson, L.E. 1983. Alaska highway gas pipeline project (Yukon) section thaw settlement design approach. In Proceedings of the Fourth International Conference on Permafrost. National Academy Press. pp. 439–444.

Johnson, T.C.E., McRoberts, E.C., et Nixon, J.F. 1984. Design implications of subgrade thawing. In Frost Action and Its Control, Technical Council on Cold Regions Engineering, ASCE. Édité par R.L. Berg et E.A. Wright. Berg, New York. pp. 45–103.

Keil, L.D., Nielsen, N.M., et Gupta, R.C. 1973. Thaw consolidation of permafrost dyke foundations at the Long Spruce Generating Station. 26th Canadian Geotechnical Conference. Toronto. pp. 134–41.

Konrad, J.-M. 1988. Influence of freezing mode on frost heave characteristics. Cold regions science and technology, 15(2): 161–175.

Konrad, J.-M. 1999. Frost susceptibility related to soil index properties. Canadian Geotechnical Journal, **36**(3): 403–417.

Konrad, J.-M. 2010. Hydraulic conductivity changes of a low-plasticity till subjected to freeze–thaw cycles. Géotechnique, 60(9): 679–690.

Konrad, J.-M., et Samson, M. 2000a. Hydraulic conductivity of kaolinite–silt mixtures subjected to closed-system freezing and thaw consolidation. Canadian Geotechnical Journal, 37(4): 857–869.

Konrad, J.-M., et Samson, M. 2000b. Influence of Freezing Temperature on Hydraulic Conductivity of Silty Clay. Journal of Geotechnical and Geoenvironmental Engineering, 126(2): 180–187.

Ladanyi, B. 1994. La conception et la réhabilitation des infrastructures de transport en régions nordiques. Manuel préparé pour le Ministère des transports du Québec.

Linell, K.A. 1973. Long-term effects of vegetative cover on permafrost stability in an area of discontinuous permafrost. Proceedings of Permafrost: North American contribution to the Second International Conference: National Academy of Sciences, National Research Council. pp. 688–693.

Luscher, U., et Afifi, S.S. 1973. Thaw consolidation of Alaskan silts and granular soils. North American Contribution to the Second International Conference on Permafrost. National Academy of Sciences, Washington, D.C. pp. 325–334.

McRoberts, E.C., et Morgenstern, N.R. 1974. The stability of thawing slopes. Canadian Geotechnical Journal, 11(4): 447–469.

Morgenstern, N.R., et Nixon, J.F. 1971. One-dimensional Consolidation of Thawing Soils. Canadian Geotechnical Journal, 8(4): 558–565.

Morgenstern, N.R., et Nixon, J.F. 1975. An analysis of the performance of a warm-oil pipeline in permafrost, Inuvik, NWT. Canadian Geotechnical Journal, 12(2): 199–208.

Morgenstern, N.R., et Smith, L.B. 1973. Thaw–Consolidation Tests on Remoulded Clays. Canadian Geotechnical Journal, 10(1): 25–40.

Nelson, R.A., Luscher, U., Rooney, J.W., et Carlson, L.E. 1983. Thaw strain data and thaw settlement predictions for alaskan soils. Proceedings of the Fourth International Conference on Permafrost. National Academy Press. pp. 439–444.

Nixon, J.F. 1973a. The consolidation of thawing soils. Doctoral Thesis, University of Alberta, Edmonton, AB.

Nixon, J.F. 1973b. Thaw–Consolidation of Some Layered Systems. Canadian Geotechnical Journal, 10(4): 617–631. doi:10.1139/t73-057.

Nixon, J.F., et McRoberts, E.C. 1973. A study of some factors affecting the thawing of frozen soils. Canadian Geotechnical Journal, 10(3): 439–452.

Nixon, J.F., et Morgenstern, N.R. 1973a. The residual stress in thawing soils. Canadian Geotechnical Journal, 10(4): 571–580.

Nixon, J.F., et Morgenstern, N.R. 1973b. Practical extensions to a theory of consolidation for thawing soils. North American Contribution to the Second International Conference on Permafrost. National Academy of Sciences, Washington, D.C. pp. 369–376.

Nixon, J.F., et Morgenstern, N.R. 1974. Thaw–Consolidation Tests on Undisturbed Fine-grained Permafrost. Canadian Geotechnical Journal, 11(1): 202–214.

O'Neill, H.B., et Burn, C.R. 2017. Impacts of variations in snow cover on permafrost stability, including simulated snow management, Dempster Highway, Peel Plateau, Northwest Territories. Arctic Science, 3(2): 150–178.

Qi, J., Yao, X., et Yu, F. 2013. Consolidation of thawing permafrost considering phase change. KSCE Journal of Civil Engineering, 17(6): 1293–1301.

Slusarchuk, W.A., Watson, G.H., et Speer, T.L. 1973. Instrumentation around a warm oil pipeline buried in permafrost. Canadian Geotechnical Journal, 10(2): 227–245.

Smith, M.W. 1985. Observations of soil freezing and frost heave at Inuvik, Northwest Territories, Canada. Canadian Journal of Earth Sciences, 22(2): 283–290.

Speer, T.L., Watson, G.H., et Rowley, R.K. 1973. Effects of ground-ice variability and resulting thaw settlements on buried warm-oil pipelines. North American Contribution to the Second International Conference on Permafrost. National Academy of Sciences. pp. 746–752.

Sykes, J.F., Lennox, W.C., et Charlwood, R.G. 1974. Finite Element Permafrost Thaw Settlement Model. Journal of Geotechnical and Geoenvironmental Engineering, 100(GT11).

Terzaghi, K. 1943. Theoretical Soil Mechanics. Wiley, New York.

Edgar, T. 2015 (conversation personnelle).

Transportation Association of Canada. 2010, July. Primer on Developing and managing transportation infrastructure in permafrost regions.

Tsytovich, N.A., Zaretsky, Yu.K., Grigoryeva, V.G., et Ter-Martirosyan, Z.G. 1965. Consolidation of thawing soils. Transaction of the 6th International Congress on Soil Mechanics. Stroiizdat.

Watson, G.H., Rowley, R.K., et Slusarchuk, W.A. 1973. Performance of a warm-oil pipeline buried in permafrost. North American Contribution to the Second International Conference on Permafrost. Yakutsk, Siberia. pp. 759–766.

Watson, G.H., Rowley, R.K., et Speer, T.L. 1972. Inuvik Frozen Core Testing. Mackenzie Valley Pipe Line Research Limited, Calgary, AB.

Zaretskii, Y.K. 1968. Calculation of the settlement of thawing soil. Soil Mechanics and Foundation Engineering, 5(3): 151–155.

Annexe A   Laying the foundations for the development of an extension to the theory of thaw consolidation

Avant-propos

Auteurs et affiliation

Simon Dumais et Jean-Marie Konrad

Département de génie civil et de génie des eaux, Université Laval.

Conférence

16th International Conference on Cold Regions Engineering, Salt Lake City, Utah, 19-22 juillet 2015

Titre français

Poser les fondations pour le développement d'une extension à la théorie de consolidation au dégel

Résumé français

Plusieurs théories ont été proposées afin de modéliser le comportement de consolidation au dégel. Cependant, elles ne sont pas applicables pour un large éventail de problèmes plus complexes en raison de leurs formulations simplifiées. La pertinence de développer une extension à la théorie de consolidation au dégel existante est étudiée dans ce document. Les théories disponibles sont d'abord présentées. Les deux composantes principales d'une théorie de consolidation au dégel, à savoir le dégel du sol et la consolidation, sont discutées avec des égards particuliers pour les lacunes des théories actuellement disponibles. Le couplage de ces deux composantes au sein d'une théorie unifiée est examiné. Des discussions sur les problèmes bidimensionnels et sur certaines considérations supplémentaires concernant la consolidation au dégel précèdent la conclusion.

Modifications apportées à l'article publié

L'article publié dans les actes de la conférence est reproduit intégralement ici. À la différence des articles intégrés dans le corps de la thèse, la nomenclature et les symboles utilisés dans les annexes n'ont pas été homogénéisés par rapport au reste de la thèse, car les articles

présentés aux conférences présentent des travaux préliminaires aux résultats présentés dans le corps de la thèse. Ainsi, certaines définitions ont changé par rapport aux articles de conférence et ne concordent plus avec les définitions finales adoptées et présentées aux chapitres 2 à 5 de la thèse.

A.1 Abstract

Several theories have been proposed in order to model the thaw consolidation behavior of frozen soil. However, they are not valid over a wide range of complex problems because of simplifications made in their formulation. The relevance of the development of an extension to the existing theory of thaw consolidation is discussed in this paper. The current available thaw consolidation theories are presented, focusing on their own specific insights into the thaw consolidation behavior of soil. The two main components of a thaw consolidation theory, namely thawing and consolidation, are discussed with special regards for the shortcomings of the currently used theories. The coupling of these two components into a unified theory is examined. Brief discussions on two-dimensional problems and on additional considerations regarding thaw consolidation precedes the conclusion.

A.2 Introduction

Pore pressure generation and settlement caused by the thawing of a frozen soil are major concerns in the design of infrastructure built on ice-rich permafrost. Indeed, large amount of water can be released upon thawing, generating high pore pressure that can cause instability. The settlement subsequent to consolidation of thawing soils is also troublesome. Infrastructure such as road and railway embankments, airstrips, pipelines, and building foundations, as well as thawing slopes, are affected by the thaw consolidation process. It is critical to have an efficient way to evaluate the pore pressure generated and settlement caused by the consolidation of a thawing soil. The relevance of the development of an extension to the existing theories of thaw consolidation will be discussed in this paper. Existing theories of thaw consolidation will be used to outline the impact of the different factors involved in the thaw consolidation process. First, the main thaw consolidation theories will be presented with special regards to Morgenstern and Nixon works (Morgenstern and Nixon 1971). The two main components constituting a thaw consolidation theory will be analyzed: the thawing of frozen soil and the consolidation of post-thawed soil. Coupling of the thawing and of the

consolidation processes will be examined. Finally, the specific aspects of two-dimensional problems of thaw consolidation and additional considerations regarding thaw consolidation theories will be discussed.

A.3 Thaw consolidation theories

The first complete one-dimensional thaw consolidation theories were proposed around the end of the 1960s. Over the years, a number of additional works on the subject have been published trying to amend for the shortcomings of the previously proposed theories. They are all based on the same basic principle of solving a problem of consolidation within a thawed region which size is increasing with time as the thaw penetrates the initially completely frozen soil. Each thaw consolidation theory brings additional insights into the process of thaw consolidation.

A.3.1 Morgenstern and Nixon's theory of thaw consolidation

Most thaw consolidation theories are based on the same basic principles as the ones proposed by Morgenstern and Nixon in 1971. Furthermore, their work is still widely used because of its simplicity and efficient calculation tools in spite of being one of the oldest thaw consolidation theory. It is thus convenient to use it as a point of reference in this paper.

The basic equations and boundary conditions of the theory are shown in Figure A.1. Neumann solution to the heat conduction problem is used to describe the movement of the thaw plane within the frozen ground and Therzaghi's theory of consolidation is used to describe the compressive behavior of the soil. The surface of the ground is assumed to be free-draining while no pore pressure is transmitted through the incompressible and impermeable frozen ground below the position of the thaw plane. A load, P_0, is applied at the surface of the ground. The top boundary, the surface of the ground, is fixed in space while the moving bottom boundary is set at the thaw plane. The pore pressure condition at the thaw plane is described by the equation found in Figure A.1.
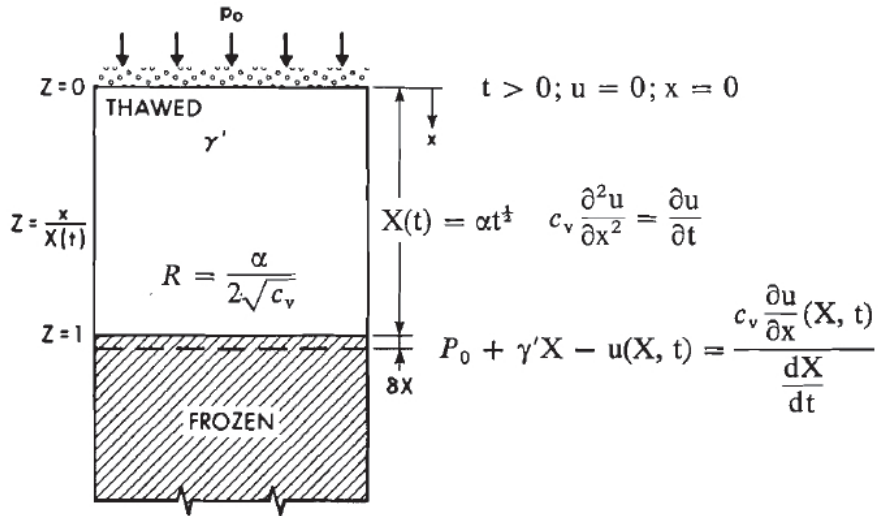
Figure A.1 : Schematics of one-dimensional thaw consolidation including boundary conditions (modified from Morgenstern and Nixon 1971)

The extended use of Morgenstern and Nixon's theory can be explained mostly by the proposed calculation tools based on the thaw consolidation ratio (R). The thaw consolidation ratio is used to describe the soil behavior under thaw consolidation using the two main analytic parameters responsible for the generation and dissipation of pore pressure: α, the thermal parameter describing the movement of the thaw plan, and c_v, the coefficient of consolidation. For example, a large thaw consolidation ratio, whether caused by a large α and/or by a small c_v, indicates that pore pressure within the thawed soil will be higher than for a smaller thaw consolidation ratio.

Simplifications were made in the development of the theory in order to find an analytical solution to the theory with the limited calculation tools available at the time. Consequently, the theory is only valid for engineering problems with simple load and thermal conditions. The shortcomings of the theory caused by these simplifications will be outlined throughout this paper.

A.3.2 Other thaw consolidation theories

The first attempt at a one-dimensional theory of thaw consolidation was proposed a few years before Morgenstern and Nixon by Tsytovich et al. in 1965. It provides a good analysis of the soil properties and of the soil behavior during the thaw consolidation process based on laboratory experiments. Improvement on boundary conditions were

made by Zaretskii in 1968. The main contribution of these authors was to determine that the thaw consolidation obeys the law of filtration consolidation as proposed by Terzaghi.

Two-dimensional finite element models have been proposed in order to improve the precision of the thaw consolidation theory proposed by Morgenstern and Nixon (Sykes et al. 1974a, Foriero and Ladanyi 1995). These models contained fewer simplifications but failed to provide efficient calculation tools such as the ones provided in Morgenstern and Nixon's works. Nevertheless, they provide interesting insights into the thaw consolidation process and provide a two-dimensional basis for an extension to the thaw consolidation theory.

In recent years, a more complex 3D model of thaw consolidation has been proposed (Yao et al. 2012, Qi et al. 2013). The development of such a model have been made possible by the powerful computation tools available nowadays. This model is more complete but doesn't offer a stand-alone easy-to-use solution to the model and still makes some simplifications in its resolution that are likely to influence its validity and precision.

All theories and models proposed up to now can accurately predict the thaw consolidation behavior of saturated frozen soil with low ice content. An extension to the theory of thaw consolidation is mainly justified in order to model the behavior of ice-rich permafrost presenting massive ice features which causes most thaw settlement problems.

Work of significant importance to the practicing engineer has been done in order to empirically describe the thaw strain behavior of soils (e.g. Nelson et al. 1983). Even if the study presented here limits itself to the theory and modelling of thaw consolidation, data from empirical work on thaw strain is highly valuable for the validation of a thaw consolidation model.

A.4   Thawing of frozen soil

The first element constituting a thaw consolidation theory is to define the boundaries of the thawed region by modelling the thawing of frozen soil. The thawing process is influenced by the geothermal properties of the soil. Finally, in presence of a large amount of water seepage the transfer of energy by advection can significantly influence thaw penetration.

A.4.1 Defining the thawed region

In most thaw consolidation theories and models, the soil is divided into two distinct regions: the thawed region and the frozen region. The process of consolidation is limited to the thawed region while the frozen region is considered impermeable and incompressible. The position of the interface between the two regions is either defined by the position of the thaw plane or by the temperature within the soil.

Neumann solution to the problem of heat conduction is often used to define the position of the thaw plane (Tsytovich et al. 1965, Morgenstern and Nixon 1971 and Foriero and Ladanyi 1995). The main advantage of this approaches is that it is very easy to implement into an analytical solution as the position of the thaw plane is defined independently of the consolidation process. The Neumann solution can also be implemented in a convective coordinate system to consider the settlement of the surface upon thawing. By using Neumann solution, the thaw consolidation process is reduced to a consolidation problem within the thawed region with a moving boundary at the bottom. However, it is an analytical solution to the heat equation, and it assumes that the thermal conductivity within the thawed region remains constant throughout the consolidation process. Furthermore, most theories don't offer a way to determine the thermal parameter of Neumann solution as they determine it experimentally or using field data.

More complex finite-element-based theories use heat transfer equations to model the thawing process (Sykes et al. 1974a and Yao et al. 2012). The thawed and frozen regions are then defined by determining if the temperature at a node is higher or lower than the melting point of the soil. A brief discussion on the melting point of soil is presented later in this paper. Problems with complex geometry are more easily analyzed using heat transfer equations. Heat transfer processes used to define the thawing of frozen soil usually include heat transfer by conduction, ice-water phase change, and sometimes, advection. The effect of advection will be discussed later in this paper. Equations of heat transfer including conduction, latent heat and advection are well documented and are easily implemented within a finite element model.

A.4.2 Thermal properties of soil

The thermal properties of the soil are key parameters in the modelling of thawing of frozen soil. The three main thermal properties of soil relevant in thaw consolidation are thermal conductivity, specific heat including latent heat and melting point. Most models use constant thermal properties even though thermal conductivity and specific heat are both temperature dependent (Yao et al. 2012). Furthermore, the thermal conductivity of the thawed soil is likely to be affected by the consolidation process. Indeed, thermal conductivity will increase as the soil densify because of the higher conductivity of the soil particles in comparison to the conductivity of water. Temperature dependence of the soil thermal properties are well documented. A thermal conductivity model such as the one proposed by Côté and Konrad in 2005 can be used to describe the thermal conductivity throughout the consolidation process.

All the models reviewed by the authors use a melting point for the soil of 0°C. However, for fine grain soils such as the ones typical of ice-rich permafrost, the melting point can be much lower and close to -1°C (Kozlowski 2003). By defining a melting temperature higher than the actual one, the actual thaw plane is ahead of the modelled thaw plane. The melting point of fine-grained soils can be determined by empirical equations using their plastic or liquid limit and their water content of the soil. The melting point can also be treated as a phase change occurring over a temperature range which is typical of soils with significant unfrozen water content. (Lunardini 1981)

A.4.3 Advection

It is generally accepted that the dominant mode of energy transfer in a frozen soil system is conduction. However, seepage of water upon thawing of frozen soil is likely to cause advective heat transfer (Lunardini 1998). Nixon (1975) indicated that free convection doesn't have a big impact on thaw penetration when the seepage flow is proportional to the rate of movement of the thaw plane. Figure A.2 shows the small influence of advection on both reducing the thaw line penetration and the settlement as calculated by Sykes et al. finite element model. They noted that for soils with low permeability including advection is unlikely to have a big impact on thaw penetration.

In permafrost and frozen soil, water flow can also be caused by a difference in potential or by gravity and can be much greater than the seepage flow upon thawing. In such cases,

advection can have a significant impact on the thawing process of frozen soils (Lunardini 1998). Linear infrastructure built on permafrost such as roads, railroads and airstrips are likely to intercept natural water ways. Even with water management systems some underwater flow can occur under these infrastructure (Zottola et al. 2012). This is likely have an impact on thaw penetration underneath these infrastructure. An extension to the theory of consolidation would benefit from the implementation of the effect of groundwater flow on the thawing process.
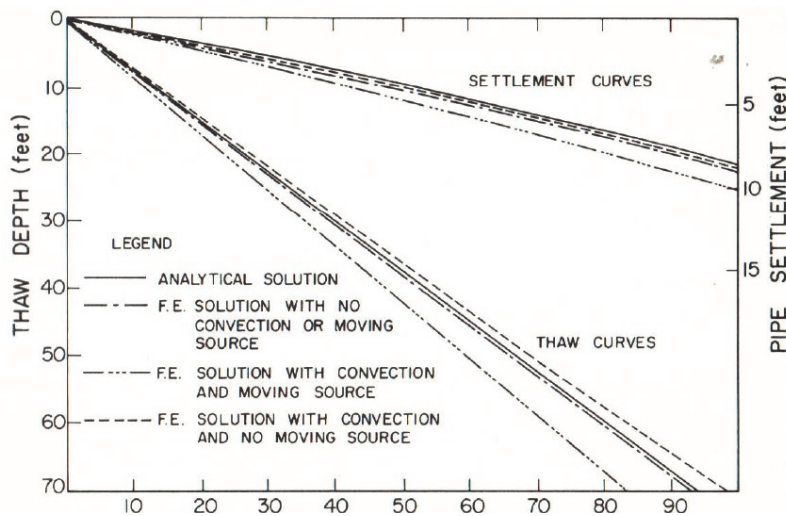

Figure A.2 : Thaw depth and settlement for the case of a buried pipeline in permafrost (Sykes et al. 1974b)

A.4.4 Movement of the heat source

In most thaw consolidation theory, the heat source inducing thawing of the frozen ground is placed at the surface of the ground. Following consolidation of the thawed soil, the surface of the ground subsides. Morgenstern and Nixon's theory did not take into account this settlement and the top boundary is fixed in space in their theory. All subsequent thaw consolidation theories recognize that this was a major conceptual issue and allowed the heat source to move along with the surface of the ground. This was achieved either by using a convective coordinate system or by allowing the nodes of the finite element mesh to move with consolidation. The impact of including the moving source in the analysis can be seen in Figure A.2. There is a difference of almost 10 feet on the thaw penetration and of more than one foot on settlement after 80 days for a thaw settlement or about 13 %. For the case illustrated in Figure A.2, the difference or including the movement

of the heat source is only significant after a long period of time. However, the impact is likely to be much greater even for a short period of time for ice-rich soil that can present thaw settlement values of well over 50%.

A.5   Consolidation of thawed soils

The second key element of a thaw consolidation theory is describing the consolidation behavior within the thawed region. Most of the focus regarding the consolidation element has been put towards selecting an appropriate theory of consolidation and establishing the pore pressure conditions at the thaw plane. However, additional considerations regarding the permeability of thawed permafrost would be of benefit to an extension to the theory of thaw consolidation.

A.5.1 Compressive behavior of thawing soil

The compressive behavior of frozen soil can be illustrated schematically by the curve presented in Figure A.3 (Tsytovich et al. 1995 and Sykes et al. 1974a). The portion a-b of the curve represents the compression when the frozen soil is submitted to an increase loading. This compression of frozen soil is usually ignored in thaw consolidation theories. The portion b-c represents the variation in void ration upon thawing. The last portion c-d represents the variation in void ratio caused by filtration consolidation when the thawed soil is submitted to an increasing load. The magnitude of the variation in void ratio of the portions b-c and c-d is a function of the soil properties. For ice-rich thaw unstable soils, the thaw consolidation behavior is mainly due to filtration consolidation occurring in the c-d portion. A soil is said to be thaw unstable when the amount of ice present is such that upon melting the water can't be held into the voids of the soil (Sykes at al. 1974a).

A.5.2 Consolidation theory

Most theories and model introduced earlier small strain consolidation theory to model the compressibility of the soil skeleton. Terzaghi's theory of filtration consolidation is used in one-dimensional models while Biot's theory is being used in multi-dimensional models. Consolidation behavior of an ice-rich thawed soil is, however, more likely to be a large-strain consolidation. Accordingly, Foriero and Ladanyi used Gibson et al. (1967) model of large-strain consolidation in their finite element model. The main advantage of using

Gibson's theory is that it takes into account the variation of soil compressibility and permeability during the consolidation process. Furthermore, ice-rich soils and frozen soils with massive ice are likely to experience large strains upon thawing so imposing the limitation of small strains leads to an underestimation of the progress of consolidation settlement (Foriero and Ladanyi 1995). Implementation of Gibson's theory within a thaw consolidation can be done after the work of Foriero and Ladanyi.

A.5.3 Compressibility and permeability of thawed soil

The compressibility of a soil is closely linked with its permeability. Except for the theories using Gibson's theory of consolidation, permeability of the thawed soil is kept constant in most thaw consolidation theories. It should be noted that the permeability of a thawed soil is different than the permeability of the same soil in the unfrozen state. Indeed, freeze thaw cycles causes an increase in both vertical and horizontal permeability (Chamberlain and Gow 1979). Upon thawing the soil will thus show a high permeability because of the fissures and failures planes left by the melting of ice lenses or massive ice (Watson et al. 1973). However, the reduction of permeability caused by consolidation will be higher in thawed soils than for unfrozen soils. A relationship between permeability and void ratio should be used to describe the behavior of the soil during consolidation. Furthermore, there is an anisotropy in the permeability of the thawed state of a frozen soil that presented oriented ice features such as horizontal ice lenses.
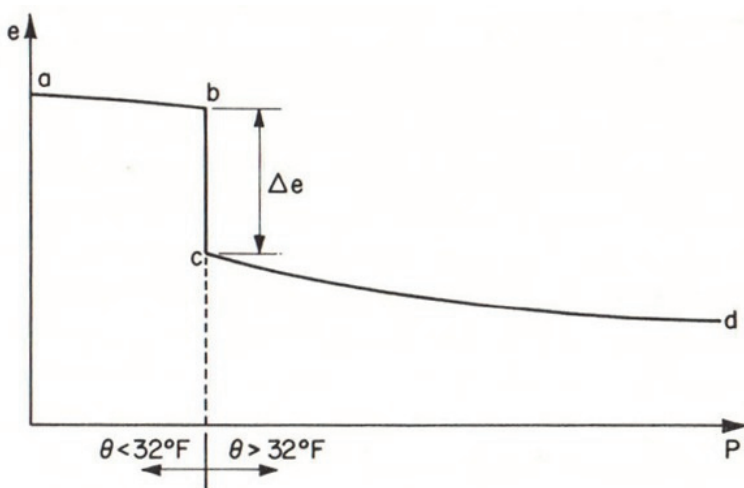

Figure A.3 : Compressive behavior of a frozen soil upon thawing (Sykes et al. 1974a modified from Tsytovich et al. 1965)

A.5.4 Settlement of the surface

The impact of the settlement of the ground surface on the movement of the heat source has already been discussed. Moreover, the settlement of the surface has an impact on consolidation. Indeed, in Morgenstern and Nixon's theory the length of the path of drainage is always equal to the thaw penetration. However, for a high value of thaw settlement, the length of the path of drainage could be reduced by more than 50% compared to with Morgenstern and Nixon's theory if the movement of the surface is considered. However, it is important to note that part of this extra dissipation of pore pressure caused by the reduction of the length of the path of drainage is compensated by the fact that upon consolidation the permeability of the thawed soil will decrease greatly especially for an ice-rich soil. Furthermore, the permeability is not constant as a function of depth within the thawed region. Indeed, the soil closer to the surface of the ground thaws first and thus consolidates before the soil deeper below the surface. The permeability of the soil within the thawed region will then increase as a function of depth.

A.5.5 Super moistened layer

Tsytovich et al. introduced the interesting concept of a super-moistened layer in their theory. At the thawing front, the water that is not immediately absorbed within the voids of the soil is creating a super-moistened layer were the mineral aggregates are in a suspended space. The effective stress closed to the thaw line is consequently very small and is considered to be zero at the thaw line by Tsytovich et al. This layer varies in thickness as a function of the type of soil and the permeability within this layer is much lower than the permeability of the soil in the rest of the thawed region. Introduction of such a layer in a thaw consolidation theory would probably allow to describe the behavior upon thawing of soils containing massive ice.

A.6 Coupling of thawing and consolidation

To develop a theory of thaw consolidation the two elements of thawing and consolidation needs to be coupled. Coupling represents a challenge especially for increasingly complex description of each element. Earlier theories such as the one proposed by Morgenstern and Nixon could be coupled into an analytical solution to which a close form solution could be found. This allows the theory to be easily usable in practice. However, compromise

in the formulation of these theories have to be made to simplify the problem and to obtain such solutions.

More complex theories need to be coupled using more advance computation tools. The latest theory proposed by Yao et al. is coupled using a finite-element method and an iterative process. Indeed, the thawing process and the consolidation process can't be solved simultaneously so a matching time step process is used to solve each element separately. In order words, the consolidation element is being solved n times for each iteration of the thermal element. When both elements are coupled after each matching time step, the soil properties are updated. However, even if coupling the thawing and consolidation processes using finite-element modelling yields good results for specific analysis, it fails to provide close form solutions that are of great use in practice.

A.7 Two-dimensional problems

Most parameters in this paper where discussed from a one-dimensional point of view. However, a multi-dimensional extension of the theory of consolidation would allow to analyze more complex problems.

For example, the behavior of a thawing bulb created around a buried heat source can hardly be describe using a one-dimensional theory (Sykes et al. 1974b). First of all, the shape of the thawing bulb is both created by the radial heat transfer around the buried heat source and by the thermal conditions at the surface of the ground. Second, the drainage of pore pressure created upon thawing can only be achieved through a limited length at the surface of the ground. Furthermore, the settlement at the surface caused by the consolidation of the soil within the thaw bulb has to be expressed by considering more than a one-dimensional vertical consolidation because of the particular shape of the bulb.

The description of the seepage of water mentioned earlier in this paper would also greatly benefit from an extension to a two-dimensional theory. This would not only allow to better integrate the heat transfer by advection but also to describe the migration of water of more complex situations. For example, in the case of a thawing slope, excess water driven by a gravity could also migrate parallel to the surface of the ground and have an impact on slope stability.

Finally, permafrost is a highly nonhomogeneous and anisotropic material (Sykes et al. 1974a). Using a two-dimensional model could certainly help to get a more accurate description of the thaw consolidation behavior of permafrost. It is surely the case of the thawing of a frozen soil presenting oriented ice features and a high anisotropy in permeability.

A.8 Additional considerations

Many more parameters involved in the thaw consolidation process have not been mentioned in this paper. Nevertheless, they are of certain importance and should be considered in an extension to the theory of consolidation. These parameters include but are not limited to: permeability and compressibility of the frozen region, swelling of soil upon thawing, thawing of frozen soil submitted to multiple thaw planes, impact of cryostructure such as ice lenses and massive ice on the thaw consolidation behavior, impact of freezing and thawing cycles on soil properties, etc.

A.9 Conclusion

In conclusion, the relevance of an extension to the theory of thaw consolidation was discussed using available theories and models. The thawed region should be defined using heat transfer equations including conduction, ice-water phase change, and advection, as well as temperature-dependent and time-dependent soil thermal properties. Special attention should be placed towards the movement of the heat source, especially for ice-rich soils presenting high thaw settlement values. Furthermore, a large-strain consolidation theory should be used to describe the compressive behavior within the thawed soil. Special care should be used to describe the evolution of permeability of the thawed soil during consolidation. Coupling of the thawing and of the consolidation behavior should be performed using a matching time-step iterative process. A close form solution should be provided in order to ease practical use of the theory. The development of a multi-dimensional theory would allow more complex problems to be analyzed. Finally, there are a few additional considerations that need to be studied in order to evaluate their impact on the thaw consolidation behavior.

A.10 Acknowledgments

A.10 References

Chamberlain, E. J., and Gow, A. J. (1979) Effect of Freezing and Thawing on the Permeability and Structure of Soils. Engineering Geology, 19, 73-92.

Côté, J., and Konrad, J.-M. (2005). A Generalized Thermal Conductivity Model for Soils and Construction Materials. Canadian Geotechnical Journal, 42(2), 443-458.

Foriero, A., and Ladanyi, B. (1995). FEM Assessment of Large-Strain Thaw Consolidation. Journal of Geotechnical Engineering, 121(2), 126-138.

Gibson, R. E., England, G. L., and Hussey M. J. L. (1967). Theory of one-dimensional consolidation of saturated clays – 1. Finite Non-Linear Consolidation of Thin Homogeneous Layers. Géotechnique, 17(3), 261-273.

Kolowski, T. (2003). Soil Freezing Point as Obtained on Melting. Cold Regions Science and Technology, 38, 93-101.

Lunardini, V. J. (1981). Heat Transfer in Cold Climates. Van Nostrand Reinhold Co. 731 p.

Lunardini, V J. (1998). Effect of Convective Heat Transfer on Thawing of Frozen Soil. Permafrost – Proceedings of the Seventh International Conference, Yellowknife, Collection Nordicana, 55, 689-695.

Morgenstern, N. R., and Nixon, J. F. (1971). One-Dimensional Consolidation of Thawing Soils. Canadian Geotechnical Journal, 8(4), 558-565.

Morgenstern, N R., and Smith, L. B. (1973). Thaw-Consolidation Tests on Remoulded Clays. Canadian Geotechnical Journal, 10(1), 25-40.

Nelson, R.A., Lucher, U., Rooney, R.A., and Stramler, A.A, (1983). Thaw Strain Data and Settlement Predictions for Alaskan Soils. Fourth International Permafrost Conference.

Nixon, J F. (1973). Thaw-Consolidation of Some Layered Systems. Canadian Geotechnical Journal, 10(4), 617-631.

Nixon, J. F. (1975). The Role of Convective Heat Transport in the Thawing of Frozen Soils. Canadian Geotechnical Journal, 12(3), 425-429.

Qi, J., Yao, X., and Yu, F. (2013). Consolidation of Thawing Permafrost Considering Phase Change. KSCE Journal of civil engineering, 17(6), 1293-1301.

Sykes, J F., Lennox, W. C., and Charlwood, R. G. (1974a). Finite Element Permafrost Thaw Settlement Model. Journal of the Geotechnical Engineering Division, 100(11).

Sykes, J F., Lennox, W. C., and Charlwood, R. G. (1974b). Two-Dimensional Heated Pipeline in Permafrost. Journal of the Geotechnical Engineering Division, 100(11).

Tsytovich, N. A., Zaretsky, Y. K., Grigoryeva, V. G., and Ter-Martirosyan, Z. G. (1965). Consolidation of Thawing Soils. Proceedings of the Sixth International Conference on Soil Mechanics and Foundation Engineering, 1, 390-394.

Watson, G. H., Slusarchuk, W. A., and Rowley, R. K. (1973). Determination of Some Frozen and Thawed Properties of permafrost Soils. Canadian Geotechnical Journal, 10, 592-606.

Yao, X., Qi, J., and Yu, F. (2012). Three Dimensional Analysis of Large Strain Thaw Consolidation in Permafrost. Acta geotechnica, 7(3), 193-202.

Zaretskii. Y. K. (1968). Calculation of the Settlement of Thawing Soil. Fundamenty I Mekhanika Gruntov, 3, 3-6.

Zottola, J., Darrow, M., Daanen, R., Fortier, D., and de Grandpré, I. (2012). Investigating the Effects of Groundwater Flow on the Thermal Stability of Embankments over Permafrost. Cold Regions Engineering 2012, American Society of Civil Engineers, 601-611.

Annexe B Compressibility and hydraulic conductivity of thawed fine-grained permafrost

Avant-propos

Auteurs et affiliation

Simon Dumais et Jean-Marie Konrad

Département de génie civil et de génie des eaux, Université Laval.

Conférence

Titre français

La compressibilité et la conductivité hydraulique des pergélisols à grains fins

Résumé français

La compressibilité et la conductivité hydraulique des sols à grains fins gouvernent en grande partie le comportement de consolidation au dégel. Cette étude présente d'abord une analyse d'une base de données des propriétés des sols dégelés provenant de la littérature des propriétés des sols dégelés. La conductivité hydraulique et la compressibilité des pergélisols dégelés sont estimées à partir des propriétés de sols dégelés provenant d'essais de gel et de dégel. Des relations entre les propriétés d'indice et la conductivité hydraulique et la compressibilité des sols dégelés sont proposées. Ces relations permettent d'analyser le coefficient de consolidation des sols dégelés.

Notes et Modifications apportées à l'article publié

L'article publié dans les actes de la conférence est reproduit intégralement ici. À la différence des articles intégrés dans le corps de la thèse, la nomenclature et les symboles utilisés dans les annexes n'ont pas été homogénéisés par rapport au reste de la thèse, car les articles présentés aux conférences présentent des travaux préliminaires aux résultats présentés dans le corps de la thèse. Ainsi, certaines définitions ont changé par rapport aux articles de conférence et ne concordent plus avec les définitions finales adoptées et présentées aux chapitres 2 à 5 de la thèse.

B.1 Abstract

The hydraulic conductivity and compressibility largely control the thaw consolidation behaviour of fine-grained permafrost. This study first presents a brief review of the properties of thawed soils based on a compendium of data from the literature. The thawed hydraulic conductivity and compressibility of fine-grained permafrost are evaluated from the thawed soil properties derived from freeze-thaw cycling tests. Relationships between simple geotechnical index and the hydraulic conductivity and compressibility of thawed soils are proposed. Finally, the coefficient of consolidation of thawed soils is discussed.

B.2 Introduction

Infrastructures built on permafrost can disrupt the thermal regime of perennially frozen ground and trigger thawing of the soil. Large excess pore pressure can develop because of the water liberated at the thaw front from the melting ice if drainage is impeded. Significant settlement also results from the consolidation of the thawed soil. This process is called thaw consolidation, and it represents a major source of instabilities for northern infrastructures.

In addition to the geothermal properties of the soil, thaw consolidation modelling requires constitutive relationships for the hydraulic conductivity and compressibility of the soil (Gibson at al., 1981). These two properties are often combined in the coefficient of consolidation, and they are considered constant and homogeneous in traditional thaw consolidation theories (Nixon 1973). However, they are void ratio dependent and should be spatially discretized.

Furthermore, it is generally accepted that the freeze-thaw cycling affects the soil properties. A reduction in the void ratio and an augmentation of the hydraulic conductivity are typically observed upon freezing and thawing (Chamberlain and Blouin 1977). The thawed properties of the soil should be used in thaw consolidation modelling instead of the properties of the unfrozen soil.

In this study, the hydraulic conductivity and compressibility of thawed fine-grained permafrost are analyzed from a compendium of literature data. First, previous studies on the subject are presented along with the data used in this study. Then, relationships between the compressibility and hydraulic conductivity and simple geotechnical index are proposed.

191

Finally, thaw consolidation modelling is discussed through the presentation of void ratio dependent relationships of the coefficient of consolidation.

B.3 Previous studies

Figure B.1 presents typical laboratory results from freeze-thaw cycling tests on fine-grained soil. Some observations noted by Chamberlain and Blouin (1977) and Chamberlain and Gow (1979) from such results should be repeated here. Freeze-thaw cycling causes a reduction in the void ratio and an increase in the hydraulic conductivity. While these two results may seem contradictory, these changes are both attributed to a reorientation of the particles which causes a reduction of particle spacing and a reduction of the adsorbed water film. Preferential drainage paths produced by vertical shrinkage cracks developed during freezing may also contribute to the increased hydraulic conductivity. The structural changes appearing both at the macroscopic and microscopic scales are attributed to high negative pore pressures developed during freezing (Williams 1966).

The results presented in Figure B.1 suggest that linear functions can be used to characterize both the $\log \sigma_v' - e$ and $e - \log k_v$ relationships with slope parameters equal to C_c and $(S_k)^{-1}$. Because the hydraulic conductivity and void ratio changes are more important at high void ratios, both C_c and $(S_k)^{-1}$ decrease upon freeze-thaw cycling.
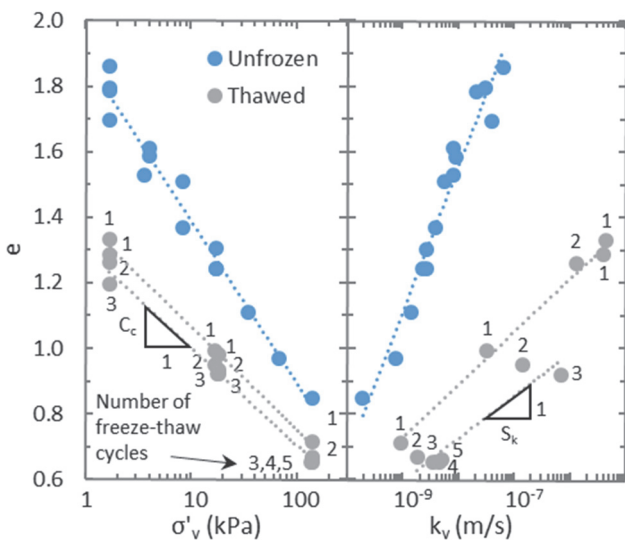

Figure B.1 : Effect of freeze-thaw cycling on the hydraulic conductivity and compressibility of Ellsworth Clay (adapted from Chamberlain and Gow 1979)

Figure B.1 illustrates how the experimental data were analyzed in the current study. The unfrozen state of the soil was characterized by performing nonlinear regressions on all available data for the unfrozen state. For the thawed state, the data from multiple freeze-thaw cycles were aggregated when the data for an individual cycle were insufficient to perform a nonlinear regression and when no void ratio or hydraulic conductivity changes were observed upon further freeze-thaw cycling. For example, the data for the Ellsworth clay presented in Figure B.1 were aggregated from cycles 2 to 5. The thawed state is thus analyzed independently of the number of freeze-thaw cycles and characterizes the state when no additional changes are expected upon further freeze-thaw cycling. The soil properties under such conditions are expected to be analogous to that of thawed permafrost.

Selected geotechnical properties and the slope parameters of the soils used in this study are presented in Table B.1. Permafrost soils are indicated in bold. Subscripts U and T are used in reference to the unfrozen and thawed soils respectively.

Limited results are available for tests performed on thawed permafrost. However, some evidences indicate that the properties of thawed fine-grained soils exposed to freeze-thaw cycles are analogous to that of fine-grained thawed permafrost soils. First, Watson et al. (1973) noted that the measured permeability of thawed permafrost core samples was one to two orders of magnitude higher than they anticipated from the grain size distribution curve. This is comparable to the ratios of thawed to unfrozen hydraulic conductivity of 4 to 300 measured by Chamberlain and Gow (1979) for fine-grained soils. Furthermore, the discrete ice features that create preferential drainage paths upon thawing are also typical of perennially frozen sediments (French and Shur 2010). The presence of segregated ice is an indication that permafrost was subjected to freezing forces similar to the ones observed during seasonal freezing (Mackay 1972).

Table B.1 : Compendium of soil data used in this study

Soil	ID	C_{cU}	C_{cT}	S_{kU}	S_{kT}	Clay (%)	Silt (%)	Sand (%)	d_{50}(FF)* (mm)	w_L (%)	w_P (%)	I_P (%)
Inuvik Silt[a]	**IS-A1**	-	0.36	-	2.99	39	54	7	2.5E-03	50	32	18
Inuvik Silt[a]	**IS-A2**	-	0.43	-	2.86	39	54	7	2.5E-03	50	32	18
Inuvik Silt[a]	**IS-B1**	-	0.30	-	4.72	39	54	7	2.5E-03	55	30	25
Fort Norman Silt[b]	**NS**	-	0.17	-	2.47	39	54	7	2.5E-03	55	30	25
Fort Edwards Silt[c]	FE	-	-	2.33	6.16	45	55	0	2.7E-03	43	20	24
Morin Clay[d]	MC	0.38	0.18	1.44	7.43	35	65	0	5.0E-03	26	19	7
Hanover Silt[d]	HS	0.10	0.03	1.83	26.14	5	95	0	3.4E-02	25	-	-
Ellsworth Clay[d]	EC	0.50	0.30	2.15	4.75	41	48	11	3.1E-03	45	25	20
Toldedo Island[e]	TI	0.82	0.39	1.22	4.68	37	57	6	4.2E-03	71	30	41
Toledo Penn 7[e]	TP	0.94	0.61	1.20	3.84	39	49	12	3.2E-03	61	28	34
Athabasca Clay[f,g]	AC	0.53	0.34	-	-	45	54	1	2.7E-03	40	20	20
Norman Wells[f]	NW	0.45	0.16	-	-	23	67	10	-	29	19	10
Mountain River[f]	MR	0.50	0.25	-	-	55	44	1	-	40	20	20
S75/K25[h]	SK-25	0.16	0.11	2.65	6.50	25	75	0	7.8E-03	32	22	10
S65/K35[h]	SK-35	0.20	0.12	2.82	4.45	35	65	0	5.0E-03	34	23	11
S50/K50[h]	SK-50	0.27	0.14	2.53	3.75	50	50	0	1.9E-03	38	24	14
Péribonka Till[i]	PG	0.09	0.03	4.67	8.75	14	29	57	6.6E-03	15	-	-

*Median particle diameter of the fine fraction
[a]Watson et al. 1973, [b]McRoberts and Morgenstern (1974,1975), [c]Chamberlain et al. (1990), [d]Chamberlain and Gow (1979), [e]Chamberlain and Blouin (1977), [f]Smith (1972), [g]Nixon (1973), [h]Konrad and Samson (2000a) and Wagg (1991), [i]Konrad (2010)

B.4   Compressibility of thawed soils

It is generally accepted that the compressibility of unfrozen soils is correlated with the liquid limit (Skempton and Jones 1944). Additionally, Chamberlain and Gow (1979) noted a link between the Atterberg limits and the magnitude of the void ratio changes observed upon freezing and thawing. It is thus justified to seek a correlation between the compression index of the thawed soils and the liquid limit.

Figure B.2 presents the compression index of the unfrozen and thawed soil as a function of the liquid limit. There is a linear relationship between the compression index and the liquid limit for both the unfrozen and thawed soils that can be defined by equations:

Equation B-1 $C_{cU} = 0.016(w_L - 11)$

and

Equation B-2 $C_{cT} = 0.011(w_L - 18)$,

where w_L is the liquid limit of the soil in percentage.
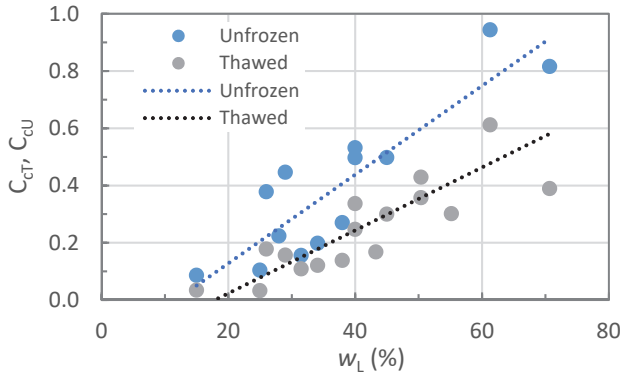
Figure B.2 : Relationship between the compression index and the liquid limit

B.5 Hydraulic conductivity of thawed soils

The hydraulic conductivity of soils is largely controlled by the size of the particles and the soil fabric (Mitchell and Soga 2015). Chamberlain and Gow (1979) indicated that most of the destructuration upon freezing happens at the level of the finer particles whose size controls the permeability of fine-grained thawed soils. It is thus convenient to work with the hypothesis that the hydraulic conductivity of fine-grained thawed soil is mostly controlled by the particle sizes and that the impact of the arrangement of the particles is limited. Accordingly, the median grain size of the fine fraction ($d_{50}(FF)$) can be used because it provides a convenient assessment of the relative size of clay and silt in the fines fraction (Konrad 2005).

Figure B.3 presents $(S_k)^{-1}$ as a function of the $d_{50}(FF)$ in mm for thawed soils. A predictive relationship can thus be defined by equation:

Equation B-3 $(S_{kT})^{-1} = 0.0042 \left(\frac{d_{50}(FF)}{1\,mm}\right)^{-0.70}$

or by inverse function

Equation B-4 $S_{kT} = 240 \left(\frac{d_{50}(FF)}{1\,mm}\right)^{0.70}$

with $d_{50}(FF)$ expressed in mm.
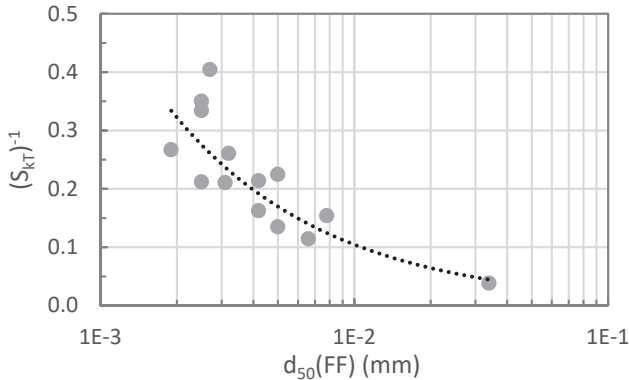
Figure B.3 : Relationship between the slope of the log(σ'$_v$) – e relationship and the median grain size of the fine fraction

B.6   Coefficient of consolidation of thawed soils

The coefficient of consolidation (c_v) can be defined by equation:

Equation B-5 $$c_v = -\frac{(1+e_0)\cdot k_v}{\gamma_w \cdot \frac{de}{d\sigma'_v}},$$

where γ_w is the unit weight of water.

By using void ratio dependent values of the hydraulic conductivity (k_v) and for the compressibility ($\frac{de}{d\sigma'_v}$), void ratio dependent values of c_v can be calculated.

Figure B.4 presents calculated values of c_v as a function of the void ratio for the Ellsworth Clay and for the Morin Clay in the unfrozen and the thawed states. By inspection, it is clear that freeze-thaw cycling has a significant impact on c_v. Indeed, c_v is orders of magnitude higher for the thawed soil and the rate of consolidation of thawed soil is expected to be much larger than for unfrozen soil (Chamberlain and Blouin 1977). This confirms the absolute importance of using the properties of the thawed soil rather than the properties of the unfrozen soil when modelling the consolidation of thawing soil.
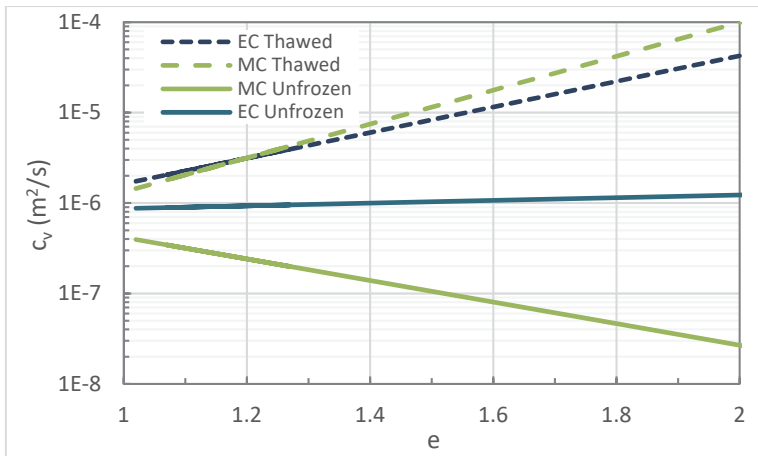
Figure B.4 : Derived values of the unfrozen and thawed coefficient of consolidation of selected soils

Figure B.5 presents the calculated values of c_v as a function of the void ratio of the different Inuvik Silt samples. The three soils were sampled at the same site in order to investigate the effect of a warm-oil pipeline built on ice-rich permafrost (Watson et al. 1973). The IS-A1 and IS-A2 cores were sampled at an average depth of 1.6 m while the B core was sampled slightly deeper at 1.85 m. A stratigraphic change was identified at a depth of about 1.8 m between a very ice-rich silty clay and an underlying ice-rich silt (Rowley et al. 1973). The data suggest that the difference between the coefficient of consolidation of the A and B samples would be considerable at high void ratios and that the coefficient of consolidation would increase with increasing depth. The spatial variation of the coefficient of consolidation would also be exacerbated by the thaw consolidation process. The thawing soil at the surface will initially consolidate quickly because of the small length of the drainage path. However, the soil subsequently liberated at the thaw front will have a higher void ratio and the drainage will be impeded by the presence of a low permeability consolidated layer at the surface. The consolidation rate will thus decrease with increasing thaw depth causing more disparity between the void ratio near the surface and near the thaw front.

The coefficient of consolidation and by extension the compressibility and hydraulic conductivity of thawed soils are not only void ratio dependent but in certain cases they also vary as a function of depth and time throughout the consolidation process. This discussion on the coefficient of consolidation supports that spatially discretized void ratio dependent properties of thawed soils should be used when modelling thaw consolidation in lieu of constant homogeneous values.
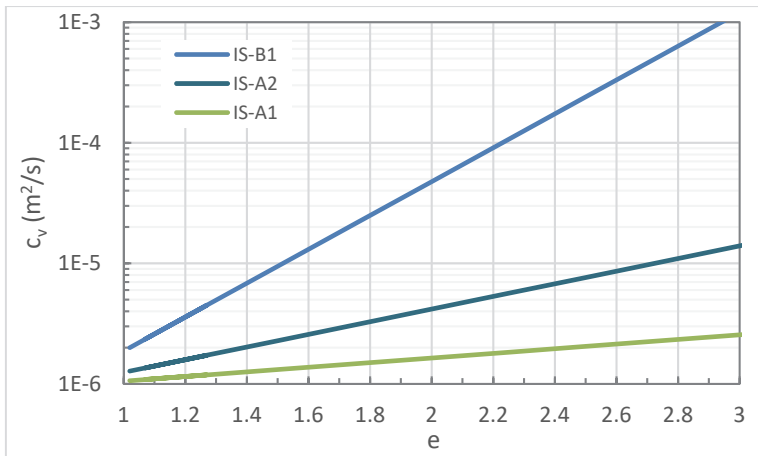
Figure B.5 : Derived values of the coefficient of consolidation of selected permafrost soils

B.7 Conclusion

A compendium of data from the literature was used in order to investigate the compressibility and hydraulic conductivity of thawed fine-grained permafrost. This study led to the following results:

1- The compressibility of thawed soil is correlated with the liquid limit while the hydraulic conductivity is correlated with the median particle diameter of the fine fraction.

2- The compressibility and hydraulic conductivity of fine-grained soils are highly affected by freeze-thaw cycling. The consolidation rate of unfrozen and thawed soil is thus expected to be drastically different. The properties of the thawed soil rather than the ones of the unfrozen soil should be used when modelling thaw consolidation.

3- Spatially discretized and void ratio dependent soil properties should be used when modelling thaw consolidation.

B.8 Acknowledgements

B.9   References

Chamberlain, E., Iskandar, I., Hunsickert, S.E. (1990) "Effect of freeze-thaw cycles on the permeability and macrostructure of soils", In *Proceedings of the International Symposium on Frozen Soil Impacts on Agricultural, Range, and Forest Lands*, Spokane, Wa, pp. 145–155.

Chamberlain, E.J. and Blouin, S.E. (1977) "Freeze-thaw enhancement of the drainage and consolidation of fine-grained dredged material in confined disposal areas", *Technical Report D-77-16*. Foundations and Materials Research Branch, U.S. Army Cold Regions Research and Engineering Laboratory, Hanover, N.H.

Chamberlain, E.J. and Gow, A.J. (1979) "Effect of freezing and thawing on the permeability and structure of soils", *Engineering Geology*, Vol. 13, pp. 73–92.

French, H. and Shur, Y. (2010) "The principles of cryostratigraphy", *Earth-Science Reviews*, Vol. 101, pp. 190–206.

Gibson, R.E., Schiffman, R.L., Cargill, K.W. (1981) "The theory of one-dimensional consolidation of saturated clays. II. Finite nonlinear consolidation of thick homogeneous layers", *Canadian Geotechnical Journal*, Vol. 18, pp. 280–293.

Konrad, J.-M. (2005) "Estimation of the segregation potential of fine-grained soils using the frost heave response of two reference soils", *Canadian Geotechnical Journal*, Vol. 42, pp. 38–50.

Konrad, J.-M. (2010) "Hydraulic conductivity changes of a low-plasticity till subjected to freeze–thaw cycles", *Géotechnique*, Vol. 60, pp. 679–690.

Konrad, J.-M. and Samson, M. (2000) "Hydraulic conductivity of kaolinite-silt mixtures subjected to closed-system freezing and thaw consolidation", *Canadian Geotechnical Journal*, Vol. 37, pp. 857–869.

Mackay, J.R. (1972) "The world of underground ice", *Annals of the Association of American Geographers*, Vol. 62, pp. 1–22.

Mitchell, J.K. and Soga, K. (2005) "Fundamentals of Soil Behavior, 3rd Edition", Wiley.

McRoberts, E.C. and Morgenstern, N.R. (1973) "A study of landslides in the vicinity of the Mackenzie River mile 205 to 660". *Report No. 73-3,* Environmental-Social Committee, Northern Pipelines, Task Force on Northern Oil Development.

McRoberts, E.C. and Morgenstern, N.R. (1974) "The stability of thawing slopes", *Canadian Geotechnical Journal*, Vol. 11, pp. 447–469.

Nixon, J.F. (1973) "The consolidation of thawing soils", Doctoral Thesis, University of Alberta, Edmonton, Alberta, Canada.

Rowley, R.K., Watson, G.H., Wilson, T.M., Auld, R.G. (1973) "Performance of a 48-in. warm-oil pipeline supported on permafrost", *Canadian Geotechnical Journal*, Vol. 10, pp. 282–303.

Skempton, A.W. and Jones, O.T. (1944) "Notes on the compressibility of clays", *Quarterly Journal of the Geological Society*, Vol. 100, pp. 119–135.

Smith, L.B. (1972) "Thaw consolidation tests on remoulded clays", Master Thesis, University of Alberta, Edmonton, Alberta, Canada.

Wagg, B.T. (1991) "Undrained behaviour of clay-silt mixtures during cyclic loading", M.Sc. Thesis, University of Waterloo, Waterloo, Ontario, Canada.

Watson, G.H., Slusarchuk, W.A., Rowley, R.K. (1973) "Determination of some frozen and thawed properties of permafrost soils", *Canadian Geotechnical Journal*, Vol. 10, pp. 592–606.

Williams, P.J. (1966). "Pore pressures at a penetrating frost line and their prediction.", *Géotechnique*, Vol. 16, pp.187–208.